

Characterization of the prelytic active egress of a non-enveloped virus.

Inauguraldissertation
der Philosophisch-naturwissenschaftlichen Fakultät
der Universität Bern

vorgelegt von
RAPHAEL WOLFISBERG

von Neuenkirch, LU

Leiter der Arbeit
Prof. Dr. Christoph Kempf
and
Dr. Carlos Ros

Departement für Chemie und Biochemie

Characterization of the prelytic active egress of a non-enveloped virus.

Inauguraldissertation

der Philosophisch-naturwissenschaftlichen Fakultät
der Universität Bern

vorgelegt von

RAPHAEL WOLFISBERG

von Neuenkirch, LU

Leiter der Arbeit

Prof. Dr. Christoph Kempf
and
Dr. Carlos Ros

Departement für Chemie und Biochemie

Von der Philosophisch-naturwissenschaftlichen Fakultät angenommen.

Bern, DATUM!!

Der Dekan:

Prof. Dr. Gilberto Colangelo

Abstract

The active egress of enveloped viruses is well-characterized and involves budding through host cell membranes. The release of non-enveloped viruses is associated with cellular lysis, thus considered a passive process. This basic principle in virology has recently been challenged by several studies suggesting that non-enveloped viruses may also egress by an active process. However, the mechanisms involved remain largely unknown. Due to their simplicity, the non-enveloped parvoviruses strongly depend on host cell functions for their replication and proliferation. Therefore, they represent ideal tools to study virus host-cell interactions. In order to gain insights into the mechanisms involved in the egress of parvoviruses, the late virus maturation steps preceding virus release were studied in two different cell lines.

Minute virus of mice (MVM) is a well characterized model parvovirus. Assembly of structural capsid proteins occurs in the nucleus giving rise to icosahedral empty capsid (EC) precursors which are subsequently filled with the viral single-stranded DNA to generate full capsids (FC). By applying anion-exchange chromatography, intranuclear MVM progeny particles were separated based on their net surface charge. Apart from EC, two distinct FC progeny populations arose in the nuclei of infected cells. The first FC population to appear was fully infectious but was deficient for nuclear export. In order to acquire egress potential, this early FC progeny underwent further maturations involving the exposure of the N-termini of the major capsid protein VP2 (N-VP2), as well as phosphorylations of surface residues. While the surface phosphorylations were strictly associated to nuclear export capacity, mutational analysis revealed that the phosphoserine-rich N-VP2 was dispensable. N-VP2 was found to mainly assist virus entry as judged by a less efficient delivery of the viral genome to the nucleus for mutants with modified N-VP2. The fact that only the mature phosphorylated population of FC was able to escape from the cells before detectable cell lysis confirms the existence of an active process of virus egress. During cell entry a reverse situation was observed. During endocytic trafficking, incoming virions lost both the N-VP2 termini and the additional surface phosphorylations.

Taken together, these temporally and spatially controlled changes in capsid surface phosphorylation would provide nuclear import and export potential required to complete the life cycle of the karyophilic virus. Further studies are required to identify the corresponding phosphorylations on the capsid surface and to demonstrate their specific role in the active egress of the non-enveloped parvovirus.

Zusammenfassung

Behüllte Viren werden von ihrer Wirtszelle sezerniert, indem sie bei der Knospung Stücke von deren Zellmembran als Bestandteil in die Virushülle integrieren. Für behüllte Viren ist die aktive Freisetzung von Virionen aus infizierten Wirtszellen bereits gut dokumentiert. Die Freisetzung von unbehüllten Viren wird als passiver Vorgang beschrieben, bei dem die Zellmembran durch Zelllyse aufgelöst wird, was zur Absonderung der neu gebildeten Virionen führt. Dieser Grundsatz der Virologie wurde in jüngster Zeit durch mehrere Studien in Frage gestellt, die für unbehüllte Viren einen aktiven Mechanismus zur Freisetzung der Virionen aufzeigten. Aufgrund ihrer Einfachheit sind die unbehüllten Parvoviren zur eigenen Vermehrung und Verbreitung stark von ihrer Wirtszelle abhängig. Daher eignen sie sich gut um die Interaktionen zwischen Viren und ihren Wirtszellen zu studieren. Um die Freisetzung von Parvoviren aus ihrer Wirtszelle besser zu verstehen, wurden späte Maturationsschritte im Kern von infizierten Zellen untersucht, welche der Absonderung der neu gebildeten Virionen unmittelbar bevorstehen. Zur Verstärkung der Aussagekraft wurden die Experimente an zwei verschiedenen Zelllinien durchgeführt.

Minute virus of mice (MVM) ist ein gut charakterisiertes Parvovirus, das sich als Modell für diese Studie eignet. Das Kapsid von Parvoviren wird aus Strukturproteinen, den sogenannten Kapsomeren, gebildet. Beim Vorgang der Selbstassemblierung lagern sich im Zellkern 60 solcher Kapsomere spontan und ohne Energieverbrauch zusammen und bilden ein Kapsid mit ikosaedrischer Symmetrie. Diese leeren Kapside werden anschliessend mit der einzelsträngigen viralen DNA bepackt. Neu generierte Virus Partikel wurden in dieser Studie mittels Anionenaustausch Chromatographie nach deren Oberflächenladungen aufgetrennt. Neben den leeren Kapsiden wurden auf diese Weise zusätzlich zwei unterschiedliche Populationen DNA-bepackte virale Partikel separiert. Die erste Population bepackter Viren im Zellkern war infektiös, wurde allerdings nicht ins Zytoplasma exportiert. Der Export aus dem Zellkern wurde der zweiten Population durch weitere Maturation ermöglicht. Die Maturationsschritte beinhalteten die Externalisierung der Amino-Termini des Hauptstrukturproteins VP2 (N-VP2) durch die Poren an den 5-fach Symmetriearchsen des Kapsids, sowie Phosphorylierungen von Aminosäuren auf der Oberfläche der Kapside. Die Phosphorylierungen auf der Kapsideoberfläche wurden jeweils nur bei den Kapsiden beobachtet, die aus dem Kern exportiert wurden. Mutanten mit modifizierten N-VP2 Termini konnten hingegen ungehindert aus dem Zellkern exportiert werden. Dies impliziert, dass N-VP2 für diesen Vorgang entbehrlich ist. Es zeigte sich, dass N-VP2 vor allem zur Initiierung der viralen Infektion, sowie zur Reorganisation des Zytoskeletts während der Freisetzung der

Viren erforderlich war. Die N-VP2 Mutanten wiesen einen erschwerten Transport des Kapsids zum Zellkern auf. Im Kern wurde weniger mutierte virale DNA quantifiziert was eine verzögerte Replikation zur Folge hatte. Zudem war die Zytolyse infizierter Zellen deutlich verzögert.

Weil vor der Zelltlyse ausschliesslich der vollständig maturierte Virus im Überstand der Zellkultur nachgewiesen wurde, konnte ein aktiver Mechanismus zur Freisetzung der neu gebildeten Virionen bestätigt werden. Obwohl zuerst eine Segregation beider DNA-bepackten Populationen beobachtet wurde konnte die frühe, unreife virale Population durch virus-induzierte Zelltlyse passiv freigesetzt werden. Interessanterweise wurde beim Eindringen der Viren in die Wirtszelle die umgekehrte Situation beobachtet. In den Endosomen wurde N-VP2 proteolytisch abgebaut und saure Phosphatasen entfernten die Phosphorylierungen auf der Kapsidoberfläche.

In dieser Arbeit wurden Phosphorylierungen auf der Kapsidoberfläche eines unbehüllten Virus identifiziert welche zeitlich und räumlich streng kontrolliert werden. Diese Modifikationen auf der Kapsidoberfläche könnten unbehüllten Viren den Import in den Zellkern, beziehungsweise deren Export aus dem Zellkern, ermöglichen. Der Transport in und aus dem Zellkern ist für karyophile Viren unabdingbar zur Vollendung ihres Lebenszyklus. Zur Identifizierung der entsprechenden Phosphorylierungen auf der Kapsidoberfläche sind in Zukunft weitere Untersuchungen notwendig. Zudem bleibt deren spezifischer Einfluss in der aktiven Freisetzung der neu generierten Virionen von der Wirtszelle weiterhin unklar.

Acknowledgements

The present thesis would not have been possible without the support and guidance that I received from many individuals. All of them contributed in one way or another and extended their valuable assistance during the preparation and completion of this study. It is a great pleasure to express my gratitude to all of them in my humble acknowledgement.

Foremost I want to thank Prof. Dr. Christoph Kempf for providing me with the opportunity to complete my PhD in his research group. Thank you very much for your active support and the freedom you gave me during the time in your lab.

I feel deeply indebted and honored to be mentored by Dr. Carlos Ros, my direct supervisor, who believed in my abilities and patiently guided me through the whole thesis. I am always grateful for his encouragement and for inspiring me with numerous clever experiments which helped to substantiate my scientific outlook. The joy and enthusiasm he has for our research was exemplary, contagious, and motivated me greatly during my PhD. I received constructive and competent feedback with regards to critical reading of papers as well as coherent presentation and skeptical interpretation of my results. His helpfulness and great sense of humor helped me to overcome experimental setbacks and provided a nice working atmosphere.

I would like to thank all the former and current co-workers in our laboratory: Aurélie Allemann, Chiarina Di Tommaso, Remo Leisi, Nico Ruprecht, Marcus von Nordheim, and Seline Zürcher. Our group has been a source of friendships as well as good collaboration. It was very pleasant to work in such a friendly and helpful environment.

I gratefully acknowledge the funding received towards my PhD from the university of Bern as well as CSL Behring AG.

Further thanks go to Achim Stocker and Walter Aeschimann for their advice and kind help with the Äkta chromatography system and for optimizing the chromatography protocols. It has been always interesting to gain further insight into the field of virology from totally different perspectives.

My time at the university of Bern was made enjoyable in large part due to the many friends at the department of chemistry and biochemistry (DCB). I am grateful for the time I spent

with you, for partying together and for the time we spent in the city, on the Gurten or down by the Aare. Special thanks go to Christof Wyss and his family for annually offering us a royal residence in their lovely chalet in Grindelwald during our memorable skiing vacations!

I want to thank Dr. Shweta Kailasan and Dr. Pamela Nicholson for critical review of parts of the present PhD thesis and for their helpful annotations in revising my English language.

Many thanks go to my best friends Martin Buob and Christian Schnyder for frequently distracting me from work and always giving me a warm welcome back at home in Neuenkirch. They always kept me well informed about the most recent happenings in Lucerne, thus I never felt fully disconnected. I really enjoyed the countless amazing moments I could share together with you whether it be just having a beer in a bar, enjoying the atmosphere at an open-air concert, or traveling around and discovering new places. In addition, I really appreciate the many barbecues I had together with you and our friends at Sagiweg 3 in Neuenkirch!

I would like to thank Stefan Hofstetter for pitching L^AT_EX to me and for rescuing me from the flaws of Microsoft word. I appreciate his invaluable advice and his patient help with the organization of the template file. It helped me definitely to save a lot of time, energy and pain!

I want to thank Markus Antener, my long-standing flat mate, for the funny time we had together and for bearing me for eight years! Thanks a lot for all the computer support and for providing me always with the latest software. I thank Marion Landolt for always arranging our flat with many flowers, paintings, pictures, and photos, thus making it a pleasant and comfortable place to live. I loved a lot her "bündnerische" nature and her crazy ideas. Thank you both for regularly taking me out and for all the relaxing activities we undertook together.

Last but definitely not least I would like to express my sincere gratitude to my lovely family. A special thanks to my parents Beat and Pia for all of the sacrifices that you have made on my behalf. Your faith in me was what sustained me thus far. Thanks for your thoughtfulness, encouragement, and financial support. You were all the time on hand with help and advice for me. I further thank Chantal, Nadine, and Anja for being the best sisters and for their warmth and words of advice. Thank you.

To my friends in Madrid

Un agradecimiento profundo al profesor José María Almendral del Río por su colaboración y por hacer posible mi breve estancia en el Centro de Biología Molecular Severo Ochoa (CBMSO) en la Universidad Autónoma de Madrid (UAM). Muchas gracias por hacer los días tan agradables en tu laboratorio y por periódicamente sacarnos a pasear para comer en el centro. Quedo en deuda contigo por haber puesto a mi disposición gran cantidad de material, anticuerpos y mutantes incluso, después de mi partida.

Especial mención merecen Nooshin Bayat y Lorena Gallego Villar por todas las chulas actividades que hicimos juntos en Madrid. Ha sido un verdadero placer conocerlos y descubrir parte de Madrid con vosotros. Fue muy divertido e interesante conocer Madrid, la comida rica, la cultura y las fiestas españolas! Muchas gracias por todos los buenos momentos que compartimos.

Quiero agradecer a mis queridos compañeros que trabajan en Madrid. A Carlos Dominguez Redondo, Jon Gil Ranedo, Josefa González Nicolás, Marta Pérez Illana y Aroa Tato de la Torre por haberme acogido tan amablemente en el grupo y por el ambiente de trabajo muy divertido y socorrido. Muchas gracias a Sandra Arduim Brasil, Celia Medrano Rodríguez, Alfonso Oyarzabal Sanz, Pablo Pérez Carillo y Patricia Yuste Checa por las conversaciones interesantes a la hora de comer y la paciencia que tuvieron con mi pobre español.

Raphael Wolfisberg
University of Bern
August 2015

Nomenclature

AAV	Adeno-associated virus	FCS	Fetal calf serum
AMDV	Aleutian mink disease virus	FGFR1	Fibroblast growth factor receptor 1
ATP	Adenosine triphosphate	FPV	Feline parvovirus
ATPase	Adenosine triphosphatase	Gb4Cer	Globotetraosyl ceramide
B19V	Human parvovirus B19	GmDNV	Galleria mellonella densovirus
BC	Basic cluster	H1-PV	Parvovirus H1
Bp	Base pair	HBoV	Human Bocavirus
BPV	Bovine parvovirus	HGFR	Hepatocyte growth factor receptor
CD	Cytochalasin D	HIV	Human immunodeficiency virus
ChPV	Chicken parvovirus	hpi	Hours post-infection
CLIC	Clathrin-independent carrier	HRP	Horseradish peroxidase
CPV	Canine parvovirus	HSPG	Heparan sulphate proteoglycan
CRE	cAMP-responsive element	IF	Immunofluorescence microscopy
cRF	Closed replicative form DNA	Ig	Immunoglobulin
CRM1	Chromosome region maintenance 1	IgG	Immunoglobulin G
CV	Column volume	IP	Immunoprecipitation
DCB	Department of Chemistry and Biochemistry	ITR	Inverted terminal repeat
DMEM	Dulbecco modified Eagle's medium	kb	Kilobase
DNA	Deoxyribonucleic acid	kDa	Kilodalton
dRF	Dimeric replicative form DNA	LamR	Laminin receptor
dsDNA	Double-stranded DNA	LMB	Leptomycin B
EC	Empty capsid	m. u.	Map unit
EGFR	Epidermal growth factor receptor	mAb	Monoclonal antibody
EM	Electron microscopy	mRF	Monomeric replicative form DNA
ER	Endoplasmic reticulum		
FC	Full capsid		

mRNA	messenger RNA	PPV	Porcine parvovirus
MVM	Minute virus of mice	pre-mRNA	messenger RNA precursor
MVMi	Immunosuppressive strain of MVM	PTM	Post-translational modification
MVMp	Prototype strain of MVM	qPCR	Quantitative PCR
MW	Molecular weight	RF	Replicative form
ND	Nocodazole	RHR	Rolling hairpin replication
NHP	Nonhuman primate	RNA	Ribonucleic acid
NIH	National institutes of health	RSS	Runting-stunting syndrome
NLM	Nuclear localization motif	SA	Sialic acid
NLS	Nuclear localization signal	SAT	Small alternatively translated protein
NPC	Nuclear pore complex	SCID	Severe combined immunodeficiency
NS	Non-structural (protein)	SN	Supernatant
nt	Nucleotide	sPLA ₂	Secretory PLA ₂
ORF	Open reading frame	ssDNA	Single-stranded DNA
PARV4	Human parvovirus 4	SV40	Simian vacuolating virus 40 or Simian virus 40
PCNA	Proliferating cell nuclear antigen	TfR	Transferrin receptor
PCR	Polymerase chain reaction	TGN	Trans Golgi network
PDGFR	Platelet-derived growth factor	TuPV	Turkey parvovirus
PEC	Poult enteritis complex	VLP	Virus-like particle
PEMS	Poult enteritis mortality syndrome	VP	Viral protein
PFU	Plaque-forming unit	VP1u	VP1 unique region
pI	Isoelectric point	WB	Western blotting
PIF	Parvovirus initiation factor		
PLA ₂	Phospholipase A ₂		

Contents

Abstract	i
Zusammenfassung	iii
Acknowledgements	v
Nomenclature	vii
I. Introduction	1
1. Discovery and brief history	3
2. Taxonomy	5
2.1. The <i>Parvovirinae</i> subfamily	6
2.1.1. <i>Amdoparvovirus</i>	6
2.1.2. <i>Aveparvovirus</i>	7
2.1.3. <i>Bocaparvovirus</i>	7
2.1.4. <i>Copiparvovirus</i>	8
2.1.5. <i>Dependoparvovirus</i>	9
2.1.6. <i>Erythroparvovirus</i>	9
2.1.7. <i>Protoparvovirus</i>	10
2.1.8. <i>Tetraparvovirus</i>	10
3. Morphology	15
4. The rugged virion	17
4.1. Physicochemical Properties	17
4.2. Atomic Model	17
4.3. Structural Proteins	18
4.4. Functional Domains	20
4.4.1. The Phospholipase A ₂ (PLA ₂) Motif	20

Contents

4.4.2. The Nuclear Localization Signal (NLS)	21
4.4.3. The Nuclear Localization Motif (NLM)	22
5. Genome Architecture	25
5.1. The MVM Left- and Right-End Telomeres	25
5.1.1. Terminal Resolution <i>versus</i> Asymmetric Junction Resolution	26
5.2. Genetic variability	27
6. Host Range and Specificity	29
6.1. Tissue Tropism Determinants	29
6.2. Pathogenicity Determinants	30
6.3. Comparison of Tissue Tropism and Pathogenicity Determinants among Parvoviruses	30
7. The Parvovirus Life Cycle	33
7.1. Receptor Binding	34
7.2. Receptor-mediated Endocytosis	36
7.3. Endosomal Trafficking and Capsid Rearrangements	37
7.4. Endosomal Escape	38
7.5. Cytosolic Trafficking and Interactions with the Proteasome	39
7.6. Nuclear Targeting	40
7.6.1. Nuclear Translocation of the Incoming Virion	40
7.6.2. Nuclear Translocation of the Structural Proteins	42
7.7. Non-structural (NS) proteins	43
7.7.1. Non-structural protein 1 (NS1)	43
7.7.2. Non-structural protein 2 (NS2)	44
7.7.3. Small alternatively translated (SAT) protein	44
7.8. Replication	45
7.9. Transcription and RNA processing	47
7.10. Assembly	50
7.11. DNA Packaging	51
7.12. Nuclear Export	52
7.13. Egress	53
8. Aim of the thesis and experimental strategy	55
8.1. Goals	55
8.2. Experimental strategy	55

II. Methods	57
9. Methods	59
9.1. Cell Cultures	59
9.1.1. Freezing and thawing of cells	59
9.2. Virus Stocks	59
9.2.1. Separation of empty and full capsids	60
9.3. Freezing bacteria stocks in glycerol	60
9.4. Fast protein liquid chromatography (FPLC)	60
9.4.1. Anion-exchange chromatography (AEX)	61
9.4.2. Chromatofocusing (CF)	61
9.5. Quantitative PCR (qPCR)	62
9.6. Virus infection	63
9.7. Transfection	63
9.8. Cell fractionation	64
9.8.1. Nuclei isolation	64
9.8.2. Extraction of the cytoplasm	64
9.9. Immunoprecipitation (IP)	64
9.10. Dot Blot	64
9.11. SDS-PAGE and Western blotting (WB)	65
9.12. Enzymatic reactions	65
III. Publication	67
1. Wolfisberg et al., Journal of Virological Methods, 2013	71
Impaired genome encapsidation restricts the <i>in vitro</i> propagation of human parvovirus B19.	71
IV. Results	83
2. Supplementary Data	85
2.1. The phosphoserine-rich N-VP2 of MVM facilitates nuclear targeting and contributes to cytotoxicity.	85
2.1.1. Isolation and characterization of empty capsids (EC)	87
2.2. Full capsids (FC) bind preferentially to murine fibroblasts	88
2.2.1. N-VP2 is not sufficient to provide an advantage in binding for FC	90
2.3. Anion-exchange chromatography (AEX) can be applied on other parvoviruses	93

V. Discussion	95
3. Conclusion	97
VI. Appendix	99
9. Materials	101
9.1. Infectious clone of MVMp (pIC_MVMp)	101
9.1.1. Plasmid map of pIC_MVMp	101
9.1.2. Complete sequence of pIC_MVMp	102
9.2. Chemicals and compounds	105
9.3. Buffers	107
9.3.1. General buffers	107
9.3.2. Chromatography buffers	108
9.3.3. Agarose gel electrophoresis	109
9.3.4. Western blot	109
9.4. Kits	110
9.5. Enzymes	110
9.6. Antibodies	111
9.6.1. Primary antibodies	111
9.6.2. Secondary antibodies	112
9.7. Media	112
Bibliography	113
Declaration	138

List of Figures

2.1. The <i>Parvovirinae</i> subfamily	6
3.1. Parvovirus surface topology groups	16
4.1. Structure of MVM	19
4.2. The cleavage sites of different types of PLAs	21

4.3. Nuclear localisation signal (NLS)	22
4.4. Nuclear localisation motif (NLM)	23
5.1. Genome architecture of minute virus of mice (MVM).	28
7.1. Life cycle of MVM	33
7.2. Rolling hairpin replication (RHR)	46
7.3. Transcription map of MVM	49
9.1. Schematic outline of the ÄKTA purifier FPLC chromatography system.	60
S1. Kinetics of nuclear export depends on the input virus.	86
S2. Purification and analysis of FC and EC.	89
S3. FCs are preferentially bound to the SA residues on the cell surface.	91
S4. N-VP2 exposure alone is not sufficient for the better binding to SA moieties.	92
3.1. Schematic representation of nuclear import and export of MVM.	98
9.1. Plasmid map of the infectious clone of MVMp	101

List of Tables

2.1. Taxonomy for the subfamily <i>Parvovirinae</i>	12
7.1. Parvoviruses and their receptors	35
9.1. Master mix for quantitative PCR	62
9.2. PCR conditions	62
9.3. Primers	63
9.1. Chemicals and compounds	106
9.2. General buffers	107
9.3. Anion-exchange chromatography (AEX) buffers	108
9.4. Chromatofocusing (CF) buffers	108
9.5. Agarose gel electrophoresis buffers	109
9.6. Western blot buffers	109
9.7. Ready-to-use Reaction Systems (Kits)	110
9.8. Enzymes	110

List of Tables

9.9. Primary antibodies	111
9.10. Secondary antibodies	112
9.11. Media	112

Part I

Introduction

1. Discovery and brief history

Minute virus of mice (MVM) is a small, non-enveloped autonomous replicating parvovirus. Two variant forms of MVM that share 96 % nucleotide (nt) sequence identity [393] have been discovered. MVMP, the prototype strain, was isolated and characterized by Crawford in 1966. It originated from a contaminated murine adenovirus stock and was shown to replicate efficiently in mouse fibroblasts [137]. The virus was plaque purified in 1972 [438] and the resulting strain was designated MVM(p) for prototype [426]. Another strain was recovered from the culture fluid of infected murine EL-4 T-cell lymphoma cells by Bonnard and colleagues in 1976 [57]. This strain efficiently replicates in lymphocytes and is immunosuppressive for allogeneic mixed leukocyte cultures as it inhibits the generation of cytolytic T lymphocytes [163]. Therefore, it was referred to as immunosuppressive strain MVMi [304]. Both strains are well characterized and reciprocally restricted for growth in each other's murine host cell.

Since its discovery nearly 50 years ago, MVM served as an interesting model virus to dissect the molecular mechanisms of tissue tropism, capsid dynamics associated with endosomal trafficking, as well as viral deoxyribonucleic acid (DNA) replication and packaging. Furthermore, it gained increasing interest as an important tool for cancer therapy due to its oncolytic capabilities and currently represents a commonly accepted parvovirus model.

2. Taxonomy

The classification of the *Parvoviridae* family is based on morphological and functional characteristics. Parvoviruses are ubiquitous pathogens that belong to one of the smallest DNA-containing viruses. Hence, the prefix "parvum" that means small in Latin. The name "parvovirus" was first introduced to the literature by Carlos Brailovsky, in an early attempt to establish a latinized binomial taxonomy system for viruses, in 1966 [63]. The age of the *Parvoviridae* family may exceed 40 to 50 million years [39]. Apart from their ancient history, the genomes of parvoviruses were affirmed to display similar high mutation rates to ribonucleic acid (RNA) viruses [172, 184, 410, 411, 430, 485]. Such high mutation rates in conjunction with the long history might be a reason for the vast genetic divergence and extensive diversity seen within the family. The *Parvoviridae* family comprises of non-enveloped, isometric viruses that contain linear single-stranded DNA genomes. Indeed, parvoviruses are the only viruses in the known biosphere that have both single-stranded and linear DNA genomes. The encapsidated single genomic molecule is 4-6 kilobase (kb) in length and terminates in palindromic duplex hairpin telomers. In general, there are two large open reading frames (ORF1 and ORF2) encoding for the non-structural (NS) protein(s) and the viral capsid protein(s) (VPs), respectively. In some cases, an additional ORF3 has been identified that encodes an accessory protein, such as NP1, a NS protein only found in members of the genus *Bocaparvovirus* and in porcine parvovirus (PPV) a member of the genus *Copiparvovirus* [88, 89, 261]. As a consequence of such a simple genome, parvoviruses are highly dependent on their host for diverse functions in their reproduction [109, 450]. The terminal hairpins are fundamental for their unique replication strategy and serve as an invariant hallmark for classification. Members of the family *Parvoviridae* infect a wide variety of hosts, ranging from insects to primates. Depending on their host range, the *Parvoviridae* are subdivided into *Parvovirinae* infecting vertebrates and *Densovirinae* infecting insects and other arthropods, respectively. The *Parvovirinae* subfamily is further subdivided into eight genera: *Amdoparvovirus*, *Aveparvovirus*, *Bocaparvovirus*, *Copiparvovirus*, *Dependoparvovirus*, *Erythroparvovirus*, *Protoparvovirus*, and *Tetraparvovirus* (see Figure 2.1, p. 6) [136]. The subdivision into the eight genera is based on differences in transcription maps, organization of the inverted terminal repeats (ITRs), the ability to replicate efficiently either autonomously or with helper virus, the sense of the single-stranded DNA (ssDNA) that is packaged into separate virions, and sequence homology amongst the *Parvovirinae* subfamily [240, 285].

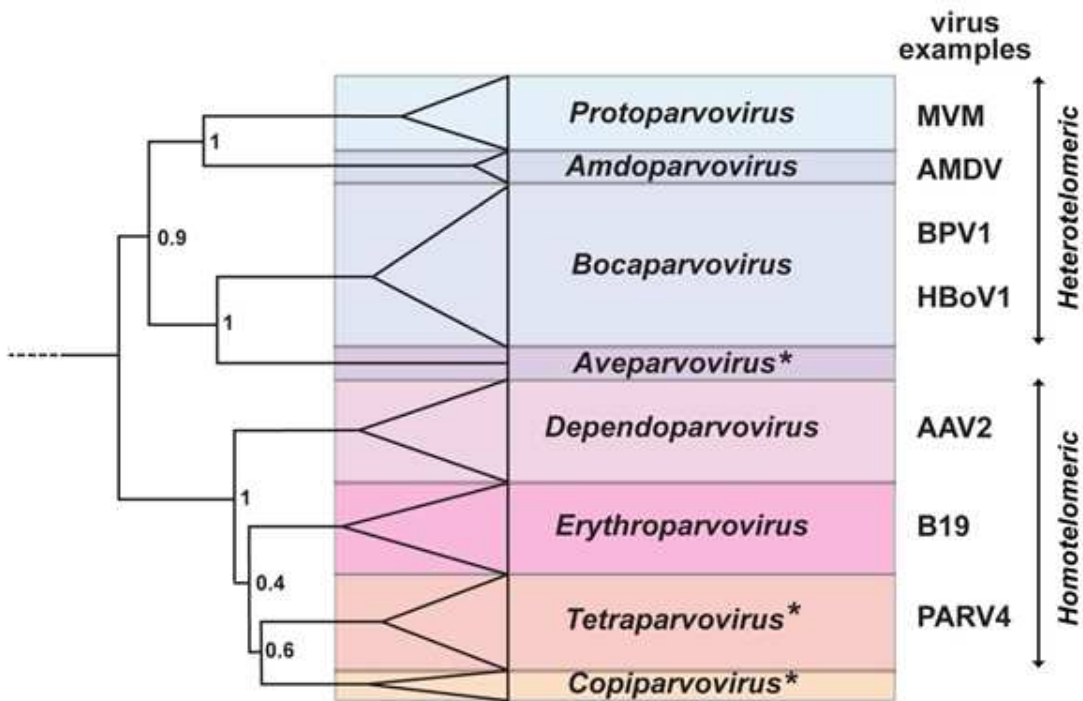


Figure 2.1.: The *Parvovirinae* subfamily. The genera of the *Parvovirinae* subfamily are depicted in a phylogenetic tree. Phylogenetic analysis is based on the amino acid sequence of NS1. The size of the color block for each genus indicates the relative number of species currently recognized, as an indicator of its diversity. Asterisks denote the names of new genera.

2.1. The *Parvovirinae* subfamily

2.1.1. *Amdoparvovirus*

Mature virions exclusively contain negative strand genomic DNA of approximately 4.8 kb in length harbouring dissimilar palindromic sequences at each end [9, 50]. A single promoter located at map unit (m. u.)¹³ at the left end of the genome generates all messenger RNA (mRNA) transcripts of Aleutian mink disease virus (AMDV). Polyadenylation may occur at either the proximal site or at the distal site of the genome. Thus, the transcription profile of the genus *Amdoparvovirus* most closely resembles that of the genus *Erythroparvovirus* [376]. Only two distant species have been reported. Firstly, *Carnivore amdoparvovirus 1*, which comprises only AMDV and secondly, *Carnivore amdoparvovirus 2*, which encompasses solely gray fox amdovirus [266]. Permissive replication is tightly restricted to Crandell feline kidney cells. The virion surface displays three mounds elevated around the threefold icosahedral axis of symmetry. Several structure features

¹ Map units are commonly accepted units that relate to the position in the genome. The parvoviral genomes are arbitrarily subdivided into 100 m. u.

were ascertained to be similar to those found in human parvovirus B19 (B19V), canine parvovirus (CPV), feline parvovirus (FPV), and MVM. Such appearance is comparable to those observed for the genus *Dependoparvovirus* [302]. Remarkably, there is no evidence of a phospholipase 2A enzymatic core within the naturally truncated N-VP1 terminus of members belonging to the genus *Amdoparvovirus* as it is common to the other genera of the subfamily *Parvovirinae* [240].

2.1.2. *Aveparvovirus*

Aveparvovirus is a new genus within the *Parvovirinae* subfamily that comprises of the species chicken parvovirus (ChPV) and turkey parvovirus (TuPV). The name *Aveparvovirus* is derived from avian parvoviruses, referring to the hosts from which the members were isolated. Although these viruses were identified for years in the intestinal tracts of poultry [243, 244, 452], analysis of the complete sequence has been reported only recently. Phylogenetic study of the genomic sequences revealed that interestingly, ChPV and TuPV do not group phylogenetically with goose parvovirus and duck parvovirus, that are members of the genus *Dependoparvovirus*. It has been clearly demonstrated that ChPV, along with the closely related TuPV, represents the prototype of a novel genus within the *Parvovirinae* subfamily [247, 514]. Identical direct repeat sequences flank the genome at both the 3' and the 5' end. Each of which contains a 39 nt ITR that is predicted to form a hairpin structure. ChPV and TuPV feature an overall genome organization similar to that of members of the genus *Bocaparvovirus* [142]. Although it has been demonstrated that ChPV can induce clinical signs in broiler chickens that show characteristics of the runting-stunting syndrome (RSS) [242], the role of avian parvoviruses in the aetiology of enteric diseases in poultry still remains to be demonstrated. RSS, also referred to as malabsorption syndrome, is characterized by significantly decreased egg hatchability, poorly developed hatched chickens, serious growth retardation, diarrhoea, enteritis, disturbed feathering, low vitality, and bone disorders [183, 349, 362]. Currently, the pathogenicity of TuPV has not been investigated yet. The predominant enteric diseases in turkeys are known as poult enteritis complex (PEC) [29] or the more drastic poult enteritis mortality syndrome (PEMS) [394]. Understanding the role of avian parvoviruses in PEMS, PEC, and RSS is of great interest due to the economic losses resulting from enteric diseases in poultry. [514].

2.1.3. *Bocaparvovirus*

The name of the genus is derived from bovine and canine, referring to the two hosts of the first identified members of this genus. The genomes of members of the genus *Bocaparvovirus* are quite distinct from all other viruses in the subfamily *Parvovirinae*. As the members of the genera *Protoparvovirus* and *Amdoparvovirus* they contain non-identical imperfect palindromic sequences at both ends of their 5.5 kb genome. Mature virions contain mainly, but not exclusively, negative strand ssDNA [86, 402]. All RNA transcripts are generated from a single P4 promoter at

the left-hand end of the genome. The transcripts are alternatively spliced and polyadenylated either at an internal site or at the 3'-end of the genome [377]. Noteworthy, bovine parvovirus (BPV), the main representative, encodes a 22.5 kilodalton (kDa) nuclear phosphoprotein, NP1, whose function still remains unknown. This protein is distinct from any other parvovirus-encoded polypeptide [261]. A human bocavirus (HBoV) was first described in 2005, when it was detected in nasopharyngeal aspirates of young children with respiratory tract infection [10, 11]. More recently, HBoV has been identified in diarrheal feces of children with gastroenteritis [465]. HBoV infection is associated with acute respiratory symptoms and is usually detected in children under 2 years of age [35, 290, 295]. HBoV infections have been reported world-wide and HBoV was often isolated in respiratory samples of diseased as well as asymptomatic patients sometimes long after the primary infection. Therefore, it can be frequently detected even though it is not likely acting as a pathogen, thus complicating the use of polymerase chain reaction (PCR) in diagnostics. Furthermore, long-term persistence may explain that HBoV infection among adults was predominantly reported in association with immunosuppression or immunodeficiency [255, 295].

2.1.4. *Copiparvovirus*

Based on phylogenetic analysis, the genus *Copiparvovirus* encompasses PPV4 and BPV2. PPV4 was identified in clinical samples from swine herds [49, 89, 217] and represents a distinct branch together with BPV2 [10]. The name *Copiparvovirus* refers to cows and pigs, the hosts from which members of that genus were isolated. PPV4 is unique in that it is phylogenetically most closely related to BPV2 but the coding capacity and genome organization resemble more those of viruses of the genus *Bocaparvovirus*. While the ORF3 encoded proteins of the three recognized *Bocaparvovirus* members share amino acid identities of 43.3-47.0 % among themselves, the PPV4 ORF3 encoded protein does not display homology with any protein in the GenBank database [89, 217]. Recently, two novel porcine parvoviruses, PPV5 and PPV6, were discovered [333, 499]. Characterization of their sequences revealed that their full-length genomes are approximately 6 kb in length. As a consequence of this capacious genome size, especially their capsid protein encoding genes are exceptionally large. Interestingly, the genomic organization of PPV5 and PPV6 is different from PPV4 in that they lack the extra ORF3 in the middle of the genome. Moreover, PPV5 as well as PPV6 possess the conserved putative secretory phospholipase A₂ (sPLA₂) motif which is present in the capsid protein of most parvoviruses but is lacking in PPV4. In spite of considerable differences in the genomic organization between BPV2, PPV5, and PPV6 on the one hand and PPV4 on the other hand, phylogenetic analysis revealed a close evolutionary relationship of these viruses, suggesting that they share the same immediate ancestor [333, 498]. Since members of the genus *Copiparvovirus* were discovered quite recently, their biological characteristics, relatedness to disease, and potential clinical manifestations are

still not fully understood [89, 217, 333, 498]. Especially, Kresse strain of porcine parvovirus belonging to the genus *Protoparvovirus* is known to be an important pathogen responsible for embryonic and fetal death in piglets, resulting in considerable losses in the pig industry worldwide [252, 306, 307, 461]. In order to clarify the precise role of the most recently discovered members of the genus *Copiparvovirus* as causative agents of reproductive failure in breeding animals, more comprehensive epidemiologic studies are required in the future [333].

2.1.5. *Dependoparvovirus*

Positive and negative strand ssDNA is distributed indifferently among mature virions belonging to the genus *Dependoparvovirus* [41, 388]. The 4.7 kb DNA molecule contains identical ITRs of 145 nt, the first 125 nt of which form a palindromic sequence [287]. Three mRNA promoters that are located at m. u. 5, 19, and 40 initiate transcription that can be terminated in two polyadenylation sites located at the right-hand end or alternatively, in the middle of the genome [187, 288]. Common for all currently accepted replication-defective members of the genus *Dependoparvovirus* is their strict dependence upon helper adenoviruses or herpesviruses [21, 73, 211]. Therefore, their host range tropism strongly depends on the one of the helper virus. The only exceptions are the autonomously replicating duck and goose parvoviruses which are also comprised within the *Dependoparvovirus* genus based on phylogenetic analysis [240]. The most important members of this genus are the adeno-associated viruses (AAV). They attract considerable interests since some of them, including AAV-2, have been reported to integrate site-specifically into the human genome [249–251, 398]. This characteristic makes AAV a promising candidate for creating viral vectors for gene therapy [143, 312]. As a well characterized member of the *Dependoparvoviruses*, AAV-2 represents the model virus among this genus.

2.1.6. *Erythroparvovirus*

Equivalent numbers of positive and negative sense ssDNA are packaged into infectious virions of the genus *Erythroparvovirus*. As in the case with the genus *Dependoparvovirus*, the 5.5 kb ssDNA molecule contains identical ITRs of 383 nt in length at both the 3' and the 5' end. The first 365 nt of those secondary elements form palindromic sequences [145]. Transcription is regulated by a single mRNA promoter located at m. u. 6 [153]. A distal polyadenylation site for use in termination of RNA synthesis is located at the far right side. Additionally, transcripts may be terminated at an unusual internal polyadanylation site in the middle of the genome [346]. Viruses belonging to this genus are highly erythrotropic, meaning that efficient replication only occurs in rapidly dividing erythroid progenitor cells, such as erythroblasts and megakaryocytes present in the bone marrow. B19V, a widespread human pathogen that causes fifth disease, polyarthropathia, anemic crises in children with underlying hematological diseases (e.g. sickle cell anemia or thalassemia) and intrauterine infections (with hydrops fetalis in some cases) [206]

represents the model virus among the genus *Erythroparvovirus*.

2.1.7. *Protoparvovirus*

Kilham Rat virus, a member of the genus *Protoparvoviruses* was the first member of the subfamily *Parvovirinae* to be discovered in 1959 [238]. Some members of the genus contain positive strand DNA in variable proportions up to 50 % [36]. However, in mature virions of most members, virtually only negative strand DNA occurs. What they have in common are their hairpin structures at both the 5' and 3' ends of the linear 5 kb ssDNA molecule that differ in both sequence and predicted structure [18]. Transcription of the genome is regulated by two mRNA promoters at m. u. 4 and 38 [367]. There is only one polyadenylation site at the 3' end. Viral replication provokes characteristic cytopathic effects in cell culture. Many species display hemagglutination with erythrocytes of one or several species, but not enforcedly of their natural host [193]. The genus *Protoparvovirus* is primarily represented by MVM [240, 439].

2.1.8. *Tetraparvovirus*

The genus *Tetraparvovirus* is a genus that has been recently described. To date, six species have been discovered, which were isolated from humans [226], chimpanzees, baboons [412], cows, pigs [2, 258, 265], as well as sheep [457]. RNA transcripts that encode the NS proteins or the VPs are generated from two promoters that are located at m. u. 6 and 38, respectively. Transcription can be terminated in two polyadenylation sites located at the right-hand end of the genome or alternatively, at an internal polyadenylation site. Since the full-length genome has not been sequenced yet, information of the terminal repeats is still lacking [283]. Analysis of the NS1 protein revealed a G2/M cell cycle arrest induced in NS1-expressing hematopoietic stem cells that clearly involved the predicted helicase motifs [224, 316, 471] of NS1. To date, no phospholipase A₂ (PLA₂)-like activity of expressed VP1 unique region (VP1u) polypeptides has been demonstrated for any member of the genus *Tetraparvovirus* [283]. Human parvovirus 4 (PARV4) is one of the only four groups of parvoviruses that is known to infect humans besides B19V, HBoV, and AAV. It was first reported in an intravenous drug user who was positive for hepatitis B virus infection in 2005. The patient suffered from arthralgia, confusion, diarrhea, fatigue, neck stiffness, night sweat, pharyngitis, and vomiting. PARV4 represents a phylogenetic deeply rooted lineage between avian dependoviruses and BPV type 3 [226]. So far, most evidence about PARV4 transmission comes from patients who had engaged in high risk behaviour for blood borne viral infections, where PARV4 infection basically was observed to be strongly associated with hepatitis C virus and human immunodeficiency virus (HIV) infection [296, 416, 505]. However, there are several reports of parenteral transmission in the absence of HIV, hepatitis B virus, or hepatitis C virus. PARV4 immunoglobulin G (IgG) has been documented independently from other blood borne viruses among injecting drug users [417], in haemophilia patients [413], and in patients who were

subjected to intra-muscular injections in the past [260]. Currently, no definitive clinical syndrome has been associated with PARV4 infection and there is no evidence for a potential pathogenicity of related members of the genus *Tetraparvovirus* in animals [258]. PARV4 viraemia appears to be asymptomatic [351] and co-existing blood borne viruses do not increase severity [505].

Table 2.1.: Taxonomy for the subfamily *Parvovirinae*

Genus	Species	Virus / virus variants	Abbr.	ACNO²
<i>Amdoparvovirus</i>	<i>Carnivore amdoparvovirus 1</i>	Aleutian mink disease virus	AMDV	JN040434
	<i>Carnivore amdoparvovirus 2</i>	Gray fox amdovirus	GFAV	JN202450
<i>Aveparvovirus</i>	<i>Galliform aveparvovirus 1</i>	Chicken parvovirus	ChPV	GU214704
		Turkey parvovirus	TuPV	GU214706
<i>Bocaparvovirus</i>	<i>Carnivore bocaparvovirus 1</i>	Canine minute virus	CnMV	FJ214110
	<i>Carnivore bocaparvovirus 2</i>	Canine bocavirus 1	CBoV	JN648103
<i>Bocaparvovirus</i>	<i>Carnivore bocaparvovirus 3</i>	Feline bocavirus	FBoV	JQ692585
	<i>Pinniped bocaparvovirus 1</i>	California sea lion bocavirus 1	CslBoV1	JN420361
<i>Bocaparvovirus</i>	<i>Pinniped bocaparvovirus 2</i>	California sea lion bocavirus 2	CslBoV2	JN420366
	<i>Primate bocaparvovirus 1</i>	California sea lion bocavirus 3	CslBoV3	JN420365
<i>Bocaparvovirus</i>	<i>Primate bocaparvovirus 2</i>	Human bocavirus 1	HBoV1	JQ923422
		Human bocavirus 3	HBoV3	EU918736
<i>Bocaparvovirus</i>		Gorilla bocavirus	GBoV	HM145750
		Human bocavirus 2a	HBoV2a	FJ973558
<i>Bocaparvovirus</i>		Human bocavirus 2b	HBoV2b	FJ973560
		Human bocavirus 2c	HBoV2c	FJ170278
<i>Bocaparvovirus</i>		Human bocavirus 4	HBoV4	FJ973561
		Bovine parvovirus	BPV	DQ335247
<i>Ungulate bocaparvovirus</i>	<i>Ungulate bocaparvovirus 1</i>	Porcine bocavirus 1	PBoV1	HM053693
	<i>Ungulate bocaparvovirus 2</i>	Porcine bocavirus 2	PBoV2	HM053694
<i>Ungulate bocaparvovirus</i>	<i>Ungulate bocaparvovirus 3</i>	Porcine bocavirus 6	PBoV6	HQ291309
	<i>Ungulate bocaparvovirus 4</i>	Porcine bocavirus 5	PBoV5	HQ223038
<i>Ungulate bocaparvovirus</i>	<i>Ungulate bocaparvovirus 5</i>	Porcine bocavirus 7	PBoV7	HQ291308
		Porcine bocavirus 3	PBoV3	JF429834
<i>Ungulate bocaparvovirus</i>		Porcine bocavirus 4-1	PBoV4-1	JF429835
		Porcine bocavirus 4-2	PBoV4-2	JF429836
<i>Copiparvovirus</i>	<i>Ungulate copiparvovirus 1</i>	Bovine parvovirus 2	BPV2	AF406966
	<i>Ungulate copiparvovirus 2</i>	Porcine parvovirus 4	PPV4	GQ387499
<i>Dependoparvovirus</i>	<i>Adeno-associated dependoparvovirus A</i>	Adeno-associated virus-1	AAV1	AF063497
		Adeno-associated virus-2	AAV2	AF043303
		Adeno-associated virus-3	AAV3	AF028705
		Adeno-associated virus-4	AAV4	U89790
		Adeno-associated virus-6	AAV6	AF028704
		Adeno-associated virus-7	AAV7	AF513851
		Adeno-associated virus-8	AAV8	AF513852
		Adeno-associated virus-9	AAV9	AX753250
		Adeno-associated virus-10	AAV10	AY631965
		Adeno-associated virus-11	AAV11	AY631966
		Adeno-associated virus-12	AAV12	DQ813647
		Adeno-associated virus-13	AAV13	EU285562
		Adeno-associated virus-S17	AAVS17	AY695376
	<i>Adeno-associated dependovirus B</i>	Adeno-associated virus-5	AAV5	AF085716
<i>Anseriform dependoparvovirus</i>		Bovine adeno-associated virus	BAAV	AY388617
		Caprine adeno-associated virus	CapAAV	DQ335246
	<i>Anseriform dependoparvovirus 1</i>	Duck parvovirus	DPV	U22967
		Goose parvovirus-PT	GPV2	JF92695
		Goose parvovirus	GPV	U25749
		Avian adeno-associated virus	AAAV	AY186198
		Bat adeno-associated virus	BtAAV	GU226971
		California sea lion adeno-associated virus	CslAAV	JN420372
		Snake adeno-associated virus	SAAV	AY349010
		Human parvovirus B19-Au	B19V-Au	M13178
<i>Erythroparvovirus</i>	<i>Primate erythroparvovirus 1</i>	Human parvovirus B19-J35	B19V-J35	AY386330
		Human parvovirus B19-Wi	B19V-Wi	M24682
		Human parvovirus B19-A6	B19V-A6	AY064475
		Human parvovirus B19-Lali	B19V-Lali	AY044266
		Human parvovirus B19-V9	B19V-V9	AJ249437
		Human parvovirus B19-D91	B19V-D91	AY083234
		Simian parvovirus	SPV	U26342
		Rhesus macaque parvovirus	RhMPV	AF221122
		Pig-tailed macaque parvovirus	PtMPV	AF221123
		Chipmunk parvovirus	ChpPV	GQ200736
<i>Protoparvovirus</i>	<i>Rodent erythroparvovirus 1</i>	Bovine parvovirus 3	BPV3	AF406967
	<i>Ungulate erythroparvovirus 1</i>	Feline parvovirus	FPV	EU659111
	<i>Carnivore protoparvovirus 1</i>	Canine parvovirus	CPV	M19296
		Mink enteritis virus	MEV	D00765
		Raccoon parvovirus	RaPV	JN867610
	<i>Primate protoparvovirus 1</i>	Bufavirus 1a	BuPV1a	JX027296

Table 2.1 continued

Genus	Species	Virus / virus variants	Abbr.	ACNO
<i>Rodent protoparvovirus 1</i>	Bufavirus 1b	BuPV1b	JX027295	
	Bufavirus 2	BuPV2	JX027297	
	H-1 parvovirus	H1	X01457	
	Kilham rat virus	KRV	AF321230	
	LuIII virus	LuIII	M81888	
	Minute virus of mice (prototype)	MVMP	J02275	
	Minute virus of mice (immunosuppressive)	MVMi	M12032	
	Minute virus of mice (Missouri)	MVMm	DQ196317	
	Minute virus of mice (Cutter)	MVMc	U34256	
	Mouse parvovirus 1	MPV1	U12469	
<i>Rodent protoparvovirus 2</i>	Mouse parvovirus 2	MPV2	DQ196319	
	Mouse parvovirus 3	MPV3	DQ199631	
<i>Ungulate protoparvovirus 1</i>	Mouse parvovirus 4	MPV4	FJ440683	
	Mouse parvovirus 5	MPV5	FJ441297	
	Hamster parvovirus	HaPV	U34255	
	Tumor virus X	TVX	In preparation	
	Rat minute virus 1	RMV1	AF332882	
	Rat parvovirus 1	RPV1	AF036710	
	Porcine parvovirus Kresse	PPV-Kr	U44978	
	Porcine parvovirus NADL-2	PPV-NADL2	L23427	
	Eidolon Helvum (bat) parvovirus	Ba-PARV4	JQ037753	
	Human parvovirus 4 G1	PARV4G1	AY622943	
<i>Tetraparvovirus</i>	Human parv4 G2	PARV4G2	DQ873391	
	Human parv4 G3	PARV4G3	EU874248	
	Chimpanzee parv4	Ch-PARV4	HQ113143	
	Bovine hokovirus 1	B-PARV4-1	EU200669	
<i>Ungulate tetraparvovirus 1</i>	Bovine hokovirus 2	B-PARV4-2	JF504697	
	Porcine hokovirus	P-PARV4	EU200677	
	Porcine Cn virus	CnP-PARV4	GU938300	
<i>Ungulate tetraparvovirus 2</i>	Ovine hokovirus	O-PARV4	JF504699	

The type species for each genus is indicated in bold type. [136]

² NIH GenBank accession number

3. Morphology

Parvoviruses belong to the smallest of isometric viruses. A linear single-stranded DNA genome of about 5 kb is packaged into the virus capsid [42, 138, 388]. They are non-enveloped and their diameters range from 215 Å (*Penaeus stylirostris* densovirus) to 255 Å (CPV) [240, 450].

The icosahedral nature of parvoviruses was shown unambiguously by a combination of electron microscopy (EM) and, latterly, X-ray crystallography [455]. Interpretation of the structural data gave rise to three distinct types of surface topology among parvoviruses (see Figure 3.1, p. 16) [348]. The icosahedral twofold axes and the protrusions surrounding the icosahedral threefold axes display profound surface topology differences between each group. Types I and III comprise members of the *Parvovirinae* subfamily described in Section 2.1, see p. 6. They share in common the following surface features: a protrusion at the 3-fold axis, depressed regions between the 3-fold elevated regions at the 2-fold axis, and another depressed region encircling the 5-fold axis. These two groups mainly differ in the shape of the 3-fold elevated region.

Members of the genus *Protoparvovirus*, as for example CPV, FPV, MVM, and PPV, represent the first topology group that is characterized by a single, relatively flat, pinwheel-shaped protrusion at the icosahedral threefold axes and a wider twofold dimple. The third topology group encompasses the AMDV, B19V, AAV2, AAV4, and AAV5 capsids, which show three distinct mounds at a distance of ~20-26 Å from the icosahedral threefold axes. In addition, the depression at the twofold axis appears to be slightly deeper, particularly for B19V [4, 190, 502]. In contrast to the vertebrate parvoviruses, no large surface protrusions or depressions are present in *Densovirus* capsids that appeared to be relatively spherical and featureless, adopting a second topology group [71, 418].

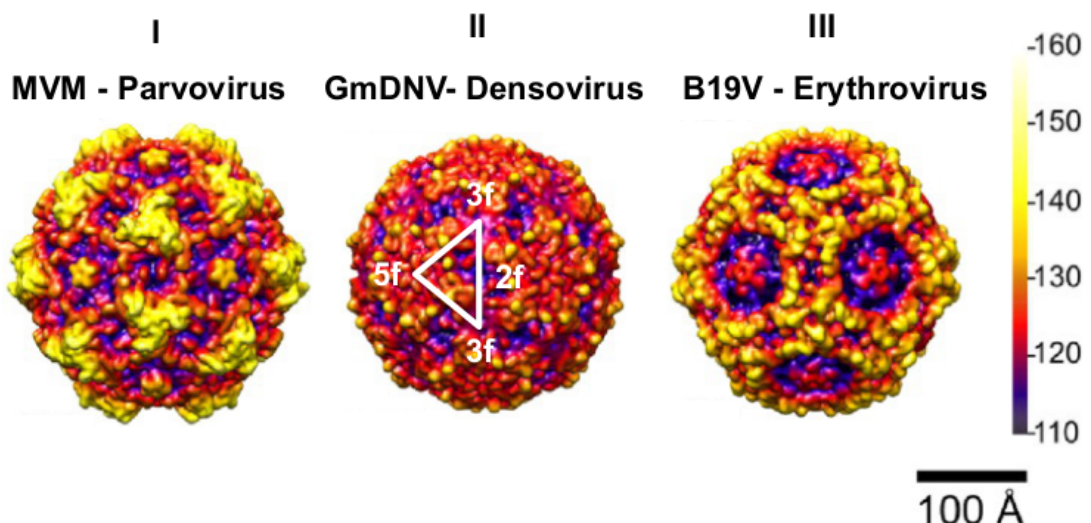


Figure 3.1.: Surface topology groups among members of the *Parvoviridae* family. Stereo, depth cued (blue-red-yellow-white), and space-filling capsid surface illustration of representative members of the two subfamilies of the parvoviruses. Type viruses representing the three surface topology groups (I-III) and the genus to which they belong are indicated. A viral asymmetric unit bound (white triangle) is shown by a 2-fold (2f), two 3-folds (3f) and a 5-fold (5f) axis on the GmDNV image. A horizontal scale bar (100 Å) for diameter measurement and a vertical color bar depicting color cueing as a function of particle radius in Å are shown on the right hand side. These images were computed from atomic coordinates using the UCSF-Chimera program [366], and all are rendered at the same resolution (7.9 Å) and magnification. The figure was adapted from [190].

4. The rugged virion

4.1. Physicochemical Properties

The extracellular infectious virus entity is defined as virion. An infectious parvovirus virion only consists of two components, namely of about 75 % protein and 25 % DNA. Their molecular weight (MW) is approximately $5.5\text{--}6.2 \times 10^6$ dalton. The virion buoyant density is 1.39 to 1.43 gcm⁻³, measured in CsCl gradients [212, 396]. Since parvoviruses are devoid of a lipid envelope, mature virions are stable in the presence of lipid solvents. In particular, animal parvoviruses show considerable heat resistance. Most species resist alcohol or ether treatment, exposure to pH 3-10, or incubation at 60 °C for 60 min [53, 58, 79, 208, 209, 293, 399], hence they are clearly more stable compared to most other, especially enveloped, viruses. Only harsh conditions, such as treatment with formalin, β -propiolactone, hydroxylamine, ultraviolet light, and oxidizing agents as for example sodium hypochlorite, ensure effective virus inactivation [65, 200, 395, 403]. Accordingly, the capsid effectively protects the fragile, condensed genome from detrimental biological, chemical, and physical agents, thus ensuring efficient transmission of the virion through the extracellular environment.

4.2. Atomic Model

Currently, there is no crystal structure available for MVMp DNA containing particles. Only baculovirus-expressed MVMp-like particles and empty capsids (ECs) have been determined at a resolution of 3.25 Å and 3.75 Å, respectively [246]. For MVMi both DNA-containing full and empty particles were crystallized and determined at 3.5 Å resolution. The known CPV structure [286] was used as a phasing model with 52 % of the 587 amino acids in VP2 of MVMi being identical to CPV. Following molecular replacement and refinement, the resulting electron density map was interpreted with respect to the amino acid sequence of MVMi. The polypeptide chain of the major structural protein, VP2, could be traced from residue 39 to residue 587 at the C-terminus (see Figure 4.1, p. 19) [274]. The N-terminal extensions of VP1 and VP2 are not visible in the electron density map. The capsid displays a T=1 icosahedral symmetry, thus having a 5-3-2 point group symmetry containing 31 rotational symmetry axes that intersect at the center: six fivefolds, ten threefolds, and fifteen twofolds. The C-terminal part in common of the structural proteins has an eight-stranded (β B to β I) antiparallel β -barrel topology, referred to as jellyroll

motif (reviewed in [202, 389]). This structural motif is frequently found in other virus capsid proteins. Additionally, like many other viruses, parvoviruses have a ninth β A-strand which is hydrogen-bonded to the β B-strand. The high structural conservation of the jellyroll motif among parvoviruses is remarkable considering the low sequence homology between members of this family. Large loops between the β -strands of the β -barrel that form the principal surface features, particularly the threefold spikes, confer the surface biological properties of the capsid, such as determination of host tropism [23, 359] and sites of antigenicity [52, 361]. Such loops were found to be quite dissimilar in different parvoviruses (see Figure 4.1, p. 19) [84].

The lack of the first 38 amino acids of VP2 indicates a highly disordered structure for N-VP2 [274]. Indeed, a glycine-rich conserved sequence at the N-terminal part of VP2 contributes to its flexibility. In virions, but not in ECs, additional density seen within the fivefold channels was modeled and found to represent the predominantly poly-glycine conserved sequence [495, 501]. These findings suggest that the N-terminus of VP2 is highly dynamic as DNA packaging triggers externalization of one in five N-termini along the pores of the fivefold axis [5].

A substantial amount of electron density in the capsid interior was built as 10 DNA nts which were located at equivalent positions to those previously found in the analysis of the structure of CPV [85, 456]. For MVM, 19 additional nts were identified in a difference electron-density map with respect to the data of empty particles. Altogether, these 29 ordered, or partially ordered, nts per icosahedral asymmetric unit imply that approximately 34 % of the total viral genome display icosahedral symmetry. These findings, and the conservation between the base-binding sites of MVMi and CPV, has led to the identification of a DNA-recognition site on the parvoviral capsid interior [5].

4.3. Structural Proteins

The MVM capsid is made up of 60 copies of a single polypeptide sequence. The virion contains structural proteins of three size classes (VP1-VP3) that constitute a nested set. These share the same C-terminal core structure, but differ in the sequence length on their N-termini. The capsid is assembled from about 10 copies per particle of VP1 (83 kDa), whereas VP2 (64 kDa) represents the major species [445]. In DNA containing virions, the N-terminal region of VP2 is cleaved during cell entry by intracellular proteolytic digestion to generate VP3 (60 kDa), which displays a truncation of approximately 25 amino acids at its N-terminus (see Section 7.3, p. 37) [99, 446, 458, 476]. The N-terminal cleavage of VP2 does not occur in ECs, suggesting that DNA packaging into the particle allows the N-VP2 terminus to be externalized [109, 354, 446]. The processing of VP2 in full virions can be mimicked *in vitro* by digestion with trypic proteases, as for instance chymotrypsin or trypsin. However, the proteolytic site *in vivo* is different to the chymotrypsin- or trypsin-sensitive site [354, 446, 458]. Although containing the identical amino

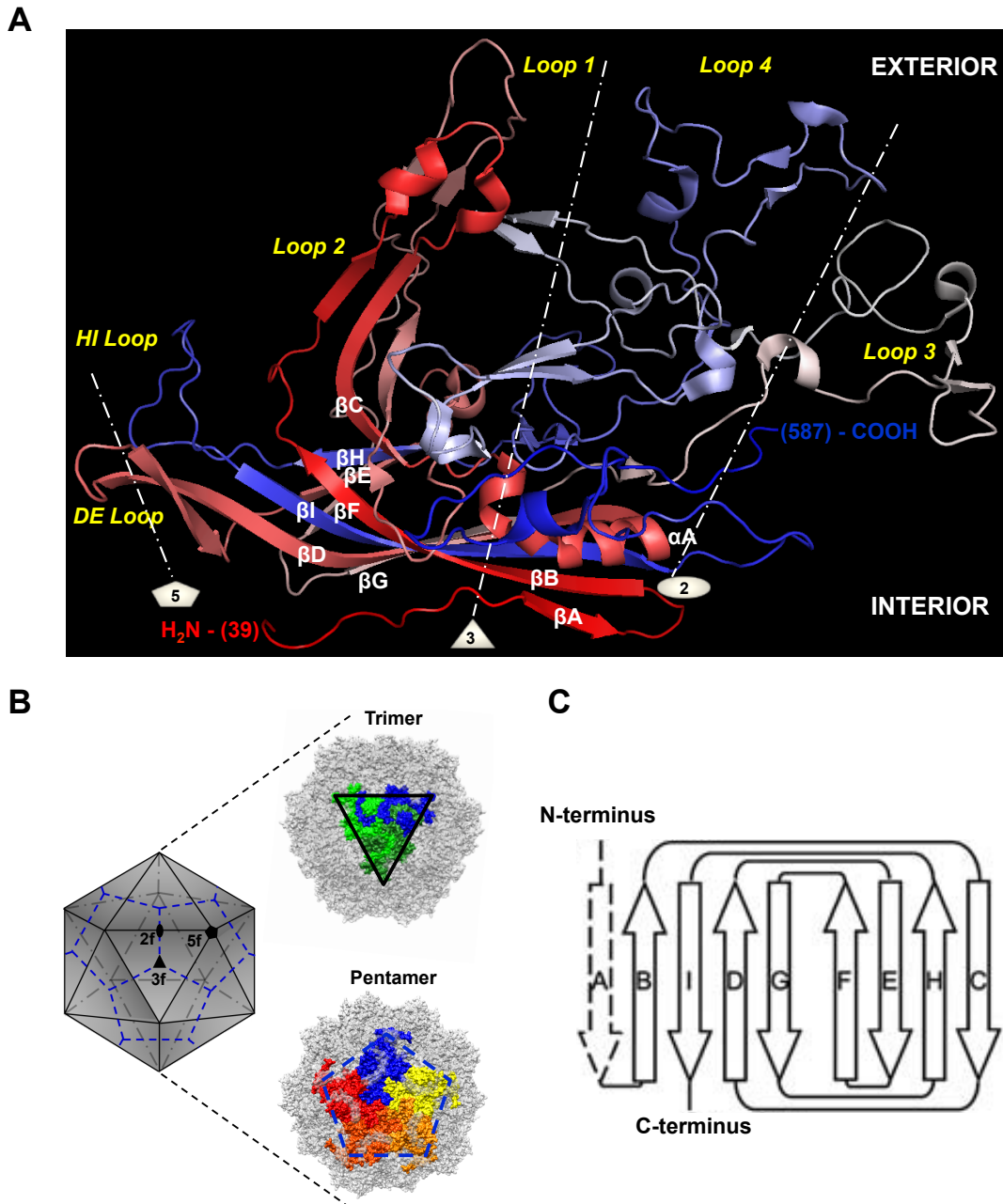


Figure 4.1.: Atomic model of MVM. (A) Ribbon diagram of MVMP VP2 illustrating β-strands, helical and loop regions. The amino acid sequence is gradually colored in a red–white–blue spectrum, beginning at residue 39 and ending at the C-terminal residue 587. The highly conserved αA-helix β-barrel motif, consisting of two antiparallel β-sheets (βABIDG-βFEHC), are labeled. The icosahedral twofold (oval), threefold (triangle), and fivefold (pentagon) axes are indicated. Atomic coordinates for MVMP were obtained from RSCB protein database (PDB accession number 1Z14). The illustration was generated using the PyMol program [146]. **(B)** 60 copies of the capsid proteins form a T=1 icosahedral structure. Each triangle of the icosadeltahedron designates a virus capsid protein subunit. Rotational symmetry axes are referred to as 5f, 3f and 2f, representing 5-folds, 3-folds, and 2-folds, respectively. A VP trimer (assembly intermediate) and a VP pentamer are represented on the right hand side, superimposed on the capsid surface. The representation was generated using the UCSF-Chimera program [366] by computing the same atomic coordinates as mentioned in (A). **(C)** The connectivity of the antiparallel β strands (arrows) of the jellyroll β-barrel is schematically indicated. Strand A is dashed because it is conserved among parvoviruses and a number of other viruses but it is not present in all viruses. This illustration was adapted from [83]

acid sequence that is cleaved in VP2, VP1 does not appear to be cleaved at this position in either type of particle, *in vivo* or *in vitro*. VP2 is both necessary and sufficient for the assembly and encapsidation of viral ssDNA (see Sections 7.10 and 7.11, p. 50 - 51) [208]. However, VP1 is required to produce an infectious particle since capsids that lack VP1 were blocked subsequent to cell binding and prior to the initiation of DNA replication, thus they are unable to fulfill a complete viral life cycle [459]. Indeed, the 142 amino acid N-terminal extension of VP1 which is referred to as VP1 unique region (VP1u) harbors several important motifs to initiate viral infection. Two of which are a PLA₂ motif as well as a nuclear localization signal (NLS), elaborated in Section 4.4, p. 20. Since VP1u initially is sequestered within the viral shell, the incoming virion must undergo important structural changes *in vivo* in order to expose its functional domains on the capsid surface. By treatment of purified virions under controlled temperature or with urea, VP1u exposure could be demonstrated *in vitro* [132, 470].

4.4. Functional Domains

From the atomic model of parvoviruses it can be estimated that structural proteins of 25-30 kDa theoretically suffice to constitute a capsid to protect the viral genome. However, this minimum size is generally enlarged among parvoviruses. VP1 and VP2 exceed the minimum size more than twice as much. The additional parts of the structural proteins harbor essential functional motifs that mediate a number of processes in the infectious viral life cycle. These include host cell surface receptor recognition (see Section 7.1, p. 34), entry and escape from endosomes (see Sections 7.2 to 7.4, pp. 36 - 38), nuclear localization (see Section 7.6, p. 40), DNA packaging, nuclear export, tropism and pathogenicity determinants (see Chapter 5, p. 25), immune surveillance and final maturation of particles to produce infectious virus progeny [451].

4.4.1. The Phospholipase A₂ (PLA₂) Motif

In the VP1u region of all parvoviruses, except AMDV and the members of the genus *Brevidensivirus*, as well as *Tetraparvovirus*, a PLA₂ motif has been identified [506]. The calcium binding loop (YXGXG) and the catalytic histidine-aspartic acid dyad (HDXXY) of parvoviral phospholipases are related to Ca²⁺-dependent extracellular or secretory sPLA₂s which are found for example in bee and snake venoms. Unlike all previously characterized sPLA₂s, the viral sPLA₂ motifs show very weak sequence similarity and lack the characteristic multiple disulfide bonds, thus analogy is mainly restricted to the catalytic units. PLA₂s specifically catalyze the hydrolysis of phospholipid substrates at the 2-acyl ester (*sn*-2) position to release free fatty acids and lysophospholipids. The viral sPLA₂s hydrolyze all major classes of glycerophospholipids, except phosphatidylinositol, without displaying a preference for unsaturated *versus* saturated *sn*-2 fatty acyl chains [78]. The catalytic activity of the PLA₂ is dependent on Ca²⁺ in mM concentrations and reaches a maximum

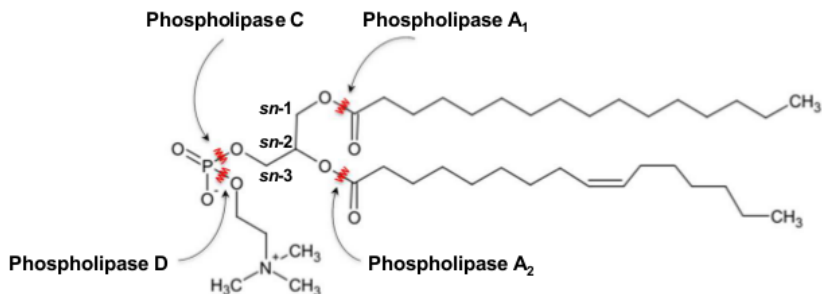


Figure 4.2.: The cleavage sites of the different PLAs are illustrated using phosphatidylcholine (PC), a common phospholipid, as an example. Phospholipase A₁, A₂, C, and D specifically cleave different ester bonds in the phospholipid. Their respective sites of attack are represented by red staggered lines.

at a pH range 6-7, presumably associated with the deprotonation of the His residue in the catalytic dyad at such pH [37, 178].

The biological importance of the viral PLA₂ motif was demonstrated by mutational analyses with AAV2, MVM, and PPV [166, 427, 506]. Viruses lacking a functional PLA₂ motif were not infectious as they failed to escape from endosomes [155, 166, 182, 434].

4.4.2. The Nuclear Localization Signal (NLS)

In addition to the PLA₂ motif [506], the VP1u region of MVM contains four basic clusters (BCs) of amino acids, referred to as BC1 to BC4. These are highly conserved among parvoviruses and moreover, even in some other DNA viruses. BC1 and BC2 represent conventional NLS which are characterized by a short stretch of basic amino acids [228, 229]. BC3 and BC4, which are separated by a short spacing sequence in between, may rather be arranged as a bipartite NLS domain [384]. The clustered basic amino acids interact with transport receptors of the importin/karyopherin family which mediate nuclear import [300, 335, 481]. Nuclear transport activity has been demonstrated for BC1 in the context of a singly expressed VP1 protein [277] and as NLS-peptide coupled to an heterologous carrier protein [466]. Furthermore, it is proven to be essential for CPV infectivity [469] and for MVM to initiate infection [277]. In contrast, BC3 and BC4 did not show such capacity to import VP1 either expressed alone [466] or in the context of the complete MVM genome [277]. Alternatively, these BCs may be involved in the tethering of the ssDNA genome to the capsid inner surface. Such function has been demonstrated for two basic, significantly homologous DNA-binding domains of the protein J of the ϕ X174 bacteriophage [191].

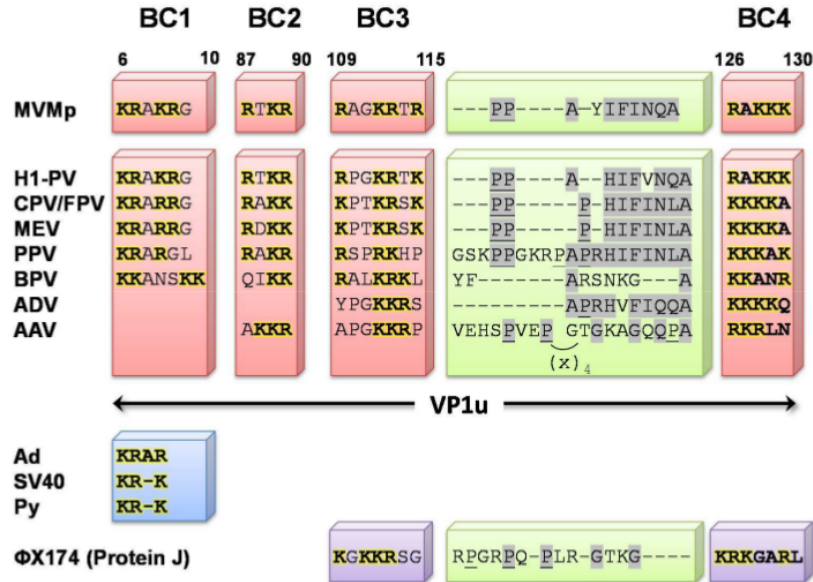


Figure 4.3.: VP1 nuclear targeting sequences. The alignment of BCs (BC1 to BC4), which are conserved in the VP1u region among parvoviruses, is boxed in red. Amino acid residues are abbreviated using the single letter code. Sequence homology between BC1 and other karyophilic double-stranded DNA (dsDNA) viruses is shaded in blue on the left-hand side. Conservation of BC3 and BC4 with the protein J of the ssDNA bacteriophage ϕ X174 is boxed in magenta on the right-hand side. Basic residues of the BC boxes are represented in bold face and possible homologous residues in the spacing region (boxed in green) between BC3 and BC4 are shadowed. Characteristic proline residues which are scattered along the space region are underlined. This illustration was adapted from [277, 460].

4.4.3. The Nuclear Localization Motif (NLM)

Since both VP1 and VP2 singly expressed proteins efficiently target the nucleus of transfected cells [277, 459] each protein must carry its own nuclear transport sequence. The common C-terminal sequence of VP1 and VP2 lacks a conventional consensus NLS. However, VP2 contains one single region which is enriched in basic amino acids (528-KGKLTMR~~A~~KLR-538) near its C-terminus. Based on the crystal structure [5, 455], analysis revealed that this sequence is structurally ordered as a β -sheet which forms the carboxy half of the β I strand (residues 520 to 538) of the eight-stranded antiparallel β -barrel (see Figure 4.4, p. 23). Moreover, the β I-strand shows marked amphiphatic characteristics, exposing all the basic amino acids to the solvent in the interior surface of the capsid while the hydrophobic residues face toward the protein core. Mutational analysis revealed that the basic nature of the exposed face of β I, as well as the hydrophobic residues on the opposite face, conferred a nuclear localization capacity to the VP2 protein. Accordingly, this sequence in β I which only functions under a precise conformation, but not in a linear form, is referred to as the VP2 nuclear localization motif (NLM) [276].

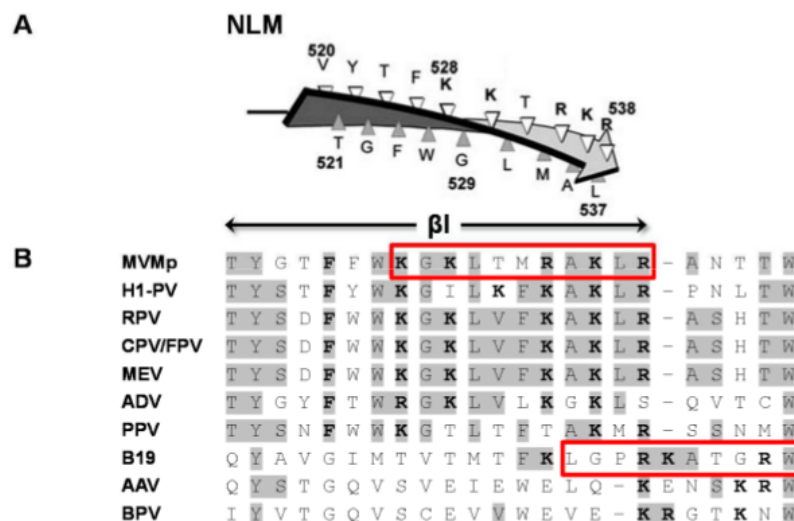


Figure 4.4.: Nuclear localization motif (NLM). (A) Schematic representation of the VP2 NLM of MVM as disposed on the β -strand I of the antiparallel, eight-stranded β -barrel topology in the common C-terminal part of VP1 and VP2. Basic amino acids which are exposed to the solvent are represented in bold. (B) Alignment of the NLM that is conserved among parvoviruses. Homologous positions are shadowed and basic residues are in bold. Sequences with proven nuclear localization capacity are boxed in red. This illustration was adapted from [276, 460].

5. Genome Architecture

The MVM genome is a small, non-permuted, linear, single-stranded DNA molecule [16, 60, 444, 475] that is 5 085 nt in length for MVMi and 5 149 nt for MVMP [20]. The relatively long coding sequence of approximately 4.8 kb contains two major, monosense ORFs that span most of the viral genome, with some regions having overlapping coding regions [18]. The ORFs encode a non-structural (NS) gene and a structural (VP) gene, by convention termed as occupying the "left" or the "right" half of the coding sequence, respectively. The NS gene encodes four proteins that are required for the replication of the viral genome and are referred to as NS1, NS2^P, NS2^Y, and NS2^L. The VP gene encodes an overlapping set of capsid proteins, VP1 the minor capsid protein and VP2 the major capsid protein [107, 227, 367]. A representation of the genomic organization of MVM is illustrated in Figure 5.1 A, p. 28.

5.1. The MVM Left- and Right-End Telomeres

The coding sequence is bracketed by short, imperfect palindromes which form back on themselves to secondary structured duplex telomeres. Both telomeres differ considerably from each other in size, primary sequence and secondary structure [18]. Hence, they are physically and functionally disparate and vary in their terminal resolution strategies at the two sites (see Section 5.1.1, p. 26), although the molecular principles that underlie both strategies are very similar [123].

Firstly, the MVM left-end telomere is 121 nt in length and forms into a Y-shaped configuration. Its structure is depicted in Figure 5.1 B (left panel), p. 28. The stem region which contains 43 base pairs (bp) only is interrupted by a mismatched bubble sequence where a triplet GAA on the inboard arm is opposed to the dinucleotide sequence GA on the outboard arm. Additionally, an asymmetric thymidine residue is located within the stem on the outboard arm in the immediate proximity to the "ears" that are generated by small internal palindromes. These "ear"-like structures give rise to the Y-shaped configuration of the left-end terminus [16, 18, 19, 115]. A single DNA sequence, designated the "flip" sequence, is conserved in the progeny viral left-end telomere, as is observed *in vivo* [19].

Secondly, the MVM right-end telomere is 248 nt in length and is most simply depicted as an almost perfect duplex stem structure of 121 bp. The palindrome only is interrupted by a triplet of unpaired nts that forms a small asymmetric bubble near the distal end of one strand, along with three unpaired bases which form the cross-link at the palindrome axis [18, 19]. As in

homotelomeric parvoviruses, two distinct forms of the MVM right-end terminus, referred to as "flip" and "flop", are generated in equimolar amounts *in vivo* (see Figure 5.1 D (i) and (ii), p. 28) [116, 123]. These two forms are the inverted complements of one another and both give rise to viral origins, dubbed *oriR* [117, 128, 133]. A small internal palindrome, surrounding the three-nt bubble, thermodynamically enables an alternative, asymmetric cruciform configuration of the right-end telomere (see Figure 5.1 D (iii), p. 28) [17].

5.1.1. Terminal Resolution *versus* Asymmetric Junction Resolution

As is the case for most of the heterotelomeric parvoviruses, MVM shows packaging bias with minus strands preferentially encapsidated to plus strands by a 10-100-fold margin (see Section 7.11, p. 51) [109, 367]. This results from differences in the efficiency of their two DNA replication origins at both ends of their genomes, rather than any strand-specific packaging sequence. In particular, the efficient nick site of the *oriR* dictates the negative polarity of the packaged strand which is encapsidated in MVM virions [120].

Given the fact that alike their homotelomeric cousins, the right-end hairpin of MVM exists as an equimolar mix of flip and flop sequence orientations, it is processed by a similar terminal resolution strategy. Nicking of the hairpin near the junction between palindromic and non-palindromic sequences and subsequent extension of the right-end terminus allows an efficient inversion of the palindrome (see step iii and iv in Figure 7.2, p. 46). On the contrary, the MVM left-end hairpin predominates in the flip orientation, indicating its generation by an asymmetric junction resolution mechanism [119]. Briefly, the asymmetric bubble sequence in the stem of the MVM left-end telomere (see Figure 5.1 B, p. 28) prevents assembly of an active nicking complex. Thus, the left-end telomere cannot function as a replication origin in its hairpin conformation [22]. During rolling hairpin replication (RHR) (see Section 7.8, p. 45), the hairpin is unfolded, extended, and copied to form the fully basepaired, imperfect palindromic junction sequence which bridges adjacent genomes in an intermediate dimer replicative form (dRF) (see Figure 5.1 B (right panel), p. 28). It was demonstrated that such junctions can initiate DNA replication in a NS1-dependent manner [113, 114]. Formation of the dimer junction effectively segregates two potential origins of DNA replication, one derived from each arm of the hairpin, on either side of the junction's symmetry axis. However, only one of these is active. The activity is regulated by the sequence of the asymmetric bubble which serves as a precise spacer between the NS1 binding site and the parvovirus initiation factor (PIF). Binding of which stabilizes the interaction of NS1 with the active (TC) origin (*OriL_{TC}*) but not with the inactive (GAA) origin (*OriL_{GAA}*) [95]. The minimal left-end origin of replication, dubbed *oriL*, is illustrated in figure 5.1 C, p. 28. It extends from two 5'-ACGT-3' motifs which represent binding sites for PIF [92–94], to a 5'-(ACCA)₂-3' binding site for the viral initiator nickase, NS1 [130], to the active nick site [114]. Recent studies revealed that MVM tolerates both sequence and orientation changes in its left-end hairpin. From

this follows that maintaining the flip orientation of the left-end telomere is a consequence of, but not the reason for, asymmetric dimer junction resolution. However, the same study indicated that asymmetric left-end processing is crucial for MVM replication [267].

In summary, the heterotelomeric hairpins, together with a few adjacent nts, provide all of the *cis*-acting information required for both efficient genome replication and encapsidation. In particular, these terminal nts, representing less than 10 % of the entire genome, create the replication origins by providing nicking sites that are used as a primer for DNA synthesis and to effectively separate unit-length genomes for DNA packaging. Additionally, they function as flexible hinge regions used to establish and re-orient the replication fork, allowing it to roll back and forth along the linear viral DNA [116, 122, 323, 449].

5.2. Genetic variability

When compared with cellular DNA, the genome of MVM has a relatively high GC-content (42 %), partially reflecting its high density of regulatory elements. The complexity of the viral genome is increased by transcriptional promoter sequences and various splicing signals that lie embedded within the same primary sequence, beyond the encoded proteins which are organized in multiple overlapping ORFs. Nevertheless, following inoculation of clonal populations of MVMi stocks in mice, genetically disparate antibody-escape variants emerged *in vivo*. This indicates that viral replication appears to support the generation of heterogeneity [278]. Another example concerns the emergent branch of CPV during its evolution from FPV in 1978 that allowed the virus to expand its host range to canines. The substitution rate of CPV resembles that seen in rapidly evolving RNA viruses, as for example HIV-1 and human influenza A virus [411]. Remarkably, such diversity occurred despite the fact that the viral genome is multiplied by a subset of the host's DNA replication machinery, hence the mutation rates would be expected to be low. Probably, the unidirectional strand-displacement mechanism may exhibit lower fidelity compared to the bidirectional replication of eukaryotic genes. Additionally, the concatemeric duplex intermediates may allow for inter- and intramolecular recombination during replication of the viral DNA. Moreover, there are several lines of evidence that MVM exploits the DNA damage response machinery early in infection in order to enhance its replication and to ameliorate virus-induced cell cycle arrest in the S-phase [1]. Therefore, it seems possible that under such conditions the replication forks appear error-prone. Finally, environmentally induced changes in the viral DNA sequence, such as depurination or deamination, cannot be corrected because virions contain ssDNA and hence do not provide a template for excision or mismatch repair systems. Nonetheless, the genetic complexity, in consequence of the constrained genome size, severely and selectively restricts the types of tolerated modifications [124].

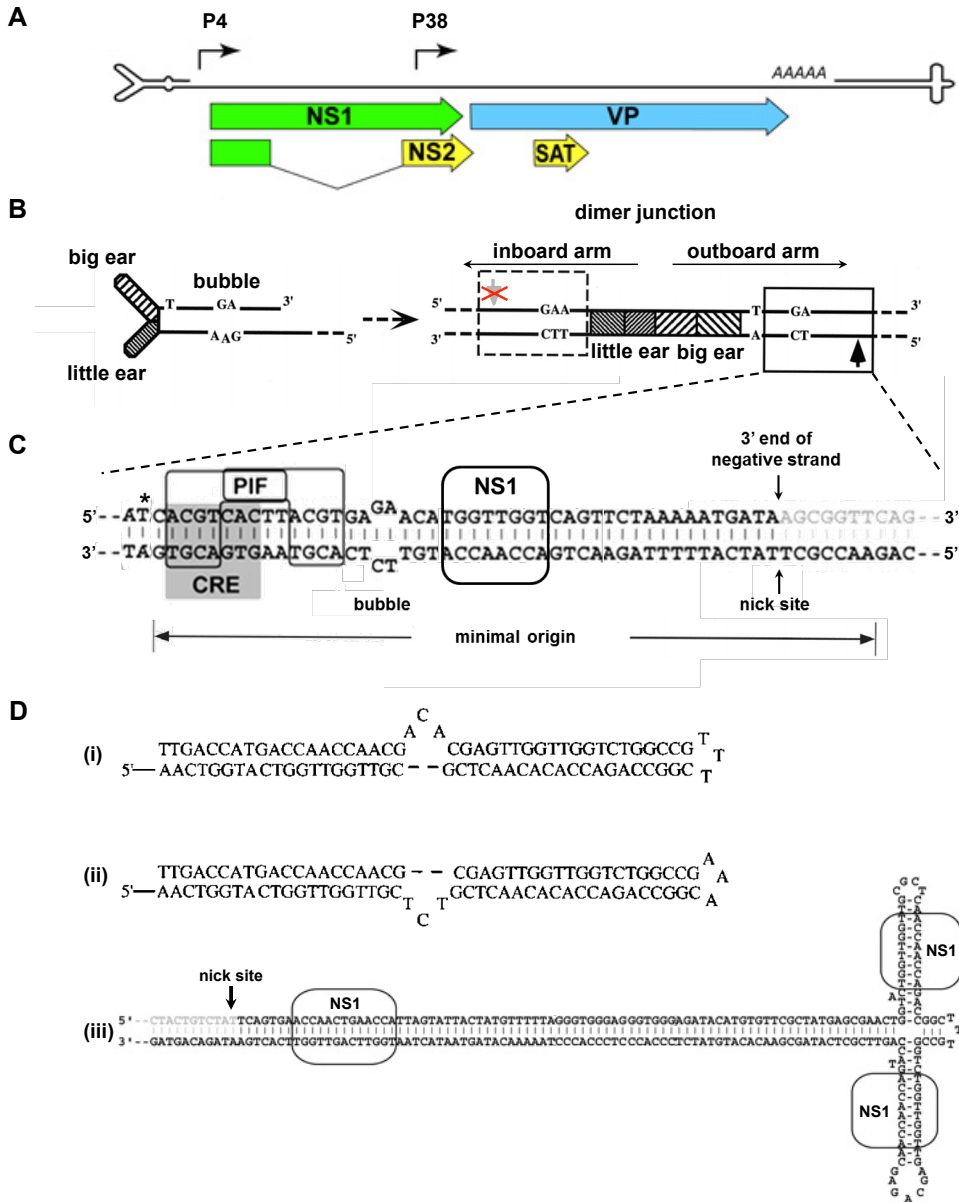


Figure 5.1.: Genome architecture of MVM. (A) The terminal hairpins, drawn to represent their predicted structures, are scaled approximately 20x relative to the rest of the genome. Major ORFs are represented by arrowed boxes and alternative RNA splicing for NS2 is indicated. Proteins are shaded green for the major replication initiator protein (NS1), blue for the structural (VP) proteins of the capsid, and yellow for sequences unique to the ancillary NS proteins. The two transcriptional promoters, P4 and P38, are indicated by rightward arrows and the polyadenylation site by the AAAAA-sequence block [125]. (B) The left-end hairpin of MVM and the dimer junction are shown in diagrammatic form. Asymmetries, such as the "ear"-like structures, extra-helical T, and bubble sequence are indicated. The fully duplex, dimer junction, generated by RHR (see Section 7.8, p. 45), is shown on the right hand side. The short, palindromic sequences derived from the hairpin ears are represented by cross-hatched boxes. The active *OriL_{TC}* is boxed, with an arrow indicating the nick site. The equivalent sequence generated on the GAA side of the bubble is framed by a dashed box with an arrow at the potential nick site that is crossed out to indicate that *OriL_{GAA}* is not active [75, 76]. (C) Sequence details of the active left-end origin (approx. 50 bp) are shown, with an arrow indicating the active nick site. The minimal sequence required for origin activity is indicated by the double-headed arrow. Sequences of the bubble and the PIF, cAMP-responsive element (CRE), and NS1 binding sites are indicated. An asterisk represents the position of the extra-helical T, now base paired, and the gray box below it indicates the CRE consensus sequence [75]. (D) Alternate conformations of the right-end hairpin sequences of MVM. The right-end terminus can form a hairpin structure in either the flip (i) or flop (ii) sequence orientation or a cruciform structure (iii). In the cruciform configuration, the binding sites for the replicator protein, NS1, are boxed and their site of nucleolytic cleavage is represented by a vertical arrow [105].

6. Host Range and Specificity

6.1. Tissue Tropism Determinants

Concerning their host range, most parvoviruses, such as MVM, CPV, and FPV, are tightly restricted to specific receptors of their particular hosts. However, some parvoviruses, as for example many of the AAVs, infect human cells by primary attachment to a variety of receptors (see Section 7.1, p. 34).

As outlined in Chapter 1 (see p. 3), two distinct strains of the parvovirus MVM have been described to occur in mice. On the one hand, MVMP, the prototype strain, replicates efficiently in mouse fibroblasts [137]. On the other hand, MVMi, the immunosuppressive strain, replicates in T lymphocytes [57, 304]. Both strains display disparate *in vitro* tropism and *in vivo* pathogenicity despite differing by only 14 amino acids in their capsid proteins [24], thus providing a useful model for in-depth characterization of the role of virus-receptor interaction (see Section 7.1, p. 34) in parvovirus infection. Beyond that, MVMP and MVMi are serologically indistinguishable, bind to sialic acid (SA), and are internalized in both fibroblasts and lymphocytes [425]. Consequently, it could be demonstrated that both viruses propagate in hybrids of the two cell types [440].

In order to map the allotropic determinants of MVM, chimeric viral genomes were constructed *in vitro* from infectious genomic clones of both strains. By mutagenesis and selective plaque assays, the major determinants for the acquisition of fibrotropism for MVMi have been mapped onto the capsid [14, 24, 103], in particular to the VP2 residues 317 and 321 [23, 301]. Both residues are located at the base of the threefold spike of the virion [14, 175, 176]. Interestingly, these two VP2 residues structurally localize nearby some of the important amino acids determining CPV, FPV, and PPV host range [185, 219, 464]. Further residues (VP2 residues 339, 399, 460, 553, and 558) were identified in MVMi to be able to confer fibrotropism to forward second-site mutants when either residues 317 or 321 are mutated. Those residues cluster around the twofold dimple-like depression [5]. In contrast, the switch to lymphotropism for MVMP is more complex and requires both an equivalent region of the major MVMi capsid protein gene VP2 and a segment of the NS protein genes [103].

6.2. Pathogenicity Determinants

MVMi appears to be more pathogenic in mice than MVMp. Oronasal inoculation of MVMi in most neonatal mice resulted in lethal phenotype or severe growth-retardation in survivors [239], as observed for other parvoviruses (see Section 2.1, p. 6). MVMp infection appears to be asymptomatic in newborn mice [70]. In contrast, MVMi infection in neonatal mice of some inbred strains caused renal papillary hemorrhage and viral replication in endothelia [69], hematopoietic precursors [404], and neuroblasts [379]. Following *in utero* inoculation of MVMi or MVMp into developing embryo, a broad set of cell types were infected that partially overlapped. Nevertheless, the tissue tropism of MVMp for fibroblasts and of MVMi for endothelium, as well as the higher virulence of MVMi was preserved [223]. By reason of the complexity of MVMi pathogenesis in the neonatal mouse, a more adequate model was required to investigate the virulence of MVMi *in vivo*.

Severe combined immunodeficiency (SCID) mice [59] represent such a model since they lack an antigen-specific immune response, thus allowing the study in adult mice and circumventing the complex situation of heterogenous viral multiplication in embryonic developing tissue. MVMi infection of adult SCID mice gave rise to the suppression of long-term repopulating hemopoietic stem cells in the bone marrow [406], leading to an acute lethal leukopenia and accelerated erythropoiesis [405]. In addition, it has been reported that MVMp evolved in intravenously inoculated SCID mice. Different variants, isolated from single plaques, carried only one of three single amino acid changes at position 325, 362, or 368 in the major VP2 capsid protein. These variants sustained their fibrotropism *in vitro*, but unlike MVMp, they propagated in mouse tissues following oronasal inoculation, eventually causing death [279, 390]. Two of the three invasive fibrotropic MVMp strains, I362S and I368R, were shown to induce lethal leukopenia in oronasal inoculated SCID mice. Emerging viral populations in leukopenic mice displayed altered sequences in the MVMi genotype at position 321 and 551 of VP2 for infections with the I362S variant or changes at position 551 and 575 in the K368R virus infections. In general, a high level of genomic heterogeneity in the DNA sequence encoding the VP2 protein was observed and was found to be clustered at the twofold depression of the viral capsid [280].

6.3. Comparison of Tissue Tropism and Pathogenicity Determinants among Parvoviurses

Significantly, the amino acids dictating *in vitro* tropism (317 and 321), *in vivo* pathogenicity (325, 362, and 368), fibrotropism on MVMi (339, 399, 460, 553, and 558), and those involved in the development of leukopenia (321, 551, and 575) were found to be located on, or near the capsid surface. Structurally, these residues cluster mainly by raised elements around the twofold axes of

symmetry, in close vicinity of the SA binding pocket (see Section 7.1, p. 34) [279, 280].

Differences in the tissue tropisms and the pathogenic phenotypes have also been mapped to the capsid proteins of Aleutian mink disease parvovirus [51], PPV [40], CPV [82, 360], and FPV [454] in a capsid region analogous to that observed for MVM (reviewed in [4]). These pronounced *in vitro* tropism and *in vivo* pathogenicity disparities between the highly homologous viruses can occur at any of the various stages of the infectious viral life cycle, including cell receptor binding, internalization, capsid uncoating, DNA replication or transcription. Studies of the strain-specific tissue tropism conducted on members of other virus families have mainly shown that each strain recognizes a different specific cell surface receptor [168, 213, 318, 319, 421, 479, 480]. This receptor is only present on the target cell for that strain, but absent on the surface of other potential host cells. Although the same structural elements of parvoviruses are involved in mediating host and tissue tropisms, each appears to be affecting a different mechanism. Host ranges of CPV and FPV are controlled by receptor binding, as observed for many other viruses, whereas the cell tropisms of MVM appear to be due to restrictions of interactions with intracellular factors [5, 218, 425]. For MVM it was suggested that the point of restriction appeared after nuclear targeting and conversion of genomic ssDNA to replicative form (RF) intermediates but prior to viral genome replication. Most likely, the restraint occurs due to a block in capsid uncoating [215, 373].

As discussed in this section the functional regions among the subfamily *Parvovirinae* co-localize to similar capsid surface regions albeit three general parvovirus topology groups with characteristic local morphological surface differences emerged (see Chapter 3, p. 15). A profound understanding of functional domains that are involved in fundamental steps of the viral life cycle, particularly receptor attachment, *in vitro* tropism, *in vivo* pathogenicity, and antigenicity are essential for infection and disease control. Hence, showing great promise to allow genetic engineering of parvovirus capsids for the therapeutic delivery to be controlled or modified in gene therapy applications and to develop foreign antigens [4, 218].

7. The Parvovirus Life Cycle

As previously mentioned, parvoviruses are heavily dependent on their cellular systems to ensure productive infection. A plethora of molecular interactions between the virus and the host cell allow the recruitment of cellular machinery to provide an environment for optimal progeny morphogenesis. These numerous interactions include binding to the cell surface determining primary attachment and internalization, cytoplasmic interactions controlling intracellular trafficking and eventual maturation, and nuclear interactions regulating uncoating, replication, transcription, assembly, and packaging of progeny particles. Some of the viral mechanisms and interactions underlying the parvovirus life cycle are introduced in this chapter in further detail keeping MVM as the main focus.

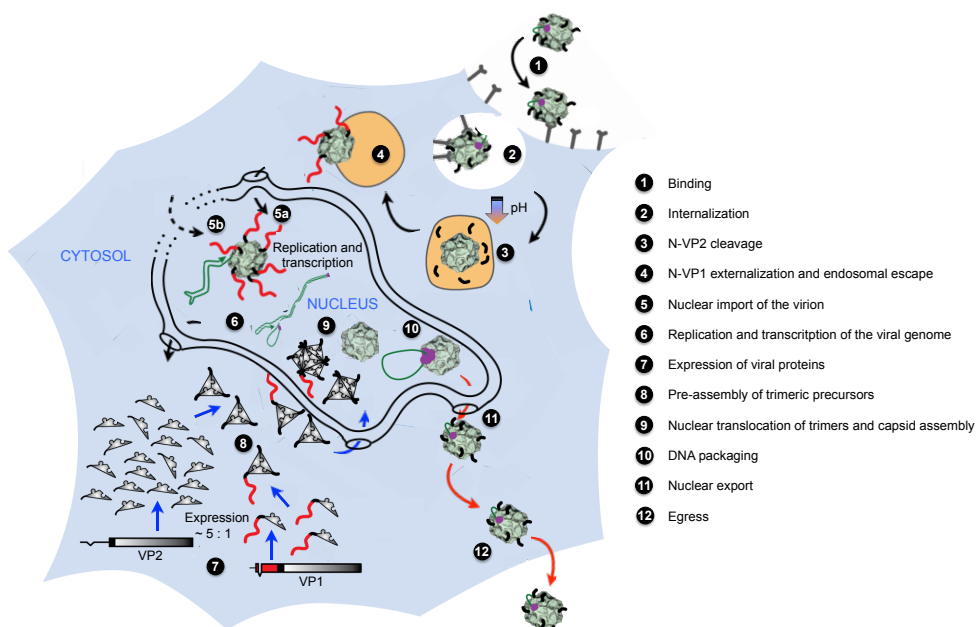


Figure 7.1.: Schematic view of the life cycle of MVM. Cell entry (black arrows), protein expression and progeny assembly (blue arrows), and DNA packaging, nuclear export and egress (red arrows) are illustrated. The unknown sialylated cell surface receptors are indicated as extended Y shapes and acidic late endocytic vesicles are colored in orange. Colored lines associated with virus particles represent the flexible N-VP2 termini (black), the VP1u region (red), and the viral genomic DNA (green). The number of externalized N-VP1 termini is not known and might vary between one and ten. Currently, nuclear targeting (step 5) of the virion is controversial and remains unclear. Due to its small size, MVM could physically traverse the nuclear pore complex (NPC) fully intact (step 5a). Alternatively, MVM was suggested to enter the nucleus in an NPC-independent manner by partial disruption of the nuclear envelope (step 5b). Horizontal bars represent primary VP gene transcripts and jigsaw triangles indicate the folded core containing the jellyroll motif common to all VP polypeptides. The multifunctional NS1 protein, which assists DNA replication and packaging, is represented as purple sphere. The amounts and the ratio of the represented viral proteins do not correspond to those of the natural capsids. This figure was adapted from reference [125].

7.1. Receptor Binding

Recognition of cell surface receptors by a virus enables the first step of infection and hence, represents a key parameter of tropism and pathogenesis (see Chapter 5, p. 25). Different biomolecules, such as proteins, carbohydrates, and glycolipids can serve as primary attachment factors. To date, a variety of different receptor molecules with specific binding properties or functional activities have been identified for some members of the subfamily *Parvovirinae* (see Table 7.1, p. 35. For a review see reference [491]). Examples include the AMDV-binding protein for AMDV [169], the globoside erythrocyte P antigen, along with $\alpha_5\beta_1$ -integrin and Ku80 for B19V [68, 235, 322, 477, 478], transferrin receptors (TfRs) for CPV, FPV and mink enteritis virus [356, 358] and heparan sulfate proteoglycan (HSPG), $\alpha_V\beta_5$ -integrin, and growth factor receptors for AAVs [148, 234, 314, 375, 435, 436]. However, a recent study from our lab conducted on B19V failed to verify the interaction between B19V and $\alpha_5\beta_1$ -integrin. Instead, purified, recombinant VP1u was demonstrated to bind and internalize independently of the B19V capsid. VP1u binding and internalization was tightly restricted to only a few cell lines of the erythroid cell lineage only. These results, together with the ability of recombinantly expressed VP1u to efficiently prevent B19V endocytosis, indicate that an unknown receptor with an expression pattern confined to few erythroid cell types mediates B19V internalization [264].

For most of the parvoviruses only the glycan component of their specific receptor is known. Glycans are carbohydrate polymers and represent the major components of the cell surface. Thus they provide a vast collection of important cellular attachment factors for viruses in general. They may be conjugated with cell surface proteins or membrane lipid head groups to form glycoproteins and glycolipids, respectively, or constitute glycosaminoglycan chains attached to proteoglycans [343]. The extensive heterogeneity of the carbohydrate polymers which are expressed across different species, and even across different tissues within the same species, creates an immense variability in viral tissue tropism. This diversity is even further enlarged by various glycosidic linkage positions between each individual monosaccharide and by the high degree of chemical modifications of hydroxyl groups [13, 463]. Most commonly, SA or sulfated oligosaccharide motifs of glycosaminoglycans (e.g. heparan sulfate) form the distal and hence most surface exposed units of glycoepitopes [231].

Biochemical studies utilizing neuraminidase and proteinase K treatment have shown that SA is a common primary attachment factor for several parvoviruses infecting different species, as for example MVM [109, 279], parvovirus H1 (H1-PV) [12], BPV [45, 225, 448], PPV [56], AAV1 [496, 497], AAV4, AAV 5 [87, 230, 407, 472], CPV and FPV [28, 32]. However, SA-CPV and SA-FPV interactions are not sufficient for infectivity but require additional binding to their respective TfRs on canine and feline cells [28, 220, 350, 358]. More than 60 analogues of SA occur in nature which result from modifications to the nine-carbon backbone [231] and are estimated to be present at 5×10^5 copies per cell on A9 mouse fibroblasts [271, 425]. The SA binding

pocket of MVM was identified by analysis of SA soaked into preformed crystals of virus-like particles (VLPs)³ of MVMp. Structurally, the SA electron density is associated with the dimple-like depression located at the icosahedral two-fold axis in the MVM capsid (see Figure 3.1, p. 16). The binding pocket exposes highly positive charges which interact with SA moieties on the cell surface [279]. Interestingly, the localization of the SA binding domain in MVM is proximal to the CPV and FPV determinants of SA binding to erythrocytes [3, 28, 419, 453]. Significantly, the amino acids determining *in vitro* tropism (317 and 321) and *in vivo* pathogenicity (325, 362, and 368) for MVM invariably localize in close vicinity of the SA binding pocket (see Chapter 5, p. 25) [246].

The identification of virus receptors and the characterization of virus-receptor interactions are of great relevance for understanding virus evolution, host tropism, and pathogenesis. A profound knowledge of the first steps of viral infections on the host cell surface is essential for the development of antiviral therapies and for the construction of gene therapy vectors with determined targeting.

Table 7.1.: Parvoviruses and their receptors

Virus	Receptor	Coreceptor	Host	Reference
AAV1	α 2-3 and α 2-6 N-linked SA	-	Human	[497]
AAV2	HSPG	Integrin $\alpha_5\beta_1$, $\alpha_V\beta_5$, FGFR1, HGFR, LamR	Human	[8, 15, 234, 375, 435, 436]
AAV3	HSPG	HGFR, LamR, FGFR1	Human	[8, 46, 270]
AAV4	α 2-3 O-linked SA	-	NHP	[230]
AAV5	α 2-3 and α 2-6 N-linked SA	PDGFR	Human	[148, 230, 407, 472]
AAV6	α 2-3 and α 2-6 N-linked SA, HSPG	EGFR	Human	[483, 496, 497]
AAV8	-	LamR	NHP	[8]
AAV9	Galactose	LamR	Human	[8, 38, 415]
Bovine	Gangliosides, chitotriose	-	Bovine	[149, 400]
AAV				
AMDV	AMDV-binding protein	-	Mink	[169]
BPV1	SA	Glycophorin A	Bovine	[45, 448]
B19V	Erythrocyte P antigen	Integrin $\alpha_5\beta_1$, ku80	Human	[68, 235, 322, 477, 478]

³ VLPs are non-infectious particles which do not contain any viral genetic material. The expression of parvoviral structural proteins results in a spontaneous self-assembly of VLPs. Since VLPs mimic the organization and conformation of viral surface epitopes, they can elicit strong B cell and T cell immune responses. Therefore, they provide a useful tool for the development of vaccines.

Table 7.1 continued

Virus	Receptor	Coreceptor	Host	Reference
MVM	SA	-	Rodent	[109, 232, 328]
CPV/FPV	SA	TfR	Cat, dog	[220, 358]
PPV	SA	-	Swine	[56]

This Table was adapted from reference [192]

7.2. Receptor-mediated Endocytosis

All known parvoviruses enter the host cell by receptor-mediated endocytosis, using a wide variety of partially unknown glycosylated receptor molecules, exposed on the cell surface [198] (see Table 7.1, p. 35). The endocytic route is advantageous for karyophilic viruses. On the one hand, endosomes provide a rapid and efficient transport towards the nuclear periphery. On the other hand, the exposure to low pH enables the capsid to undergo conformational changes which are required for further stages of infection (see Section 7.3, p. 37), such as endosomal escape, uncoating, and nuclear localization. Recent research has demonstrated that, in addition to the classical clathrin-mediated endocytosis [56, 158, 357], several alternative endocytic routes can be used by parvoviruses. For example, AAV2 utilizes clathrin-independent carriers (CLICs) [336], AAV5 uses caveolae-dependent endocytosis [25], and PPV utilizes macropinocytosis [56] as additional endocytic pathways. Most recently, Garcin and Panté showed that MVM enters its host cell by at least three potential endocytic routes. Inhibition of various endocytic pathways with specific drugs in combination with EM, immunofluorescence microscopy (IF), and fluorescence-activated cell sorting, identified clathrin-, caveolin-, and CLIC-mediated endocytosis for MVM. However, the latter endocytic uptake mechanism was restricted to transformed cells only, but did not occur in murine A9 fibroblasts. This observation was confirmed in further experiments which demonstrated that dynasore, an inhibitor of dynamins, completely blocked MVMP uptake in A9 mouse fibroblasts, whereas its inhibitory effect was incomplete in transformed cells. These results indicate that both clathrin- and caveolin-mediated MVMP endocytosis is dependent on dynamin in murine A9 fibroblasts, but transformed cells allow for the dynamin-independent CLIC-mediated uptake of MVMP [174]. Although parvoviruses share some general features in receptor binding and in their routes of cellular entry, each appears to display their own unique mechanistic details.

7.3. Endosomal Trafficking and Capsid Rearrangements

Endosomal trafficking of parvovirus virions is thought to be a slow and rate-limiting process in viral infection [159, 194, 195, 292]. The delayed progression to infection allows parvoviruses the opportunity to undergo important structural transitions and prolonged processing within endosomes. For instance, AAVs escape from early endosomes but only reach the nucleus after 40 min to 2 hours post-infection (hpi) [30, 500]. MVM is exceptionally well characterized with respect to endosomal trafficking in spite of the rapid dynamics and complexity of viral movement within and between endosomal compartments. It has been reported to traffic even slower through the endocytic pathway and only reaches the cell nucleus after 8 hpi when DNA replication was detected [387].

Several lines of evidence confirm that endosomal processing of incoming parvovirus particles is essential. First, virions with or without exposed N-VP2 termini failed to confer a nuclear localization phenotype to AAV2 when directly injected into the cytoplasm to bypass the endocytic pathway [152, 424]. Similarly, low pH pre-treated CPV capsids were unable to accumulate in the nucleus following injection into the cytoplasm [467]. Also, for MVM all structural rearrangements were equally impaired by lysosomotropic drugs, thereby preventing infection [292, 387]. These drugs, such as bafilomycin A₁ or the weak base chloroquine diphosphate, raise the endosomal pH by inhibiting the vacuolar-type H⁺-adenosine triphosphatase (ATPase) [62, 207, 216] or by accumulation inside acidic compartments [144, 340, 369], respectively. Finally, endosomal acidification has been demonstrated to be essential for the infection of AAV [30, 48, 156, 195], CPV [31, 357, 467], and MVM [292, 387].

Already 30 min after endocytosis, three considerable structural rearrangements of the MVM capsid occurred simultaneously. Specifically, the capsid transitions include the cleavage of the exposed N-VP2 termini, the externalization of originally sequestered N-VP1 termini, and the release of the full-length viral DNA genome without the loss of capsid integrity [292]. The conformational changes of parvovirus capsids, which are induced by endosomal trafficking *in vivo*, can be partially mimicked *in vitro*. Treatment of CPV particles under acidic conditions mimicking endosomal pH induced VP1u exposure [434]. However, in the case of MVM full capsids (FC), prior cleavage of N-VP2 termini to VP3 is a prerequisite for VP1u externalization under such conditions [132, 167]. Contrarily, the N-VP2 termini remained buried in the interior of ECs and thus they were not accessible to proteolytic digestion [292]. Surprisingly, EC exposed the N-VP1 termini with similar kinetics to FC, indicating that at least for EC, neither the genomic DNA nor the cleavage of N-VP2 is involved in the extrusion of N-VP1 [132, 292]. Harsh conditions, such as exposure to heat or urea, trigger VP1u externalization in AAV [253], CPV [469, 476], and MVM particles [132, 135]. Characterization of the biochemical and structural capsid dynamics was enabled by artificial *in vitro* treatments although they cannot directly reproduce physiological conditions [132, 135, 253, 469]. The differences observed in the *in vitro* and *in vivo* studies imply

that a combination of several factors, such as receptor binding, low endosomal pH, or interactions with unknown host factors play a role in these structural transitions of parvoviruses.

The study of the infectious pathway of parvoviruses is impeded by the fact that the bulk of incoming particles are retained within lysosomal compartments and only a minority escapes the endocytic route (see Section 7.4, p. 38). Moreover, the lack of dynamic information in fixed cell samples has complicated the examination of virus trafficking through the highly dynamic and overlapping vesicular endocytic pathway. However, emerging advances in time-lapse microscopy make live-cell imaging an important complementary method to study the complex nature of endosomal trafficking in the future.

7.4. Endosomal Escape

The high particle to infection (P/I) ratio⁴ of most parvoviruses (100:1 to >1000:1) [353, 438, 462] indicates that most of the incoming viruses fail to enter the nucleus. Indeed, a substantial portion of the incoming MVM virions was demonstrated to follow a non-infectious pathway ending up in lysosomal compartments where they co-localized with co-endocytosed dextrans which had a MW of 10 kDa and were used as lysosomal markers. Hence, the endosomal escape represents the major barrier for the subsequent steps of MVM infection. However, the inability to escape from the endocytic route was not due to a failure in endosomal processing of MVM since all virions retained in lysosomal compartments underwent the required structural transitions. MVM VLPs or ECs that accumulated in lysosomes remained intact up to 50 hpi but the exposed, capsid-tethered viral DNA of FCs was degraded 21 hpi, most probably, by the lysosomal endonuclease DNase II activity [292].

Unlike enveloped viruses, non-enveloped viruses are unable to deliver their genomes into the host cell by fusion with the cellular plasma or endosomal membrane [201]. They must employ alternative strategies to breach their host cell's delimiting membrane. Although MVM has not yet been directly demonstrated to permeabilize endosomal membranes, there is evidence that parvoviruses have the capability to disrupt membranes. Labeled dextrans with a MW of 3 kDa were progressively liberated into the cytosol 8–20 h after co-endocytosis with CPV virions. However, despite the apparent change in the permeability of endosomal membranes, there is no complete disintegration of endosomal vesicles since larger dextrans with a MW of 10 kDa, as well as α -sarcin, were mainly retained in vesicles at the same time post-infection [357, 434].

Several arguments speak in favor of the N-VP1 terminal PLA₂ activity (see Section 4.4.1, p. 20) mediating endosomal escape of parvoviruses. Firstly, N-VP1 becomes exposed in early

⁴ The P/I ratio is the number of virus particles per plaque-forming unit (PFU).

endocytic vesicles [132, 166, 182, 292, 427, 434, 506]. Secondly, VP1 has been demonstrated to be essential for productive infection of parvoviruses in a step prior to the initiation of DNA replication [30, 31, 156, 195, 357, 387, 459, 467]. Lastly, pre-incubation of N-VP1-exposing CPV virions with PLA₂ inhibitors, such as quinacrine and manoalide, significantly reduced or completely abolished infectivity, respectively [434]. For MVM [166] and AAV2 [427], complementation assays between wild-type and mutant particles have been used to demonstrate that the lipolytic PLA₂ function is mediating phospholipid bilayer penetration. Accordingly, mutants with amino acid substitutions within their catalytic dyad (see Section 4.4.1, p. 20) were constructed. Their enzymatic activity was severely impaired and viral infectivity was completely abrogated. Polyethyleneimine-induced endosomal rupture or co-infection with wild-type or mutant virions could partially rescue the mutant phenotype. Similarly, co-infection with endosomolytically active adenoviral variants resulted in a partial complementation of the mutant phenotype. Contrarily, endosomolytically inactive adenoviral variants, as well as wild-type ECs carrying sequestered VP1u sequences, were unable to restore infectivity of the PLA₂-negative mutants. Thus, the capsid-tethered PLA₂ motif seems to be either directly or indirectly required for successful penetration of the endosomal membranes.

Information about the site of endosomal escape for MVM is still lacking. Previous *in vitro* experiments showed that the optimal pH for the parvoviral PLA₂ enzymatic activity ranges between pH 6 to 7, but drastically decreases at a pH below 5 [78]. Correspondingly, the acidic, lysosomal environment would not provide optimal conditions for PLA₂-mediated escape from the degradative pathway. Therefore, it is tempting to speculate that only a few viruses manage to escape the endocytic route from a pre-lysosomal compartment in the absence of vesicle disintegration. This hypothesis is supported by the fact that MVM externalizes N-VP1 already within the first minutes of infection, thus exposing the functional PLA₂ enzymatic activity on its surface. Additionally, brefeldin A, a fungal antibiotic that blocks the transition between early and late endosomes [272], has been demonstrated to abrogate MVM infection [387]. In summary, these results collectively suggest that the minority of virions that enter the cytosol escape from an intermediate pre-lysosomal vesicle, namely late endosomes [292].

7.5. Cytosolic Trafficking and Interactions with the Proteasome

Free diffusion of macromolecular complexes, such as viruses, is strictly limited in the lattice-like mesh of actin microfilaments, intermediate filaments, and microtubules present in the cytoplasm [284, 409]. Karyophilic viruses require active transport through the cytoplasm in order to reach the perinuclear area. CPV has been demonstrated to depend on active, dynein-mediated retrograde transport along the microtubules. Nocodazole (ND), a highly specific antimicrotubular drug promoting tubulin depolymerization in mammalian cells, prevented nuclear translocation of CPV.

Similarly, an antibody against the intermediate chain of the motor protein dynein also reduced the nuclear accumulation of CPV capsids. EM based studies and co-immunoprecipitations (IPs) of CPV with the intermediate chain of dynein reinforced a dynein-mediated transport of CPV along the microtubules toward the nucleus [432, 433, 468]. For MVM similar observations were reported. Intracellular transport requires a functional cytoskeleton and particularly depends on both microfilaments and microtubules. Both compounds cytochalasin D (CD), a drug inhibiting actin filament function, and ND had a moderate decreasing effect on nuclear viral DNA amplification [387].

Parvoviruses likely undergo further processing in the cytoplasm because microinjection of virions with or without externalized N-termini did not confer a nuclear translocation phenotype [357, 424, 432, 434]. For AAV2 and AAV5 it has been demonstrated that phosphorylation of surface exposed tyrosine residues followed by ubiquitination targets viral capsids for proteasomal degradation [503, 511, 512]. Correspondingly, co-administration of proteasome inhibitors, such as e.g. the tripeptidyl aldehyde MG-132, enhances AAV2 and AAV5 transduction efficiency. In contrast, proteasome inhibition was detrimental to infection for the autonomous parvoviruses PPV, CPV, and MVM. In particular, the chymotrypsin-like activity of the proteasome appeared to be essential for infection. While PPV capsid proteins were ubiquitinated early during the course of infection, no particle ubiquitinylated or degradation was observed for CPV and MVM [56, 386, 387].

7.6. Nuclear Targeting

In addition to the plasma membrane, the nuclear envelope constitutes a second barrier to karyophilic viruses. They need to enter the host's nucleus in order to profit from the replication and transcription machinery for their own multiplication. In fact, viral structural components enter the nucleus at two stages of their life cycle. At the start of infection the incoming virion delivers its genome and late in infection viral subunits accumulate in the nucleus for self-assembly leading to the generation of virus progeny. Small molecules freely diffuse through the nuclear pore complex (NPC). In contrast, nuclear import of larger macromolecules, between 9 and 39 nm in diameter [352], is highly selective and depends on energy and temperature [466]. Nuclear translocation across the NPC is mediated through import signals exposed on the cargo molecules in conjunction with soluble transport receptors [164, 170, 363].

7.6.1. Nuclear Translocation of the Incoming Virion

Interestingly, the functional diameter of the NPC central channel which has been reported to be 23–39 nm [160, 352] is in the range of the diameter of the parvovirus capsids [441]. Therefore, incoming parvoviruses could physically traverse the NPC fully intact unlike influenza- or retroviruses

which partially or completely uncoat their capsids [61, 72, 233, 342, 484]. In the absence of nuclear membrane disintegration, the transport of viral particles must proceed across the NPC [141, 392, 429], as it is the case for cellular proteins. However, there is other evidence that MVM enters the host's nucleus in a NPC-independent way (see step 5b in Figure 7.1, p. 33) [101]. When microinjected into the cytoplasm of *Xenopus oocytes*, MVM has been shown to cause damage to the nuclear envelope in a time- and concentration-dependent manner [100]. It has been proposed that MVM hijacks a cellular pathway to disrupt the nuclear envelope of the host cell. The exact mechanism remains elusive but appears to involve the re-localization of caspase-3 from the cytoplasm to the nucleus without its activation above basal levels in MVM infected cells. In the nucleus, caspase-3 was demonstrated to cleave lamin B2, resulting in a sustained disruption of the nuclear lamina structure and progression of nuclear envelope rupture. MVM-mediated, non-apoptotic caspase-3 activity induces nuclear entry of MVM capsids and possibly the nuclear targeting of further accessory proteins required for replication. Inhibition of caspase-3 during MVM infection resulted in a significant reduction of nuclear entry of MVM capsids and delayed expression of early viral gene products. These results support the possibility of a caspase-facilitated disruption of the nuclear envelope [102].

Several observations are in line with the nuclear translocation of MVM as an intact particle. CPV particles microinjected into the cytoplasm slowly entered the nucleus, possibly crossed the NPC, and were detected by antibodies against intact capsids, indicating that nuclear entry occurs without extensive uncoating [433, 468]. Other reports describe alternative NPC-independent nuclear import mechanisms for intact AAV particles when co-infected with adenoviruses [196, 500]. However, nuclear translocation of intact AAV particles was inefficient [30, 289, 408] or even not detected [424] in the absence of the helper virus, suggesting viral uncoating before or during nuclear entry.

Despite the fact that the NLM domain (see Section 4.4.3, p. 22) is disposed of the inner surface of the capsid [5], the structural rearrangements of MVM during the early endosomal trafficking (see Section 7.3, p. 37) allow the externalization of the VP1u sequence. In this way, the basic NLS sequences (see Section 4.4.2, p. 21) become exposed on the capsid surface. The exposed BC sequences may direct the incoming particle toward the nucleus. Accordingly, deletions of BC1 to BC4 sequences within VP1u completely abrogated MVM infectivity [277]. Similarly, cytoplasmic microinjection of VP1u-specific antibodies was able to neutralize CPV infection [469]. However, nuclear translocation of MVM as a stable disassembly intermediate remains possible since the generation of BC1-4 mutant virions required nuclear localization competent, NLM-harboring VP subunits. Therefore, the NLM within the common part of VP1 and VP2 may act together with the BC sequences in the process of nuclear localization since MVM particles composed of only VP2 subunits are insufficient for MVM infection [277, 459].

7.6.2. Nuclear Translocation of the Structural Proteins

Although sharing a common C-terminal sequence, with VP1 extending along additional 142 amino acids at its N-terminus, the structural proteins of MVM (see Section 4.3, p.18) translocate to the nucleus using different mechanisms. Deletions in any part of the VP2 sequence prevented the major VP from nuclear import, indicating that nuclear translocation is mediated by the conformational NLM (see Section 4.4.3, p. 22) requiring the correct cytoplasmic folding of the whole polypeptide. In contrast, in spite of harboring the same deletions within the common amino acid sequence to VP2, VP1 was not retained in the cytoplasm [276]. VP1 was actively imported using its NLS (see Section 4.4.2, p. 21), located within the VP1u region [277]. The NLS comprised of BCs shows high homology to conventional NLS of many karyophilic polypeptides (see Figure 4.3, p. 22) [173, 228].

Lombardo *et al.* demonstrated that VP1 was able to co-operatively interact with NLM incompetent VP2 subunits, resulting in a predominant accumulation of VP2 in the nucleus in approximately 40 % of the transfected cells. Such coupling of capsid proteins and co-operative nuclear import has also been shown for AAV2 [391]. The efficient nuclear import of NLM-deficient VP2 is surprising because MVM VP1 and VP2 subunits are expressed in a 1:5 stoichiometry. Correspondingly, there is evidence that each VP1 subunit interacts with two VP2 subunits to form a trimer which represents the stable precursor in the MVM assembly pathway [276]. Large insertion loops between the β G and β H strands (see Figure 4.1, p. 19) of threefold symmetry-related subunits extensively interact with each other [494, 501] to form the threefold spikes of parvoviral virions [5, 455]. This observation reinforces the hypothesis of a stable VP trimer as assembly precursor [276]. Indeed, covalent crosslinking of assembly intermediates revealed two types of oligomeric assembly units. The larger species, a heterotrimer, contains one VP1 and two VP2 subunits whereas the smaller homotrimer consist of only VP2 subunits [383]. Moreover, the stable trimeric assembly intermediates have been directly demonstrated by the use of atomic force microscopy [80].

Nuclear translocation of the viral structural proteins depends on the cell cycle. In human and mouse fibroblasts synchronized at G₀, G₁, and G₁/S transition, VPs accumulated in the cytoplasm. Upon arrest release, VPs translocated to the nucleus contemporaneously when the cell entered S phase. In the nucleus they immediately assembled into capsids (see Section 7.10, p. 50) [181].

The NLS and NLM may be involved as major regulatory elements at several levels of MVM morphogenesis because they maintain the stoichiometry between the VP subunits in the host's nucleus. Moreover, nuclear translocation capacity is only conferred to a specific subviral assembly intermediate, namely the VP trimer, thus organizing capsid assembly in the nucleus. Finally, correct folding of the polypeptide chains is a prerequisite for efficient nuclear translocation. Misfolded proteins are excluded from nuclear entry, hence preventing from detrimental interference with MVM capsid assembly in the nuclei [276].

7.7. Non-structural (NS) proteins

The strong dependence of parvoviruses upon host cell “factories” is due to their restricted complexity and strictly limited coding capacity. Parvoviruses do not encode for their own DNA synthesis machinery like large DNA viruses, such as poxviruses, but instead they interfere with the host cell physiology at several distinct stages. Only a few pleiotropic, multifunctional NS proteins suffice to orchestrate the host’s DNA replication, protein synthesis, and transport systems for their own benefit. By this mean parvoviruses ensure the efficient production of all the required viral components necessary for the morphogenesis of progeny virions. Moreover, eventual antiviral responses of the host cell are efficiently evaded. During the course of parvovirus infection, this overwhelming adaptation of the host cell environment is mediated by only five tightly regulated NS proteins. Regulation of the NS proteins involves post-translational modifications (PTMs), re-organization of their cellular compartmental distribution, and interactions with specific cellular partner proteins. Such changes ultimately lead to the formation of novel protein complexes with distinct functions and activities [329].

7.7.1. Non-structural protein 1 (NS1)

NS1 (83 kDa) is a multifunctional, regulatory, nuclear phosphoprotein that consists of several distinct domains. These include ATPase [490], endonuclease [90, 111, 338, 488], and 3’ to 5’ helicase [224] activities, as well as sequence-specific DNA recognition motifs [130, 134, 320], oligomerization domains [374], and an NLS [337]. The functional domains of NS1 act in concert or alone to control and orchestrate a variety of activities essential for viral genome amplification [114, 128, 129], transcriptional regulation [154, 197, 281], interactions with the host cell environment, and mediation of cytotoxicity [64, 77, 262, 268]. NS1 is required in stoichiometric amounts in order to ensure such a fine-tuned control of the virus life cycle. The steady-state level of the major regulatory protein NS1 is controlled by alternative splicing events (see Section 7.9, p. 47) and by its relatively long half-life (> 6 h) [112, 310], thus ensuring a progressive accumulation of NS1 throughout the course of infection. Moreover, specific activities of each individual functional domain can be regulated by PTMs, particularly phosphorylations at serine and threonine residues [108, 315], which are even temporally regulated.

An example for the functional interplay between different NS1 domains is represented by adenosine triphosphate (ATP) binding to the nucleoside triphosphate binding domain which promotes oligomerization of NS1 proteins [337], thus enhancing its site-specific binding to the consensus duplex DNA recognition motif (ACCA)₂₋₃ (see Figure 5.1 C and D, p. 28) [130] and contributing to its cytotoxic potential [104, 263, 268]. In contrast, hydrolysis of bound ATP releases energy [490] which is essential for duplex DNA unwinding activity [91, 222, 338, 490] during replication (see Section 7.8, p. 45 and Figure 7.2 (step iii-iv), p. 46). Thereby, NS1

liberates separated ssDNA strands of the duplex replication origin, which subsequently allow an NS1-mediated introduction of a site and strand specific nick at the consensus nick site via an energy-neutral *trans*-esterification reaction (see Section 5.1.1, p. 26) [66, 339, 423].

7.7.2. Non-structural protein 2 (NS2)

Three forms of the small MVM NS2 proteins (25 kDa) are generated during a productive infection. Each protein harbors a slightly different C-terminal peptide (see Section 7.9, p. 47). Only a little amount of mutant dsDNA RF and no accumulation of progeny unit-length ssDNA genomes were detected following infection or transfection of restrictive murine cells with NS2-null mutants [81]. However, the restricted replication of MVM genomes was less evident in transformed permissive human cells [325]. Therefore, NS2 was demonstrated to have a critical role in MVM replication, depending on the infected cell type. NS2 lacks any enzyme activities but it mediates regulatory functions through multiple interactions with cellular partner proteins in restrictive murine cells. Such cellular interaction partners include the nuclear export factor chromosome region maintenance 1 (Crm1) as well as 14-3-3 protein family members [55, 67, 341]. Since Crm1 functions as a nuclear export receptor and 14-3-3 proteins directly or indirectly regulate cellular protein kinases and phosphatases (reviewed in references [7] and [74]), NS2 is most likely involved in the modulation of cellular signaling of the host cell. Therefore, NS2 plays a central role in the control of nuclear export and progeny virion egress (see Sections 7.12 and 7.13, pp. 52 - 54). Similar to NS1, NS2 can be phosphorylated at multiple residues. Phosphorylation and dephosphorylation influences the subcellular distribution of both viral NS proteins [112] and their ability to interact with cellular partner proteins [55]. Several functions have been attributed to NS2, such as capsid assembly (see Section 7.10, p. 50) [131], genome replication (see Section 7.8, p. 45), mRNA translation, virus production (see Sections 7.10 and 7.11, pp. 50 - 51) [325, 327], and nuclear export of progeny virions (see Section 7.12, p. 52) [55, 161, 311, 341]. Interference with these NS2-mediated functions will cause changes in viral tropism, pathogenesis (see Chapter 6, pp. 29 - 31), and NS1-mediated cytotoxicity (see Section 7.7.1, p. 43) [64, 70, 103, 140, 263].

7.7.3. Small alternatively translated (SAT) protein

The SAT protein is encoded within the capsid gene and is conserved across all members of the *Protoparvovirus* genus. As for the capsid proteins (see Section 4.3, p. 18), expression of the SAT protein occurs late in infection from the same mRNA as VP2 (see Section 7.9, p. 47). Currently, its role during viral infection remains elusive. SAT has been shown to localize to the endoplasmic reticulum (ER) and to affect virus spreading in cell culture by an unknown mechanism [507]. It has been suggested to prevent major histocompatibility complex type I processing [313, 355] and/or cause ER stress-induced cell lysis, which is in line with other ER-targeted viral proteins [151, 269, 431, 437].

7.8. Replication

The coding capacity of MVM genomic DNA is strictly limited due to the small capsid size of an approximate maximum external radius of 140 Å [274]. Consequently, viral genes do not code for their own DNA- and RNA polymerases and relevant accessory proteins. In order to efficiently initiate replication, MVM must recruit and assemble crucial cellular host factors at one of its active origins of replication. Thus, viral proliferation depends heavily on ancillary cellular factors that are essentially involved in viral genome replication and transcription. These factors are transiently supplied by proliferating host cells during the S-phase in the nucleus [109, 147, 385, 425, 438, 442, 447]. In contrast to other host cell dependent, small DNA viruses, such as simian vacuolating virus 40 (SV40) [180, 203], MVM does not have the capability to stimulate resting cells and to initiate its DNA replication. Infection of resting host cells results in an initial latent period until infected cells enter S-phase in order to amplify their DNA [33, 97, 438]. For these reasons, MVM, and parvoviruses in general, show a pronounced predilection for rapidly dividing cell populations [109].

Parvoviruses are unique among all known viruses in having a DNA genome that is both linear and single-stranded. Thus, it is not surprising that they evolutionary adapted their own exclusive replication strategy. Their method to amplify the ssDNA genome resembles an ancient mechanism, called rolling circle replication. This is utilized by many other small, circular prokaryotic and viral replicons [221, 248, 259, 305, 345] but in parvoviruses it is modified and adapted for the replication of a linear chromosome. The parvoviral replication strategy, termed rolling hairpin replication (RHR), proceeds by a single-strand displacement mechanism. Thus, there is no lagging-strand synthesis and the integrity of the terminal hairpin sequences is maintained [443]. The unidirectional progression of the replication fork results in the synthesis of a single, continuous DNA strand. In addition, MVM replication forks are aphidicolin-sensitive and require the proliferating cell nuclear antigen (PCNA). These findings suggest a DNA polymerase δ -mediated DNA replication [33, 90, 334]. Initiation of parvovirus replication induces the reorganization of the host cell nucleus, leading to formation of distinct nuclear foci, referred to as autonomous parvovirus-associated replication bodies [34, 139, 504]. These bodies were shown to be active sites of viral replication and to accumulate essential cellular replication proteins, such as cyclin A, DNA polymerases α and δ , PCNA, and replication protein A [33].

In the initial stage of the RHR, complementary strand synthesis starts from the left-end snap-back telomere, which serves as a primer for the generation of double-stranded monomeric replicative form (mRF) DNA (see step (i) in Figure 7.2, p. 46). Subsequently, the growing complementary strand is ligated to the flipped-back right-end telomere by a host ligase, generating a covalently continuous closed replicative form DNA (cRF) species (see step (ii) in Figure 7.2, p. 46) [127, 275]. This monomer-length turnaround intermediate functions as a transcription template for NS1 (see Section 7.7.1, p. 43) expression. NS1 is essential for all further stages

of the RHR pathway because the cellular replication machinery is unable to melt, copy, and re-orient the left-end telomere [22]. Specifically, NS1 nicks the right-end telomere (*OriR*) of the cRF intermediate [488], assisted by a host DNA-bending protein from the high-mobility group 1/2 family (see step (iii) in Figure 7.2, p. 46) [117]. The resulting, liberated, 3' nt at the nick site serves as a platform for the assembly of a new replication fork. NS1 remains covalently attached to the 5' end of the mRF DNA, where it also functions as the 3' to 5' replicative helicase [90, 110, 189]. The next step (see step (iv) in Figure 7.2, p. 46), called "hairpin transfer", involves reopening and copying of the right-end hairpin sequence in order to generate a right-end extended duplex molecule, replacing the original sequence of the right-end telomere (R) with its inverted complement (r). The two previous steps (iii and iv) of the RHR are commonly referred to as "terminal resolution" [116]. In a NS1 dependent reaction, the extended duplex RF is melted and refolded into two hairpins, creating a "rabbit-ear" structure (see step (v) in Figure 7.2, p. 46) [282, 489]. In this way, the path of the replication fork is reversed effectively, redirecting it back along the internal coding sequences (see step (vi) in Figure 7.2, p. 46). Finally, this results in the generation of dimeric RF and higher-order concatemeric molecules (see steps (vii-ix) in Figure 7.2, p. 46), in such a way that the viral coding sequence is replicated twice as frequently as the telomeres. Viral genomes are fused through a single palindromic junction, in either a left-end:left-end or right-end:right-end orientation. In a last step, individual, unit-length, ssDNA genomes are excised and displaced from the concatemeric RF intermediates. Initially, they feed back as new templates into the replicative pool to promote exponential DNA amplification but later they are consumed by encapsidation [120, 123].

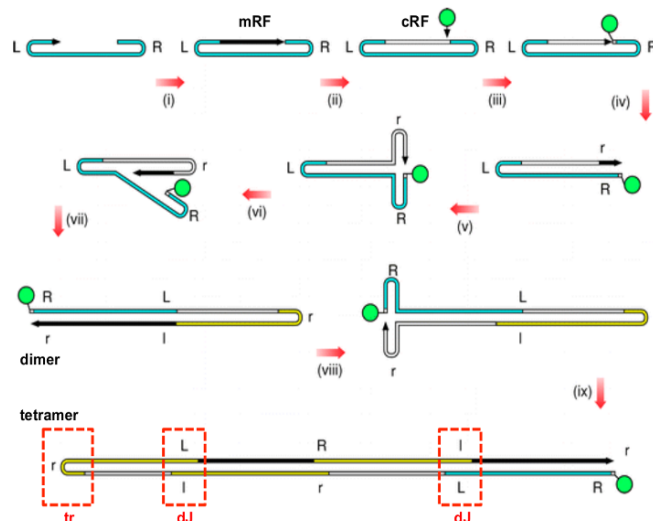


Figure 7.2.: Modified rolling hairpin model for MVM DNA replication. The sequence of the parvoviral genome is illustrated by a continuous line, colored blue for the parental genome, yellow for progeny genomes, and black for newly synthesized DNA, the 3' end of which is capped by an arrowhead. The green sphere represents NS1, which nicks the covalently closed monomer (cRF) and remains attached to its 5' end. The letters L and R depict the palindromic sequences at each terminus, with their inverted complements represented by l and r, respectively. Red dashed boxes depict the turnaround (tr) form of the right-end and the dimer junction (dJ) form of the left-end palindrome [118].

7.9. Transcription and RNA processing

Parvoviruses use a wide variety of alternative RNA processing strategies in order to exploit the strictly limited coding capacity of their small genomes. Alternative splicing of messenger RNA precursors (pre-mRNA) provides a powerful mechanism to generate structurally related but distinct proteins from a single gene, hence contributing to a complex but efficient and compact genome organization [303, 422]. The complex nature of MVM RNA processing of primary transcripts is summarized and simplified in Figure 7.3, p.49. The genome of MVM is transcribed in overlapping transcription units from two promoters located at m. u. 4 and 38, termed P4 and P38, respectively (see Figure 7.3 A, p. 49) [367]. Products of these promoters are three major transcript classes, R1 (4.8 kb) and R2 (3.3 kb), generated from P4, as well as R3 (2.8 kb), generated from P38 [256]. All MVM mRNAs are polyadenylated at a single polyadenylation site at the far right-hand end of the genome (see Figure 7.3 B, p. 49) [20, 96]. On the one hand, transcripts R1 and R2 encode the viral NS proteins NS1 and NS2, respectively, utilizing the ORF in the left half of the genome [107]. On the other hand, the R3 transcripts encode the overlapping viral capsid proteins VP1 and VP2, utilizing the ORF in the right half of the genome. Additionally, the non-structural SAT protein (see Section 7.7.3, p. 44) lies embedded within the capsid genes and likewise, is expressed from the P38 promoter [507]. Transcription from the viral early and late promoters is accomplished by the host RNA polymerase II [106, 367] and accompanied by various cellular transcription factors [6, 165, 177, 188, 368].

All MVM pre-mRNAs contain an overlapping set of downstream small introns in the center of the genome (m. u. 44-46) that is alternatively spliced using two donor sites (D1 and D2) and two acceptor sites (A1 and A2) [98, 112, 227, 317]. In addition to the small downstream intron, P4-generated transcripts also have a large upstream intron, located between m. u. 10 and 39. Intron splicing events are represented by the thin-lined carets in Figure 7.3 B, p. 49. Excision of the large intron is required to produce the R2 transcripts which encode the three NS2 protein isoforms [126, 227, 367]. Splicing at this site is critical in determining the steady state levels of NS1 and NS2 (see Section 7.7, p. 43) [112, 401]. Since R1 and R2 transcripts have similar stabilities [401], and are transported equally to the cytoplasm [326], the ratio of accumulated levels of R1 transcripts relative to R2 directly depends upon the percentage of P4-generated R2 transcripts which lack the large intron. In this way, MVM manages to maintain the optimal balance between the crucial roles which NS1 and NS2 play in viral replication and cytotoxicity [109]. On the contrary, alternative splicing of the small downstream intron from P4-generated pre-mRNAs leads to the production of three isoforms of NS2 [98, 112, 317] of the one part and the two structural capsid proteins, derived from P38-generated R3 transcripts, of the other part. The joining of donor D1 to acceptor A1 [major, M (~70 %)] produces an mRNA which encodes the major capsid protein VP2, or a mRNA encoding NS2^P from R3 or R2 transcripts, respectively. Alternatively, joining of D2 to A2 [minor, m (~25 %)] generates an mRNA encoding the minor capsid protein

VP1, or an mRNA that encodes NS2^Y from R3 or R2 transcripts, respectively. Finally, a rare splicing pattern that joins D1 to A2 [rare, r (~5 %)] is required for the production of NS2^L encoding mRNAs from R2 transcripts [20, 227, 256, 317]. The fourth splicing pattern that joins D2 to A1 is not detected *in vivo* [317], presumably because the distance between this sites (60 nts) is too short to enable successful excision of introns in mammalian cells [347]. To date, only a few examples of small overlapping introns with two donors and two acceptors have been described in literature [186, 294, 303]. For MVM, the small central intron, which is excised efficiently from all classes of MVM pre-mRNA transcripts, appears to be the entry of the spliceosome. In addition, it dictates the relative amounts of VP1 and VP2 or of the three isoforms of NS2 produced during infection. Splicing of the large upstream intron occurs subsequent to small intron recognition and splicing. This second processing step is slowed to make sure that the spliced RNA can leave the nucleus to encode NS1. This delay is most likely ensured by the large non-consensus donors and acceptors of the splice site of the large intron [378]. However, the determinants governing the alternative excision of the large and small intron from MVM pre-mRNAs are poorly understood [179, 204, 205, 508–510]. Nonetheless, it is known that wild-type patterns of alternative splicing of MVM pre-mRNAs are achieved exclusively by cellular splicing factors without the involvement of auxiliary viral proteins [326]. Moreover, it has bee shown that polyadenylation of MVM RNAs precedes splicing of the small intron since unspliced polyadenylated molecules can be detected in the nucleus. In contrast, no detectable accumulation of unspliced MVM RNAs were observed in the cytoplasm of infected cells [97]. This does not apply for the large intron which is only spliced in a proportion of the pre-mRNAs prior to its export from the nucleus. Once in the cytoplasm, R1 transcripts are prevented from further splicing to R2 transcripts. The mechanisms that regulate the export of R1 versus its nuclear retention and further splicing to R2 remain elusive [378]. All aforementioned splicing patterns are exemplified in Figure 7.3 B, p. 49.

Although viral proteins are not participating in the regulation of alternative splicing, they are indispensable for controlling transcription, along with relevant cellular transcription factors and viral *cis*-acting sequences. Interestingly, there is a chronological order to the production of MVM RNA transcripts. It was demonstrated that R1 and R2, the P4-generated pre-mRNAs, precede the P38-generated R3 transcripts during synchronous infection [97]. This temporal phasing is the result of NS1-dependent up-regulation of transcription from the P38 promoter [154, 381]. The acidic C-terminal domain of NS1 acts as a classical transcriptional activator that can potentiate P38 transcription approximately 100-fold [262]. In this way, the NS proteins, particularly NS1 that is essential for MVM DNA replication (see Section 7.8, p. 45) are available prior to the structural capsid proteins in order to initiate early events in parvoviral infection and to stimulate the transcription of the VP and SAT genes under the control of the late P38 promoter. An example for viral *cis*-acting sequences that regulate infection can be found in the left-end hairpin sequence, where both transcription and replication factors compete for specific recognition elements distal to

the bubble sequence. Binding of cAMP-responsive element (CRE) to this sequence has been shown to contribute to maintaining basal levels of P4 activity and also to the up-regulation of P4 activity in transformed cells [171, 365]. CRE binding overlaps with the distal of the two 5'-ACGT-3' half sites needed to bind PIF (see Figure 5.1 C, p. 28) which is essential for stabilizing NS1 binding to the active left-end origin (*OriL_{TC}*) for replication initiation (see Section 5, p. 25) [90]. In this way, replication and transcription are in competition with each other co-ordinate viral infection.

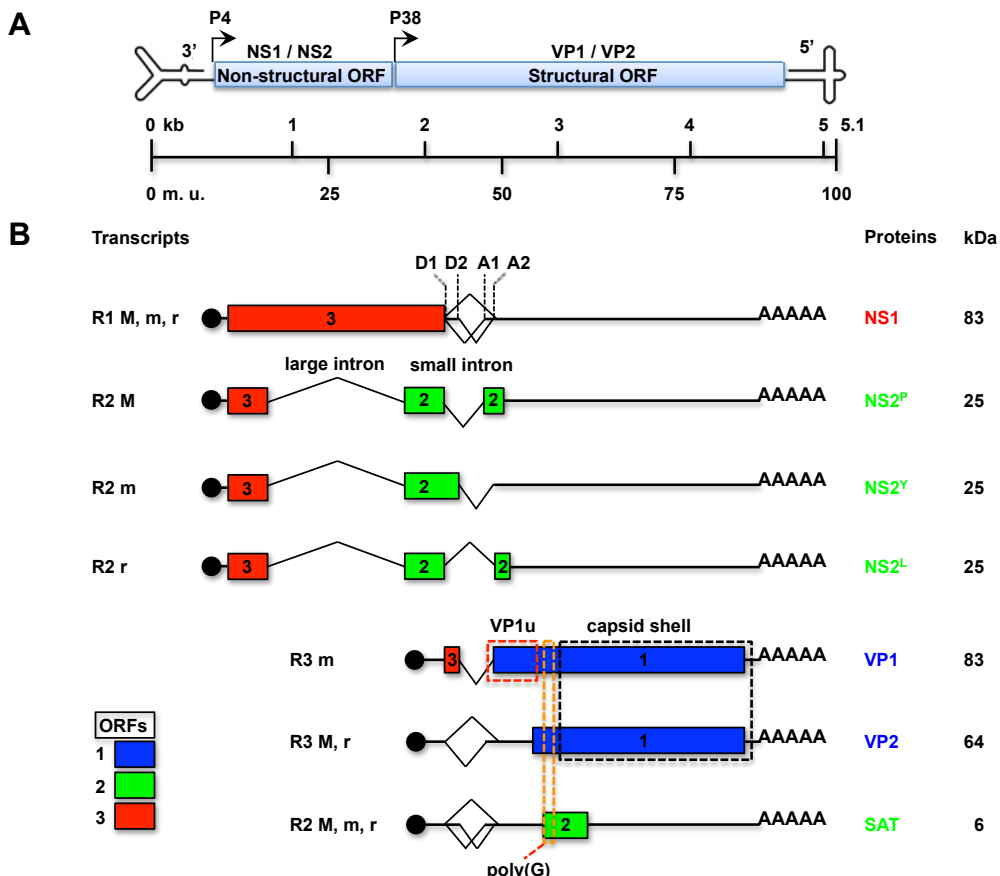


Figure 7.3.: Transcription map of MVM. (A) The single-stranded, negative-sense DNA genome of MVM is illustrated by a single line terminating in dissimilar hairpin telomeres. The two major ORFs are boxed in light blue and the proteins which they encode are indicated above. The two viral promoters, P4 and P38 are shown by rightward arrows. Below, arbitrary m. u. are diagrammed relative to the 5.1 kb genome. (B) The three major cytoplasmic transcript classes R1, R2, and R3 are displayed. A black sphere indicates the capped 5' ends and (AAAAA) denotes their polyadenylated tails near the far right-hand end of the genome. ORFs encoding the viral proteins, named on the right, are displayed in different coloring according to their reading phase. Their spliced-out large or small introns are indicated by thin-lined carets. The small intron is excised from each transcript class by the alternative use of three different splicing patterns, denoted M (major), m (minor), and r (rare). Splice donor and acceptor sites for splicing of the small intron are denoted D1, D2 and A1, A2, respectively. On the one hand, alternative splicing of the small intron generates the R3 transcripts encoding VP1 and VP2, the two structural capsid proteins, and the R2 transcripts encoding three C-terminally distinct isoforms of NS2, referred to as NS2^P, NS2^Y, and NS2^L. On the other hand, excision of the large intron is critical in determining the steady state levels of NS1 and NS2 transcripts. The N-terminal protein sequence boxed in red represents VP1u which harbors the PLA₂ motif that is involved in entry functions. Sequences boxed in black, comprising the C-terminal region common to all VP polypeptides, assemble to form the capsid shell. Poly(G), boxed in orange, identifies a short glycine-rich region present in all VPs that can be modeled into X-ray density occupying the fivefold pores in virions. This Figure was adapted from [125]

7.10. Assembly

The assembly of MVM capsids occurs in the nucleus and involves cytoplasmic trimerization of viral structural proteins and subsequent nuclear translocation of those trimers (see Section 7.6.2, p. 42) [383]. The formation of trimers results from extensive intertwining of the VP polypeptides through extended surface loops which form tight, convoluted intratrimer interactions (see Figure 4.1, p. 19) [274, 364]. These trimers are incompetent for capsid assembly in the cytoplasm. In order to confer nuclear assembly, the trimeric precursors undergo a global conformational rearrangement on top of the 3-fold spike at the center of each trimer [236, 278, 383]. Nuclear association of trimeric assembly intermediates is mainly mediated by quasi-linear, hydrophobic interactions between trimeric subunits. Polar interactions only marginally contribute to capsid assembly and stability [380].

Currently, it remains uncertain whether auxiliary nuclear factors are required for the final steps of parvovirus assembly and maturation. There is evidence that the formation of MVM capsids requires both nuclear factors and the major capsid protein VP2. Expressed capsid proteins that were incompetent for nuclear localization, as well as singly expressed nuclear transport competent VP1 proteins in the absence of VP2 proteins, were not able to assemble [214, 276, 277]. In the case of B19V it was demonstrated that VP1 deletion mutants formed morphologically normal capsids but only a limited extension of VP1 was tolerated. Further lengthening of VP1 versions resulted in less efficient assembly and any assembled particles showed dysmorphic appearance [493]. Truncations beyond 30 amino acids at the N-terminus of VP2 prevented assembly because they affected the β A-strand of the conserved β -barrel motif which constitutes the core of the capsid shell (see Figure 4.1, p. 19) [237].

Nuclear assembly occurs regardless whether the host cell is in S-phase. Inhibition of DNA synthesis resulted in a reduction of mature virions. Nonetheless, ECs accumulated in the nucleus of infected cells [245, 382]. The viral NS2 protein was reported to play a host-range specific role in MVM capsid assembly. On the one hand, MVM expressing truncated forms of NS2 was able to give rise to progeny virus in transformed human cells, albeit with reduced efficiency. On the other hand, they were unable to assemble in their restrictive murine host cells in spite of properly expressing NS1 and the structural proteins in early stages post-infection. The involvement of NS2 in virus assembly remains elusive but is likely to be indirect, since an appropriate cellular environment can complement the defect [131].

A better understanding of the mechanisms underlying capsid assembly and disassembly will be fundamental to the development of antiviral drugs. Virus propagation may be prevented by interference with capsid assembly or by promoting or inhibiting capsid disassembly [372, 513]. Further applications include the use of self-assembling viral nanoparticles for biomedical and nanotechnological applications [157, 299].

7.11. DNA Packaging

Commonly, viruses use two alternative strategies to package their genomes into the capsids. On the one hand, viruses containing circular dsDNA genomes assemble their protein shell around the genome, driven by interactions between protein capsid subunits and nucleic acids and assisted by auxiliary scaffolding proteins [43, 47, 344]. Moreover, several ssDNA or ssRNA viruses, such as tobacco mosaic virus, F1, and M13 bacteriophage follow the same assembly pathway via association of structural proteins around the genome [241]. On the other hand, viruses with double-stranded linear genomes translocate their genetic material into pre-assembled ECs. This process is ATP-dependent and involves auxiliary non-structural packaging enzymes [44]. The presence of a large excess of ECs in parvovirus stocks and the fact that recombinant expression of their structural proteins is sufficient for capsid formation [391] implies that the viral DNA is not required for capsid assembly. Thus, parvoviruses use the latter mechanism for genome translocation into their pre-formed capsids which accumulate in the cell nucleus (see Section 7.10, p. 50). Significantly, the encapsidation process has been visualized by EM in an *in vitro* assembly and packaging reaction of LuIII parvovirus [321].

In the case of MVM, partially or fully packaged capsids were demonstrated to interact with NS1. The NS protein was covalently attached to the 5' termini of unit-length ssDNA genomes. These structures may represent intermediates of the packaging process and NS1, particularly its 3' to 5' helicase activity (see Section 7.7.1, p.43) may support genome translocation into the pre-assembled capsid [111]. Similar observations were reported for AAV2 capsids which were shown to interact with the homologous *rep* proteins [371, 492]. DNase protection studies in AAV [241] and binding experiments between DNA and capsids of autonomous parvoviruses [309, 487] suggest a 3' to 5' packaging direction for parvoviruses. According to the directionality of the encapsidation process, the 3' to 5' processivity of the virus-encoded helicase, rather than the strand displacement 5' to 3' RHR synthesis, seem to drive the translocation of the genome into pre-formed capsids [241].

Initiation of the encapsidation process involves viral *cis*-acting elements. The ITRs of AAV contain a packaging signal which is both required and sufficient for genome encapsidation [397]. So far, a direct, specific interaction of AAV ITRs with capsids has not been demonstrated [473, 474]. In contrast, specific binding of the 3' terminal repeat of MVM to VP1 [486] and to particles composed only of VP2 [487] have been reported. However, interaction with VP1 is not essential for genome translocation since VP1 is dispensable for MVM assembly and packaging [459].

Cross-packaging of LuIII-derived vector genomes into capsids of MVM reinforced the observation that strand selection for packaging occurs due to varying efficiency of excision from replicated genomes of one strand polarity *versus* the other rather than differences in packaging preference [121]. This phenomenon is further elucidated in Section 5.1.1, p. 26.

7.12. Nuclear Export

Besides having the possibility to passively egress the host cell by NS1-induced cellular lysis, the latest data of several research groups propose an active, pre-lytic egress for MVM (see Section 7.13, p. 53) [26, 27, 298]. In order to actively egress the host cell, progeny particles of karyophilic viruses need to cross considerable cellular barriers. Apart from the plasma membrane, the nuclear envelope constitutes a second barrier to MVM. Although the mechanism for nuclear export and subsequent release of MVM virions remains unknown, several important viral and cellular effectors involved in PV egress have been identified and characterized.

MVM is supposed to be exported from the host's nucleus by a Crm1 dependent mechanism. A stable interaction between NS2 and Crm1 has been documented [55, 341]. Classical nuclear export signals (NES) exhibit low affinity for Crm1 in order to prevent the formation of the Crm1/cargo complex in the cytoplasm where RanGTP is absent [324]. Surprisingly, the NES of NS2 belongs to the supraphysiological NES which tightly bind to Crm1 regardless of the presence of RanGTP. Therefore, NS2 competitively inhibits Crm1 function by sequestering endogenous nuclear export receptors. MVM mutant genomic clones generating NS2 proteins harboring either regular NES, or substitutions which abrogated Crm1 interaction were shown to be compromised in viral nuclear export and productive infection [162]. As expected, NS2-Crm1-mutants showed nuclear accumulation of export deficient NS2 in transfected cells. Surprisingly, the nuclear retention of mutant NS2 proteins came along with a substantial accumulation of progeny virions in the nucleus of infected cells, suggesting a NS2-dependent export of progeny virions. Additionally, an indirect involvement of NS2 in viral egress was demonstrated using the closely related H1-PV. For this virus, an in-frame deletion of 38 amino acids within the common coding sequence of NS1 and NS2 was demonstrated to beneficially influence infectivity *in vitro*, indicated by a lower particle-to-infectivity (P/I) ratio and a larger plaque phenotype. The increase in infectivity which resulted from an accelerated egress of the mutant progeny virions, positively affected tumor growth suppression *in vivo* [482]. However, approaches to demonstrate a direct interaction between NS2 and the viral capsid and/or individual structural proteins *in vitro* have not yet been successful despite extensive attempts. Such interactions might be very weak and highly dynamic, thus it is difficult to demonstrate them.

The differences in nuclear export observed during productive MVM infection in either permissive human cells or restrictive murine cells may be due to cell-type-specific use of alternative strategies for nuclear export. They became particularly apparent when the different cell types were treated with the anti-fungal antibiotic leptomycin B (LMB) to inhibit Crm1-dependent nuclear export [254]. LMB treatment of susceptible murine cells resulted in a significant but not complete inhibition of nuclear export of MVM progeny virions. In contrast, even high doses of LMB did not inhibit nuclear export of MVM in transformed human cells, indicating that Crm1 is not required for the nuclear export of MVM in these cells [298]. The observed differences may

result from a cell-type dependent phosphorylation status of MVM. Generally, MVM capsids derived from permissive human cells displayed prominent phosphorylation compared to the decent phosphorylation status of capsids isolated from restrictive murine fibroblasts [297]. Significantly, the three distal serine residues at position 2, 6, and 10 of the unordered N-VP2 terminus showed high phosphorylation levels in permissive cells. Site-directed mutagenesis studies discovered an important role of these phosphorylations in the Crm1-independent nuclear export of MVM in permissive human cells. When the N-terminal phosphorylations were diminished, progeny virions were predominantly retained in the nucleus and the corresponding mutants displayed a small plaque phenotype, indicating the importance of those phosphorylations in viral spread [298].

7.13. Egress

MVM transport from the nucleus to the cell periphery is associated with the degradation of actin fibers and the formation of “actin-patches”. These alterations to the filamentous network were attributed to a virus-induced imbalance between the actin polymerization factor neural Wiskott-Aldrich syndrome protein and gelsolin, a member of the actin-severing protein family [331]. Indeed, the MVM titer in the culture medium following MVM infection drastically declined when gelsolin function was diminished. During MVM infection, gelsolin activity is regulated by the CKII α /NS1 complex which was demonstrated to be capable of phosphorylating gelsolin. Consequentially, inhibition of CKII α correlated with prolonged persistence of actin fibers and delayed formation of the characteristic “actin patches” [26, 330]. A great deal of experimental data would point to an active, vesicle-associated, gelsolin-dependent export of MVM. Progeny virions were shown to co-localize with exocytic, endosomal, and lysosomal markers in immunofluorescent experiments [26, 150]. Cell fractionation experiments confirmed this observation by demonstrating a co-migration of viral particles with cytosolic vesicles rather than free, vesicle-independent localization in the soluble cytosolic fraction. Furthermore, dynamin was found to accumulate in the perinuclear region where it co-localized with *de novo* synthesized MVM capsids. A co-operative cross-talk between actin- and microtubule dependent transport [370, 420, 428] might be involved in MVM transport from the nucleus to the cell periphery, resulting in the destruction of actin filaments and the stabilization of microtubules [26].

The secretory pathway has been proposed as the route for active egress of MVM. Progeny virions would become engulfed by COPII-vesicle formation in the perinuclear ER where they accumulated with dynamin. Accordingly, a dramatic retention of virions in the perinuclear area and inhibition of virion release into the medium was observed in cells lacking functional effectors of the secretory pathway [27]. However, no significant co-localization between MVM progeny virions and representative markers of the recycling pathway or the Trans Golgi Network (TGN) were evident [27]. Radixin and moesin were shown to play a role in virus maturation and spreading

capacity, as judged by their impact on MVM plaque morphology [332]. Indeed, dominant negative mutants failed in wrapping progeny virions into transport vesicles, resulting in a marked reduction of egressed virions in the culture medium. As a consequence, corresponding markers for alternative export routes, e.g. direct transport from the TGN to the PM or through recycling endosomes, exhibited increased co-localization with progeny virions. Finally, active egress promotes cellular lysis as demonstrated by the prolonged viability of cells wherein vesicular transport was either inhibited or by-passed the Golgi apparatus. In addition, the involvement of progeny particles in cytolysis was demonstrated by the prolonged survival of murine cells transduced with a viral vector deficient for the production of progeny virion particles [27].

8. Aim of the thesis and experimental strategy

8.1. Goals

Viral egress affects the transmission and proliferation of virus progeny through the host's tissue. For enveloped viruses, the late maturation steps and final egress via budding through the plasma membrane are well characterized. However, the current knowledge about late maturation, nuclear export, and egress of non-enveloped viruses remains largely unknown.

The present thesis aims for a better understanding of the critical maturation steps leading to nuclear export and egress of a non-enveloped virus. The following issues are the main subject of this study:

1. Confirmation of the existence of an active process of nuclear export and egress of virions prior to passive release through cell lysis.
2. Characterization of the critical capsid maturation steps that trigger active prelytic egress.

8.2. Experimental strategy

Three main experimental procedures were used:

1. Fast protein liquid chromatography (FPLC) was used in order to separate, concentrate, and purify different intracellular virus populations representing distinct maturation intermediates of the parvovirus life cycle. Minute virus of mice (MVM) served as a model parvovirus to study late maturation steps, nuclear export, and egress of non-enveloped viruses. All experiments were performed using a restrictive murine cell line and/or a transformed human cell line.
2. Standard biochemical and molecular biological methods were performed to investigate the structural and functional characteristics of the isolated virus populations.
3. Site-directed mutagenesis on an infectious clone of MVM was applied to study the role of different capsid regions in active egress.

Part II

Methods

9. Methods

9.1. Cell Cultures

A9 ouab^rl1 cells, a derivative from the original HGPRT⁻ L-cell line A9 represent a clone resistant to 10⁻³ M ouabain after nitrosoguanidine mutagenesis [273, 440]. NB324K cells are a clone of SV40-transformed human newborn kidney cells [414]. The SV40 large T antigen was detected by immunofluorescent staining with monoclonal antibodies (mAb) [199]. However, NB324K cells do not produce infectious SV40 spontaneously. Both cell lines, A9 mouse fibroblasts and NB324K cells, were routinely propagated under a minimal number of passages in Dulbecco's Modified Eagle Medium (DMEM) (see Table 9.11, p. 112) supplemented with 5 % of heat inactivated fetal calf serum (FCS) at 37 °C in 5 % CO₂ atmosphere.

9.1.1. Freezing and thawing of cells

Before use, the A9 mouse fibroblasts or NB324K cells were thawed at 37 °C and cultured in 5 mL of pre-warmed DMEM (see Table 9.11, p. 112) supplemented with 5 % FCS. The medium was replaced every 3 to 4 days. In order to freeze the cells for long storage in liquid nitrogen they were passed the day before in DMEM containing 10 % FCS, to ensure exponential growth. Subsequently, 7.5 % DMSO was added and the cells were frozen slowly at -70 °C over night before transfer to liquid nitrogen.

9.2. Virus Stocks

Stocks of MVM without detectable levels of VP3 were propagated on A9 mouse fibroblast monolayers. As soon as the cytopathic effect was complete (7-8 days post-infection), the supernatant (SN) was collected and pre-cleared from cell debris by low-speed centrifugation. Thereby, intracellular VP3 rich capsids were discarded. In order to remove low-molecular contaminants, virus containing SN was pelleted through 20 % sucrose cushion in PBS by ultra-centrifugation. Virus titers were determined by quantitative PCR (qPCR) (see Section 9.5, p.62) as DNA-packaged particles per microliter.

9.2.1. Separation of empty and full capsids

Sucrose purified capsids were prepared as previously described in Section 9.2, p. 59. The virus pellet was resuspended in 10 mL PBS. Caesium chloride was added to a density of 1.38 g/mL adjusted by refractometry ($\eta=1.371$) at 4 °C. The gradient was centrifuged to equilibrium for 24 h at 41 000 rpm and 4 °C in a Beckman SW-41 Ti swinging bucket rotor. Gradients were fractionated and tested for intact capsids by dot blot analysis using B7 mAb (see Table 9.9, p. 111). CsCl was depleted from the corresponding fractions by size-exclusion chromatography through PD-10 desalting columns (GE Healthcare) and the capsids were concentrated in Amicon® centrifugal filter devices (Merck Millipore) when required.

9.3. Freezing bacteria stocks in glycerol

Bacteria were frozen in dry ice. A volume of 700 μ L of the bacteria culture that was grown over night in LB-medium (see Table 9.11, p. 112) was mixed with 300 μ L of 50 % glycerol in a cryotube. In order to mix well the glycerol the cryotube was vortexed intensively. Following snap-freeze in dry ice the bacteria were stored at -70 °C.

9.4. Fast protein liquid chromatography (FPLC)

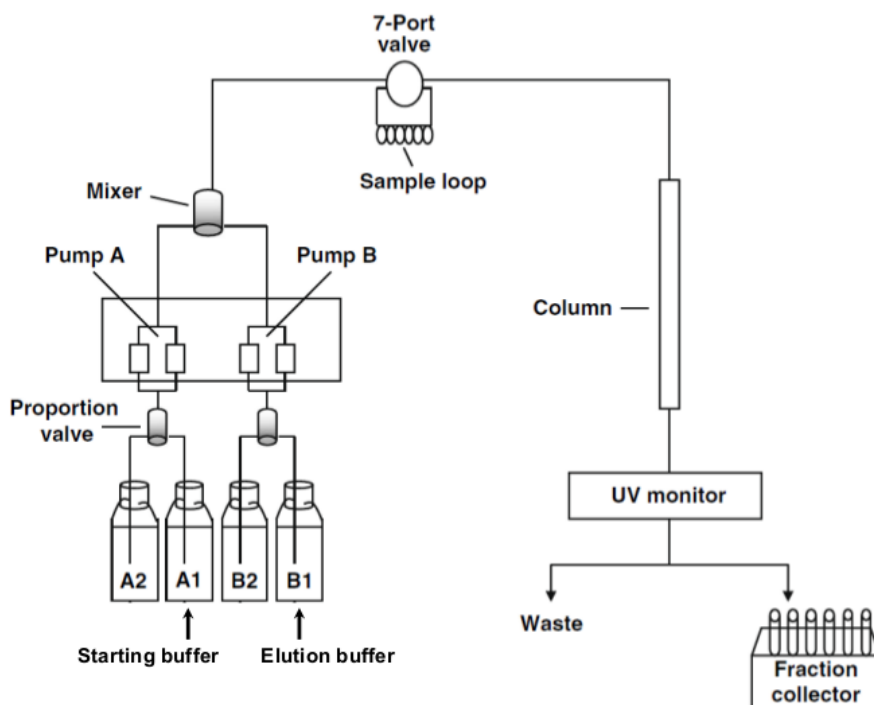


Figure 9.1.: Schematic outline of the ÄKTA purifier FPLC chromatography system. This figure was adapted from [291].

9.4.1. Anion-exchange chromatography (AEX)

A Mono QTM HR 5/5 (Pharmacia) column (5 x 50 mm) was used to analyse virus samples. The Mono Q column was connected to the ÄKTA purifier 10 chromatography system (GE Healthcare) that was operated by the unicorn control software (GE Healthcare). The Mono QTM column was equilibrated with five column volumes (CV) starting buffer (see Table 9.3, p. 108). Samples (1 mL) containing at least 10^{10} DNA-containing virus particles in sample buffer (see Table 9.3, p. 108) were applied to the Mono QTM column through a 2 mL injection loop. Following sample application the loop and the column were rinsed with six CV starting buffer. In order to elute the bound proteins, a linear salt gradient (0-2 M NaCl) was applied by gradually increasing the concentration of the elution buffer (see Table 9.3, p. 108). The total elution volume of 24 CV was split into fractions of 185 μ L which were collected in 96-well plates. The flow rate was constantly kept at 1.5 mL/min and the salt concentration was monitored by measuring the electrical conductivity. Viral genomes in each fraction were quantified by qPCR (see Section 9.5, p. 62).

Occasionally, the Mono QTM column needed to be washed. Increased back-pressure, color change at the top of the column, decreased sample recoveries, or loss of resolution indicate that the column matrix requires regeneration. In order to circumvent such problems, the column was washed every tenth run. To elute contaminants that tightly stick to the column the following harsh conditions were applied to the reversed (bottom to top) Mono QTM column. 500 μ L 2 M NaCl solution was injected and subsequently, the column was rinsed with water. Then, 500 μ L 2 M NaOH solution was injected and the column was rinsed with water. Finally, 500 μ L 75 % acetic acid was injected before the column was re-equilibrated with starting buffer (see Table 9.3, p. 108).

All runs were performed at 6 °C. Buffers were filtered and degassed before application to the Mono QTM column.

9.4.2. Chromatofocusing (CF)

A Mono PTM 5/200 GL (GE Healthcare) column (5 x 200 mm) was used to determine the isoelectric points (pI) of virus samples. The column was connected to the ÄKTA purifier 10 chromatography system (GE Healthcare) that was operated by the unicorn control software (GE Healthcare). The Mono PTM column was equilibrated with two CV of buffer A (see Table 9.4, p. 108). Samples (500 μ L) containing 10^{10} DNA-containing virus particles in buffer A (see Table 9.4, p. 108) were applied to the Mono PTM column through a 1 mL injection loop. Following sample application, the loop and the column were rinsed with 10 mL buffer A (see Table 9.4, p. 108). Bound viruses were eluted by applying buffer B (see Table 9.4, p. 108) to the column. Buffer B contains the acidic ampholyte solution, thus gradually lowering the pH within the column. The total elution volume of 7 CV was split into fractions of 250 μ L which were collected in 96-well plates. The flow rate was constantly kept at 0.5 mL/min and the pH was monitored. Viral genomes in each

fraction were quantified by qPCR (see Section 9.5, p. 62).

All runs were performed at 6 °C. Buffers were filtered and degassed before application to the Mono PTM column.

9.5. Quantitative PCR (qPCR)

Amplification of MVM DNA and real-time detection of PCR products were performed by using CFX96 technology (BioRad) with iTaqTM Universal SYBR[®] Green Supermix (see Table 9.7, p. 110). PCR was carried out by using the hot-start iTaqTM DNA polymerase (BioRad) following the manufacturer's guide-lines. Viral DNA was isolated using the DNeasy blood and tissue kit (see Table 9.7, p. 110). Elution of the purified vDNA was carried out using 100 µL elution buffer. As templates 2 µL of the isolated viral DNA were used for the PCR reaction as outlined in Table 9.1.

Component	Amount	Final concentration
dH ₂ O, PCR grade	6 µL	-
Forward primer (CR3), 10 pM	1 µL	0.5 pM
Reverse primer (CR4), 10 pM	1 µL	0.5 pM
2x IQ TM SYBR [®] Green Supermix	10 µL	1×
Total volume	18 µL	

Table 9.1.: Master mix for quantitative PCR. In order to minimize pipetting errors a master mix was prepared. Following preparation the master mix was distributed across the 96 well plates. The master mix contains all the ingredients which are required for the DNA amplification except the initial DNA template that differs among the samples.

To ensure accurate quantification, the 96-well plates containing master mix and template DNA were shortly spun and transferred into the BioRad CFX96 unit. The PCR program used for quantification of viral DNA is depicted in Table 9.2.

Cycles	Step	Temperature	Time
1x	Initial denaturation	95 °C	300 s
40x	Denaturation	95 °C	15 s
	Annealing	61 °C	15 s
	Extension	72 °C	15 s
1x	Final denaturation	95 °C	60 s
1x	Melting curve	65 °C up to 95 °C	0.1 °C/s

Table 9.2.: PCR conditions for the amplification and real-time detection of MVM DNA.

To provide standards for sample quantification, serially diluted plasmids containing the entire

MVM genomic DNA were used. For cell number variations that may exist between the samples, the number of applied cells per PCR reaction needed to be quantified for normalization as well. For this purpose quantification of cellular β -actin gene was performed. After normalization, direct comparison of the results is possible. β -actin quantification was carried out with the same PCR conditions outlined in Table 9.2, p. 62 with the annealing temperature ($60\text{ }^{\circ}\text{C}$) as the only exception.

In Table 9.3 all primers are listed which were used for MVM genome or β -actin gene quantification.

Primer	Sequence
CR3	5'-GACGCACAGAAAGAGAGTAACCAA-3'
CR4	5'-CCAACCATCTGCTCCAGTAAACAT-3'
Mouse β -actin forward	5'-TGGCACCAACACCTTCTACAATGA-3'
Mouse β -actin reverse	5'-CCGCTCGTTGCCAATAGTGA-3'
Human β -actin forward	5'-TGCTGTCCCTGTATGCCTCTG-3'
Human β -actin reverse	5'-AATGCCTGGGTACATGGTGGT-3'

Table 9.3.: Different primers that were used for qPCR.

9.6. Virus infection

A9 or NB324K cells (10^5 for qPCR, IF, and Western blotting (WB) or 3×10^6 for AEX) were infected with MVM (5 000 DNA-containing particles per cell, corresponding to approximately 10 PFU/cell [438]) for 1 h at $4\text{ }^{\circ}\text{C}$ for binding. Unbound virus was removed by washings and the cells were incubated at $37\text{ }^{\circ}\text{C}$ to initiate infection. At progressive times post-internalization total cellular DNA was extracted for qPCR analysis (see Section 9.5, p. 62) or cells were fractionated (see Section 9.8, p. 64) and subjected to AEX (see Section 9.4.1, p. 61).

9.7. Transfection

NB324K cells at a confluence of 70 % were trypsinized and resuspended in 10 mL of DMEM (see Table 9.11, p. 112) supplemented with 10 % FCS. A total amount of 10^6 cells were used for transfection with the AMAXATM nucleofectorTM II device following the manufacturer's instructions. Transfection was carried out with 5 μg of the infectious clone of MVM (see Section 9.1, p. 101, [308]) using the V-001 program. As a transfection reagent, AMAXA[®] Cell Line Nucleofector[®] Kit V (see Table 9.7, p. 110) was used. Following transfection the weakened cells were maintained in 1.5 mL of pre-warmed culture medium and after 6 h, the culture medium was replaced with an equal amount of pre-warmed culture medium. The cells were further incubated for the required times.

9.8. Cell fractionation

9.8.1. Nuclei isolation

Isolation of A9 and NB324K nuclei was performed by using the Nuclei EZ Prep Nuclei Isolation Kit (see Table 9.7, p. 110) following the manufacturer's instructions. In order to obtain highly pure nuclear fractions, the isolated nuclei were pelleted through a sucrose gradient by low speed centrifugation at 500 g for 10 min. Extracted nuclei were lysed in nuclei lysis buffer (see Table 9.2, p. 107) at 4 °C for 30 min. Following vortexing thoroughly the nuclear lysate was passed through a 27 G needle 10 times. Debris was removed by centrifugation at 10 000 rpm for 10 min at 4 °C.

9.8.2. Extraction of the cytoplasm

Cytoplasmic fractions were extracted in cell lysis buffer (see Table 9.2, p. 107) at 4 °C for 30 min. Following vortexing thoroughly, intact nuclei and cell debris was removed by centrifugation at 10 000 rpm for 10 min at 4 °C.

9.9. Immunoprecipitation (IP)

In vitro treated viruses or viruses from cell extracts were transferred to LoBind tubes that were pre-blocked with PBS containing 1 % bovine serum albumin (PBSA 1 %). The volume was adjusted to 200 µL with PBSA 1 %. The antibody was added in excess and incubated with the viral capsids for 1 h at 4 °C on a rotary shaker. Subsequently, 20 µL protein G-agarose beads were added. Following overnight incubation at 4 °C and centrifugation at 2 500 rpm for 5 min the supernatant was discarded. The beads were washed 4 times with PBSA 1 %. To remove the BSA an additional wash step was carried out with PBS. Finally, the beads were frozen at -20 °C until further use or immediately processed.

9.10. Dot Blot

Viruses (10^8 in 2 µL) were spotted on a nitrocellulose membrane. The membrane was blocked for 20 min with TBST containing 5 % milk. The primary antibody was diluted in TBST supplemented with 1 % milk and incubated for 30 min at room temperature. Unbound antibody was removed by washing the membrane 3 times for 5 min with TBST containing 1 % milk. The horseradish peroxidase (HRP)-coupled secondary antibody was diluted 1:20 000 in TBST supplemented with 1 % milk and added to the membrane for 30 min. Excess secondary antibody was removed by the same procedure as aforementioned for the primary antibody. The membrane was developed by exposure to photo films.

9.11. SDS-PAGE and Western blotting (WB)

Immunoprecipitated capsids were dissolved in 20 μL 1 \times protein loading buffer (see Table 9.6, p. 109) containing 2 % SDS and 10 % glycerol. The samples were boiled at 96 °C for 8 min. Viral proteins were separated through a NuPAGE® 10 % Bis-Tris Gel (Invitrogen). The XCell Sure Lock™ Electrophoresis Cell (Invitrogen) was used to separate the proteins. The gel was first run at 30 V for 10 min to stack the proteins. In this way, sharper bands could be achieved. Separation of the different proteins was accomplished at 200 V. Following separation, the proteins were blotted on a methanol activated, porous, 0.2 μm polyvinylidene fluoride (PVDF) Immobilon® Transfer Membrane (EMD Millipore). Blotting was carried out at 30 V for 1 h 10 min using XCell II™ Blot Module (Invitrogen). The membrane was blocked in TBS-T buffer (see Table 9.6, p. 109) supplemented with 5 % milk overnight at 4 °C. Subsequently, the membrane was probed with a polyclonal rabbit antibody against linear MVM-VP epitopes (see Table 9.9, p. 111) that was diluted 1:2 000 in 3 mL TBS-T containing 1 % milk. The first antibody was incubated for 1 h at room temperature. The PVDF membrane was washed in TBS-T for a total 90 min with many buffer replacements. Subsequently, the horseradish peroxidise conjugated secondary antibody (goat α -rabbit-HRP, (see Table 9.10, p. 112) was added for 1 h at room temperature. This secondary goat anti-rabbit antibody was diluted 1:20 000 in TBS-T supplemented with 1 % milk. To deplete remaining antibodies, the membrane was washed in the same way as described above except for a final wash step with TBS (see Table 9.6, p. 109). VP1, VP2, and possibly VP3 were visualized by a chemiluminescence system (SuperSignal® West Femto Maximum Sensitivity Substrate, see Table 9.7, p. 110) following the manufacturer's instructions. After this treatment, the PVDF membrane was exposed to a film (Amersham Hyperfilm™ ECL, see Table 9.7, p. 110). Finally, the film was developed using Anatomix Developer Replenisher Solution and Fixer and Replenisher Solution (see Table 9.7, p. 110).

9.12. Enzymatic reactions

All enzymatic reactions were performed with 10^8 virus particles in a reaction volume of 50 μL . Viruses were incubated in PBS for 1.5 h at 37 °C with 0.5 mg/mL chymotrypsin (see Table 9.8, p. 110). The reaction was blocked by adding 100 μM chymostatin (see Table 9.1, p. 106).

Phosphatase lambda treatment (2 000 Units, see Table 9.8, p. 110) was performed in 50 mM Tris-HCl, 100 mM NaCl, 2 mM MnCl₂, 5 mM DTT, pH 7.8 for 3 h at 37 °C in PBSA 1 % pre-blocked Protein LoBind eppendorf tubes. Phosphatase lambda was inactivated by supplementing the enzymatic reaction with 1 mM Na₃VO₄ and 1 mM NaF.

Free DNA was digested using 50 Units DNaseI (see Table 9.8, p. 110) in 1 \times incubation buffer according to the manufacturer's protocol. DNaseI was inhibited by incubation at 75 °C for 15 min.

Negative controls were incubated in the same buffers for the same time.

Part III

Publication

1. Wolfisberg et al., Journal of Virological Methods, 2013

Impaired genome encapsidation restricts the *in vitro* propagation of human parvovirus B19.

Raphael Wolfisberg, Nico Ruprecht, Christoph Kempf and Carlos
Ros



Impaired genome encapsidation restricts the *in vitro* propagation of human parvovirus B19



Raphael Wolfisberg^a, Nico Ruprecht^a, Christoph Kempf^{a,b}, Carlos Ros^{a,b,*}

^a Department of Chemistry and Biochemistry, University of Bern, Freiestrasse 3, 3012 Bern, Switzerland

^b CSL Behring AG, Wankdorffstrasse 10, 3000 Bern 22, Switzerland

ABSTRACT

Article history:

Received 7 March 2013

Received in revised form 24 May 2013

Accepted 3 June 2013

Available online 10 June 2013

Keywords:

Parvovirus B19
UT7/Epo cells
Erythroid progenitor cells
EPCs
VP1u
Hypoxia

The lack of a permissive cell culture system hampers the study of human parvovirus B19 (B19V). UT7/Epo is one of the few established cell lines that can be infected with B19V but generates none or few infectious progeny. Recently, hypoxic conditions or the use of primary CD36+ erythroid progenitor cells (CD36+ EPCs) have been shown to improve the infection. These novel approaches were evaluated in infection and transfection experiments. Hypoxic conditions or the use of CD36+ EPCs resulted in a significant acceleration of the infection/transfection and a modest increase in the yield of capsid progeny. However, under all tested conditions, genome encapsidation was impaired seriously. Further analysis of the cell culture virus progeny revealed that differently to the wild-type virus, the VP1 unique region (VP1u) was exposed partially and was unable to become further externalized upon heat treatment. The fivefold axes pore, which is used for VP1u externalization and genome encapsidation, might be constricted by the atypical VP1u conformation explaining the packaging failure. Although CD36+ EPCs and hypoxia facilitate B19V infection, large quantities of infectious progeny cannot be generated due to a failure in genome encapsidation, which arises as a major limiting factor for the *in vitro* propagation of B19V.

© 2013 Elsevier B.V. All rights reserved.

1. Introduction

Human parvovirus B19 (B19V) is spread worldwide and typically causes a mild self-limiting infection in children known as *erythema infectiosum*. B19V has also been associated to myocarditis, acute and chronic arthropathies in adults, transient aplastic crisis and chronic anemia in individuals with altered immunologic or hematologic conditions, hydrops fetalis and intrauterine fetal death (Heegaard and Hornsleth, 1995; Heegaard and Brown, 2002; Survey et al., 2007).

Considering its worldwide distribution, prevalence and associated disorders, B19V is regarded as a prominent human pathogen and the only parvovirus undoubtedly linked to human disease. However, the experimental research with B19V is hampered seriously due to the lack of an appropriate and sufficiently permissive cell system to propagate the virus and study its biology. The reason for this is the rigorous replication requirements of the virus. B19V has an extraordinary tropism for erythroid progenitor cells in the bone marrow at a particular differentiation stage corresponding to BFU-E and CFU-E (Takahashi et al., 1990; Ozawa et al.,

1986, 1987). The narrow tropism of B19V is mediated, at least in part, by its particular uptake mechanism. B19V utilizes globoside (Gb4Cer) as a primary attachment receptor, which is expressed in few cell types (Brown et al., 1993) and a co-receptor (Weigel-Kelley et al., 2003) to initiate the internalization process. However, cells expressing the required receptors and co-receptors are not always permissive, suggesting that the selective replication of B19V is determined by additional intracellular factors restricted to erythroid cells (Pallier et al., 1997; Bruneck et al., 2000; Gallinella et al., 2000; Guan et al., 2008; Chen et al., 2010; Luo et al., 2011). The high viremia that is typically associated to B19V acute infections, exceeding occasionally 10^{13} genome equivalents (geq) per ml of plasma (Kooistra et al., 2011), suggests that the virus can replicate efficiently in the target cells when all the required elements are present. However, despite continuous efforts, the specific cellular factors that control B19V infection in the natural target cells have not yet been reproduced adequately in an established cell line. Some erythropoietin-dependent leukemic cell lines, notably UT7/Epo (Shimomura et al., 1992) and KU812Ep6 (Miyagawa et al., 1999), have been shown to be semi-permissive to B19V infection, producing in general none or minor amounts of infectious progeny. The permissivity of non-erythroid cells, such as HepG2 cells has produced contradictory results (Caillet-Fauquet et al., 2004a; Bonvicini et al., 2008). Considering all these limitations, highly viremic donors without B19V neutralizing antibodies remain the only source of infectious B19V. Thus, the need to develop

* Corresponding author at: Department of Chemistry and Biochemistry, University of Bern, Freiestrasse 3, 3012 Bern, Switzerland. Tel.: +41 31 6314349; fax: +41 31 6314887.

E-mail address: carlos.ros@ibc.unibe.ch (C. Ros).

a cell culture method capable of producing large amounts of infectious B19V remains a major challenge.

Recently, the use of cells cultured under hypoxic conditions has been described as a promising method to produce high quantities of infectious particles (Caillet-Fauquet et al., 2004b; Pillet et al., 2004; Chen et al., 2011). Similarly, the use of *ex vivo* expanded CD36+ primary human erythroid progenitor cells (CD36+ EPCs), previous CD34+ *in vitro* preselection (Pillet et al., 2008; Wong et al., 2008), has also been described as a highly permissive system, based on the expression of B19V non-structural and capsid proteins. A simplified approach to generate CD36+ EPCs directly from ordinary blood samples, without *ex vivo* stem cell mobilization has been reported (Filippone et al., 2010). The combination of both approaches, primary CD36+ EPCs cultured under hypoxic conditions, has been shown to enhance remarkably B19V infection (Chen et al., 2011). Hypoxia, which mimics the oxygen microenvironment in the bone marrow, seems to promote B19V infection by the direct stimulating effect of HIF1 α on the B19V p6 promoter (Pillet et al., 2004). However, an alternative HIF1 α -independent mechanism based on STAT5A and MEK signaling has been proposed recently (Chen et al., 2011).

These novel approaches based on hypoxia and primary CD36+ EPCs have been compared systematically in infection and transfection experiments with the established erythroid cell line UT7/Epo. In all cases, a substantial amount of capsid progeny was obtained. The use of the novel approaches resulted in a significant acceleration of the infection and the augmentation in the number of infected cells resulting in a modest but noticeable increase in virus progeny production. However, in all tested cells and under all conditions genome encapsidation was impaired seriously generating an empty non-infectious virus progeny. Differently to the wild-type virus, the VP1 unique region (VP1u) of the virus progeny was exposed partially and upon heat treatment did not undergo the expected conformational change that renders VP1u fully externalized. The abnormal configuration and rigidity of VP1u, which utilizes the genome encapsidation portal for its externalization, might constrict the fivefold axes channel impeding the translocation of the viral genome into the pre-assembled capsid.

2. Materials and methods

2.1. Cells and viruses

UT7/Epo cells were maintained in Eagle's minimum essential medium (MEM) supplemented with 5% heat-inactivated fetal calf serum (FCS) and 2 U/ml of recombinant human erythropoietin (Epo; Janssen-Cilag, Midrand, South Africa) at 37 °C with 5% CO₂. For hypoxic conditions the oxygen tension was lowered to 1%. Cells with adherent phenotype were selected by removing the non-adherent cells in every passage. CD36+ erythroid progenitor cells (CD36+ EPCs) were obtained from ordinary blood samples and cultured as described previously (Filippone et al., 2010). A B19V-infected plasma sample (Genotype 1; CSL Behring AG, Charlotte, NC), without detectable B19V-specific IgM or IgG antibodies, was used as a source of native infectious virus. The virus was pelleted by ultracentrifugation through 20% (w/v) sucrose and the concentration of virions was determined by quantitative PCR (qPCR).

2.2. Antibodies and chemicals

Two human monoclonal antibodies (mAb), one directed to a conformational epitope in the major capsid protein VP2 (mAb 860-55D), which detects exclusively intact capsids, and the other against the N-terminal region of VP1, also known as VP1 unique region (VP1u) (mAb 1418), were provided by S. Modrow

(Regensburg, Germany). These antibodies were produced from peripheral blood mononuclear cells of normal, healthy individuals with high titers of serum antibodies against B19 virus proteins (Gigler et al., 1999). A rabbit antibody against the C-terminal region of VP1u was described earlier (Bönsch et al., 2008). A mouse mAb against B19V capsids (mAb 521-5D) was purchased from Millipore (Billerica, MA). A globoside-specific mouse IgM mAb (AME-2) was provided by J. de Jong (The Netherlands Red Cross, Amsterdam, Netherlands). Mouse IgG mAb against Ku80 and CD49e were purchased from BD Biosciences (San Jose, CA). A mouse antibody against B19V proteins was obtained from US biologicals (Swampscott, MA). Chloroquine diphosphate (CQ) was purchased from Sigma (St. Louis, MO) and dissolved in water.

2.3. Flow cytometry

The presence of B19V receptors and co-receptors on the cell surface of UT7/Epo cells was analyzed quantitatively by flow cytometry. UT7/Epo cells were incubated with either an anti-Ku80 or an anti-Gb4Cer antibody at 4 °C for 1 h in PBS containing 2% fetal calf serum, followed by incubation with fluorescein isothiocyanate (FITC)-conjugated rat anti-mouse IgG or IgM, respectively (BD Biosciences). Additionally, UT7/Epo cells were stained with R-phycocerythrin conjugated anti-human CD49e (BD Biosciences). The cells were analyzed on a BD FacsCanto II (Becton Dickinson, San Jose, CA). Data acquisition and analysis were conducted with a software (BD FacsDivा, BD Biosciences).

2.4. Infection

UT7/Epo and primary CD36+ EPCs (3×10^5) cultured under normoxia or hypoxia (1% O₂) during 2 days, were infected with B19V at 10^4 geq per cell for 1 h at 4 °C. The cells were washed to remove unbound viruses and further incubated at 37 °C. At different post-infection (p.i.) times, cells and supernatants were collected. The cells were washed and processed for immunofluorescence (IF), immunoprecipitation (IP), as well as DNA and RNA extraction. The supernatant was used for IP and DNA extraction.

2.5. Transfection

A total of 5×10^6 UT7/Epo cells, cultured under normoxia or hypoxia (1% O₂) during 2 days, were transfected using the AMAXA nucleofector™ II device (Lonza, Cologne, Germany) following the manufacturer's instructions. Transfection was carried out with 5 µg of the B19V genome excised from a B19V infectious clone (pB19-M20) (Zhi et al., 2004) or with 2 µg of a GFP-control plasmid, using the T-20 program. As a transfection reagent, AMAXA™ Cell Line Nucleofector™ Kit R (Lonza) was used. After transfection, the cells were maintained in 20 ml of pre-warmed culture medium. A volume of 5 ml of fresh MEM culture medium supplemented with 5% FCS and Epo (2 U/ml) was added to the cells 24 h post-transfection (p.t.). At increasing times p.t., the cells and supernatant were collected for further analysis.

2.6. Quantitation of B19V DNA and NS1 mRNA

Total DNA was extracted from cells or from the supernatant by using the DNeasy blood and tissue kit (Qiagen, Valencia, CA). For the isolation of total mRNA, cells were transferred to RNase-free tubes (Safe-Lock Tubes 1.5 ml, Eppendorf Biopur) and washed twice with PBS. Total poly-A-mRNA was isolated with the Dynabeads mRNA direct kit (Roche Diagnostics, Mannheim, Germany). The RNA preparations were used for reverse transcription as described previously (Bönsch et al., 2010a). Amplification of DNA or cDNA and real-time detection of PCR products were performed by qPCR

with the iQ SYBR Green Supermix and the CFX96 device (Bio-Rad, Cressier, Switzerland). Primers used for amplification were described elsewhere (Bönsch et al., 2010a).

2.7. Immunoprecipitation of B19V particles and quantitation of virions

Viral particles were immunoprecipitated from cell extracts or from the supernatant of infected cells with a human mAb against intact capsids (860-55D) (Gigler et al., 1999). As reference control, a known amount of virions was added to the uninfected cell extracts or to the supernatant. After overnight incubation at 4 °C in the presence of 20 µl of protein G agarose beads (Santa Cruz Biotechnology, Heidelberg, Germany) the supernatant was discarded and the beads were washed four times with PBSA. Immunoprecipitated viral capsids were detected by SDS-PAGE. To verify the presence of the viral genome, DNA was extracted from the immunoprecipitated virions by using the DNeasy blood and tissue kit (Qiagen) and quantified as specified above.

2.8. Immunofluorescence

Cells or purified viruses were fixed on coverslips by using acetone/methanol (1:1 [v/v]) solution at -20 °C for 4 min. Following blocking with goat serum diluted in PBS (20% [v/v]), the samples were incubated with the primary antibodies in PBS containing 2% goat serum for 1 h at room temperature (RT). The samples were washed and the appropriate fluorescently labeled secondary antibody in 2% goat serum was added for 1 h at RT. Nuclei was stained with 4',6-diamidino-2-phenylindole (DAPI). Mowiol supplemented with 2.5% 1,4-Diazabicyclo[2.2.2]octan (DABCO) was used to maintain the fluorescent signal. Samples were examined by confocal laser scanning microscopy (Axiovert 200M, Carl Zeiss A.G., Feldbach, Switzerland).

2.9. Fluorescence *in situ* DNA hybridization

The presence of newly replicated viral genomes in the infected cells was examined by fluorescence *in situ* DNA hybridization (FISH). Biotinylated probes specific for B19V DNA were generated from PCR products by nick translation (Roche), according to the manufacturer's instructions. The size of the hybridization probes was 200–500 nucleotides in length, as confirmed by agarose gel electrophoresis. Cells were fixed and immunostained with mAb 860-55D against capsids and incubated in a humid chamber at 37 °C for 18 h with a volume of 20 µl hybridization mix (5 ng/µl biotinylated probe in 60% deionised formamide, 300 mM NaCl, 20 mM sodium citrate, 10 mM EDTA, 25 mM NaH₂PO₄ pH 7.4, 5% dextran sulfate and 250 ng/µl sheared salmon sperm DNA). Subsequently, the cells were washed (50% deionized formamide, 25 mM NaCl and 2.5 mM sodium citrate pH 7.4) three times for 5 min at RT and once at 37 °C. The samples were blocked for 30 min with 1% blocking solution (Roche) in 150 mM NaCl, 100 mM Tris-HCl pH 7.4. Biotin was detected with avidin-rhodamine (Roche) 1:500 in blocking solution for 45 min. Finally, the cells were washed three times 10 min (200 mM Tris-HCl pH 7.4, 1.5 M NaCl and 0.05% Tween-20), mounted with mowiol supplemented with DABCO and examined by confocal laser scanning microscopy.

3. Results

3.1. General profile of B19V infection in UT7/Epo cells

UT7/Epo cells have been used extensively to study B19V infection. However, intracellular factors restrict severely the infection of B19V in these and other cells, resulting in the production of

none or few infectious progeny (Pallier et al., 1997; Brunstein et al., 2000; Gallinella et al., 2000; Guan et al., 2008). In order to better identify which steps of the infection are deficient, different parameters of B19V infection in UT7/Epo cells have been analyzed. Analysis of the expression profile of B19V receptor and co-receptors over a period of six weeks showed a high and stable expression of Gb4Cer and CD49e along the specified period. In contrast, expression of Ku80, which may have a similar role to Gb4Cer in certain cells (Munakata et al., 2005), was not significant (Fig. 1A). IF microscopy examination of infected cells confirmed that B19V can attach and internalize cells, adopting the typical intracellular distribution around the microtubule organizing center (MTOC) observed in other parvovirus infections (Fig. 1B). The kinetics of viral transcription and replication were analyzed quantitatively. The synthesis of viral RNA (NS1 mRNA) was already detectable by 3 h p.i. and reached a plateau by 24 h p.i. (Fig. 1C). Viral replication started later and reached a plateau by the third day p.i. (Fig. 1D). Expression of viral proteins became detectable after 24 h and reached a plateau after 2 days (Fig. 1E). Immunoprecipitation at 3 days p.i. with an antibody against intact viral particles (mAb 860-55D) (Gigler et al., 1999) demonstrated that virus assembly occurred and that a significant amount of capsid progeny was produced (Fig. 1F). Quantitative determination of the viral DNA from the immunoprecipitated capsids revealed that the virus progeny was essentially empty (Fig. 1G). Mature virion progeny was not either detected in the supernatant of the infected cells (Fig. 1H). These results together indicate that despite the substantial amount of capsid progeny produced, deficiencies in genome packaging and capsid egress limit the progression of B19V infection in UT7/Epo cells.

3.2. B19V infection of UT7/Epo cells, under normoxia or hypoxia, generates mostly empty capsids

Infected cells were collected at progressive days, washed and lysed. Viral particles were immunoprecipitated from the cell lysate with the antibody 860-55D, against assembled capsids. The results confirmed that under hypoxic conditions, the capsid progeny was more abundant but also appeared earlier (after 48 h p.i. under normoxia and after 24 h p.i. under hypoxia) (Fig. 2A and B). These results confirmed previous observations indicating that hypoxia enhances B19V infection (Cailliet-Fauquet et al., 2004b; Pillet et al., 2004; Chen et al., 2011). The virus progeny generated under hypoxic or normoxic conditions was further characterized. The amount of viral genomes in the immunoprecipitated viral particles from the experiment shown in Fig. 2A and B was analyzed quantitatively. The results revealed that independently of the oxygen environment, a limited number of progeny capsids (<1% of the reference control) contained the viral DNA (Fig. 2C and D). Quantitation of the viral DNA in the supernatant of the infected cells showed no increase over the background signal (day 0 p.i.) under normoxia and modestly under hypoxic conditions (Fig. 2E and F). Capsid proteins in the supernatant were undetectable by IP and Western blot (data not shown). These results indicate that although hypoxic conditions result in the acceleration of the infection and an augmented capsid production, the improvement of the genome encapsidation step was not significant.

3.3. Hypoxia enhances significantly the transfection efficiency, however genome packaging and egress remained restricted

In a control transfection experiment in UT7/Epo cells, the oxygen level did not influence the transfection efficiency with a control plasmid expressing green fluorescent protein (GFP) (Fig. 3A). However, the transfection efficiency increased drastically under hypoxic conditions with an infectious clone of B19V (pB19-M20)

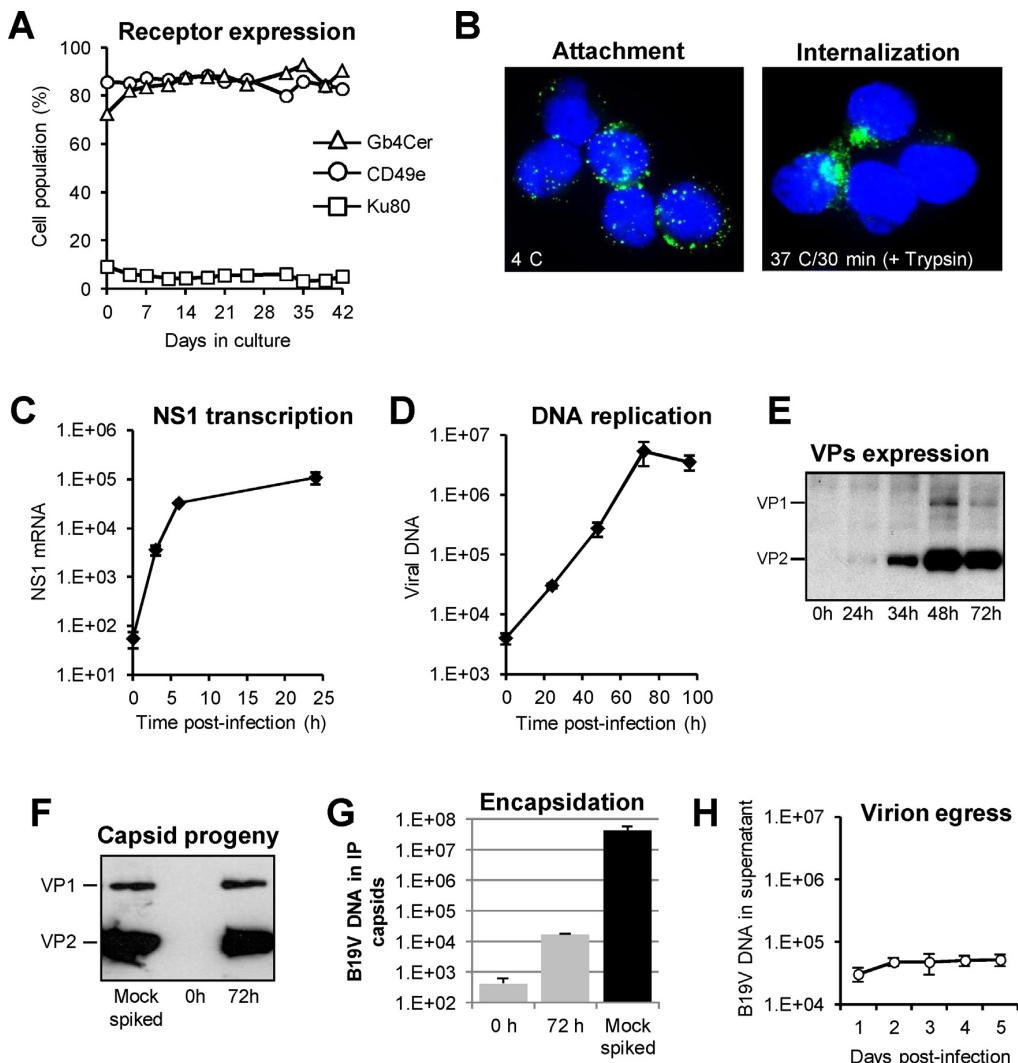


Fig. 1. Characterization of B19V infection in UT7/Epo cells. (A) Expression of B19V-related receptors in UT7/Epo cells. The presence of B19V receptors and co-receptors on the cell surface of UT7/Epo cells was quantitatively analyzed by flow cytometry during a period of 6 weeks. (B) Binding and internalization of B19V in UT7/Epo cells. B19V was added to the cells at 4 °C for 2 h, washed, fixed and stained with an antibody against intact capsids. For internalization, the cells were further incubated for 30 min at 37 °C, washed and trypsinized to remove uninternalized particles. (C) Kinetics of NS1 mRNA synthesis in infected cells. At increasing times p.i., total mRNA was isolated and NS1 mRNA quantified. Samples taken 10 min p.i. served as background controls. (D) Kinetics of viral DNA replication. At increasing times p.i., total DNA was isolated and viral DNA quantified. Samples taken prior to virus internalization served as background controls. (E) Kinetics of B19V capsid proteins expression. (F) Production of assembled capsid progeny in UT7/Epo cells. B19V capsids were immunoprecipitated from cell extracts with mAb 860-55D against intact capsids. As a reference control, B19V (4×10^{10}) was added to mock-infected cell extracts. (G) B19V capsids were immunoprecipitated and B19V DNA was quantified. As a reference control, B19V (4×10^{10} virions) was added to mock-infected cell extracts. (H) Quantitation of virus egress. B19V DNA was quantified from the supernatant of the infected cells.

(Fig. 3B). Immunoprecipitation experiments confirmed that assembled capsids were generated (Fig. 3C) and similarly to the infection experiments, progeny capsids were slightly more abundant and appeared earlier under hypoxic conditions.

As shown in Fig. 3D, at progressive times p.t. no viral DNA above the input signal was detected in the immunoprecipitated capsids. Additionally, virions were not detectable in the supernatant of the transfected cells (Fig. 3E).

3.4. Chloroquine enhances B19V infection in UT7/Epo cells but has no influence in genome encapsidation and egress

It has been shown previously that chloroquine (CQ) enhances B19V infection. In the presence of CQ, an increased production of

viral DNA, RNA and proteins was observed and the infection was accelerated (Bönsch et al., 2010b). The production of mature virions in CQ-treated UT7/Epo cells was examined. The results confirmed, that in the presence of CQ, an increased amount of assembled capsids was produced (Fig. 4A). However, similar to untreated cells, most of the progeny capsids remained empty (Fig. 4B). Viral DNA or capsid proteins were not detected in the supernatant of infected cells (data not shown).

3.5. B19V infection is enhanced in CD36+ EPCs, in particular under hypoxia, but genome encapsidation remains restricted

Immunofluorescence microscopy examination of infected primary CD36+ EPCs confirmed that B19V can attach and internalize

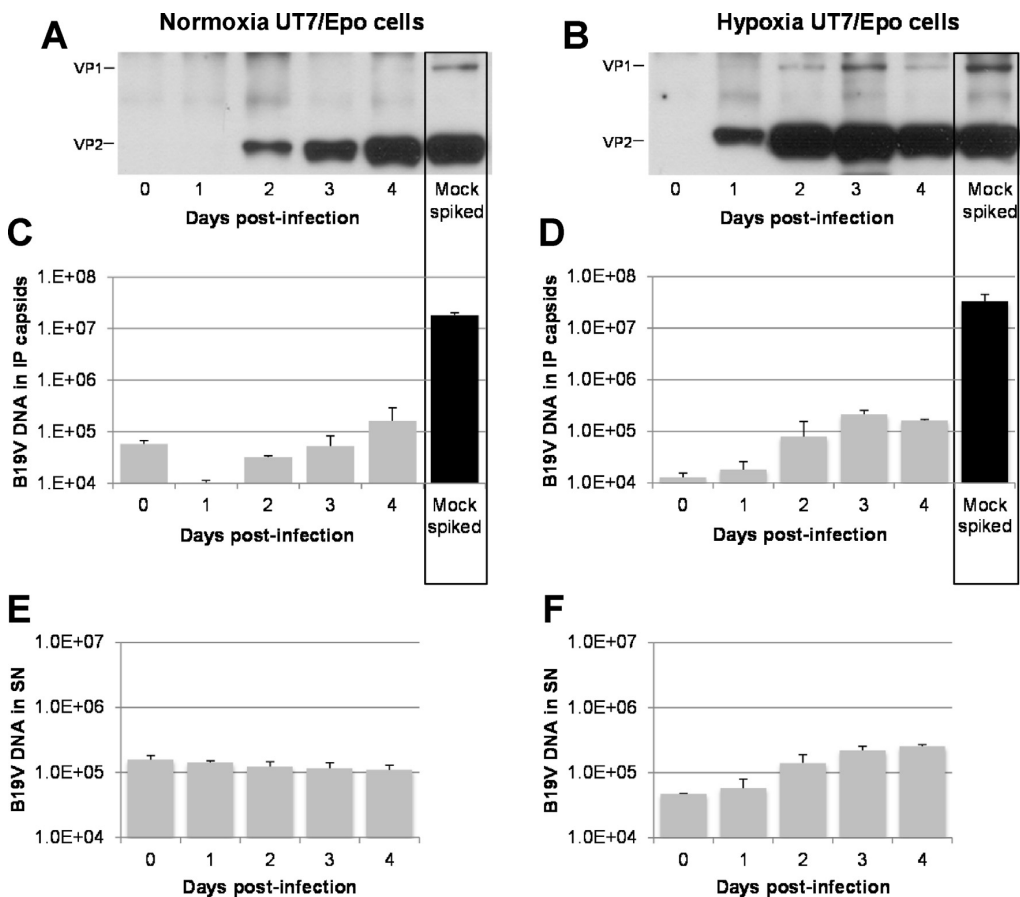


Fig. 2. Capsid progeny and quantitation of virions in UT7/Epo cells. Cells (3×10^5) were infected with B19V under normoxia or hypoxia. At progressive times p.i., the supernatant was collected and the cells were lysed. (A and B) B19V capsids were immunoprecipitated from the cell extracts with mAb 860-55D. As a reference control, B19V (4×10^{10}) was added to mock-infected cell extracts. (C and D) B19V DNA was quantified from the immunoprecipitated capsids. As a reference control, B19V (4×10^{10} virions) was added to mock-infected cell extracts. (E and F) B19V DNA was quantified from the supernatant of the infected cells. Data are the mean \pm SD of two independent experiments.

EPCs without noticeable differences to UT7/Epo cells or between normoxic and hypoxic conditions (Fig. 5A). However, the oxygen environment had an important influence in the number of cells infected by B19V. By 2 days p.i., the number of UT7/Epo cells with detectable capsid progeny was 1–5% and 15–20% under normoxia and hypoxia, respectively. In CD36+ EPCs, the number of infected cells increased to approximately 25% under normoxia and above 70% under hypoxic conditions (Fig. 5B).

Immunoprecipitation experiments with the antibody 860-55D (against intact capsids) at progressive days p.i. showed, that regardless the oxygen conditions, progeny capsids appeared earlier in CD36+ EPCs than in UT7/Epo cells. While in UT7/Epo cells, capsid progeny production reached a plateau on day 4 under normoxia and on day 2–3 under hypoxia, in CD36+ EPCs, maximal capsid progeny was observed already after 24 h p.i. (compare Fig. 6A and B and Fig. 2A and B). The amount of viral DNA in the immunoprecipitated samples from the experiment shown in Fig. 6A and B was analyzed quantitatively. The results revealed that a limited number of capsids containing the viral DNA were produced after 24 h p.i. and did not increase subsequently (Fig. 6C and D). The presence of viral DNA in the supernatant increased and reached similarly a plateau already after 24 h p.i. (Fig. 6E and F).

Capsid progeny was detectable in the supernatant of infected EPCs, in particular under hypoxic conditions (Fig. 7A and B).

However, quantitation of their DNA content and comparison with the reference control revealed that only a modest proportion of the particles represented mature infectious virions (Fig. 7C and D). The IP of capsid-associated DNA increased and reached a plateau by 24 h p.i. At this time, the capsid progeny was undetectable under normoxia and hardly detectable under hypoxia (Fig. 7A and B). Therefore, the increase of capsid progeny observed in the following days represented essentially empty particles. These results indicate that despite the augmented and earlier production of virus progeny, the deficient packaging step remains the limiting factor for the propagation of B19V in CD36+ EPCs.

3.6. Intracellular distribution of viral genomes and capsids

The presence and distribution of the viral genomes and capsids in the infected UT7/Epo cells was examined by FISH. In some cells, assembled capsids and viral genomes colocalized within large intranuclear clusters (Fig. 8A, panel i) resembling the nuclear compartments described earlier in AAV, containing non-structural proteins, capsids, and viral genomes and where presumably encapsidation takes place (Hunter and Samulski, 1992; Wistuba et al., 1997). However, in a larger proportion of cells the viral genomes appeared isolated in the nucleus, while the assembled capsids were detected in the cytoplasm (Fig. 8A, panel ii).

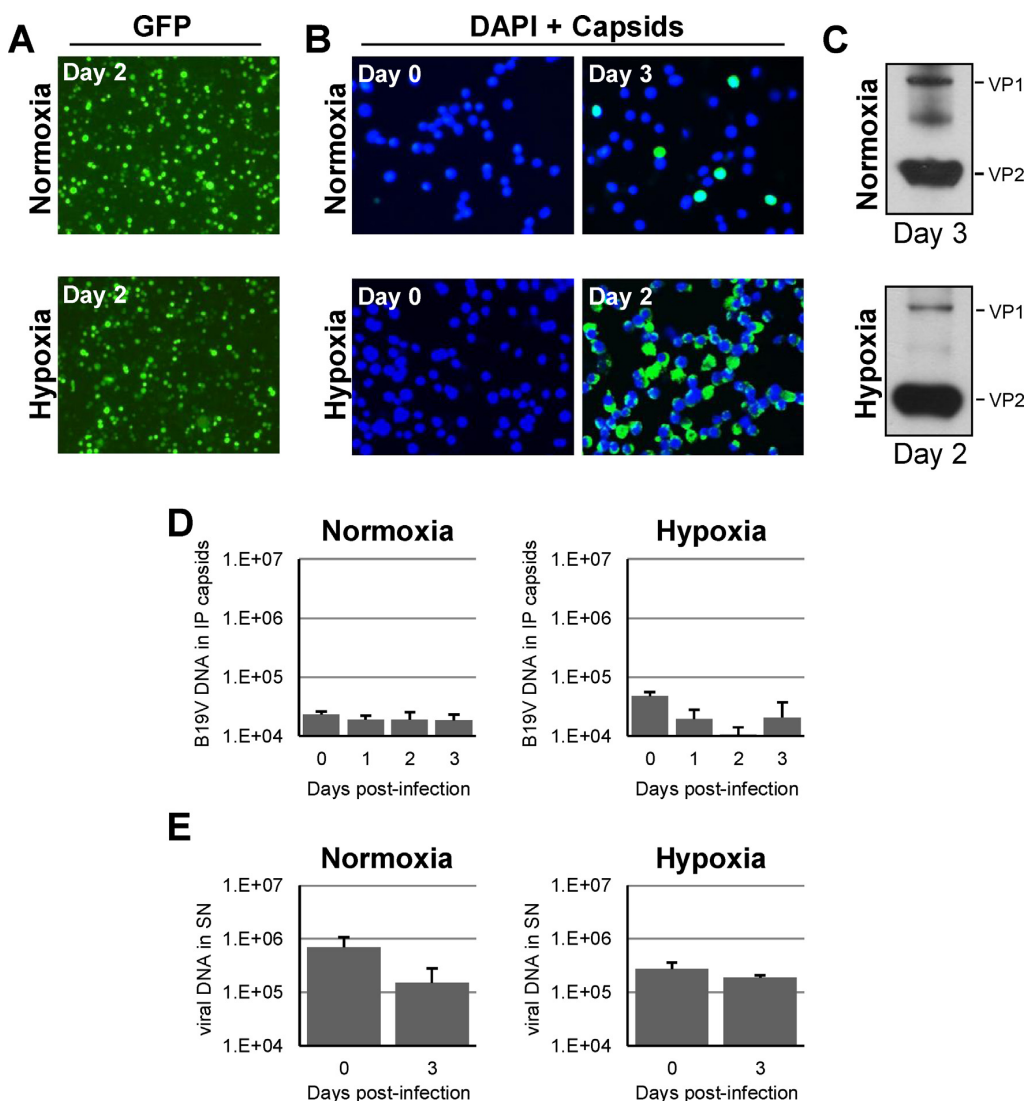


Fig. 3. Transfection of UT7/Epo cells with a B19V infectious clone under normoxia and hypoxia. (A) Transfection of UT7/Epo cells with a control plasmid expressing GFP is not influenced by normoxia or hypoxia. (B) Detection of B19V capsids by IF following transfection with a B19V infectious clone (pB19-M20). (C) Detection of B19V capsids by IP with mAb 860-55D from pB19-M20 transfected cells. (D) At progressive days p.i. B19V capsids were immunoprecipitated from cell lysates and B19V DNA was quantified. (E) B19V DNA was quantified from the supernatant of the infected cells. Data are the mean \pm SD for two independent experiments.

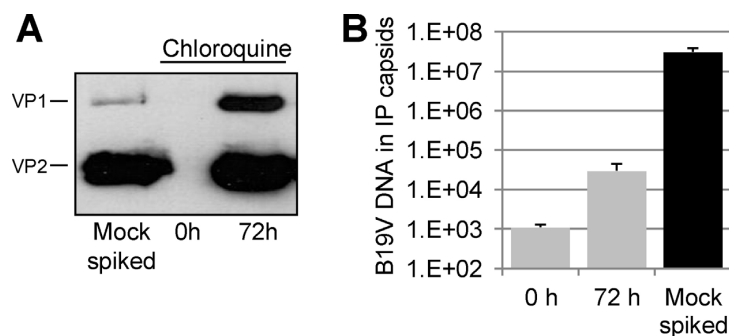


Fig. 4. Effect of chloroquine (CQ) in B19V infection in UT7/Epo cells. (A) Production of capsid progeny in UT7/Epo cells treated with CQ (25 μ M). B19V capsids were immunoprecipitated from the cell extracts with mAb 860-55D. As a reference control, B19V (4×10^{10}) was added to mock-infected cell extracts. The production of capsid progeny in untreated UT7/Epo cells is shown in Fig. 1F. (B) B19V DNA was quantified from the immunoprecipitated capsids. As a reference control, B19V (4×10^{10} virions) was added to mock-infected cell extracts. Data are the mean \pm SD for two independent experiments.

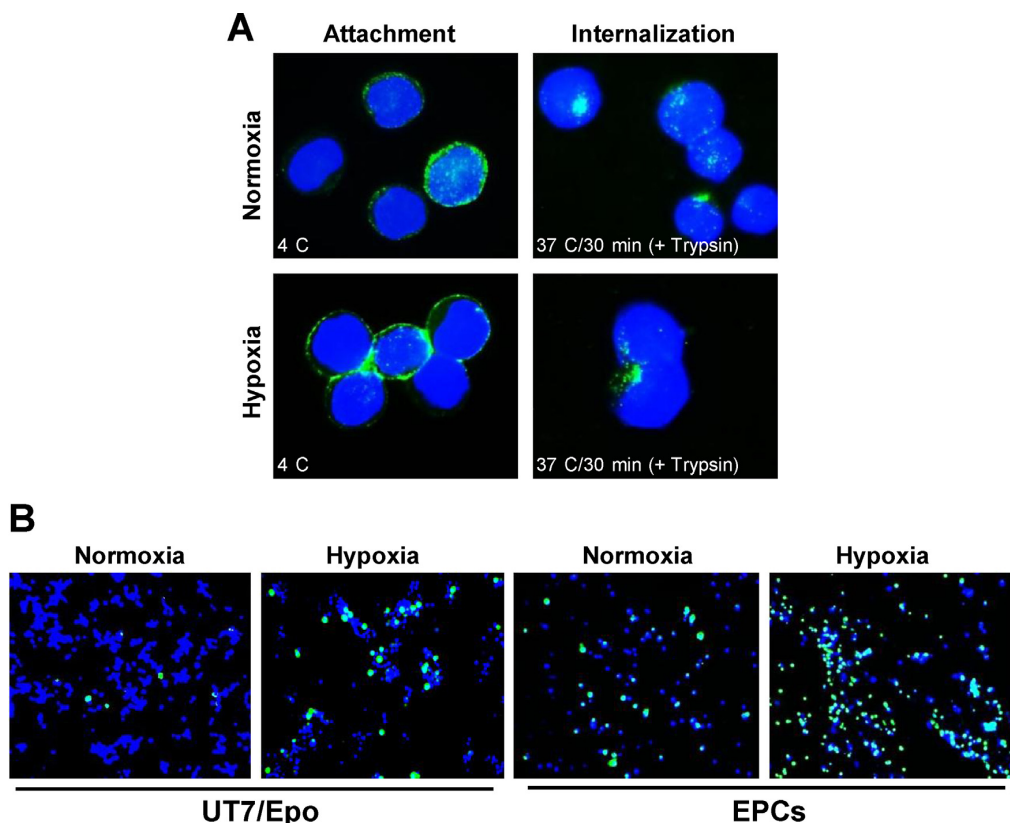


Fig. 5. Attachment, internalization and infection of B19V in EPCs under normoxia and hypoxia. Cells (3×10^5) were infected with B19V under normoxia or hypoxia. (A) Binding and internalization of B19V in EPCs. B19V was added to the cells at 4 °C for 1 h, washed, fixed and stained with an antibody against intact capsids. For internalization, the cells were further incubated for 30 min at 37 °C, washed and trypsinized to remove uninternalized particles. (B) Detection of virus progeny by IF 2 days p.i. in UT7/Epo cells and EPCs cultured under normoxic and hypoxic conditions.

3.7. VP1u conformation in the virus progeny differs from that of wild-type virus

The pores at the fivefold symmetry axis are the portals for the encapsidation of the viral genome but also for the externalization of VP1u. The fivefold cylinder is narrow and constrictions of the channel impair the encapsidation of the viral genome and the externalization of VP1u (Farr and Tattersall, 2004; Bleker et al., 2005, 2006; Plevka et al., 2011). Examination of the VP1u conformation in the mostly empty virus progeny revealed, that differently to the wild-type virus, VP1u was partially exposed. The most N-terminal part was accessible to antibodies, while the C-terminal region remained internal and inaccessible (Fig. 8B and C). Similar to other parvoviruses (Cotmore et al., 1999; Viihinen-Ranta et al., 2002), exposure to mild temperature triggers the externalization of the N-terminal and C-terminal regions of VP1u from B19V without capsid disassembly (Ros et al., 2006). In clear contrast to the wild-type virus, heat treatment did not trigger the externalization of the C-terminal region of VP1u from the capsid progeny generated under normoxia and only discretely from capsids generated under hypoxia (Fig. 8D). Therefore, the failure to encapsidate the viral genome is possibly due to the constriction of the fivefold axis channel by a partially exposed and inflexible VP1u.

4. Discussion

Discovered in 1975 (Cossart et al., 1975), today B19V is recognized as a major human pathogen involved in multiple syndromes.

However, the lack of a suitable cell culture system or an animal model restricts the availability of infectious virus and hampers seriously the studies with B19V. The virus has an extraordinary tropism for human erythroid progenitor cells (EPCs) in the bone marrow (Mortimer et al., 1983) where it can infect cells at the BFU-E and CFU-E stages of differentiation (Takahashi et al., 1990). During a natural infection B19V is able to replicate efficiently in the target cells, as judged by the typical high viremia observed in the infected individuals. However, the efficient B19V replication *in vivo* has not yet been mimicked *in vitro* with an established cell line, indicating the existence of highly restricted and still poorly understood cellular factors required for B19V replication. Some erythroleukemia cell lines, such as UT7/Epo (Shimomura et al., 1992) and KU812Ep6 (Miyagawa et al., 1999), have been shown to support B19V replication to a certain level, but none of them can produce significant quantities of infectious progeny. The human megakaryoblastic cell line UT7/Epo, has been shown to be the most permissive system for the *in vitro* replication of B19V (Wong and Brown, 2006) and it is used widely to study B19V infection.

The reason for the defective replication of B19V in these cells has been shown to be multifactorial. Restrictions occur already at the cell surface, by the variable and limited expression of receptors and co-receptors required for binding and internalization of B19V (Brown et al., 1993; Munakata et al., 2005; Weigel-Kelley et al., 2003), but also by required intracellular factors restricted mainly to the erythroid lineage. Those intracellular factors can operate at the level of transcription, controlling the generation of sufficient full-length capsid-encoding transcripts (Guan et al., 2008; Liu et al.,

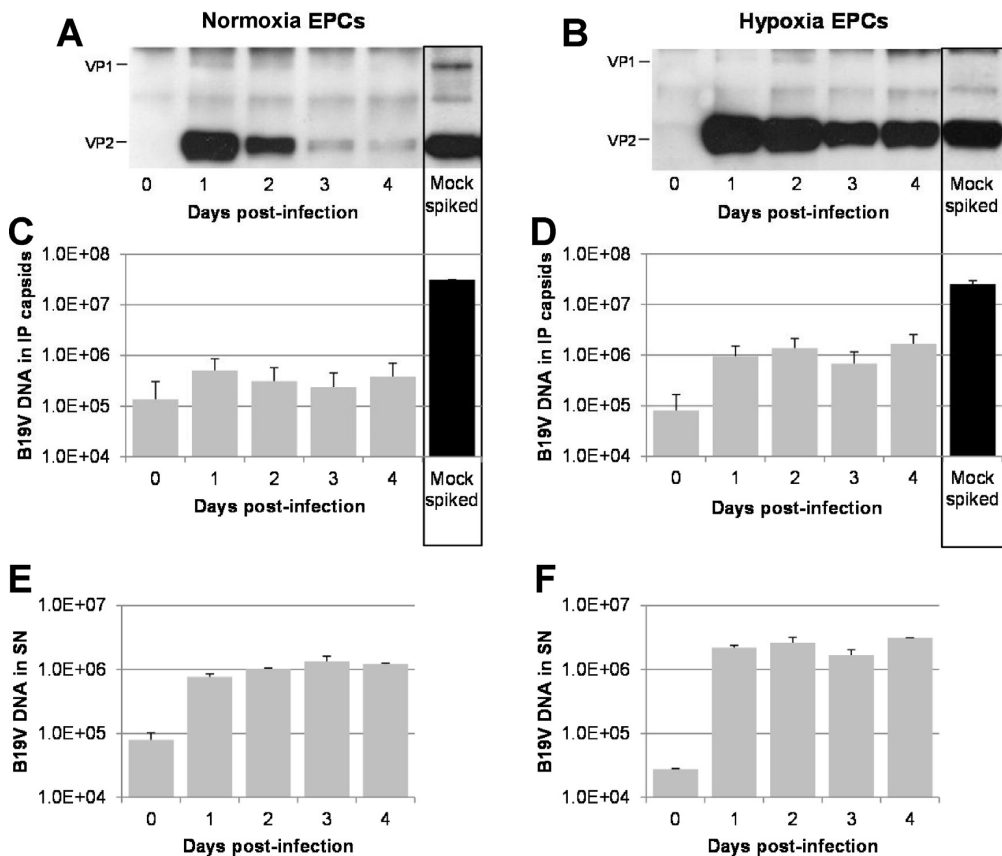


Fig. 6. Capsid progeny and quantitation of virions in EPCs. Cells (3×10^5) were infected with B19V under normoxia or hypoxia. At progressive times p.i., the supernatant was collected and the cells were lysed. (A and B) B19V capsids were immunoprecipitated from the cell extracts with mAb 860-55D, against intact capsids. As a reference control, B19V (4×10^{10}) was added to mock-infected cell extracts. (C and D) B19V DNA was quantified from the immunoprecipitated capsids. As a reference control, B19V (4×10^{10} virions) was added to mock-infected cell extracts. (E and F) B19V DNA was quantified from the supernatant of the infected cells. Data are the mean \pm SD of two independent experiments.

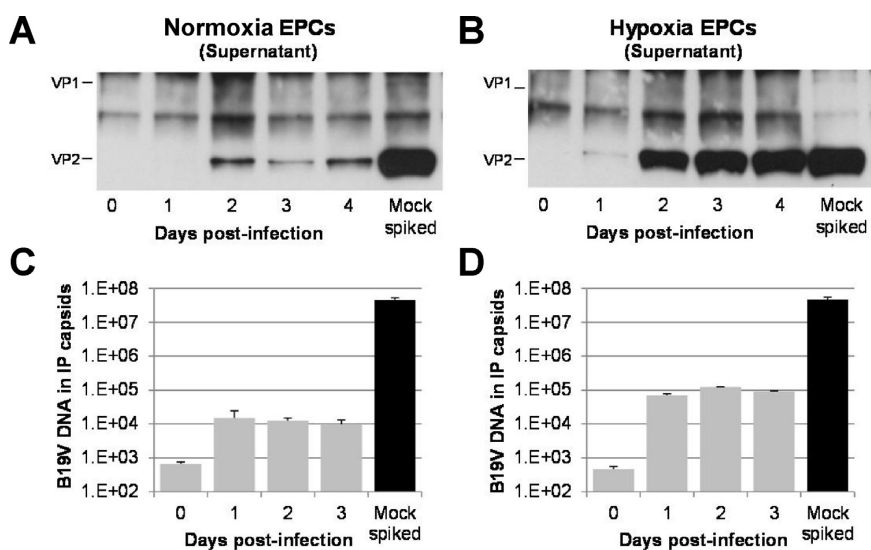


Fig. 7. Virus egress in EPCs. Cells (3×10^5) were infected with B19V under normoxia or hypoxia. (A and B) At progressive times p.i., B19V capsids were immunoprecipitated from the cell supernatant with mAb 860-55D. As a reference control, B19V (4×10^{10}) was added to mock-infected cell supernatant. (C and D) B19V capsids were immunoprecipitated and B19V DNA was quantified. As a reference control, B19V (4×10^{10} virions) was added to mock-infected cell supernatant. Data are the mean \pm SD of two independent experiments.

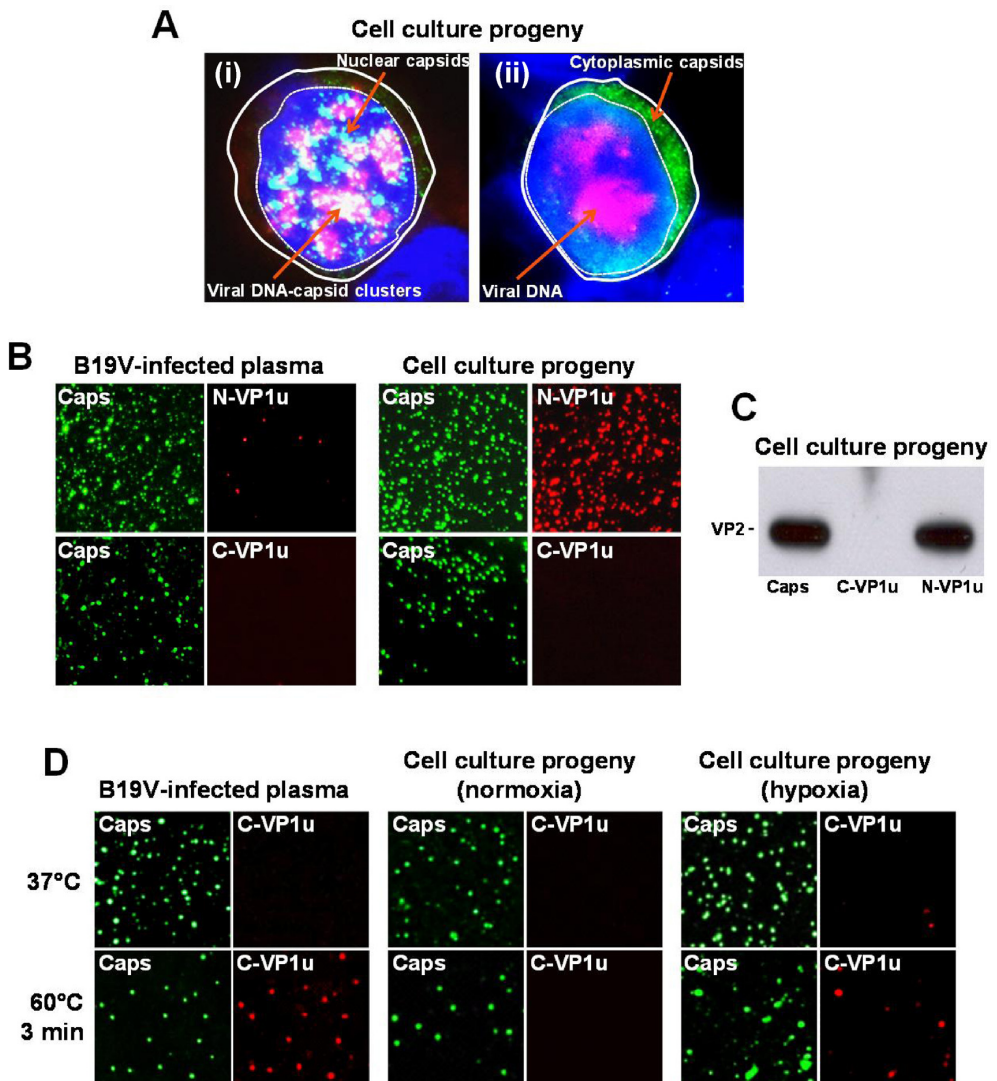


Fig. 8. Intracellular distribution of capsids and viral genomes and VP1u conformation in the capsid progeny. (A) Simultaneous detection of viral genomes and capsids in infected UT7Epo cells by FISH. Two representative cells are shown. (i) In some cells, B19V genomes and capsids were detectable in large clusters in the nucleus. (ii) In a larger proportion of cells, viral genomes were detected isolated in the nucleus while capsids were detected in the cytoplasm. (B) VP1u conformation in the plasma-derived virus differs from that of the cell culture progeny (UT7/Epo cells). Plasma-derived virus and cell culture progeny were concentrated by sucrose cushion centrifugation, spotted onto coverslips, fixed and detected by IF with mAb 860-55D or mAb 521-5D (Caps) and antibodies against the N-terminal and C-terminal regions of VP1u. (C) Immunoprecipitation of the cell culture progeny (UT7/Epo cells, 3 days p.i.) with mAb 860-55D (Capsids) and antibodies against the N-terminus and C-terminus of VP1u. (D) Flexibility of VP1u in the plasma-derived virus and cell culture progeny obtained under normoxia or hypoxia. Viruses were untreated (37 °C) or heat-treated (60 °C for 3 min) to trigger the exposure of VP1u and detected by IF with the indicated antibodies.

1992). In non-permissive cells the majority of viral mRNAs encode for NS1, with only limited production of the capsid-encoding transcripts. NS1 causes cell death by its cytotoxic or apoptotic characteristics (Moffatt et al., 1998). In contrast, more B19V RNAs are read through the multiple polyadenylation sites in permissive cells, which results in sufficient full-length capsid-encoding mRNAs (Liu et al., 1992). Studies have also shown that B19V replication and transcription were restricted to a small subset of cells but without production of capsid proteins, while in other cells, the single-stranded viral DNA was not converted to the double-stranded form (Gallinella et al., 2000). All the described restrictions at early (receptor/co-receptor) and late (replication/transcription) stages of the infection result in none or limited production of virus progeny.

Recently, two novel approaches based on hypoxic conditions (Caillet-Fauquet et al., 2004b; Pillet et al., 2004) and the use of *ex vivo* expanded CD36+ primary human erythroid progenitor cells (CD36+ EPCs), previous CD34+ *in vitro* preselection (Pillet et al., 2008; Wong et al., 2008), or directly from unselected peripheral blood mononuclear cells (Filippone et al., 2010), have been shown to improve B19V infection. The obtained results are in agreement with previous observations, which showed that B19V replicates better in CD36+ EPCs, in particular under hypoxia (Chen et al., 2011). However, despite these improvements, the final genome encapsidation step was still insufficient, producing abundant but mostly non-infectious empty capsids. In the study by Chen et al. (2011), the use of EPCs under hypoxia was shown to improve B19V infection, however large quantities of infectious virus were not

recovered from the supernatant of the infected cells, as it should be expected for a lytic virus. Therefore, CD36+ EPCs cannot yet be considered as a highly permissive cell culture system to propagate B19V and a robust source of infectious virus. Moreover, compared to UT7/Epo cells, the generation of primary CD36+ EPCs remains time-consuming, requires large quantities of expensive growth factors and the permissivity to B19V is limited within a narrow and variable time-frame when B19V receptor and co-receptors are expressed in concert with a favorable intracellular microenvironment (Wong et al., 2008).

Parvoviruses pack their single-stranded, linear DNA genome into the pre-assembled capsids in the nucleus (Cotmore and Tattersall, 2005; King et al., 2001; Timpe et al., 2005). The helicase activity of the parvovirus nonstructural protein, which is present in the encapsidation complexes, functions as a molecular motor to translocate the viral genome into the empty capsid through the fivefold symmetry axes pore, a process that is also mediated by the terminal telomeric structures of the viral genome (Cotmore and Tattersall, 2005; King et al., 2001). Besides genome encapsidation, the channels at the fivefold symmetry axis are also used for the externalization of VP1u during the infection process (Bleker et al., 2005, 2006; Cotmore and Tattersall, 2012; Farr and Tattersall, 2004; Plevka et al., 2011). The channel is narrow and minor modifications of its diameter result in defective genome encapsidation and VP1u externalization (Bleker et al., 2005; Cotmore and Tattersall, 2012). Therefore, specific capsid and genome conformations play a critical role in the packaging step. VP1u from parvoviruses is not accessible, but can become exposed *in vitro* by mild heat or low pH treatments and *in vivo* during the intracellular trafficking of the virus (Cotmore et al., 1999; Kronenberg et al., 2005; Mani et al., 2006; Ros et al., 2006; Viñinen-Ranta et al., 2002) or upon receptor binding in the case of B19V (Bönsch et al., 2010a). In clear contrast to natural plasma-derived virus, VP1u was exposed partially in the capsid progeny. While the most N-terminal region was externalized and accessible to antibodies, the C-terminal region remained internal (Fig. 8). This particular conformation was irreversible and did not change upon heat treatment. The aberrant conformation and rigidity of VP1u might explain the encapsidation failure in semi-permissive cell systems. Further studies will elucidate whether the VP1u conformation in the virus progeny is due to an aberrant assembly or the lack of a final maturation step.

5. Conclusions

When compared to UT7/Epo cells and normoxia, hypoxic conditions or the use of CD36+ EPCs resulted in a significant acceleration of the infection/transfection, an increase in the number of infected cells and a modest increase in the yield of capsid progeny. However, despite these improvements, genome encapsidation was impaired seriously under all tested conditions and cells. The fivefold axes channel might be constricted in the virus progeny by the atypical partial exposure of VP1u hindering the packaging step, which arises as a major limiting factor for the *in vitro* propagation of B19V.

Acknowledgments

We are grateful to M. Bärtschi for performing the flow cytometry assay and S. Bieli for the technical assistance in the fluorescence *in situ* DNA hybridization experiments.

References

- Bleker, S., Pawlita, M., Kleinschmidt, J.A., 2006. Impact of capsid conformation and Rep-capsid interactions on adeno-associated virus type 2 genome packaging. *J. Virol.* 80, 810–820.
- Bleker, S., Sonntag, F., Kleinschmidt, J.A., 2005. Mutational analysis of narrow pores at the fivefold symmetry axes of adeno-associated virus type 2 capsids reveals a dual role in genome packaging and activation of phospholipase A2 activity. *J. Virol.* 79, 2528–2540.
- Bönsch, C., Zuercher, C., Lieby, P., Kempf, C., Ros, C., 2010a. The globoside receptor triggers structural changes in the B19 virus capsid that facilitate virus internalization. *J. Virol.* 84, 11737–11746.
- Bönsch, C., Kempf, C., Mueller, I., Manning, L., Laman, M., Davis, T.M., Ros, C., 2010b. Chloroquine and its derivatives exacerbate B19V-associated anemia by promoting viral replication. *PLoS Negl. Trop. Dis.* 4 (4), e669.
- Bönsch, C., Kempf, C., Ros, C., 2008. Interaction of parvovirus B19 with human erythrocytes alters virus structure and cell membrane integrity. *J. Virol.* 82, 11784–11791.
- Bonvicini, F., Filippone, C., Manaresi, E., Zerbini, M., Musiani, M., Gallinella, G., 2008. HepG2 hepatocellular carcinoma cells are a non-permissive system for B19 virus infection. *J. Gen. Virol.* 89, 3034–3038.
- Brown, K.E., Anderson, S.M., Young, N.S., 1993. Erythrocyte P antigen: cellular receptor for B19 parvovirus. *Science* 262, 114–117.
- Brunstein, J., Söderlund-Venermo, M., Hedman, K., 2000. Identification of a novel RNA splicing pattern as a basis of restricted cell tropism of erythrovirus B19. *Virology* 274, 284–291.
- Caillet-Fauquet, P., Di Giambattista, M., Draps, M.L., Hougardy, V., de Launoit, Y., Laub, R., 2004a. An assay for parvovirus B19 neutralizing antibodies based on human hepatocarcinoma cell lines. *Transfusion* 44, 1340–1343.
- Caillet-Fauquet, P., Draps, M.L., Di Giambattista, M., de Launoit, Y., Laub, R., 2004b. Hypoxia enables B19 erythrovirus to yield abundant infectious progeny in a pluripotent erythroid cell line. *J. Virol. Methods* 121, 145–153.
- Chen, A.Y., Kleiboecker, S., Qiu, J., 2011. Productive parvovirus B19 infection of primary human erythroid progenitor cells at hypoxia is regulated by STAT5A and MEK signaling but not HIF α . *PLoS Pathog.* 7 (6), e1002088.
- Chen, A.Y., Guan, W., Lou, S., Liu, Z., Kleiboecker, S., Qiu, J., 2010. Role of erythropoietin receptor signaling in parvovirus B19 replication in human erythroid progenitor cells. *J. Virol.* 84, 12385–12396.
- Cossart, Y.E., Field, A.M., Cant, B., Widdows, D., 1975. Parvovirus-like particles in human sera. *Lancet* 1, 72–73.
- Cotmore, S.F., Tattersall, P., 2012. Mutations at the base of the icosahedral five-fold cylinders of minute virus of mice induce 3'-to-5' genome uncoating and critically impair entry functions. *J. Virol.* 86, 69–80.
- Cotmore, S.F., Tattersall, P., 2005. Encapsulation of minute virus of mice DNA: aspects of the translocation mechanism revealed by the structure of partially packaged genomes. *Virology* 336, 100–112.
- Cotmore, S.F., D'abramo Jr., A.M., Ticknor, C.M., Tattersall, P., 1999. Controlled conformational transitions in the MVM virion expose the VP1 N-terminus and viral genome without particle disassembly. *Virology* 254, 169–181.
- Farr, G.A., Tattersall, P., 2004. A conserved leucine that constricts the pore through the capsid fivefold cylinder plays a central role in parvoviral infection. *Virology* 323, 243–256.
- Filippone, C., Franssila, R., Kumar, A., Saikko, L., Kovanen, P.E., Söderlund-Venermo, M., Hedman, K., 2010. Erythroid progenitor cells expanded from peripheral blood without mobilization or preselection: molecular characteristics and functional competence. *PLoS One* 5 (3), e9496.
- Gallinella, G., Manaresi, E., Zuffi, E., Venturoli, S., Bonsi, L., Bagnara, G.P., Musiani, M., Zerbini, M., 2000. Different patterns of restriction to B19 parvovirus replication in human blast cell lines. *Virology* 278, 361–367.
- Gigler, A., Dorsch, S., Hernauer, A., Williams, C., Kim, S., Young, N.S., Zolla-Pazner, S., Wolf, H., Gorni, M.K., Modrow, S., 1999. Generation of neutralizing human monoclonal antibodies against parvovirus B19 proteins. *J. Virol.* 73, 1974–1979.
- Guan, W., Cheng, F., Yoto, Y., Kleiboecker, S., Wong, S., Zhi, N., Pintel, D.J., Qiu, J., 2008. Block to the production of full-length B19 virus transcripts by internal polyadenylation is overcome by replication of the viral genome. *J. Virol.* 82, 9951–9963.
- Heegaard, E.D., Brown, K.E., 2002. Human parvovirus B19. *Clin. Microbiol. Rev.* 15, 485–505.
- Heegaard, E.D., Hornsleth, A., 1995. Parvovirus: the expanding spectrum of disease. *Acta Paediatr.* 84, 109–117.
- Hunter, L.A., Samulski, R.J., 1992. Colocalization of adeno-associated virus Rep and capsid proteins in the nuclei of infected cells. *J. Virol.* 66, 317–324.
- King, J.A., Dubielzig, R., Grimm, D., Kleinschmidt, J.A., 2001. DNA helicase-mediated packaging of adeno-associated virus type 2 genomes into preformed capsids. *EMBO J.* 20, 3282–3291.
- Kooistra, K., Mesman, H.J., de Waal, M., Koppelman, M.H., Zaaijer, H.L., 2011. Epidemiology of high-level parvovirus B19 viraemia among Dutch blood donors, 2003–2009. *Vox Sang.* 100, 261–266.
- Kronenberg, S., Bottcher, B., von der Lieth, C.W., Bleker, S., Kleinschmidt, J.A., 2005. A conformational change in the adeno-associated virus type 2 capsid leads to the exposure of hidden VP1N termini. *J. Virol.* 79, 5296–5303.
- Liu, J.M., Green, S.W., Shimada, T., Young, N.S., 1992. A block in full-length transcript maturation in cells nonpermissive for B19 parvovirus. *J. Virol.* 66, 4686–4692.

- Luo, Y., Lou, S., Deng, X., Liu, Z., Li, Y., Kleiboecker, S., Qiu, J., 2011. Parvovirus B19 infection of human primary erythroid progenitor cells triggers ATR-Chk1 signaling, which promotes B19 virus replication. *J. Virol.* 85, 8046–8055.
- Mani, B., Baltzer, C., Valle, N., Almendral, J.M., Kempf, C., Ros, C., 2006. Low pH-dependent endosomal processing of the incoming parvovirus minute virus of mice virion leads to externalization of the VP1 N-terminal sequence (N-VP1), N-VP2 cleavage, and uncoating of the full-length genome. *J. Virol.* 80, 1015–1024.
- Miyagawa, E., Yoshida, T., Takahashi, H., Yamaguchi, K., Nagano, T., Kiriyama, Y., Okochi, K., Sato, H., 1999. Infection of the erythroid cell line, KU812Ep6 with human parvovirus B19 and its application to titration of B19 infectivity. *J. Virol. Methods* 83, 45–54.
- Moffatt, S., Yaegashi, N., Tada, K., Tanaka, N., Sugamura, K., 1998. Human parvovirus B19 nonstructural (NS1) protein induces apoptosis in erythroid lineage cells. *J. Virol.* 72, 3018–3028.
- Mortimer, P.P., Humphries, R.K., Moore, J.G., Purcell, R.H., Young, N.S., 1983. A human parvovirus-like virus inhibits haematopoietic colony formation in vitro. *Nature* 302, 426–429.
- Munakata, Y., Saito-Ito, T., Kumura-Ishii, K., Huang, J., Kodera, T., Ishii, T., Hirabayashi, Y., Koyanagi, Y., Sasaki, T., 2005. Ku80 autoantigen as a cellular coreceptor for human parvovirus B19 infection. *Blood* 106, 3449–3456.
- Ozawa, K., Kurtzman, G., Young, N., 1987. Productive infection by B19 parvovirus of human erythroid bone marrow cells in vitro. *Blood* 70, 384–391.
- Ozawa, K., Kurtzman, G., Young, N., 1986. Replication of the B19 parvovirus in human bone marrow cell cultures. *Science* 233, 883–886.
- Pallier, C., Greco, A., Le Junter, J., Saib, A., Vassias, I., Morinet, F., 1997. The 3' untranslated region of the B19 parvovirus capsid protein mRNAs inhibits its own mRNA translation in nonpermissive cells. *J. Virol.* 71, 9482–9489.
- Pillet, S., Fichelson, S., Morinet, F., Young, N.S., Zhi, N., Wong, S., 2008. Human B19 erythrovirus in vitro replication: what's new? *J. Virol.* 82, 8951–8953.
- Pillet, S., Le Guyader, N., Hofer, T., NguyenKhac, F., Koken, M., Aubin, J.T., Fichelson, S., Gassmann, M., Morinet, F., 2004. Hypoxia enhances human B19 erythrovirus gene expression in primary erythroid cells. *Virology* 327, 1–7.
- Plevka, P., Hafenstein, S., Li, L., D'Abregamo Jr., A., Cotmore, S.F., Rossman, M.G., Tattersall, P., 2011. Structure of a packaging-defective mutant of minute virus of mice indicates that the genome is packaged via a pore at a 5-fold axis. *J. Virol.* 85, 4822–4827.
- Ros, C., Gerber, M., Kempf, C., 2006. Conformational changes in the VP1-unique region of native human parvovirus B19 lead to exposure of internal sequences that play a role in virus neutralization and infectivity. *J. Virol.* 80, 12017–12024.
- Servey, J.T., Reamy, B.V., Hodge, J., 2007. Clinical presentations of parvovirus B19 infection. *Am. Fam. Physician* 75, 373–376.
- Shimomura, S., Komatsu, N., Frickhofen, N., Anderson, S., Kajigaya, S., Young, N.S., 1992. First continuous propagation of B19 parvovirus in a cell line. *Blood* 79, 18–24.
- Takahashi, T., Ozawa, K., Takahashi, K., Asano, S., Takaku, F., 1990. Susceptibility of human erythropoietic cells to B19 parvovirus in vitro increases with differentiation. *Blood* 75, 603–610.
- Timpe, J., Bevington, J., Casper, J., Dignam, J.D., Trempe, J.P., 2005. Mechanisms of adeno-associated virus genome encapsidation. *Curr. Gene Ther.* 5, 273–284.
- Vihinen-Ranta, M., Wang, D., Weichert, W.S., Parrish, C.R., 2002. The VP1 N-terminal sequence of canine parvovirus affects nuclear transport of capsids and efficient cell infection. *J. Virol.* 76, 1884–1891.
- Weigel-Kelley, K.A., Yoder, M.C., Srivastava, A., 2003. Alpha5beta1 integrin as a cellular coreceptor for human parvovirus B19: requirement of functional activation of beta1 integrin for viral entry. *Blood* 102, 3927–3933.
- Wistuba, A., Kern, A., Weger, S., Grimm, D., Kleinschmidt, J.A., 1997. Subcellular compartmentalization of adeno-associated virus type 2 assembly. *J. Virol.* 71, 1341–1352.
- Wong, S., Zhi, N., Filippone, C., Keyvanfar, K., Kajigaya, S., Brown, K.E., Young, N.S., 2008. Ex vivo-generated CD36+ erythroid progenitors are highly permissive to human parvovirus B19 replication. *J. Virol.* 82, 2470–2476.
- Wong, S., Brown, K.E., 2006. Development of an improved method of detection of infectious parvovirus B19. *J. Clin. Virol.* 35, 407–413.
- Zhi, N., Zádori, Z., Brown, K.E., Tijssen, P., 2004. Construction and sequencing of an infectious clone of the human parvovirus B19. *Virology* 318, 142–152.

Part IV

Results

2. Supplementary Data

2.1. The phosphoserine-rich N-VP2 of MVM facilitates nuclear targeting and contributes to cytotoxicity.

In order to investigate a possible involvement of the distal serine phosphorylations within N-VP2 in MVM egress, we generated a mutant, referred to as 5SG, having the corresponding serine residues substituted by glycine. In Figure S1, p. 86 several aspects of an infection with 5SG, such as cytotoxicity, nuclear targeting, and nuclear export are summarized.

In a WT infection, the cells showed reorganization of the cytoskeleton as early as 20 hpi, resulting in a rounded phenotype of affected cells. At later times, increasing amounts of cells became rounded and partially detached showing apoptotic bodies at 40 hpi, eventually resulting in cell death and cytolysis (see Figure S1 A, 1st row, p. 86). In contrast, 5SG virions were significantly less cytotoxic. Even as late as 40 hpi most of the infected cells still exhibited the typical fibroblastic phenotype and only a few cells became rounded. No signs of apoptosis and cytolysis were observed (see Figure S1 A, 2nd row, p. 86). 5SG was approximately 5× less efficient in replicating viral DNA in the nucleus, indicating that fewer virions reached the nucleus, thus delivering less DNA templates to initiate viral replication. Indeed, the amount of viral DNA in the nuclei of 5SG infected cells was similar to the quantities that were obtained when the cells were infected with 5× less WT virions (see Figure S1 B, p. 86). Nuclear export of 5SG progeny was not significantly affected. Virions were efficiently exported from the nucleus even though showing a slight delay in cytoplasmic accumulation (see Figure S1 C, p. 86). This delay is obviously caused by defects in early steps of infection prior to the initiation of DNA replication, such as binding, endosomal escape, viral uptake, or nuclear targeting.

As observed, productive MVM infection produces a strong cytopathic effect in the host cell, ultimately causing cellular lysis. Such dramatic changes in the cytoskeleton filaments involve gelsolin-mediated degradation of actin fibers resulting in the generation of characteristic “actin-patches” [26]. While the actin filaments become destabilized, the microtubule network is maintained during the course of infection [331]. The latter observation together with the previously reported capsid-dynamin co-localization [26] would be in agreement with a microtubule dependent egress of MVM. The little delay in nuclear targeting and the fewer amount of progeny DNA in the nucleus observed for an infection with 5SG virions (see Figure S1 B, p. 86) cannot explain the

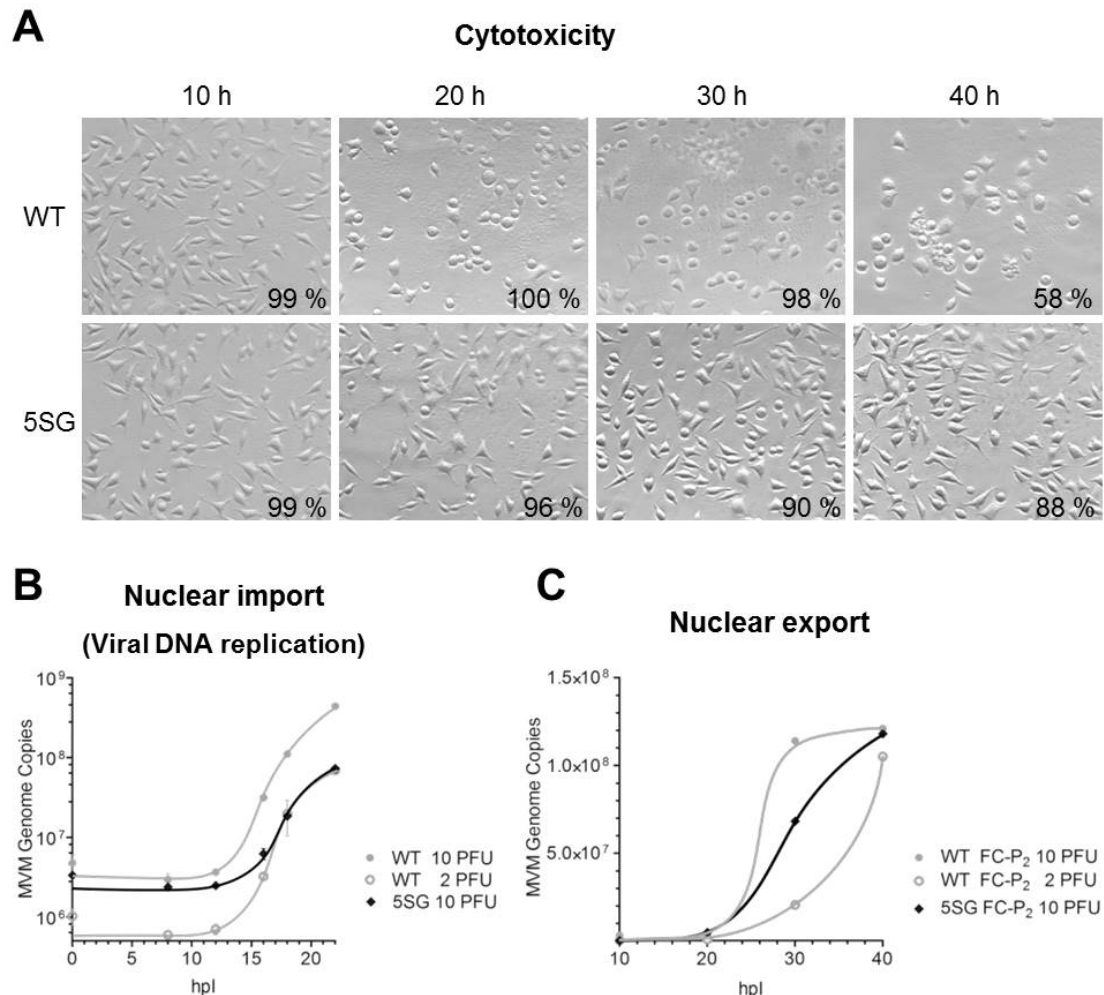


Figure S1.: Kinetics of nuclear export depends on the input virus. (A) A9 cells were infected with WT or 5SG MVM using 10 PFU per cell. Following binding at 4 °C unbound virus was removed by washings. Cells were incubated at 37 °C for the indicated times. Phase contrast pictures of the infected cells were taken using a 20× magnification objective built in a Zeiss Axiovert 35 microscope. Cell viability was assessed via trypan blue exclusion using the TC10™ automated cell counter (BioRad). The average of three independent measurements is indicated. (B) A9 cells (8×10^3) were infected with the indicated PFU of WT or 5SG virus. Following binding at 4 °C unbound viruses were removed. Viral DNA was extracted and quantified at the indicated times post-infection. (C) A9 cells (3×10^6) were infected using the indicated viruses and PFU. Binding was performed at 4 °C. Unbound virus was removed prior to incubation at 37 °C for the indicated times. Cytosolic fractions were isolated and applied for AEX-qPCR. Exported FC-P2 virions were quantified using qPCR. All infections were performed in the presence of α -capsid mAb (B7) and neuraminidase in order to prevent re-infections.

2.1. The phosphoserine-rich N-VP2 of MVM facilitates nuclear targeting and contributes to c87otoxicity.

considerable delay of the cytopathic effect of more than 20 h. N-VP2 is removed by proteolytic digestion during endosomal uptake. Hence, it is not involved in important signaling for replication or progeny morphogenesis. Additionally, it has been demonstrated that there are no significant differences in the cytoplasmic accumulation of WT and 5SG progeny virions (see Figure S1 C, p. 86). Therefore, the phosphorylations on N-VP2, which represent the only difference between the WT and 5SG progeny, are likely involved in late events mediating the rearrangement of the cytoskeleton during egress. 5SG seems to be defective for severing the actin filaments resulting in prolonged maintenance of the cytoskeleton and cell integrity.

Similar observations have been reported by G. E. Tullis *et al.* [458] for a MVM mutation affecting the sequence but not the phosphorylations within N-VP2. Their results suggest that the trypsin-sensitive RVER region is important for both binding and a subsequent step prior to the onset of DNA replication. A 7 amino acid deletion mutant lacking the trypsin-sensitive residues 17-23 within N-VP2 was slightly defective for binding and approximately 10× deficient, compared to the WT, in initiating a productive infection. However, *in vivo* processing of N-VP2 was still achieved. Because this mutation affects both structural proteins VP1 and VP2, it is difficult to distinguish their relative contribution to the mutant phenotype. However, the binding defect is more likely a VP2 effect since virions lacking VP1 are not defective in binding to susceptible cells [459]. In addition to its defect in cell binding, the mutant produced approximately 10× less viral DNA in the nuclei of infected cells, suggesting that fewer mutant virions, on the average, reached the nucleus where they can initiate DNA replication. Nonetheless, those that managed to reach the nucleus, replicated normally. Similar to 5SG, this mutant was delayed in egress from the cells late in asynchronous infections. However, mutant progeny virions efficiently egress early in the infection, as well as in highly synchronized infections. Therefore, this effect might be a nonspecific defect in some aspect of cytolysis rather than a defect in an active egress mechanism. A less efficient cytolysis would hamper the passive release and spread of intracellular progeny virions, thus preventing their contribution in a next round of infection.

Altogether, these results strongly suggest an involvement of N-VP2 late in infection. N-VP2 appears to orchestrate the reorganization of the cytoskeleton late in infection facilitating passive release of progeny virions. However, since early active egress remains unaffected [458], N-VP2 does not seem to actively participate in the transport mechanism underlying active egress.

2.1.1. Isolation and characterization of empty capsids (EC)

As previously mentioned, DNA packaging and the recently discovered capsid surface phosphorylations are a prerequisite for the externalization of N-VP2. ECs lack both a viral genome and the late phosphorylations, thus having their N-VP2 termini buried in the interior of the capsid. Therefore, EC represent an useful tool to study the role of N-VP2 during early steps in infection, such as binding and endosomal uptake. In addition to the previously characterized FC populations

(FC-P₁ and FC-P₂), infected cells also produce a considerable amount of ECs. Due to the lack of DNA, EC band at lower density compared to FC following differential centrifugation in CsCl. While FC entered the gradient to a density of 1.46 gcm⁻³, EC already banded at 1.32 gcm⁻³, as determined by refractometry (see Figure S2 A, p. 89). A quantitative PCR analysis of the corresponding fractions confirmed that viral DNA containing particles were depleted from ECs to almost a thousand times (see Figure S2 B, p. 89). Approximately half of the overall viral progeny population represents ECs. Therefore, it is of interest to characterize their role during the course of infection. First of all, we verified their N-VP2 conformation and the binding specificity to SA moieties. In Figure S2 C and D, p. 89 it is shown that N-VP2 is not accessible to specific antibodies and proteolytic digestion by chymotrypsin (CHT), respectively. Figure S2 E and F, p. 89 demonstrates that both EC and FC restrictively bind to SA moieties on the surface of murine A9 cells. Binding of both capsid species can be efficiently prevented by pre-treatment of A9 cells using neuraminidase (Neur, see Table 9.8, p. 110) at doses higher than 50 U/mL. Neuraminidase specifically hydrolyzes glycosidic linkages of neuraminic acids. These results confirm that both capsid species bind to the same class of receptor molecules on the surface of susceptible murine cells.

2.2. Full capsids (FC) bind preferentially to murine fibroblasts

In order to characterize the binding specificity of FC and EC, both capsid types were allowed to bind discretely to susceptible, restrictive murine fibroblasts. It was important to minimize uptake of virus into cells to exclusively study virus-receptor interactions. Viral entry can be prevented at reduced temperatures. At 4 °C, active cell-mediated uptake through endocytosis is prohibited, thus bound viral particles remain attached to their receptor molecules on the cell surface but do not internalize [271]. The differences for N-VP2 accessibility can be used to distinguish FCs and ECs in IF experiments. Staining of FCs results in co-localization of α -capsid and α -N-VP2 antibodies whereas ECs are detected by α -capsid antibodies only (see Figure S3 A, upper rows, p. 91). When FCs and ECs were bound to cells at equal stoichiometry, FCs preferentially bound to the cell surface, indicating a higher binding affinity for FCs compared to ECs. Co-localization of both antibodies was higher than 95 % in the absence and in the presence of ECs. Even under non-saturated conditions, ECs were detected rarely when applied as mixed populations (see Figure S3 A, 3rd row, p. 91). Only when an equal amount of ECs was added prior to the FCs a slight increase in bound ECs was observed. Nevertheless, ECs did not represent as much as 50 % of the bound population but only reduced co-localization marginally to approximately 75 % (see Figure S3 A, lowest row, p. 91). *In silico* quantification of co-localization by scatter plot analysis in representative IF pictures revealed that binding of FCs was not disturbed in the presence of ECs (see Figure S3 B, p. 91). Hence, N-VP2 might assist during binding providing an advantage

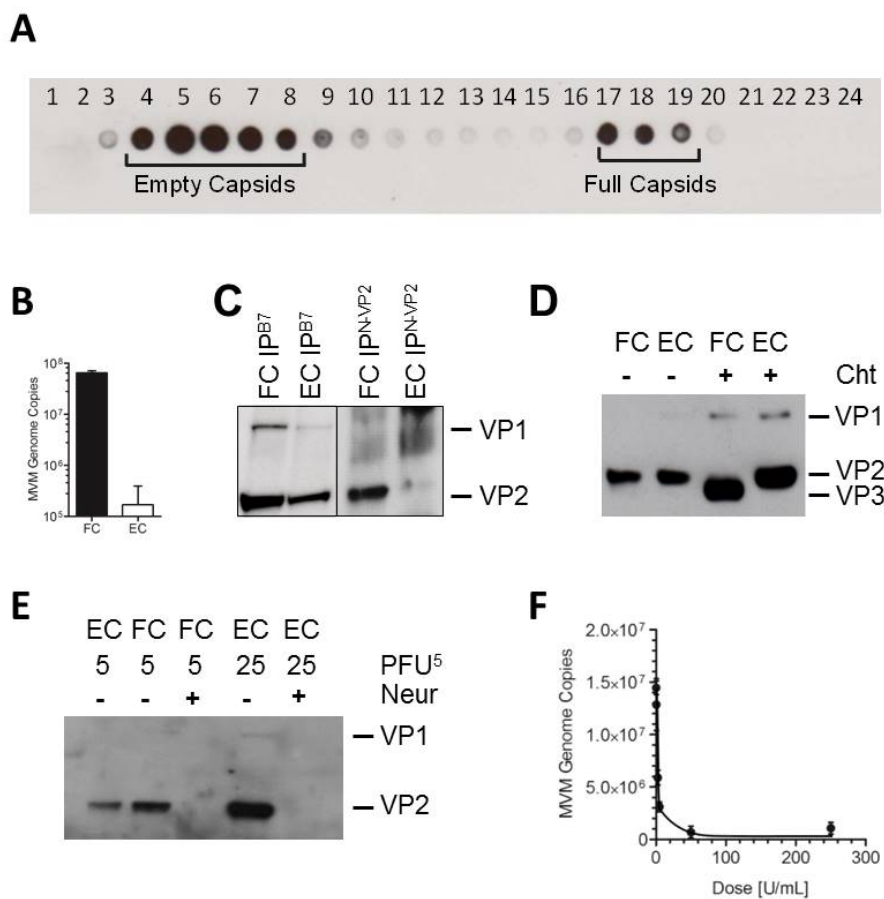


Figure S2.: Purification and analysis of FC and EC. (A) FC and EC were separated by differential centrifugation through a CsCl gradient as described in Section 9.2.1, p. 60. Fractions (500 μ L each) are labeled from top to bottom of the gradient. 2 μ L of each fraction were spotted on a nitrocellulose membrane and probed with an α -capsid mAb (B7). A HRP-coupled secondary antibody was used and the membrane was developed by exposure to a photo film. (B) EC and FC fractions were pooled. qPCR analysis was performed to quantify DNA-containing particles. (C) N-VP2 accessibility of ECs and FCs was tested by IP using an antibody raised against the N-VP2 region. The total amount of applied viral particles was verified using an α -capsid antibody (B7 mAb). (D) ECs and FCs (10^8 particles each) were treated with 0.5 mg/mL chymotrypsin (CHT) or not. Proteolytic N-VP2 processing was analyzed by 10 % SDS-PAGE. After transfer to a polyvinylidene difluoride membrane, the blot was probed with a rabbit α -VP pAb, followed by a HRP conjugated secondary antibody. The membrane was developed by exposure to a photo film. (E) Following treatment with 50 U/mL neuraminidase (Neur) or not, A9 cells were infected at 4 °C using the indicated PFU of FCs or ECs⁵. Following washings to remove unbound viruses the cells were lysed in protein loading buffer and proteins were separated by 10 % SDS-PAGE. Membranes were probed as outlined above. (F) Estimation of the effective dose of Neur in order to completely deplete MVM binding on A9 fibroblasts. Following neuraminidase treatment using the indicated doses, virus (5 PFU) was bound to 3 \times 10⁵ cells for 1 h at 4 °C. Unbound virus was removed by washings, DNA was extracted and viral DNA was quantified by qPCR.

⁵ ECs do not contain DNA and thus, they are not infectious. As a consequence, no PFUs can be calculated for ECs. FCs were quantified by qPCR analysis and used as “external standards” for dot blot analyses. ECs were quantified by spot densitometry by comparison to serial dilutions of quantified FCs.

to cellular attachment for DNA-containing particles.

2.2.1. N-VP2 is not sufficient to provide an advantage in binding for FC

A critical criteria for studying the attachment of a virus to its surface receptor represents the binding specificity of such an interaction. In general, specific attachment is limited to the number of available receptor molecules, thus it saturates as the amount of input virus increases. For A9 cells it has been reported that they offer 5×10^5 specific binding sites per cell [271]. In Figure S4 A, p. 92 it is shown that saturation could be achieved at PFUs higher than 20, corresponding to approximately 10^4 viruses per cell. In addition, specific binding can be competed by adding an excess of particles competing for the same receptor. Linser *et al.* demonstrated that preliminary bound radio-labeled capsids were displaced by subsequently adding an excess of unlabeled particles. However, large quantities of unlabeled particles were required in order to demonstrate competition. Only by exceeding the amount of initially bound virus particles by $20\text{-}40\times$, competition was observed under saturating conditions. Due to the large amount of viral particles required, they were not able to demonstrate complete competition [271]. Even though working under similar conditions, we were not able to demonstrate competition between FC and EC, FC and proteolytically cleaved FC (FC^{CHT}), and FC^{CHT} and EC (see Figure S4 B, C, and D, respectively, p. 92). This indicates that still higher PFUs would have been required to demonstrate competition. However, it might be more difficult to compete for binding with EC or FC^{CHT} since N-VP2 might stabilize the primary attachment to the cell surface. The most clear evidence for this assumption is given by the fact that EC do not bind to the cell surface when applied together with FC as observed in IF experiments (see Figure S3 A, lower rows, p. 91). ECs might not only compete for primary receptor attachment but also for intracellular interactions required for uncoating and trafficking. Therefore, we studied the potential of EC to interfere with the progression of a natural infection. As shown in Figure S4, p. 92, even a large excess of ECs does not interfere with the infection process.

Altogether we conclude that ECs do not interfere with a productive infection, even though representing a large population in a normal infection. In order to disturb binding to cells, a huge excess of ECs would be required that is not found in nature. N-VP2 might be involved in the stabilization of primary attachment of MVM to susceptible cells as judged by IF analyses (see Figure S3 A, 3rd row, p. 91). However, besides N-VP2 exposure, the packaged ssDNA genome and the surface phosphorylations represent further known differences between EC and FC which might directly or indirectly influence receptor binding. In summary, N-VP2 might have minor importance during early steps in infection except for its own proteolytic digestion which is important to allow N-VP1 externalization. However, N-VP2 appears to mediate the rearrangement of the cytoskeleton late in infection (see Section 2.1, p. 85), thus being a key player in progeny egress.

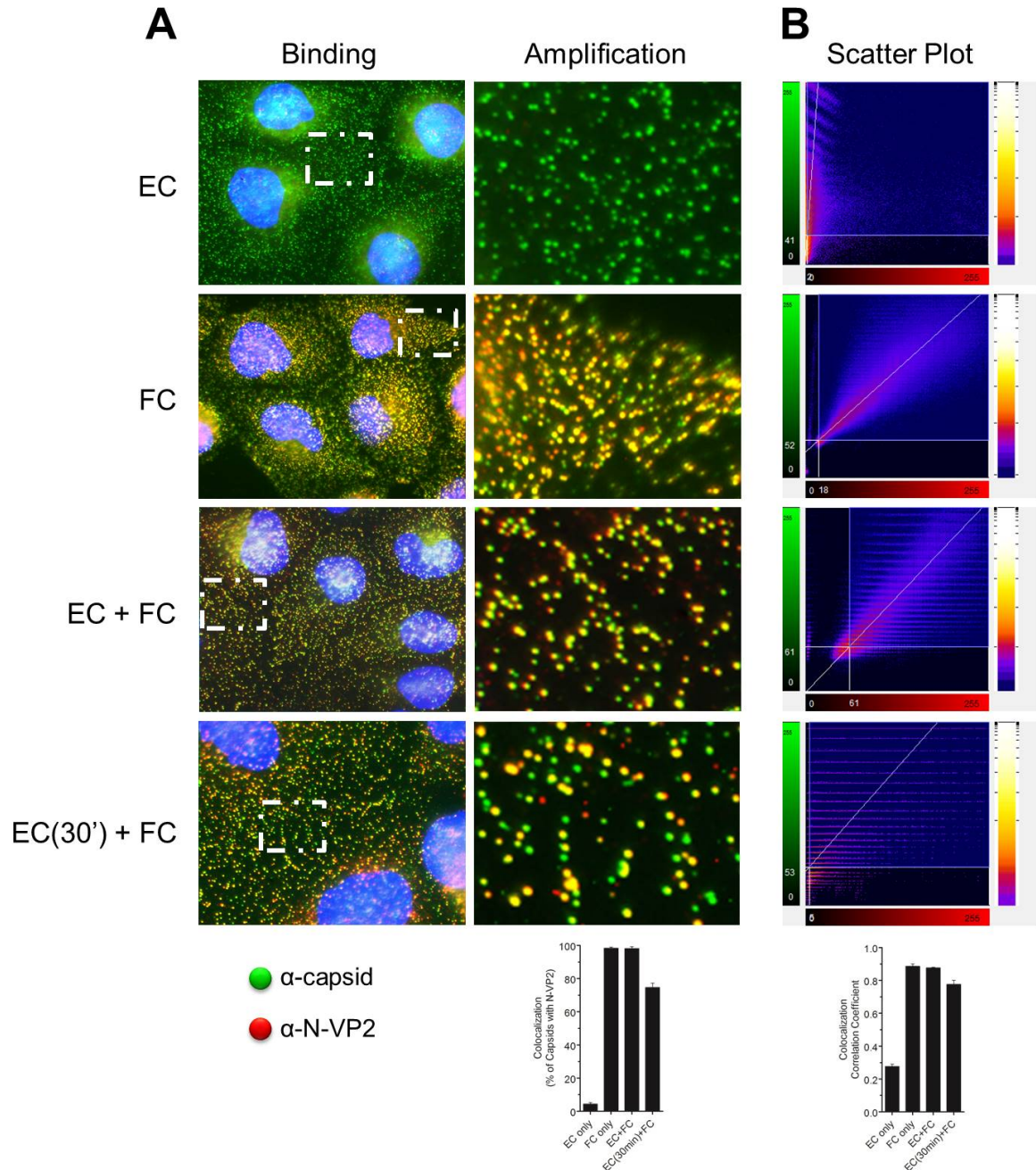


Figure S3.: FCs are preferentially bound to the SA residues on the cell surface. (A) A9 cells (3×10^5) were grown on cover slips and infected independently or combined with FC and EC (5 PFU per cell) at 4 °C. In the 4th row ECs were incubated with the cells 30 min prior to the addition of FCs. Following removal of unbound viruses the cells were fixed and stained for IF using an antibody (mAb B7) raised against assembled capsids (green) and an antibody recognizing N-VP2 (red). Percentage of capsids showing N-VP2 signal was calculated for the indicated areas of interest. (B) Scatter plots analysis showing the indicated areas of interest were used to calculate the corresponding correlation coefficient as a measurement for the degree of co-localization.

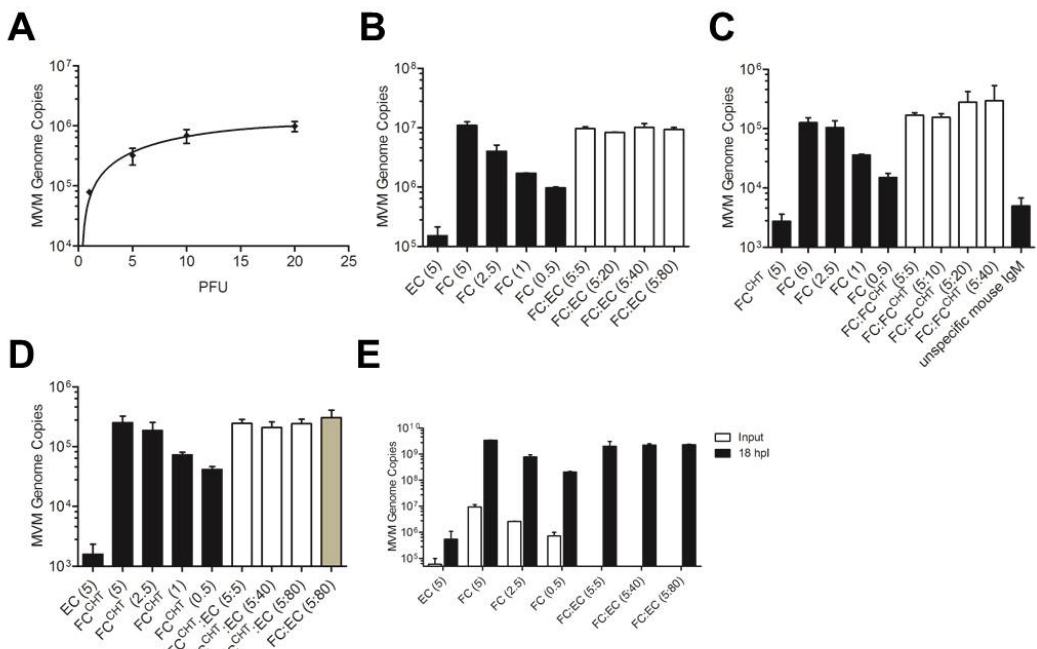


Figure S4.: N-VP2 exposure alone is not sufficient for the better binding to SA moieties. (A) A9 cells (3×10^5) were incubated with MVM at increasing PFU. Following binding at 4 °C unbound virus was removed and total amount of bound virus was quantified. (B) ECs or FCs were bound to A9 cells at the PFUs indicated in brackets (black bars). In order to compete the bound FCs (5 PFU) increasing amounts of ECs were added (5-80 PFU, white bars). (C) FC^{CHT} or FCs were bound to A9 cells at the PFUs indicated in brackets (black bars). In order to compete the bound FCs (5 PFU) increasing amounts of FC^{CHT} were added (5-40 PFU, white bars). Cells were washed and lysed in cell lysis buffer (see Table 9.2, p. 107). FC were quantified following IP using α -N-VP2 Ab (see Table 9.9, p. 111) (D) ECs or FC^{CHT} were bound to A9 cells at the PFUs indicated in brackets (black bars). In order to compete the bound FC^{CHT} (5 PFU) increasing amounts of ECs were added (5-80 PFU, white bars). Grey bar: As a negative control experiment, FCs (5 PFU) were simultaneously incubated with an excess of ECs (80 PFU). (E) A9 cells (8×10^3) were infected at the PFUs indicated in brackets. Increasing amount of ECs were added to FCs. Inputs are represented by white bars.

2.3. Anion-exchange chromatography (AEX) can be applied on other parvoviruses

As previously mentioned, parvoviruses undergo many interactions with their respective host cell due to their strong host cell dependence. Such interactions may preferentially occur on the very surface of incoming or progeny particles because it is readily accessible to the host's enzymes. Therefore, their net surface electrostatics can change as a consequence of host cell induced modifications on the capsid surface. As demonstrated in the present thesis, intranuclear virion populations representing different maturation stages of MVM were successfully separated by AEX based on different surface charges, in this case as a result of distinct surface phosphorylations. Fast protein liquid chromatography (FPLC, see Section 9.4, p. 60) is a high performance chromatography method that combines several advantages. First, the small-diameter stationary phase enables high resolution and fast flow rates. Secondly, samples can be diluted in bio-compatible aqueous buffer systems and large sample volumes can be injected to the system. Thirdly, separation is highly reproducible due to a high level of automation including gradient program control and fraction collection. Finally, a full range of chromatography modes, such as ion exchange, chromatofocusing, gel filtration, hydrophobic interaction, and reverse phase can be provided [291].

We tried to apply AEX on other parvoviruses than MVM, such as B19V and CPV. B19V is a widespread human pathogen which can cause severe disease in human beings. It belongs to the genus *Erythroparvovirus* (see Section 2.1.6, p. 9) and thus, it is highly erythrotropic. B19V efficiently replicates in rapidly dividing erythroid progenitor cells, such as erythroblasts and megakaryocytes present in the bone marrow [206]. Only fully mature virions migrate to the blood plasma of infected individuals where they can persist at high titers (see Figure S5 A, p. 94). CPV emerged in the mid-1970s as a new pathogen of dogs. Equally to MVM, it belongs to the genus *Protoparvovirus* (see Section 2.1.7, p. 10) and replicates in tissues containing rapidly proliferating cells, including the bone marrow, lymph nodes, and the spleen [210]. Stocks of CPV were generated *ex vivo* in canine A72 cells. The cells were productively infected and virus progeny was isolated by physical lysis of infected cell cultures. By doing so, pre-mature and mature virus progeny was not physically separated (see Figure S5 B, p. 94).

The AEX profiles of B19V and CPV stock virus were analyzed. As expected, there was one sharp peak in the case of B19V. Since only the fully mature virions manage to migrate from the bone marrow to the blood plasma, they eluted as a single homogeneous population from the AEX column (see Figure S5 C, p. 94). On the contrary, at least two heterogeneous populations occurred in the case of CPV stock viruses that were expected to contain a mixture of several viral precursors (see Figure S5 F, p. 94). Binding interaction is known to rearrange the VP1u conformation in the case of B19V. Upon receptor attachment, B19V exposes its VP1u on the surface of its capsid [54]. Since such a rearrangement of the capsid surface influences the surface

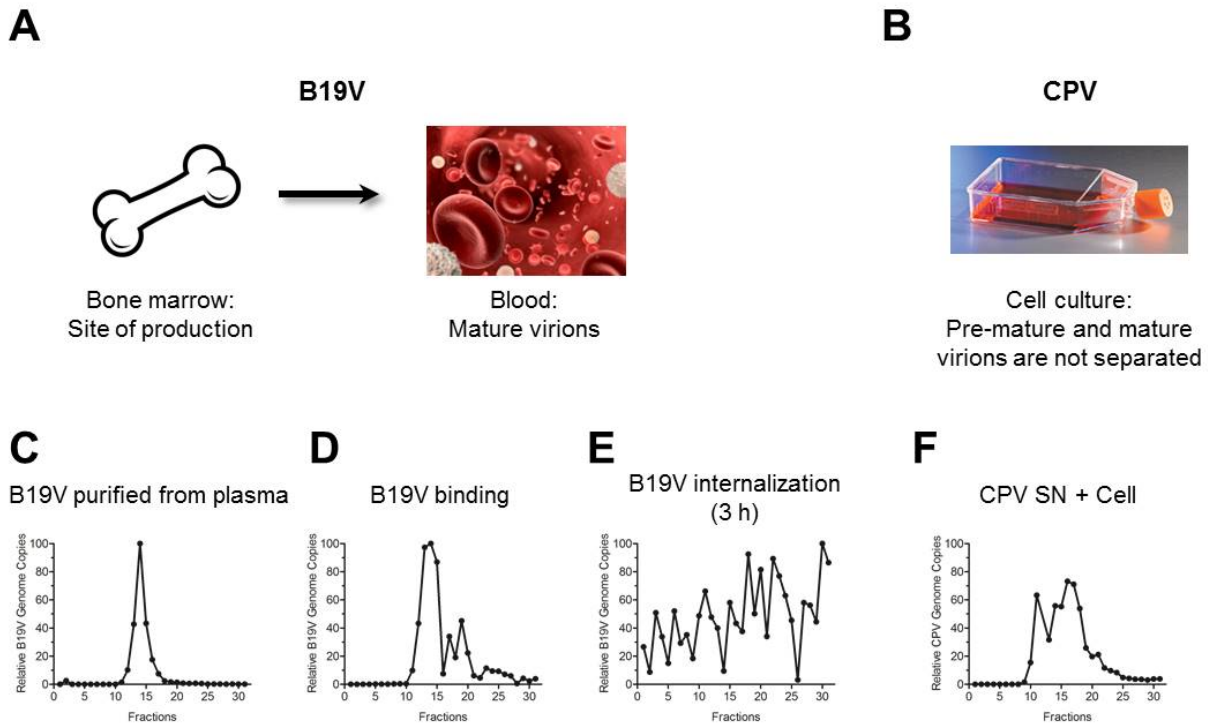


Figure S5.: Anion-exchange chromatography can be applied to study other parvoviruses. (A) B19V is produced in the bone marrow of infected individuals. Only mature particles accumulate in the blood plasma where they productively infect erythroid progenitor cells. (B) CPV was produced in tissue cell culture. Pre-mature and mature particles were not efficiently separated. (C) AEX profile of B19V derived from blood plasma. (D) AEX profile of B19V following binding to UT-7/EPO-S1 cells at 4 °C for 1h. (E) AEX profile of B19V internalized in UT-7/EPO-S1 cells for 3 h at 37 °C. (F) AEX profile of CPV produced in canine A72 cells. Virus was recovered from infected cells by repeated freeze and thaw cycles to lyse the cells.

electrostatics, the profile of bound B19V was found to be distinct from the one of the stock virus (see Figure S5 D, p. 94). The situation became even more complex when intracellular virus was analyzed. B19V undergoes complex phosphorylation and partially uncoats during entry (Ruprecht, N. *et al.*, manuscript in preparation). The formerly homogeneous stock virus displayed a highly complex AEX profile consisting of several peaks (see Figure S5 D, p. 94). In order to analyze such a complex profile, cell fractionation prior to AEX analysis might simplify the analysis. Another possibility would be to infect the cells in the presence of chemical compounds which interfere with certain maturation steps preventing such a complex AEX profile.

In summary, AEX represent a powerful tool to physically separate intracellular virus populations and to gain insights into progeny virus maturation. By performing pulse chase labeling, maturation events can even be tracked chronologically.

Part V

Discussion

3. Conclusion

The present thesis addresses late nuclear maturation steps of the non-enveloped parvovirus minute virus of mice (MVM) which ultimately precede nuclear export and egress of the virus progeny. The current knowledge about nuclear maturation, export, and egress of non-enveloped viruses is highly limited. Although non-enveloped viruses have always been thought to be passively released by virus-induced cytolysis, growing evidence suggests an active mechanism for the egress of progeny virions.

Anion-exchange chromatography (AEX) was applied to separate intracellular virus populations displaying different protein surface electrostatics. Apart from empty capsids (EC), two well defined DNA-containing populations were separated based on their net surface electrostatics. The full capsid (FC) populations, referred to as FC-P₁ and FC-P₂, differed in the conformation of their N-termini of the viral capsid protein VP2 (N-VP2), as well as in their surface phosphorylations. Nuclear export was observed only for the FC-P₂ population, resulting in distinct subcellular localization leading to a segregation of both FC populations. Thus, an active mechanism for virus egress was confirmed. While N-VP2 was not involved in the active nuclear export of MVM, the phosphorylations were strictly associated to nuclear export. During their life cycle, karyophilic viruses encounter a paradoxical situation. Early in infection, the virus has to expose nuclear localization signals (NLS) on its surface to enter the nucleus and to usurp the replication machinery of the host cell. Following assembly and DNA-packaging, progeny virions are exported from the nucleus to egress the infected cell. In order to fulfill a complete infection cycle, the virus needs to rearrange its capsid surface to switch from an import mode to an export mode and vice versa. Figure 3.1, p. 98 summarizes the spatially and temporally controlled modifications in capsid surface phosphorylation providing nuclear import and export potential required to complete the life cycle of a karyophilic virus. Significantly, the surface phosphorylations of the FC-P₂ population disappeared during endocytic trafficking of incoming virions. The FC-P₂ population adopted the surface electrostatics of the FC-P₁ population. Acidic phosphatases hydrolyzed the corresponding phosphorylations. The endocytic dephosphorylation was sensitive to basification of the endosomes by lysosomotropic compounds.

Despite previously thought to orchestrate nuclear export, N-VP2 was shown to be dispensable for this step. N-VP2 defective mutants were able to be exported from the nucleus and to egress the host cell prior to cell lysis. The phosphoserine-rich N-VP2 was demonstrated to mediate the rearrangement of the cytoskeleton late in infection. N-VP2 defective mutants showed prolonged

endocytic VP2 processing and thus delayed nuclear targeting.

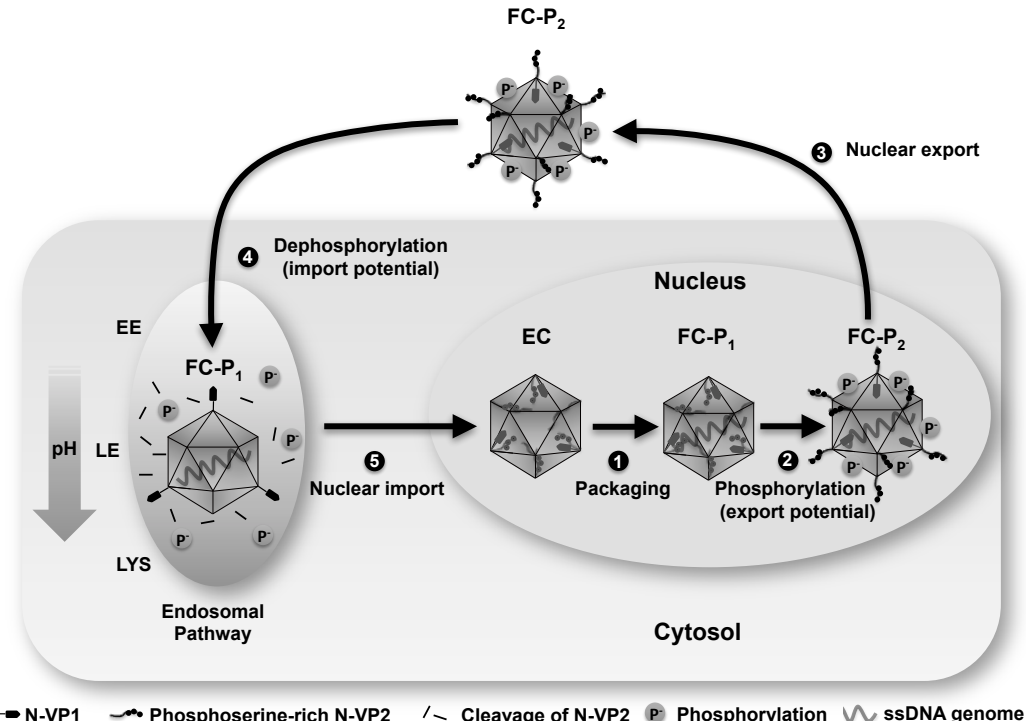


Figure 3.1.: Schematic representation of nuclear export and import of MVM. The virus life cycle is summarized in 5 steps. Following self-assembly of the structural proteins, the empty capsids (EC) are filled with a ssDNA genome, leading to the generation of FC-P₁ virions (step 1). FC-P₁ particles are phosphorylated by a nuclear kinase, resulting in the accumulation of FC-P₂ virion progeny (step 2). FC-P₂ virions are exported from the nucleus of infected cells and egress the host cell (step 3). During entry, export competent FC-P₂ virions become dephosphorylated by acidic phosphatases, adopting the FC-P₁ surface electrostatics (step 4). Infectious incoming virions escape the endosomal pathway and are imported into the nucleus (step 5). The most important capsid elements involved in the viral life cycle are explained below the representation.

Part VI

Appendix

9. Materials

9.1. Infectious clone of MVMp (pIC_MVMp)

9.1.1. Plasmid map of pIC_MVMp

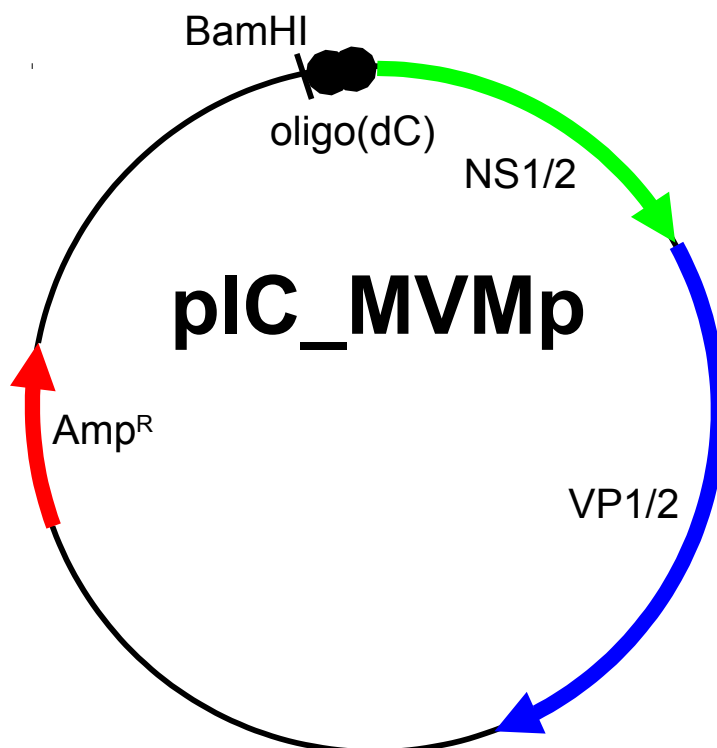


Figure 9.1.: Plasmid map of the infectious clone of MVM (pIC_MVMp). Colored arrows indicate the genes in either the MVMp genome or the pBR322 cloning vector. The circles at the left-hand end of the MVM genome represent the oligo(dC) linker sequence which was originally used for cloning [308].

9.1.2. Complete sequence of pIC_MVMp

The complete nucleotide sequence of the infectious clone of MVM (pIC_MVMp) is shown below. Sequences in black correspond to the backbone of the pBR322 cloning vector. The sequence colored red corresponds to the viral negative (-) strand in 3' to 5' direction which is predominantly packaged into MVM capsids.

```

1 AAGAACTTCT GCTTTCCCGG AGCACTATGC GGATAAAAAT ATCCAATTAC AGTACTATTA TTACCAAAGA
71 ATCTGCAGTC CACCGTAAAA AGCCCCTTA CACGCGCCTT GGGGATAAAC AAATAAAAAG ATTTATGTAA
141 GTTTATACAT AGGCGAGTAC TCTGTTATTG GGACTATTAA CGAAGTTATT ATAACCTTTT CCTTCTCATA
211 CTCATAAGTT GTAAAGGCAC AGCGGAAATA AGGGAAAAAA CGCGTAAAAA CGGAAGGACA AAAACGAGTG
281 GGTCTTTGCG ACCACTTTCA TTTTCTACGA CTTCAGTCA ACCCACGTGC TCACCCAATG TAGCTTGACC
351 TAGAGTTGTC GCCATTCTAG GAACTCTCAA AAGCGGGGCT TCTTGCAAAA GGTTACTACT CGTAAAATT
421 TCAAGACGAT ACACCGCGCC ATAATAGGGC ACAACTGCGG CCCGTTCTCG TTGAGCCAGC GGCGTATGTG
491 ATAAGAGTCT TACTGAACCA ACTCATGAGT GGTAGTGTCTTTCTAGA ATGCCTACCG TACTGTCATT
561 CTCTTAATAC GTCACGACGG TATTGGTACT CACTATTGTG ACGCCGGTTG AATGAAGACT GTTGCTAGCC
631 TCCTGGCTTC CTCGATTGGC GAAAAAACGT GTTGTACCCC CTAGTACATT GAGCGGAAC AGCAACCCCTT
701 GGCCTCGACT TACTTCGGTA TGTTTGCTG CTCGCACTGT GGTGCTACGG ACGTCGTTAC CGTTGTTGCA
771 ACGCGTTTGA TAATTGACCG CTTGATGAAT GAGATCGAAG GGCGGTTGTT AATTATCTGA CCTACCTCCG
841 CCTATTTCAA CGTCCTGGT AAGACCGCAG CGGGGAAGGC CGACCGACCA AATAACGACT ATTTAGACCT
911 CGGCCACTCG CACCCAGAGC GCCATAGTAA CGTCGTGACC CCGGTCTACC ATTGGGAGG GCATAGCATC
981 AATAGATGTG CTGCCCTCA GTCCGTTGAT ACCTACTTGC TTTATCTGTCTAGC ACTGACTCT ATCCACGGAG
1051 TGACTAATTG GTAACCATTG ACAGTCTGGT TCAAATGAGT ATATATGAAA TCTAACTAAA TTTTGAAGTA
1121 AAAATTAAT TTTCTAGAT CCACCTCTAG GAAAAACTAT TAGAGTACTG GTTTTAGGGA ATTGCACTCA
1191 AAAGCAAGGT GACTCGCAGT CTGGGGCATC TTTCTAGTT TCCTAGAAGA ACTCTAGGAA AAAAGACGCG
1261 GCATTAGACG ACGAACGTTT GTTTTTTGG TGGCGATGGT CGCCACCAAA CAAACGGCCT AGTTCTCGAT
1331 GGTTGAGAAA AAGGCTTCCA TTGACCGAAG TCGTCTCGCG TCTATGGTT ATGACAGGAA GATCACATCG
1401 GCATCAATCC GGTGGTGAAG TTCTTGAGAC ATCGTGGCGG ATGTATGGAG CGAGACGATT AGGACAATGG
1471 TCACCGACGA CGGTACCGC TATTCAAGCAC AGAATGGCCC AACCTGAGTT CTGCTATCAA TGGCTTATTC
1541 CGCGTCGCCA GCCCCACTTG CCCCCCAAGC ACAGTGTGTCG GGTGAAACCT CGCTTGCTGG ATGTGGCTTG
1611 ACTCTATGGA TGTCGCACTC GATACTTTT CGCGGTGCGA AGGGCTTCCC TCTTCCGCC TGTCCATAGG
1681 CCATTGCGCG TCCCAGCCTT GTCCCTCTCGC GTGCTCCCTC GAAGGTCCCC CTTTGCGGAC CATAGAAATA
1751 TCAGGACAGC CCAAAGCGGT GGAGACTGAA CTCGCAGCTA AAAACACTAC GAGCAGTCCC CCCGCCTCGG
1821 ATACCTTTT GCGGTGCGT CGCGGAAAAA ATGCCAAGGA CCGGAAAACG ACCGGAAAAC GAGTGTACAA
1891 GAAAGGACGC AATAGGGGAC TAAGACACCT ATTGGCATAA TGGCGAAAC TCACTCGACT ATGGCGAGCG
1961 GCGTCGGCTT GCTGGCTCGC GTCGCTCAGT CACTCGCTCC TTGCGCTTCT CGCGGACTAC GCCATAAAAG
2031 AGGAATGCGT AGACACGCCA TAAAGTGTGG CGTATACCAAC GTGAGAGTCA TGTTAGACGA GACTACGGCG
2101 TATCAATTG GTCATATGTG AGGGATAGC GATGCACTGA CCCAGTACCG ACGCGGGCT GTGGCGGTT
2171 GTGGGCGACT GCGCGGGACT GCCCCAACAG ACGAGGGCCG TAGGCGAATG TCTGTTGAC ACTGGCAGAG
2241 GCCCTCGACG TACACAGTCT CCAAAAGTGG CAGTAGTGGC TTTGCGCGCT CCGTCGACGC CATTTCGAGT
2311 AGTCGCACCA GCACCTCGCT AAGTGTCTAC AGACGGACAA GTAGGCGCAG GTCGAGCAAC TCAAAGAGGT
2381 CTTCGCAATT ACAGACCGAA GACTATTGCG CCCGGTACAA TTCCCGCCAA AAAAGGACAA ACCAGTGAAC
2451 TACGGAGGCA CATTCCCCCT TAAAGACAAG TACCCCCATT ACTATGGCTA CTTTGCTCTC TCCTACGGAGT
2521 GCTATGCCCA ATGACTACTA CTTGTACGGG CCAATGACCT TGCAACACTC CCATTGTTG ACCGCCATAC
2591 CTACGCCGCC CTGGTCTCTT TTTAGTGTGAGT CCCAGTTACG GTGCGAAGC AATTATGTCT ACATCCACAA

```

2661 GGTGTCCCAT CGGTCGTCGT AGGACGCTAC GTCTAGGCCT TGTATTACCA CGTCCCGCGA CTGAAGGCC
 2731 AAAGGTCTGA AATGCTTTGT GCCTTTGGCT TCTGGTAAGT ACAACAACGA GTCCACGCGTC TGCAAAACGT
 2801 CGTCGTCAGC GAAGTGCAAG CGAGCGCATA GCCACTAAGT AAGACGATTG GTCATTCCGT TGGGGCGGTC
 2871 GGATCGGGCCC AGGAGTTGCT GTCTCGTGC TAGTACGCGT GGGCACCGGT CCTGGGTTGC GACGGGCTCT
 2941 ACGCGGCCGA CGCCGACGAC CTCTACCGCC TGCCTACCT ATACAAGACG GTTCCAACC AACCGCGTAA
 3011 GTGTCAAGAG GCGTTCTTAA CTAACCGAGG TTAAGAACCT CACCACTTAG GCAATCGCTC CACGGCGGCC
 3081 GAAGGTAAGT CCAGCTCCAC CGGGCCGAGG TACGTGGCGC TGCGTTGCCT CCCTCCGTCT GTTCCATATC
 3151 CCGCCGCGGA TGTTAGGTAC GGTTGGGCAA GGTACACGAG CGGCTCCGCC GTATTAGCG GCACTGCTAG
 3221 TCGCCAGGTC ACTAGCTTCA ATCCGACCAT TCTCGCGCT CGCTAGGAAC TTGACAGGG ACTACCAGCA
 3291 GTAGATGGAC GGACCTGTG TACCGGACGT TGCGCCCGTA GGGCTACCGC GGCCTTCGCT CTTCTTAGTA
 3361 TTACCCCTTC CGGTAGGTG GAGCGCAGCG CTTGCGGTG TTCTGCATCG GGTGCGCAG CGGGCGGTAC
 3431 GGCGCTATT ACCGGACGAA GAGCGGCTTT GCAAACACC ACCCTGGTCA CTGCTCCGA ACTCGCTCCC
 3501 GCACGTTCTA AGGCTTATGG CGTCGCTGT CGGGCTAGTA GCAGCGCAG GTGCTTCG CCAGGAGCGG
 3571 CTTTACTGG GTCTCGCGAC CGCCGTGGAC AGGATGCTCA ACGTACTATT TCTCTGTCA GTATTACCG
 3641 CGCTGCTATC AGTACGGGGC CGGGGTGGCC TTCTCGACT GACCCAACCTT CCGAGAGTTG CCGTAGGCCAG
 3711 CTGCGAGAGG GAATACGCTG AGGACGTAAT CCTTCGTCGG GTCATCATCC AACTCCGGCA ACTCGTGGCG
 3781 GCGGCGTCTC TTACACCGTA CGTCTCTCTA CGCGGGGTTG TCAGGGGGC GGTGCCCCGG ACGGTGGTAT
 3851 GGGTGCAGGCT TTGTTCGCGA GTACTCGGCTC TTCACCGCTC GGGCTAGAAAG GGGTAGCCAC TACAGCCGCT
 3921 ATATCCGCGG TCGTTGGCGT GGACACCGCG GCACTACCG CCGGTGCTAC GCAGGCCGCA TCTCCTAGGC
 3991 CCCCCCCCCC CCCAAAATCT TGACTGGTTG GTACAAGTGC ATTCACTGCA CTACTGGCG CGACGCCGCG
 4061 GACGGAAGGCC GTCAGTGTGC AGTGAATGCA AAGTGTACCA ACCAGTCAAG ATTTTTACTA TTGCGCAAGT
 4131 CCCTCAAATT TGGTTCCGCG CTTTCTCTC ACCCGCACCA AATTTCATAT ATTCTGTGAT GACTTCAGTC
 4201 AATGAATAGA AAAGAAAGTA AGACACTCAG CTCTGCGTGT CTTTCTCTCA TTGGTTGATT GGTACCGACC
 4271 TTTACGAATG AGACTACTTC AAAACCCCTCG TTGGTTGACC AATTTCCTT TTTCATTGGT CCTTCACAAG
 4341 AGTAAACAAA AATTTTACT TTTACAAGTT GACTTACCTT TTCTATAGCC TACCTTATCA ATGTTTTTC
 4411 TCGACGTCTC CCTGCTCGAC TTAGAAATG TTGCTCTCG CTTTGTGATGA ACCCTGGTT CGCTCTGTA
 4481 CCTTACCCCTT TGGTGCACC TACTTTACTG GTTTTCTGTT CATAAGTAAA AACTAAGAAA CCAATTTTT
 4551 ACAAAATAAC TTCACGAATT GTGTTCTTA TATAAAGGAC CACTACAATT AACCAAACAC GTTGTACTTA
 4621 CCCCCTTCTT CTGTCGACCT GTGACGGTAC ATGATTAACC TCCTTCTCG AAATCAGTTC GAGTTCCCTT
 4691 TACCACTCT TCCGTTGATT TACAAATGAC CTCGTCTACC AACCAATTGTC GGACATTACA CGTTGATTGT
 4761 GGTCGACTTT CTTAATTGTA TTCTCTTCTG CGTCTCTGT TACTCACCCA ATGAGATGAA TGAATATTG
 4831 TATTGTTTG GTTTCTG ATATGGTTCA CACAAGAAAA ACCTTTGTAC TAACGAATGA TAAAAAATTG
 4901 ATTTTCTTT TATTGTTGAT CAGGTGGTTC TCTGCCTCCG ATAAAAGAAA TCGTCACTGA AACCGACCTT
 4971 TTGATTGAAA AATTTCCTTC CGCTCGCGGT AGATCACTCG TTTGATATGT GACTACTGTA CGCCGGCTT
 5041 TGCAACTTT GGTGTCATTG GTGACGGTC CTTGATTG CGCCGTCTTA AGTTGATTT TTTCTTCAAA
 5111 GATAATTGTTG ATGTGAATTG CTCGACCGACG TATTTCCTCA TTGGAGTGGT CTCTGACCT ACTACTACGT
 5181 CGGTCTGTCA ATGTAACCTT ACTACCGAGT TGGTCCACCT CTTTGGACG ACTTTTATG CGATCTCTAA
 5251 ACATGTGATT GAGATCGGTC TTGGTTTG CGTAAACTGA ATTAAAATCT TTTGACTT TGGTCGTTG
 5321 ATTGGTTGAA AAGTGACGGA CTGTGTTCTT GGACGTCTTA AAAACGAAAA GTACCGACCT TGATACAATT
 5391 TCAAACGGTA CGATAAACGA CACAAAATTT GTCTGTTCTT CCGTTTCTT TATGACAAAA TAAAGTACCT
 5461 GGTGGTCGTTG GTCCGTTAG ATAATAACGT GTTCGGTATC GTGTTGCTCA ACCGTTACAA CCAACGATAT
 5531 TACGTGCGTT ACATTGAAA GGTAATTAC TGACATGGTT GTTCTTGAAAC TAAACCCATC TTCTTCGACC
 5601 ATTGAAACCT GTCGTTCAATT TGGTCAAATT TCGGTAAACCG AGACCAGTTT GATAAGCGTA ACTAGTTT
 5671 CCTTTCTCGT CGTTGTTCTA ACTTGGTTGT GGTCACTAGT ACTGGTGTGTT ACTCTTGAA TGTCACTAGT
 5741 CTTATCCGAC GCTTCTTCTT GGTCTGTGT GAGTTGGTTA GTCTCTGTCT TACGAATTGT AAGTAGATTG
 5811 TGTATGGAAC GGACCACTGA AACCAAACCA ACTGTTTTA CTTACCGGGT ACTAAACACG AACCAACCAT

5881 TTCTTACCAA TGGTTAGATG GTACCGTCG ATGACACGAT TTACCCCGTT TCAAGGACTA ACCAGTCTTT
 5951 TGACCCGCCT CGGTTTCCAC GGTTGAGGAT ATTTAAATGA TCCAAGCCGT GCGAGTGGTA AGTGCTGTGG
 6021 CTTTCATGC GGAGAGTCGG TCTTGATACG TGATTGAGGT GAACGTAGCC TAGAGCTCCT GGACCGAAAT
 6091 CTGGAACCT CGTGTGGTTT ATGAGGACAA CGCCCGTGAC GTCTTGGGT CTTGTGACCC CTTCGACCAA
 6161 GGTTTCGGAC GGTTCTACCA GTTGAECTCGG GTTGAACCAG TCTCTAGCTC CTCTAAACT CTCGCACGAA
 6231 GCCACGCCTT GGCAACTTCT TTCTGAAAGTC GCTCGGCAC TTGAACCTGA TTCCATGCTA CCGGGGAGGT
 6301 CGATTTCTC GATTTCTCC ATTCCCAAAT TCCCTACCAA CCAACCACCC CATAATTACA AATTAAATGGA
 6371 CAAAATGTCC GGACTTTAGT GAACCAAAT CCAACCCACG GAGGACCGAT GTTCATGGAC CCTGGTCCCT
 6441 TGTCGGAACCT GGTTCCCTCTT GGTTGGTTAG GTAGACTGCG GCGACGGTTT CTCGTGCTGC TCCGGATACT
 6511 AGTTATGTAG TTTAGACCTT TTTAGGAAT GGACATGAAG AGACGACGAC TAGTTGCGAA ATAATGGTT
 6581 TGTTCCCTGC GGTTCTGAC CCCTCCGTT CAACCAACTGA TGAAAAAAATC TTGGTTCCGG CGAAAACGTG
 6651 GATTCGAACG ATGACTGAGA CTTGGACCTT GAAGACCACA TTCGTCTCGA CCATTTGCGT GATCTGGTGG
 6721 ACGAATGTA AAATAATTGG TTCGGTCTCG ATTTTTTTT GAATGAAGAA GACGACGTG CGTTTGTCA
 6791 GTTTGGTACT CACTACCGTG GTCGGTTGGA CTGTCGCCCT TGCGACAGGT GAGTCGACGT TCTCAACTTG
 6861 CTCGTCGACT GCCGGGACCT CCGAGACCCC CACCCCCGAG ACCGCCCCCA CCCAACCCAC AAAGATGACC
 6931 CAGAATACTA TTAGTTGCG TAATATCTAA GAACCCACTG CCGACCCATC TTTAATGACG TGATCGTTGA
 7001 TCTGATCATG TAAATTGTA CGGATTAGT CTTTGATAA CGTCTTAGTC TCAAGTGTAA TGTGTCTGT
 7071 GTAGTCAGTT TCCGTTGTAC CGTTTCTAC TACGAGTACT CGTTTAAACC TGTGGTACCT CGAACCCACCT
 7141 ACGATTACGA ACCCCTAAA CCGAGGTCGG TTCACTGACC GTTATGTAAA CGTTGCGTA CTCGGTCGAA
 7211 TTGAACCATA GTGAACACTGT TCTTTATAAG TTACATCACG ACTTTTGACA ATGTCTCGTT CTGAATCCCTC
 7281 CAGTTCGATA TTTTTATATG TTGTTACTGG AATGTCGAAAC GTACTACCAA CGTCATCTGA GTTTGTTGTA
 7351 AAACGGTATG TGTGGACGTC GTTTGAGTTA CCTTTGTGAA CCAAAGATGG GGACCTTGG TTGGTATCGT
 7421 AGTGGTATGT CCATGATAAA AACGCAACTG TCTCTAGAAA GTCACTGGAT GCTTTAGTT CTTCCGTGTC
 7491 AACTTGTATT ACACTACCCCT TGTGGTTTTC CTACTTAAG AGTTAAAAAA TGGTAACTCT TGTGTGTTGT
 7561 TTAGTGTAAAC GAGTCTTGTC CCCTGCTTAA ACGGTGTCCG TGAATGATGA AACTGTGTTT AGGTCAATT
 7631 GAGTGTGTGT GCACCGTTTG GTTGGCAGTT GAACCTGTGAG GAGGTGACGA CAGTTGAAA GGACTTCGAC
 7701 TGTGACTACG TCCATGTGAA TGACGAGTTC CCTCGTCTGT ACCTTGTGTT GTTTACCCCC AATTGACCCA
 7771 CTCACTTCGT TAGTCTGGT CTGGACGAGT TCATCCTAAA ACAGTTGGT TGTTACTGAA ACTTCGGTCG
 7841 TCTCGACCTG GTAAACGACG GGGTTTCAA GGTGTCAT AATGAGTTC TCATCTGTTT CTTCCGTTAC
 7911 CGTCACAATC TATGTCAATA CCGTTTGTG TACCACTTTT AACCCGAAGT GTACCTGGTC GTGGTCTCGC
 7981 GATGTGTACC CTACTTTGTT CGAAACCAAG TCCATCTCTG TGTTTCTAC CAAAATAAGT TAGTCGTGGT
 8051 GATCAACAAG GTGGTGGTGA TTTACCGTAA GAATGTTAC GTTTGGGATA ACCCTGATTT TTACTGTAAG
 8121 TAAAAAGTTT ACAAAAATTG TCGATACCAAG GTGATTGACG TAAAAGTGTG GGTTCAAGGAC ATATGGAGT
 8191 TCCTGTTTAT ACCCTGTTTC TTGATCTAGA ACTTGTGTTT GGATCTGAAG TGTATTGACG AGGTAACCAA
 8261 ACATTTTGT TACGTGGACC GTTTACAAC CAATCTAAC TCGTTTGGG TTGACTGGTT ATACTAGTT
 8331 TGCCCTGGTG TGAAAGATCT TAACAATGTA TACCATGTA AAAGACCTTT CCTTTGATT GGTACTCTCG
 8401 TTTTGAATCT CGATTGTGGT GAACCTTGGG TCACATGGTT CATTCAACGAC TTCTGTTACC GTTGAGTATG
 8471 TACTCACATT GATTTACCGA TGTTGACGA TGACCTTGT ACGTCAGACA CGGCGAATAT TGTTCTGGAC
 8541 AACGATCTT ATGAATGATT GATTGGTACG AAAAAGAAAG ACATGAAGTA TATAATAATT CTGATTATT
 8611 CTATGTTGTA TCTTTATATT ATAATGTATA TCTAAATTCT TTATCTTATT ATACCATGAA TCATTGACAA
 8681 TTTTATTAT CTTGGAAACC TTATTGTTCT ATCAATCAAC CAATTACAAT CTATCTTATT CTTCTAGTAC
 8751 ATATTACTTA TTTTCCACC TTCCACCAA CCATCCAATT ACAATCTATC TTATTCTCT AGTACATATT
 8821 ACTTATTTTC CCACCTTCCC ACCAACCATC CATAAGGGAA TCTGAACCTAC AATTCCGTGGT TTTTTTATTA
 8891 TTTTGAAAAA ATTTGAGTT GGTTCTGATG ACAGATAAGT CACTTGGTTG ACTTGGTAAT CATAATGATA
 8961 CAAAATCCC ACCCTCCAGT TAGTTAGTCC TT

9.2. Chemicals and compounds

Chemical	Provider
Acetic Acid (Glacial)	Merck
Acetone	Merck
Agarose low EEO	AppliChem
Ampicillin (Ready Made Solution, 100 g/mL, 0.2 μ M filtered)	Sigma-Aldrich
Bafilomycin A ₁	Sigma-Aldrich
Bovine Serum Albumin (BSA)	Sigma-Aldrich
Bromophenol Blue	Merck
Caesium Chloride (CsCl)	Sigma-Aldrich
Chymostatin	Sigma-Aldrich
Citric Acid	Sigma-Aldrich
Complete Mini Protease Inhibitor Cocktail Tablets	Roche
Complete Mini Protease Inhibitor Cocktail Tablets EDTA-free	Roche
1,4-diazabicyclo[2.2.2]octane (DABCO)	Sigma-Aldrich
4',6-diamidino-2-phenylindole (DAPI)	Invitrogen
Dimethyl Sulfoxide (DMSO)	Sigma-Aldrich
Dithiothreitol (DTT)	Sigma-Aldrich
1kb DNA Ladder	Invitrogen
Ethylenediaminetetraacetic Acid (EDTA)	Sigma-Aldrich
Ethanol (99.89 %)	Sigma-Aldrich
Ethanol (94 %) denat. with 2 % MEK	Grogg Chemie AG
Ethidium Bromide (10 mg/mL)	Invitrogen
EZMix™ N-Z-Amine® A (NZ Amine)	Sigma-Aldrich
Fetal Calf Serum (FCS)	Amimed
Glycerol (Anhydrous)	Sigma-Aldrich
Goat Serum	DAKO
G-Protein Agarose Beads	Santa Cruz Biotech
Hydrochloric Acid (HCl)	Sigma-Aldrich
Imidazole	Sigma-Aldrich
Iminodiacetic Acid	Sigma-Aldrich
Isopropanyl β -D-1-thiogalactopyranoside (IPTG)	Invitrogen
LB-Agar, Miller	Sigma-Aldrich
LB Broth Base	Invitrogen
L-Glutamine (200 mM)	Biochrom
Magnesium Chloride (MgCl ₂)	Sigma-Aldrich

Table 9.1 continued

Chemical	Provider
Magnesium Sulfate (MgSO_4)	Sigma-Aldrich
Manganese(II) chloride (MnCl_2)	Sigma-Aldrich
2-Mercaptoethanol	Sigma-Aldrich
Methanol HPLC grade	Fisher Chemical
Milk Powder (Adapta)	Coop
Mowiol	Calbiochem
Nitrocellulose Transfer Membranes $0.45 \mu\text{m}$	Millipore
2-(<i>N</i> -morpholino)ethanesulfonic acid (MES)	Sigma-Aldrich
3-(<i>N</i> -morpholino)propanesulfonic acid (MOPS)	Sigma-Aldrich
Nonidet P40 (NP-40)	Applichem
NuPage MOPS SDS-Running Buffer (20 \times)	Invitrogen
Nupage Transfer Buffer (20 \times)	Invitrogen
N-Z-Amine® A	Sigma-Aldrich
Penicillin/Streptomycin	Biochrom AG
Phosphate-Buffered-Saline (PBS)	Oxoid
Polybuffer® 74	Sigma-Aldrich
Precision Plus Protein Standards, Dual Color	BioRad
Sodium Acetate, anhydrous	Sigma-Aldrich
Sodium Citrate	Sigma-Aldrich
Sodium Chloride (NaCl)	Roth
Sodium dihydrogen phosphate Dihydrate ($\text{NaH}_2\text{PO}_4 \cdot 2\text{H}_2\text{O}$)	Sigma-Aldrich
Sodium dodecyl sulfate (SDS)	Sigma-Aldrich
di-Sodium hydrogen phosphate Dihydrate ($\text{Na}_2\text{HPO}_4 \cdot 2\text{H}_2\text{O}$)	Sigma-Aldrich
Sodium Fluoride (NaF)	Sigma-Aldrich
Sodium Hydroxide (NaOH)	Sigma-Aldrich
Sodium Orthovanadate (Na_3VO_4)	ICN Biomedicals Inc.
D(+)-Sucrose	Sigma-Aldrich
Sulfuric Acid 95-98 %	Sigma-Aldrich
Tris(hydroxymethyl)aminoethane (Tris Buffer)	Sigma-Aldrich
Triton X-100	Siegfried
Tween 20	Applichem
Yeast Extract	Sigma-Aldrich

Table 9.1.: List of chemicals and compounds

9.3. Buffers

9.3.1. General buffers

Buffer	Reagent	Concentration
Cell Lysis Buffer	Tris-HCl (pH 7.2)	50 mM
	NaCl	150 mM
	Nonidet P40 (NP-40)	1 % (v/v)
	EDTA	5 mM
	Sodium orthovanadate (Na_3VO_4)	1 mM
	Sodium fluoride (NaF)	1 mM
	Protease Inhibitor Cocktail	1 tablet per 10 mL
Nuclei Lysis Buffer	Tris-HCl (pH 7.2)	50 mM
	NaCl	150 mM
	Triton X-100	1 % (v/v)
	EDTA	5 mM
	Sodium orthovanadate (Na_3VO_4)	1 mM
	Sodium fluoride (NaF)	1 mM
	Protease Inhibitor Cocktail	1 tablet per 10 mL
Phosphate Buffered Saline (PBS Buffer)	PBS Tablets	1 tablet in 100 mL
		dH ₂ O
Phosphate Buffered Saline with (PBSA Buffer)	PBS Buffer	
Bovine Serum Albumin	Bovine Serum Albumin (BSA)	1% (w/v) in PBS

Table 9.2.: Buffers used for cell lysis and standard incubations.

9.3.2. Chromatography buffers

Anion-exchange chromatography (AEX)

Buffer	Reagent	Concentration
Sample Buffer	Tris-HCl (pH 8)	10 mM
	EDTA	1 mM
	Sodium orthovanadate (Na_3VO_4)	1 mM
	Sodium fluoride (NaF)	1 mM
Starting Buffer	Tris-HCl (pH 7.2)	20 mM
	EDTA	1 mM
Elution Buffer	Tris-HCl	20 mM
	EDTA	1 mM
	NaCl	2 M

Table 9.3.: Buffers used for anion-exchange chromatography (AEX).

Chromatofocusing (CF)

Buffer	Reagent	Concentration
Buffer A	Bis-Tris (pH 7, adjusted with saturated iminodiacetic acid)	25 mM
Buffer B	Polybuffer 74 (pH 4, adjusted with saturated iminodiacetic acid)	20 % in ddH ₂ O

Table 9.4.: Buffers used for chromatofocusing (CF).

9.3.3. Agarose gel electrophoresis

Buffer	Reagent	Concentration
6× DNA Loading Buffer	D(+)Sucrose	40 % (w/v)
	Bromophenol Blue	0.25 % (w/v)
10× Tris-Acetate-EDTA Buffer (TAE Buffer)	Tris Base (pH 8.0)	400 mM
	Acetic Acid (Glacial)	11.5 % (v/v)
	EDTA	10 mM

Table 9.5.: Buffers used for agarose gel electrophoresis.

9.3.4. Western blot

Buffer	Reagent	Concentration
1× NuPage MOPS Buffer	20× Buffer was diluted to 1× with dH ₂ O and used for SDS page.	
1× NuPage Transfer Buffer	20× buffer was diluted to 1× with 20 % methanol. This Buffer was used to transfer the separated proteins to the nitrocellulose membrane.	
2× Protein Loading Buffer (PLB) (non-reducing, [257])	Tris-HCl (pH 6.8)	120 mM
	Sodium Dodecyl Sulfate (SDS)	4 % (w/v)
	Glycerol	20 % (v/v)
	Bromophenol Blue	0.02 % (w/v)
10× Tris-Buffered Saline (TBS Buffer)	Tris-HCl (pH 7.3)	0.2 M
	NaCl	1.5 M
1× Tris-Buffered Saline with Tween 20 (TBST Buffer)	10× TBS	10 % (v/v)
	Tween 20	0.05 % (v/v)

Table 9.6.: Buffers used for Western blotting analysis.

9.4. Kits

Ready-to-use Reaction System (Kit)	Provider
Amaxa™ Cell Line Nucleofector™ Kit R	Lonza Group AG
Amaxa™ Cell Line Nucleofector™ Kit V	Lonza Group AG
Amersham Hyperfilm™ ECL	GE Healthcare
Carestream® Kodak® autoradiography GBX developer/replenisher	Sigma-Aldrich
Carestream® Kodak® autoradiography GBX fixer/replenisher	Sigma-Aldrich
DNeasy Blood and Tissue Kit	Qiagen
Dynabeads® mRNA DIRECT™ Kit	Invitrogen
iTaq™ Universal SYBR® Green Supermix	BioRad
Nuclei EZ Prep Kit	Sigma-Aldrich
pBluescript II KS(+) Phagemid Kit	Agilent Technologies
QIAEX II® Gel Extraction Kit	Qiagen
QIAGEN Plasmid Midi Kit	Qiagen
QIAprep® Spin Miniprep Kit	Qiagen
QIAquick® PCR Purification Kit	Qiagen
QuikChange® Site-Directed Mutagenesis Kit	Agilent Technologies
SuperSignal® West Femto Maximum Sensitivity Substrate	Thermo Scientific
XL-10 Ultracompetent Cells	Agilent Technologies

Table 9.7.: Ready-to-use kits.

9.5. Enzymes

Enzyme	Concentration	Provider
α-Chymotrypsin	10 mg/mL	Sigma-Aldrich
DNaseI, RNase free	10 000 U/mL	Roche
Neuraminidase	50 000 U/mL	New England Biolabs
λ-Phosphatase	400 000 U/mL	Merck
Trypsin/EDTA solution	0.25 % / 0.02 % (w/v)	Biochrom AG

Table 9.8.: The listed enzymes were used for *in vitro* treatments or passing tissue culture cells.

9.6. Antibodies

9.6.1. Primary antibodies

Name	Specificity	Host	Clonality	Dilution	Provider
α -VP (Jimmy)	Linear epitopes on VP1 and VP2 of MVM.	Rabbit	Polyclonal	IF: 1/800 WB: 1/2 000	J. M. Almendral [298]
α -Caps (B7)	Conformational surface epitope on intact capsids of MVM.	Mouse	Monoclonal	IF: 1/100	J. M. Almendral [278]
N-VP2	N-terminal part of VP2.	Rabbit	Polyclonal	IF: 1/200 WB: 1/1 000	J. M. Almendral [298]

Table 9.9.: The primary antibodies were used for immunolabeling, immunoprecipitation, and Western blotting analysis.

9.6.2. Secondary antibodies

Name	Target species	Host	Conjugate	Dilution	Provider
Goat α -mouse IgG	Mouse	Goat	Alexa Fluor® 488	IF: 1/500	Life Technologies
Goat α -mouse IgG	Mouse	Goat	Alexa Fluor® 594	IF: 1/500	Life Technologies
Goat α -mouse Ig	Mouse	Goat	Horseradish per-oxidase (HRP)	WB: 1/20 000	Dako
Goat α -rabbit Ig	Rabbit	Goat	Horseradish per-oxidase (HRP)	WB: 1/20 000	Dako
Goat α -rabbit IgG	Rabbit	Goat	Alexa Fluor® 488	IF: 1/500	Life Technologies
Goat α -rabbit IgG	Rabbit	Goat	Alexa Fluor® 594	IF: 1/500	Life Technologies

All secondary antibodies listed in this table are polyclonal.

Table 9.10.: The secondary antibodies were used for immunofluorescence assays and Western blotting analysis.

9.7. Media

Name	Provider
Dulbecco's Modified Eagle Medium (DMEM)	Gibco
Lysogeny Broth Agar (LB Agar)	Sigma-Aldrich
Lysogeny Broth Medium (LB Medium)	Sigma-Aldrich
SOC Medium	Sigma-Aldrich

Table 9.11.: The denoted media were used for the cultivation of A9 and NB324K cells, as well as XL1-blue and XL10-gold bacteria.

Bibliography

- [1] Adeyemi, R. O., Landry, S., Davis, M. E., Weitzman, M. D., and Pintel, D. J. Parvovirus minute virus of mice induces a DNA damage response that facilitates viral replication. *PLoS Pathog.*, 6(10):e1001141, 2010.
- [2] Adlroch, C., Kaiser, M., Ellerbrok, H., and Pauli, G. High prevalence of porcine Hokovirus in German wild boar populations. *Virol. J.*, 7:171, 2010.
- [3] Agbandje, M., McKenna, R., Rossmann, M. G., Strassheim, M. L., and Parrish, C. R. Structure determination of feline panleukopenia virus empty particles. *Proteins*, 16(2):155–171, Jun 1993.
- [4] Agbandje-McKenna, M. and Chapman, M. S. Correlating structure with function in the viral capsid. In Kerr, J. R., Bloom, M. E., Cotmore, S. F., Linden, R. M., and Parrish, C. R., eds., *Parvoviruses*, pp. 125–139. Hodder Arnold, London, UK, 2006.
- [5] Agbandje-McKenna, M., Llamas-Saiz, A. L., Wang, F., Tattersall, P., and Rossmann, M. G. Functional implications of the structure of the murine parvovirus, minute virus of mice. *Structure*, 6(11):1369–1381, Nov 1998.
- [6] Ahn, J. K., Gavin, B. J., Kumar, G., and Ward, D. C. Transcriptional analysis of minute virus of mice P4 promoter mutants. *J. Virol.*, 63(12):5425–5439, Dec 1989.
- [7] Aitken, A. 14-3-3 proteins on the MAP. *Trends Biochem. Sci.*, 20(3):95–97, Mar 1995.
- [8] Akache, B., Grimm, D., Pandey, K., Yant, S. R., Xu, H., and Kay, M. A. The 37/67-kilodalton laminin receptor is a receptor for adeno-associated virus serotypes 8, 2, 3, and 9. *J. Virol.*, 80(19):9831–9836, Oct 2006.
- [9] Alexandersen, S., Bloom, M. E., and Perryman, S. Detailed transcription map of Aleutian mink disease parvovirus. *J. Virol.*, 62(10):3684–3694, Oct 1988.
- [10] Allander, T., Emerson, S. U., Engle, R. E., Purcell, R. H., and Bukh, J. A virus discovery method incorporating DNase treatment and its application to the identification of two bovine parvovirus species. *Proc. Natl. Acad. Sci. U.S.A.*, 98(20):11609–11614, Sep 2001.
- [11] Allander, T., Tammi, M. T., Eriksson, M., Bjerkner, A., Tiveljung-Lindell, A., and Andersson, B. Cloning of a human parvovirus by molecular screening of respiratory tract samples. *Proc. Natl. Acad. Sci. U.S.A.*, 102(36):12891–12896, Sep 2005.
- [12] Allaume, X., El-Andaloussi, N., Leuchs, B., Bonifati, S., Kulkarni, A., Marttila, T., Kaufmann, J. K., Netzelbeck, D. M., Kleinschmidt, J., Rommelaere, J., and Marchini, A. Retargeting of rat parvovirus H-1PV to cancer cells through genetic engineering of the viral capsid. *J. Virol.*, 86(7):3452–3465, Apr 2012.
- [13] Angata, T. and Varki, A. Chemical diversity in the sialic acids and related alpha-keto acids: an evolutionary perspective. *Chem. Rev.*, 102(2):439–469, Feb 2002.
- [14] Antonietti, J. P., Sahli, R., Beard, P., and Hirt, B. Characterization of the cell type-specific determinant in the genome of minute virus of mice. *J. Virol.*, 62(2), Feb 1988.
- [15] Asokan, A., Hamra, J. B., Govindasamy, L., Agbandje-McKenna, M., and Samulski, R. J. Adeno-associated virus type 2 contains an integrin alapha5beta1 binding domain essential for viral cell entry. *J. Virol.*, 80(18):8961–8969, Sep 2006.
- [16] Astell, C. R., Smith, M., Chow, M. B., and Ward, D. C. Structure of the 3' hairpin termini of four rodent parvovirus genomes: nucleotide sequence homology at origins of DNA replication. *Cell*, 17(3):691–703, Jul 1979.
- [17] Astell, C. R., Thomson, M., Chow, M. B., and Ward, D. C. Structure and replication of minute virus of mice DNA. *Cold Spring Harb. Symp. Quant. Biol.*, 47 Pt 2:751–762, 1983.

- [18] Astell, C. R., Thomson, M., Merchlinsky, M., and Ward, D. C. The complete DNA sequence of minute virus of mice, an autonomous parvovirus. *Nucleic Acids Res.*, 11(4):999–1018, Feb 1983.
- [19] Astell, C. R., Chow, M. B., and Ward, D. C. Sequence analysis of the termini of virion and replicative forms of minute virus of mice DNA suggests a modified rolling hairpin model for autonomous parvovirus DNA replication. *J. Virol.*, 54(1):171–177, Apr 1985.
- [20] Astell, C. R., Gardiner, E. M., and Tattersall, P. DNA sequence of the lymphotropic variant of minute virus of mice, MVM(i), and comparison with the DNA sequence of the fibrotropic prototype strain. *J. Virol.*, 57(2):656–669, Feb 1986.
- [21] Atchison, R. W. The role of herpesviruses in adenovirus-associated virus replication in vitro. *Virology*, 42(1):155–162, Sep 1970.
- [22] Baldauf, A. Q., Willwand, K., Mumtsidu, E., Nüesch, J. P., and Rommelaere, J. Specific initiation of replication at the right-end telomere of the closed species of minute virus of mice replicative-form DNA. *J. Virol.*, 71(2):971–980, Feb 1997.
- [23] Ball-Goodrich, L. J. and Tattersall, P. Two amino acid substitutions within the capsid are coordinately required for acquisition of fibrotropism by the lymphotropic strain of minute virus of mice. *J. Virol.*, 66(6):3415–3423, Jun 1992.
- [24] Ball-Goodrich, L. J., Moir, R. D., and Tattersall, P. Parvoviral target cell specificity: acquisition of fibrotropism by a mutant of the lymphotropic strain of minute virus of mice involves multiple amino acid substitutions within the capsid. *Virology*, 184(1):175–186, Sep 1991.
- [25] Bantel-Schaal, U., Braspenning-Wesch, I., and Kartenbeck, J. Adeno-associated virus type 5 exploits two different entry pathways in human embryo fibroblasts. *J. Gen. Virol.*, 90(Pt 2):317–322, Feb 2009.
- [26] Bar, S., Daeffler, L., Rommelaere, J., and Nüesch, J. P. Vesicular egress of non-enveloped lytic parvoviruses depends on gelsolin functioning. *PLoS Pathog.*, 4(8):e1000126, 2008.
- [27] Bar, S., Rommelaere, J., and Nüesch, J. P. Vesicular transport of progeny parvovirus particles through ER and Golgi regulates maturation and cytolysis. *PLoS Pathog.*, 9(9):e1003605, Sep 2013.
- [28] Barbis, D. P., Chang, S. F., and Parrish, C. R. Mutations adjacent to the dimple of the canine parvovirus capsid structure affect sialic acid binding. *Virology*, 191(1):301–308, Nov 1992.
- [29] Barnes, H. J., Guy, J. S., and Vaillancourt, J. P. Poult enteritis complex. *Rev. - Off. Int. Epizoot.*, 19(2):565–588, Aug 2000.
- [30] Bartlett, J. S., Wilcher, R., and Samulski, R. J. Infectious entry pathway of adeno-associated virus and adeno-associated virus vectors. *J. Virol.*, 74(6):2777–2785, Mar 2000.
- [31] Basak, S. and Turner, H. Infectious entry pathway for canine parvovirus. *Virology*, 186(2):368–376, Feb 1992.
- [32] Basak, S., Turner, H., and Parr, S. Identification of a 40- to 42-kDa attachment polypeptide for canine parvovirus in A72 cells. *Virology*, 205(1):7–16, Nov 1994.
- [33] Bashir, T., Horlein, R., Rommelaere, J., and Willwand, K. Cyclin A activates the DNA polymerase delta -dependent elongation machinery in vitro: A parvovirus DNA replication model. *Proc. Natl. Acad. Sci. U.S.A.*, 97(10):5522–5527, May 2000.
- [34] Bashir, T., Rommelaere, J., and Cziepluch, C. In vivo accumulation of cyclin A and cellular replication factors in autonomous parvovirus minute virus of mice-associated replication bodies. *J. Virol.*, 75(9):4394–4398, May 2001.
- [35] Bastien, N., Chui, N., Robinson, J. L., Lee, B. E., Dust, K., Hart, L., and Li, Y. Detection of human bocavirus in Canadian children in a 1-year study. *J. Clin. Microbiol.*, 45(2):610–613, Feb 2007.
- [36] Bates, R. C., Snyder, C. E., Banerjee, P. T., and Mitra, S. Autonomous parvovirus LuIII encapsidates equal amounts of plus and minus DNA strands. *J. Virol.*, 49(2):319–324, Feb 1984.
- [37] Bayburt, T. and Gelb, M. H. Interfacial catalysis by human 85 kDa cytosolic phospholipase A2 on anionic vesicles in the scooting mode. *Biochemistry*, 36(11):3216–3231, Mar 1997.
- [38] Bell, C. L., Vandenberghe, L. H., Bell, P., Limberis, M. P., Gao, G. P., Van Vliet, K., Agbandje-McKenna, M., and Wilson, J. M. The AAV9 receptor and its modification to improve in vivo lung gene transfer in mice. *J. Clin. Invest.*, 121(6):2427–2435, Jun 2011.

- [39] Belyi, V. A., Levine, A. J., and Skalka, A. M. Sequences from ancestral single-stranded DNA viruses in vertebrate genomes: the parvoviridae and circoviridae are more than 40 to 50 million years old. *J. Virol.*, 84(23):12458–12462, Dec 2010.
- [40] Bergeron, J., Hebert, B., and Tijssen, P. Genome organization of the Kresse strain of porcine parvovirus: identification of the allotropic determinant and comparison with those of NADL-2 and field isolates. *J. Virol.*, 70(4):2508–2515, Apr 1996.
- [41] Berns, K. I. and Adler, S. Separation of two types of adeno-associated virus particles containing complementary polynucleotide chains. *J. Virol.*, 9(2):394–396, Feb 1972.
- [42] Berns, K. I. and Rose, J. A. Evidence for a single-stranded adenovirus-associated virus genome: isolation and separation of complementary single strands. *J. Virol.*, 5(6):693–699, Jun 1970.
- [43] Bina, M., Ng, S. C., and Blasquez, V. Simian virus 40 chromatin interaction with the capsid proteins. *J. Biomol. Struct. Dyn.*, 1(3):689–704, Dec 1983.
- [44] Black, L. W. DNA packaging in dsDNA bacteriophages. *Annu. Rev. Microbiol.*, 43:267–292, 1989.
- [45] Blackburn, S. D., Cline, S. E., Hemming, J. P., and Johnson, F. B. Attachment of bovine parvovirus to O-linked alpha 2,3 neuraminic acid on glycophorin A. *Arch. Virol.*, 150(7):1477–1484, Jul 2005.
- [46] Blackburn, S. D., Steadman, R. A., and Johnson, F. B. Attachment of adeno-associated virus type 3H to fibroblast growth factor receptor 1. *Arch. Virol.*, 151(3):617–623, Mar 2006.
- [47] Blasquez, V., Beecher, S., and Bina, M. Simian virus 40 morphogenetic pathway. An analysis of assembly-defective tsB201 DNA protein complexes. *J. Biol. Chem.*, 258(13):8477–8484, Jul 1983.
- [48] Bleker, S., Sonntag, F., and Kleinschmidt, J. A. Mutational analysis of narrow pores at the fivefold symmetry axes of adeno-associated virus type 2 capsids reveals a dual role in genome packaging and activation of phospholipase A2 activity. *J. Virol.*, 79(4):2528–2540, Feb 2005.
- [49] Blomstrom, A. L., Stahl, K., Masembe, C., Okoth, E., Okurut, A. R., Atmnedi, P., Kemp, S., Bishop, R., Belak, S., and Berg, M. Viral metagenomic analysis of bushpigs (*Potamochoerus larvatus*) in Uganda identifies novel variants of Porcine parvovirus 4 and Torque teno sus virus 1 and 2. *Virol. J.*, 9:192, 2012.
- [50] Bloom, M. E., Race, R. E., and Wolfenbarger, J. B. Characterization of Aleutian disease virus as a parvovirus. *J. Virol.*, 35(3):836–843, Sep 1980.
- [51] Bloom, M. E., Berry, B. D., Wei, W., Perryman, S., and Wolfenbarger, J. B. Characterization of chimeric full-length molecular clones of Aleutian mink disease parvovirus (ADV): identification of a determinant governing replication of ADV in cell culture. *J. Virol.*, 67(10):5976–5988, Oct 1993.
- [52] Bloom, M. E., Martin, D. A., Oie, K. L., Huhtanen, M. E., Costello, F., Wolfenbarger, J. B., Hayes, S. F., and Agbandje-McKenna, M. Expression of Aleutian mink disease parvovirus capsid proteins in defined segments: localization of immunoreactive sites and neutralizing epitopes to specific regions. *J. Virol.*, 71(1):705–714, Jan 1997.
- [53] Blumel, J., Schmidt, I., Willkommen, H., and Lower, J. Inactivation of parvovirus B19 during pasteurization of human serum albumin. *Transfusion*, 42(8):1011–1018, Aug 2002.
- [54] Bönsch, C., Zuercher, C., Lieby, P., Kempf, C., and Ros, C. The globoside receptor triggers structural changes in the B19 virus capsid that facilitate virus internalization. *J. Virol.*, 84(22):11737–11746, Nov 2010.
- [55] Bodendorf, U., Cziepluch, C., Jauniaux, J. C., Rommelaere, J., and Salome, N. Nuclear export factor CRM1 interacts with nonstructural proteins NS2 from parvovirus minute virus of mice. *J. Virol.*, 73(9):7769–7779, Sep 1999.
- [56] Boisvert, M., Fernandes, S., and Tijssen, P. Multiple pathways involved in porcine parvovirus cellular entry and trafficking toward the nucleus. *J. Virol.*, 84(15):7782–7792, Aug 2010.
- [57] Bonnard, G. D., Manders, E. K., Campbell, D. A., Herberman, R. B., and Collins, M. J. Immunosuppressive activity of a subline of the mouse EL-4 lymphoma. Evidence for minute virus of mice causing the inhibition. *J. Exp. Med.*, 143(1):187–205, Jan 1976.
- [58] Boschetti, N., Wyss, K., Mischler, A., Hostettler, T., and Kempf, C. Stability of minute virus of mice against temperature and sodium hydroxide. *Biologicals*, 31(3):181–185, Sep 2003.
- [59] Bosma, G. C., Custer, R. P., and Bosma, M. J. A severe combined immunodeficiency mutation in the mouse. *Nature*, 301(5900):527–530, Feb 1983.

- [60] Bourguignon, G. J., Tattersall, P. J., and Ward, D. C. DNA of minute virus of mice: self-priming, nonpermuted, single-stranded genome with a 5'-terminal hairpin duplex. *J. Virol.*, 20(1):290–306, Oct 1976.
- [61] Bouyac-Bertoia, M., Dvorin, J. D., Fouchier, R. A., Jenkins, Y., Meyer, B. E., Wu, L. I., Emerman, M., and Malim, M. H. HIV-1 infection requires a functional integrase NLS. *Mol. Cell*, 7(5):1025–1035, May 2001.
- [62] Bowman, E. J., Siebers, A., and Altendorf, K. Bafilomycins: a class of inhibitors of membrane ATPases from microorganisms, animal cells, and plant cells. *Proc. Natl. Acad. Sci. U.S.A.*, 85(21):7972–7976, Nov 1988.
- [63] Brailovsky, C. Research on the rat K virus (Parvovirus ratti). I. A method of titration by plaques and its application to the study of the multiplication cycle of the virus. *Ann Inst Pasteur (Paris)*, 110(1):49–59, Jan 1966.
- [64] Brandenburger, A., Legendre, D., Avalosse, B., and Rommelaere, J. NS-1 and NS-2 proteins may act synergistically in the cytopathogenicity of parvovirus MVMp. *Virology*, 174(2):576–584, Feb 1990.
- [65] Brauniger, S., Fischer, I., and Peters, J. The temperature stability of bovine parvovirus. *Zentralbl Hyg Umweltmed*, 196(3):270–278, Oct 1994.
- [66] Brister, J. R. and Muzyczka, N. Rep-mediated nicking of the adeno-associated virus origin requires two biochemical activities, DNA helicase activity and transesterification. *J. Virol.*, 73(11):9325–9336, Nov 1999.
- [67] Brockhaus, K., Plaza, S., Pintel, D. J., Rommelaere, J., and Salome, N. Nonstructural proteins NS2 of minute virus of mice associate in vivo with 14-3-3 protein family members. *J. Virol.*, 70(11):7527–7534, Nov 1996.
- [68] Brown, K. E., Anderson, S. M., and Young, N. S. Erythrocyte P antigen: cellular receptor for B19 parvovirus. *Science*, 262(5130):114–117, Oct 1993.
- [69] Brownstein, D. G., Smith, A. L., Jacoby, R. O., Johnson, E. A., Hansen, G., and Tattersall, P. Pathogenesis of infection with a virulent allotropic variant of minute virus of mice and regulation by host genotype. *Lab. Invest.*, 65(3):357–364, Sep 1991.
- [70] Brownstein, D. G., Smith, A. L., Johnson, E. A., Pintel, D. J., Naeger, L. K., and Tattersall, P. The pathogenesis of infection with minute virus of mice depends on expression of the small nonstructural protein NS2 and on the genotype of the allotropic determinants VP1 and VP2. *J. Virol.*, 66(5):3118–3124, May 1992.
- [71] Bruemmer, A., Scholari, F., Lopez-Ferber, M., Conway, J. F., and Hewat, E. A. Structure of an insect parvovirus (*Junonia coenia* Densovirus) determined by cryo-electron microscopy. *J. Mol. Biol.*, 347(4):791–801, Apr 2005.
- [72] Bui, M., Whittaker, G., and Helenius, A. Effect of M1 protein and low pH on nuclear transport of influenza virus ribonucleoproteins. *J. Virol.*, 70(12):8391–8401, Dec 1996.
- [73] Buller, R. M., Janik, J. E., Sebring, E. D., and Rose, J. A. Herpes simplex virus types 1 and 2 completely help adenovirus-associated virus replication. *J. Virol.*, 40(1):241–247, Oct 1981.
- [74] Burbelo, P. D. and Hall, A. 14-3-3 proteins. Hot numbers in signal transduction. *Curr. Biol.*, 5(2):95–96, Feb 1995.
- [75] Burnett, E. and Tattersall, P. Reverse genetic system for the analysis of parvovirus telomeres reveals interactions between transcription factor binding sites in the hairpin stem. *J. Virol.*, 77(16):8650–8660, Aug 2003.
- [76] Burnett, E., Cotmore, S. F., and Tattersall, P. Segregation of a single outboard left-end origin is essential for the viability of parvovirus minute virus of mice. *J. Virol.*, 80(21):10879–10883, Nov 2006.
- [77] Caillet-Fauquet, P., Perros, M., Brandenburger, A., Spegelaere, P., and Rommelaere, J. Programmed killing of human cells by means of an inducible clone of parvoviral genes encoding non-structural proteins. *EMBO J.*, 9(9):2989–2995, Sep 1990.
- [78] Canaan, S., Zadori, Z., Ghomashchi, F., Bollinger, J., Sadilek, M., Moreau, M. E., Tijssen, P., and Gelb, M. H. Interfacial enzymology of parvovirus phospholipases A2. *J. Biol. Chem.*, 279(15):14502–14508, Apr 2004.
- [79] Carreira, A., Menendez, M., Reguera, J., Almendral, J. M., and Mateu, M. G. In vitro disassembly of a parvovirus capsid and effect on capsid stability of heterologous peptide insertions in surface loops. *J. Biol. Chem.*, 279(8):6517–6525, Feb 2004.
- [80] Castellanos, M., Perez, R., Carrillo, P. J., de Pablo, P. J., and Mateu, M. G. Mechanical disassembly of

- single virus particles reveals kinetic intermediates predicted by theory. *Biophys. J.*, 102(11):2615–2624, Jun 2012.
- [81] Cater, J. E. and Pintel, D. J. The small non-structural protein NS2 of the autonomous parvovirus minute virus of mice is required for virus growth in murine cells. *J. Gen. Virol.*, 73 (Pt 7):1839–1843, Jul 1992.
- [82] Chang, S. F., Sgro, J. Y., and Parrish, C. R. Multiple amino acids in the capsid structure of canine parvovirus coordinately determine the canine host range and specific antigenic and hemagglutination properties. *J. Virol.*, 66(12):6858–6867, Dec 1992.
- [83] Chapman, M. S. and Agbandje-McKenna, M. Atomic structure of viral particles. In Kerr, J. R., Bloom, M. E., Cotmore, S. F., Linden, R. M., and Parrish, C. R., eds., *Parvoviruses*, pp. 107–124. Hodder Arnold, London, UK, 2006.
- [84] Chapman, M. S. and Rossmann, M. G. Structure, sequence, and function correlations among parvoviruses. *Virology*, 194(2):491–508, Jun 1993.
- [85] Chapman, M. S. and Rossmann, M. G. Single-stranded DNA-protein interactions in canine parvovirus. *Structure*, 3(2):151–162, Feb 1995.
- [86] Chen, K. C., Shull, B. C., Moses, E. A., Lederman, M., Stout, E. R., and Bates, R. C. Complete nucleotide sequence and genome organization of bovine parvovirus. *J. Virol.*, 60(3):1085–1097, Dec 1986.
- [87] Chen, S., Kapturczak, M., Loiler, S. A., Zolotukhin, S., Glushakova, O. Y., Madsen, K. M., Samulski, R. J., Hauswirth, W. W., Campbell-Thompson, M., Berns, K. I., Flotte, T. R., Atkinson, M. A., Tisher, C. C., and Agarwal, A. Efficient transduction of vascular endothelial cells with recombinant adenovirus-associated virus serotype 1 and 5 vectors. *Hum. Gene Ther.*, 16(2):235–247, Feb 2005.
- [88] Cheng, W. X., Li, J. S., Huang, C. P., Yao, D. P., Liu, N., Cui, S. X., Jin, Y., and Duan, Z. J. Identification and nearly full-length genome characterization of novel porcine bocaviruses. *PLoS ONE*, 5(10):e13583, 2010.
- [89] Cheung, A. K., Wu, G., Wang, D., Bayles, D. O., Lager, K. M., and Vincent, A. L. Identification and molecular cloning of a novel porcine parvovirus. *Arch. Virol.*, 155(5):801–806, May 2010.
- [90] Christensen, J. and Tattersall, P. Parvovirus initiator protein NS1 and RPA coordinate replication fork progression in a reconstituted DNA replication system. *J. Virol.*, 76(13):6518–6531, Jul 2002.
- [91] Christensen, J., Pedersen, M., Aasted, B., and Alexandersen, S. Purification and characterization of the major nonstructural protein (NS-1) of Aleutian mink disease parvovirus. *J. Virol.*, 69(3):1802–1809, Mar 1995.
- [92] Christensen, J., Cotmore, S. F., and Tattersall, P. A novel cellular site-specific DNA-binding protein cooperates with the viral NS1 polypeptide to initiate parvovirus DNA replication. *J. Virol.*, 71(2):1405–1416, Feb 1997.
- [93] Christensen, J., Cotmore, S. F., and Tattersall, P. Parvovirus initiation factor PIF: a novel human DNA-binding factor which coordinately recognizes two ACGT motifs. *J. Virol.*, 71(8):5733–5741, Aug 1997.
- [94] Christensen, J., Cotmore, S. F., and Tattersall, P. Two new members of the emerging KDWK family of combinatorial transcription modulators bind as a heterodimer to flexibly spaced PuCGPy half-sites. *Mol. Cell. Biol.*, 19(11):7741–7750, Nov 1999.
- [95] Christensen, J., Cotmore, S. F., and Tattersall, P. Minute virus of mice initiator protein NS1 and a host KDWK family transcription factor must form a precise ternary complex with origin DNA for nicking to occur. *J. Virol.*, 75(15):7009–7017, Aug 2001.
- [96] Clemens, K. E. and Pintel, D. Minute virus of mice (MVM) mRNAs predominantly polyadenylate at a single site. *Virology*, 160(2):511–514, Oct 1987.
- [97] Clemens, K. E. and Pintel, D. J. The two transcription units of the autonomous parvovirus minute virus of mice are transcribed in a temporal order. *J. Virol.*, 62(4):1448–1451, Apr 1988.
- [98] Clemens, K. E., Cerutis, D. R., Burger, L. R., Yang, C. Q., and Pintel, D. J. Cloning of minute virus of mice cDNAs and preliminary analysis of individual viral proteins expressed in murine cells. *J. Virol.*, 64 (8):3967–3973, Aug 1990.
- [99] Clinton, G. M. and Hayashi, M. The parvovirus MVM: a comparison of heavy and light particle infectivity and their density conversion in vitro. *Virology*, 74(1):57–63, Oct 1976.
- [100] Cohen, S. and Pante, N. Pushing the envelope: microinjection of Minute virus of mice into Xenopus

- oocytes causes damage to the nuclear envelope. *J. Gen. Virol.*, 86(Pt 12):3243–3252, Dec 2005.
- [101] Cohen, S., Behzad, A. R., Carroll, J. B., and Pante, N. Parvoviral nuclear import: bypassing the host nuclear-transport machinery. *J. Gen. Virol.*, 87(Pt 11):3209–3213, Nov 2006.
- [102] Cohen, S., Marr, A. K., Garcin, P., and Pante, N. Nuclear envelope disruption involving host caspases plays a role in the parvovirus replication cycle. *J. Virol.*, 85(10):4863–4874, May 2011.
- [103] Colomar, M. C., Hirt, B., and Beard, P. Two segments in the genome of the immunosuppressive minute virus of mice determine the host-cell specificity, control viral DNA replication and affect viral RNA metabolism. *J. Gen. Virol.*, 79 (Pt 3):581–586, Mar 1998.
- [104] Corbau, R., Duverger, V., Rommelaere, J., and Nuesch, J. P. Regulation of MVM NS1 by protein kinase C: impact of mutagenesis at consensus phosphorylation sites on replicative functions and cytopathic effects. *Virology*, 278(1):151–167, Dec 2000.
- [105] Cossons, N., Faust, E. A., and Zannis-Hadjopoulos, M. DNA polymerase delta-dependent formation of a hairpin structure at the 5' terminal palindrome of the minute virus of mice genome. *Virology*, 216(1): 258–264, Feb 1996.
- [106] Cotmore, S. F. Gene expression in the autonomous parvoviruses. In Tijssen, P., ed., *Handbook of parvoviruses*, vol. 1, pp. 141–154. CRC Press, Inc., Boca Raton, FL, 1990.
- [107] Cotmore, S. F. and Tattersall, P. Organization of non-structural genes of the autonomous parvovirus minute virus of mice. *J. Virol.*, 58(3):724–732, Jun 1986.
- [108] Cotmore, S. F. and Tattersall, P. The NS-1 polypeptide of the autonomous parvovirus MVM is a nuclear phosphoprotein. *Virus Res.*, 4(3):243–250, May 1986.
- [109] Cotmore, S. F. and Tattersall, P. The autonomously replicating parvoviruses of vertebrates. *Adv. Virus Res.*, 33:91–174, 1987.
- [110] Cotmore, S. F. and Tattersall, P. The NS-1 polypeptide of minute virus of mice is covalently attached to the 5' termini of duplex replicative-form DNA and progeny single strands. *J. Virol.*, 62(3):851–860, Mar 1988.
- [111] Cotmore, S. F. and Tattersall, P. A genome-linked copy of the NS-1 polypeptide is located on the outside of infectious parvovirus particles. *J. Virol.*, 63(9): 3902–3911, Sep 1989.
- [112] Cotmore, S. F. and Tattersall, P. Alternate splicing in a parvoviral nonstructural gene links a common amino-terminal sequence to downstream domains which confer radically different localization and turnover characteristics. *Virology*, 177(2):477–487, Aug 1990.
- [113] Cotmore, S. F. and Tattersall, P. In vivo resolution of circular plasmids containing concatemer junction fragments from minute virus of mice DNA and their subsequent replication as linear molecules. *J. Virol.*, 66(1):420–431, Jan 1992.
- [114] Cotmore, S. F. and Tattersall, P. An asymmetric nucleotide in the parvoviral 3' hairpin directs segregation of a single active origin of DNA replication. *EMBO J.*, 13(17):4145–4152, Sep 1994.
- [115] Cotmore, S. F. and Tattersall, P. DNA replication in the autonomous parvoviruses. *Semin. Virol.*, 6: 271–281, 1995.
- [116] Cotmore, S. F. and Tattersall, P. Parvovirus DNA replication. In DePamphilis, M. L., ed., *DNA replication in eukaryotic cells*, pp. 799–813. Cold Spring Harbor Laboratory Press, Cold Spring Harbor, NY, 1996.
- [117] Cotmore, S. F. and Tattersall, P. High-mobility group 1/2 proteins are essential for initiating rolling-circle-type DNA replication at a parvovirus hairpin origin. *J. Virol.*, 72(11):8477–8484, Nov 1998.
- [118] Cotmore, S. F. and Tattersall, P. Parvoviruses. *eLS*, Jul 2003. John Wiley and Sons Ltd, Chichester, UK.
- [119] Cotmore, S. F. and Tattersall, P. Resolution of parvovirus dimer junctions proceeds through a novel heterocruciform intermediate. *J. Virol.*, 77(11):6245–6254, Jun 2003.
- [120] Cotmore, S. F. and Tattersall, P. Genome packaging sense is controlled by the efficiency of the nick site in the right-end replication origin of parvoviruses minute virus of mice and LuIII. *J. Virol.*, 79(4):2287–2300, Feb 2005.
- [121] Cotmore, S. F. and Tattersall, P. Encapsidation of minute virus of mice DNA: aspects of the translocation mechanism revealed by the structure of partially packaged genomes. *Virology*, 336(1):100–112, May 2005.

- [122] Cotmore, S. F. and Tattersall, P. A rolling-hairpin strategy: basic mechanisms of DNA replication in the parvoviruses. In Kerr, J. R., Bloom, M. E., Cotmore, S. F., Linden, R. M., and Parrish, C. R., eds., *Parvoviruses*, pp. 171–188. Hodder Arnold, London, UK, 2006.
- [123] Cotmore, S. F. and Tattersall, P. Parvoviruses. In De-Pamphilis, M. L., ed., *DNA Replication and Human Disease*, pp. 593–608. Cold Spring Harbor Laboratory Press, Cold Spring Harbor, NY, 2006.
- [124] Cotmore, S. F. and Tattersall, P. Structure and organization of the viral genome. In Kerr, J. R., Bloom, M. E., Cotmore, S. F., Linden, R. M., and Parrish, C. R., eds., *Parvoviruses*, pp. 73–90. Hodder Arnold, London, UK, 2006.
- [125] Cotmore, S. F. and Tattersall, P. Parvoviruses: Small Does Not Mean Simple. *Annual Review of Virol.*, 1: 515–537, Jul 2014.
- [126] Cotmore, S. F., Sturzenbecker, L. J., and Tattersall, P. The autonomous parvovirus MVM encodes two nonstructural proteins in addition to its capsid polypeptides. *Virology*, 129(2):333–343, Sep 1983.
- [127] Cotmore, S. F., Gunther, M., and Tattersall, P. Evidence for a ligation step in the DNA replication of the autonomous parvovirus minute virus of mice. *J. Virol.*, 63(2):1002–1006, Feb 1989.
- [128] Cotmore, S. F., Nüesch, J. P., and Tattersall, P. In vitro excision and replication of 5' telomeres of minute virus of mice DNA from cloned palindromic concatemer junctions. *Virology*, 190(1):365–377, Sep 1992.
- [129] Cotmore, S. F., Nüesch, J. P., and Tattersall, P. Asymmetric resolution of a parvovirus palindrome in vitro. *J. Virol.*, 67(3):1579–1589, Mar 1993.
- [130] Cotmore, S. F., Christensen, J., Nüesch, J. P., and Tattersall, P. The NS1 polypeptide of the murine parvovirus minute virus of mice binds to DNA sequences containing the motif [ACCA]2-3. *J. Virol.*, 69(3): 1652–1660, Mar 1995.
- [131] Cotmore, S. F., D'Abramo, A. M., Carbonell, L. F., Bratton, J., and Tattersall, P. The NS2 polypeptide of parvovirus MVM is required for capsid assembly in murine cells. *Virology*, 231(2):267–280, May 1997.
- [132] Cotmore, S. F., D'Abramo, A. M., Ticknor, C. M., and Tattersall, P. Controlled conformational transitions in the MVM virion expose the VP1 N-terminus and viral genome without particle disassembly. *Virology*, 254(1):169–181, Feb 1999.
- [133] Cotmore, S. F., Christensen, J., and Tattersall, P. Two widely spaced initiator binding sites create an HMG1-dependent parvovirus rolling-hairpin replication origin. *J. Virol.*, 74(3):1332–1341, Feb 2000.
- [134] Cotmore, S. F., Gottlieb, R. L., and Tattersall, P. Replication initiator protein NS1 of the parvovirus minute virus of mice binds to modular divergent sites distributed throughout duplex viral DNA. *J. Virol.*, 81(23):13015–13027, Dec 2007.
- [135] Cotmore, S. F., Hafenstein, S., and Tattersall, P. Depletion of virion-associated divalent cations induces parvovirus minute virus of mice to eject its genome in a 3'-to-5' direction from an otherwise intact viral particle. *J. Virol.*, 84(4):1945–1956, Feb 2010.
- [136] Cotmore, S. F., Agbandje-McKenna, M., Chiorni, J. A., Mukha, D. V., Pintel, D. J., Qiu, J., Soderlund-Venermo, M., Tattersall, P., Tijssen, P., Gatherer, D., and Davison, A. J. The family Parvoviridae. *Arch. Virol.*, 159(5):1239–1247, May 2014.
- [137] Crawford, L. V. A minute virus of mice. *Virology*, 29 (4):605–612, Aug 1966.
- [138] Crawford, L. V., Follett, E. A., Burdon, M. G., and McGeoch, D. J. The DNA of a minute virus of mice. *J. Gen. Virol.*, 4(1):37–46, Jan 1969.
- [139] Cziepluch, C., Lampel, S., Grewenig, A., Grund, C., Lichter, P., and Rommelaere, J. H-1 parvovirus-associated replication bodies: a distinct virus-induced nuclear structure. *J. Virol.*, 74(10):4807–4815, May 2000.
- [140] D'Abramo, A. M., Ali, A. A., Wang, F., Cotmore, S. F., and Tattersall, P. Host range mutants of Minute Virus of Mice with a single VP2 amino acid change require additional silent mutations that regulate NS2 accumulation. *Virology*, 340(1):143–154, Sep 2005.
- [141] Daigle, N., Beaudouin, J., Hartnell, L., Imreh, G., Hallberg, E., Lippincott-Schwartz, J., and Ellenberg, J. Nuclear pore complexes form immobile networks and have a very low turnover in live mammalian cells. *J. Cell Biol.*, 154(1):71–84, Jul 2001.
- [142] Day, J. M. and Zsak, L. Determination and analysis of the full-length chicken parvovirus genome. *Virology*, 399(1):59–64, Mar 2010.

- [143] Daya, S. and Berns, K. I. Gene therapy using adeno-associated virus vectors. *Clin. Microbiol. Rev.*, 21(4): 583–593, Oct 2008.
- [144] de Duve, C., de Barsy, T., Poole, B., Trouet, A., Tulkens, P., and Van Hoof, F. Commentary. Lysosomotropic agents. *Biochem. Pharmacol.*, 23(18): 2495–2531, Sep 1974.
- [145] Deiss, V., Tratschin, J. D., Weitz, M., and Siegl, G. Cloning of the human parvovirus B19 genome and structural analysis of its palindromic termini. *Virology*, 175(1):247–254, Mar 1990.
- [146] DeLano, W. L. *The PyMOL Molecular Graphic System*. DeLano Scientific, San Carlos, CA, 2002.
- [147] Deleu, L., Fuks, F., Spitkovsky, D., Horlein, R., Faisst, S., and Rommelaere, J. Opposite transcriptional effects of cyclic AMP-responsive elements in confluent or p27KIP-overexpressing cells versus serum-starved or growing cells. *Mol. Cell. Biol.*, 18(1):409–419, Jan 1998.
- [148] Di Pasquale, G., Davidson, B. L., Stein, C. S., Martins, I., Scudiero, D., Monks, A., and Chiorini, J. A. Identification of PDGFR as a receptor for AAV-5 transduction. *Nat. Med.*, 9(10):1306–1312, Oct 2003.
- [149] Di Pasquale, G., Kaludov, N., Agbandje-McKenna, M., and Chiorini, J. A. BAAV transcytosis requires an interaction with beta-1-4 linked- glucosamine and gp96. *PLoS ONE*, 5(3):e9336, 2010.
- [150] Di Piazza, M., Mader, C., Geletneky, K., Herrero Y Calle, M., Weber, E., Schlehofer, J., Deleu, L., and Rommelaere, J. Cytosolic activation of cathepsins mediates parvovirus H-1-induced killing of cisplatin and TRAIL-resistant glioma cells. *J. Virol.*, 81(8): 4186–4198, Apr 2007.
- [151] Dimcheff, D. E., Askovic, S., Baker, A. H., Johnson-Fowler, C., and Portis, J. L. Endoplasmic reticulum stress is a determinant of retrovirus-induced spongiform neurodegeneration. *J. Virol.*, 77(23):12617–12629, Dec 2003.
- [152] Ding, W., Zhang, L., Yan, Z., and Engelhardt, J. F. Intracellular trafficking of adeno-associated viral vectors. *Gene Ther.*, 12(11):873–880, Jun 2005.
- [153] Doerig, C., Beard, P., and Hirt, B. A transcriptional promoter of the human parvovirus B19 active in vitro and in vivo. *Virology*, 157(2):539–542, Apr 1987.
- [154] Doerig, C., Hirt, B., Beard, P., and Antonietti, J. P. Minute virus of mice non-structural protein NS-1 is necessary and sufficient for trans-activation of the viral P39 promoter. *J. Gen. Virol.*, 69 (Pt 10):2563–2573, Oct 1988.
- [155] Dorsch, S., Liebisch, G., Kaufmann, B., von Landenberg, P., Hoffmann, J. H., Drobnik, W., and Modrow, S. The VP1 unique region of parvovirus B19 and its constituent phospholipase A2-like activity. *J. Virol.*, 76(4):2014–2018, Feb 2002.
- [156] Douar, A. M., Poulard, K., Stockholm, D., and Danos, O. Intracellular trafficking of adeno-associated virus vectors: routing to the late endosomal compartment and proteasome degradation. *J. Virol.*, 75(4): 1824–1833, Feb 2001.
- [157] Douglas, T. and Young, M. Viruses: making friends with old foes. *Science*, 312(5775):873–875, May 2006.
- [158] Duan, D., Li, Q., Kao, A. W., Yue, Y., Pessin, J. E., and Engelhardt, J. F. Dynamin is required for recombinant adeno-associated virus type 2 infection. *J. Virol.*, 73(12):10371–10376, Dec 1999.
- [159] Duan, D., Yue, Y., Yan, Z., Yang, J., and Engelhardt, J. F. Endosomal processing limits gene transfer to polarized airway epithelia by adeno-associated virus. *J. Clin. Invest.*, 105(11):1573–1587, Jun 2000.
- [160] Dworetzky, S. I. and Feldherr, C. M. Translocation of RNA-coated gold particles through the nuclear pores of oocytes. *J. Cell Biol.*, 106(3):575–584, Mar 1988.
- [161] Eichwald, V., Daeffler, L., Klein, M., Rommelaere, J., and Salome, N. The NS2 proteins of parvovirus minute virus of mice are required for efficient nuclear egress of progeny virions in mouse cells. *J. Virol.*, 76(20):10307–10319, Oct 2002.
- [162] Engelsma, D., Valle, N., Fish, A., Salome, N., Almendral, J. M., and Fornerod, M. A supraphysiological nuclear export signal is required for parvovirus nuclear export. *Mol. Biol. Cell*, 19(6):2544–2552, Jun 2008.
- [163] Engers, H. D., Louis, J. A., Zubler, R. H., and Hirt, B. Inhibition of T cell-mediated functions by MVM(i), a parvovirus closely related to minute virus of mice. *J. Immunol.*, 127(6):2280–2285, Dec 1981.
- [164] Fahrenkrog, B. and Aeby, U. The nuclear pore complex: nucleocytoplasmic transport and beyond. *Nat. Rev. Mol. Cell Biol.*, 4(10):757–766, Oct 2003.

- [165] Faisst, S., Perros, M., Deleu, L., Spruyt, N., and Rommelaere, J. Mapping of upstream regulatory elements in the P4 promoter of parvovirus minute virus of mice. *Virology*, 202(1):466–470, Jul 1994.
- [166] Farr, G. A., Zhang, L. G., and Tattersall, P. Parvoviral virions deploy a capsid-tethered lipolytic enzyme to breach the endosomal membrane during cell entry. *Proc. Natl. Acad. Sci. U.S.A.*, 102(47):17148–17153, Nov 2005.
- [167] Farr, G. A., Cotmore, S. F., and Tattersall, P. VP2 cleavage and the leucine ring at the base of the five-fold cylinder control pH-dependent externalization of both the VP1 N terminus and the genome of minute virus of mice. *J. Virol.*, 80(1):161–171, Jan 2006.
- [168] Fields, B. N. and Greene, M. I. Genetic and molecular mechanisms of viral pathogenesis: implications for prevention and treatment. *Nature*, 300(5887):19–23, Nov 1982.
- [169] Fox, J. M. and Bloom, M. E. Identification of a cell surface protein from Crandell feline kidney cells that specifically binds Aleutian mink disease parvovirus. *J. Virol.*, 73(5):3835–3842, May 1999.
- [170] Fried, H. and Kutay, U. Nucleocytoplasmic transport: taking an inventory. *Cell. Mol. Life Sci.*, 60(8):1659–1688, Aug 2003.
- [171] Fuks, F., Deleu, L., Dinsart, C., Rommelaere, J., and Faisst, S. ras oncogene-dependent activation of the P4 promoter of minute virus of mice through a proximal P4 element interacting with the Ets family of transcription factors. *J. Virol.*, 70(3):1331–1339, Mar 1996.
- [172] Gao, G., Alvira, M. R., Somanathan, S., Lu, Y., Vandenbergh, L. H., Rux, J. J., Calcedo, R., Sanmiguel, J., Abbas, Z., and Wilson, J. M. Adeno-associated viruses undergo substantial evolution in primates during natural infections. *Proc. Natl. Acad. Sci. U.S.A.*, 100(10):6081–6086, May 2003.
- [173] Garcia-Bustos, J., Heitman, J., and Hall, M. N. Nuclear protein localization. *Biochim. Biophys. Acta*, 1071(1):83–101, Mar 1991.
- [174] Garcin, P. O. and Panté, N. The minute virus of mice exploits different endocytic pathways for cellular uptake. *Virology*, 482:157–166, Apr 2015.
- [175] Gardiner, E. M. and Tattersall, P. Evidence that developmentally regulated control of gene expression by a parvoviral allotropic determinant is particle mediated. *J. Virol.*, 62(5):1713–1722, May 1988.
- [176] Gardiner, E. M. and Tattersall, P. Mapping of the fibrotropic and lymphotropic host range determinants of the parvovirus minute virus of mice. *J. Virol.*, 62(8):2605–2613, Aug 1988.
- [177] Gavin, B. J. and Ward, D. C. Positive and negative regulation of the minute virus of mice P38 promoter. *J. Virol.*, 64(5):2057–2063, May 1990.
- [178] Gelb, M. H., Jain, M. K., Hanel, A. M., and Berg, O. G. Interfacial enzymology of glycerolipid hydro-lases: lessons from secreted phospholipases A2. *Annu. Rev. Biochem.*, 64:653–688, 1995.
- [179] Gersappe, A. and Pintel, D. J. CA- and purine-rich elements form a novel bipartite exon enhancer which governs inclusion of the minute virus of mice NS2-specific exon in both singly and doubly spliced mRNAs. *Mol. Cell. Biol.*, 19(1):364–375, Jan 1999.
- [180] Gershon, D., Sachs, L., and Winocour, E. The induction of cellular DNA synthesis by simian virus 40 in contact-inhibited and in x-irradiated cells. *Proc. Natl. Acad. Sci. U.S.A.*, 56(3):918–925, Sep 1966.
- [181] Gil-Ranedo, J., Hernando, E., Riolobos, L., Dominguez, C., Kann, M., and Almendral, J. M. The Mammalian Cell Cycle Regulates Parvovirus Nuclear Capsid Assembly. *PLoS Pathog.*, 11(6):e1004920, Jun 2015.
- [182] Girod, A., Wobus, C. E., Zadori, Z., Ried, M., Leike, K., Tijssen, P., Kleinschmidt, J. A., and Hallek, M. The VP1 capsid protein of adeno-associated virus type 2 is carrying a phospholipase A2 domain required for virus infectivity. *J. Gen. Virol.*, 83(Pt 5):973–978, May 2002.
- [183] Goodwin, M. A., Davis, J. F., McNulty, M. S., Brown, J., and Player, E. C. Enteritis (so-called runting stunting syndrome) in Georgia broiler chicks. *Avian Dis.*, 37(2):451–458, 1993.
- [184] Gottschalck, E., Andersen, S., Cohn, A., Poulsen, L. A., Bloom, M. E., and Aasted, B. Nucleotide sequence analysis of Aleutian mink disease parvovirus shows that multiple virus types are present in infected mink. *J. Virol.*, 65(8):4378–4386, Aug 1991.
- [185] Govindasamy, L., Hueffer, K., Parrish, C. R., and Agbandje-McKenna, M. Structures of host range-controlling regions of the capsids of canine and feline parvoviruses and mutants. *J. Virol.*, 77(22):12211–12221, Nov 2003.

- [186] Green, M. R. Biochemical mechanisms of constitutive and regulated pre-mRNA splicing. *Annu. Rev. Cell Biol.*, 7:559–599, 1991.
- [187] Green, M. R. and Roeder, R. G. Definition of a novel promoter for the major adenovirus-associated virus mRNA. *Cell*, 22(1 Pt 1):231–242, Nov 1980.
- [188] Gu, Z., Plaza, S., Perros, M., Cziepluch, C., Rommelaere, J., and Cornelis, J. J. NF-Y controls transcription of the minute virus of mice P4 promoter through interaction with an unusual binding site. *J. Virol.*, 69(1):239–246, Jan 1995.
- [189] Gunther, M. and Tattersall, P. The terminal protein of minute virus of mice is an 83 kilodalton polypeptide linked to specific forms of double-stranded and single-stranded viral DNA. *FEBS Lett.*, 242(1):22–26, Dec 1988.
- [190] Gurda, B. L., Parent, K. N., Bladék, H., Sinkovits, R. S., DiMatta, M. A., Rence, C., Castro, A., McKenna, R., Olson, N., Brown, K., Baker, T. S., and Agbandje-McKenna, M. Human bocavirus capsid structure: insights into the structural repertoire of the parvoviridae. *J. Virol.*, 84(12):5880–5889, Jun 2010.
- [191] Hafenstein, S. and Fane, B. A. ϕ X174 genome-capsid interactions influence the biophysical properties of the virion: evidence for a scaffolding-like function for the genome during the final stages of morphogenesis. *J. Virol.*, 76(11):5350–5356, Jun 2002.
- [192] Halder, S., Ng, R., and Agbandje-McKenna, M. Parvoviruses: structure and infection. *Future Virol.*, 7(3):253–278, Mar 2012.
- [193] Hallauer, C., Siegl, G., and Kronauer, G. Parvoviruses as contaminants of permanent human cell lines. 3. Biological properties of the isolated viruses. *Arch Gesamte Virusforsch*, 38(4):366–382, 1972.
- [194] Hansen, J., Qing, K., Kwon, H. J., Mah, C., and Srivastava, A. Impaired intracellular trafficking of adeno-associated virus type 2 vectors limits efficient transduction of murine fibroblasts. *J. Virol.*, 74(2):992–996, Jan 2000.
- [195] Hansen, J., Qing, K., and Srivastava, A. Adeno-associated virus type 2-mediated gene transfer: altered endocytic processing enhances transduction efficiency in murine fibroblasts. *J. Virol.*, 75(9):4080–4090, May 2001.
- [196] Hansen, J., Qing, K., and Srivastava, A. Infection of purified nuclei by adeno-associated virus 2. *Mol. Ther.*, 4(4):289–296, Oct 2001.
- [197] Hanson, N. D. and Rhode, S. L. Parvovirus NS1 stimulates P4 expression by interaction with the terminal repeats and through DNA amplification. *J. Virol.*, 65(8):4325–4333, Aug 1991.
- [198] Harbison, C. E., Chiorini, J. A., and Parrish, C. R. The parvovirus capsid odyssey: from the cell surface to the nucleus. *Trends Microbiol.*, 16(5):208–214, May 2008.
- [199] Harlow, E., Crawford, L. V., Pim, D. C., and Williamson, N. M. Monoclonal antibodies specific for simian virus 40 tumor antigens. *J. Virol.*, 39(3):861–869, Sep 1981.
- [200] Harris, R. E., Coleman, P. H., and Morahan, P. S. Stability of minute virus of mice to chemical and physical agents. *Appl Microbiol.*, 28(3):351–354, Sep 1974.
- [201] Harrison, S. C. Viral membrane fusion. *Nat. Struct. Mol. Biol.*, 15(7):690–698, Jul 2008.
- [202] Harrison, S. C., Skehel, J. J., and Wiley, D. C. Virus structure. In Fields, B. N., Knipe, D. M., Howley, P. M., Chanock, R. M., Melnick, J. L., Monath, T. P., Roizman, B., and Straus, S. E., eds., *Fundamental Virology*, pp. 59–99. Lippincott-Raven Press, Philadelphia, PA, 1996.
- [203] Hatanaka, M. and Dulbecco, R. Induction of DNA synthesis by SV40. *Proc. Natl. Acad. Sci. U.S.A.*, 56(2):736–740, Aug 1966.
- [204] Haut, D. D. and Pintel, D. J. Intron definition is required for excision of the minute virus of mice small intron and definition of the upstream exon. *J. Virol.*, 72(3):1834–1843, Mar 1998.
- [205] Haut, D. D. and Pintel, D. J. Inclusion of the NS2-specific exon in minute virus of mice mRNA is facilitated by an intronic splicing enhancer that affects definition of the downstream small intron. *Virology*, 258(1):84–94, May 1999.
- [206] Heegaard, E. D. and Brown, K. E. Human parvovirus B19. *Clin. Microbiol. Rev.*, 15(3):485–505, Jul 2002.
- [207] Hensens, O. D., Monaghan, R. L., Huang, L., and Albers-Schönberg, G. Structure of the sodium and potassium ion activated adenosine triphosphatase inhibitor L-681,110. *J. Am. Soc.*, 105(11):3672–3679, 1983.

- [208] Hernando, E., Llamas-Saiz, A. L., Foces-Foces, C., McKenna, R., Portman, I., Agbandje-McKenna, M., and Almendral, J. M. Biochemical and physical characterization of parvovirus minute virus of mice virus-like particles. *Virology*, 267(2):299–309, Feb 2000.
- [209] Hirt, B. Molecular biology of autonomous parvoviruses. *Contrib Microbiol*, 4:163–177, 2000.
- [210] Hoelzer, K. and Parrish, C. R. The emergence of parvoviruses of carnivores. *Vet. Res.*, 41(6):39, 2010.
- [211] Hoggan, M. D., Blacklow, N. R., and Rowe, W. P. Studies of small DNA viruses found in various adenovirus preparations: physical, biological, and immunological characteristics. *Proc. Natl. Acad. Sci. U.S.A.*, 55(6):1467–1474, Jun 1966.
- [212] Hoggan, M. D., Maramorosch, K., and Kurstak, E. *Small DNA viruses*. Academic Press, New York, NY, 1971.
- [213] Holland, J. J. Receptor affinities as major determinants of enterovirus tissue tropisms in humans. *Virology*, 15:312–326, Nov 1961.
- [214] Hoque, M., Ishizu, K., Matsumoto, A., Han, S. I., Arisaka, F., Takayama, M., Suzuki, K., Kato, K., Kanda, T., Watanabe, H., and Handa, H. Nuclear transport of the major capsid protein is essential for adeno-associated virus capsid formation. *J. Virol.*, 73(9):7912–7915, Sep 1999.
- [215] Horiuchi, M., Ishiguro, N., Goto, H., and Shinagawa, M. Characterization of the stage(s) in the virus replication cycle at which the host-cell specificity of the feline parvovirus subgroup is regulated in canine cells. *Virology*, 189(2):600–608, Aug 1992.
- [216] Huang, L., Albers-Schonberg, G., Monaghan, R. L., Jakubas, K., Pong, S. S., Hensens, O. D., Burg, R. W., Ostlind, D. A., Conroy, J., and Stapley, E. O. Discovery, production and purification of the Na^+ , K^+ activated ATPase inhibitor, L-681,110 from the fermentation broth of *Streptomyces* sp. MA-5038. *J. Antibiot.*, 37(9):970–975, Sep 1984.
- [217] Huang, L., Zhai, S. L., Cheung, A. K., Zhang, H. B., Long, J. X., and Yuan, S. S. Detection of a novel porcine parvovirus, PPV4, in Chinese swine herds. *Virol. J.*, 7:333, 2010.
- [218] Hueffer, K. and Parrish, C. R. Parvovirus host range, cell tropism and evolution. *Curr. Opin. Microbiol.*, 6(4):392–398, Aug 2003.
- [219] Hueffer, K., Govindasamy, L., Agbandje-McKenna, M., and Parrish, C. R. Combinations of two capsid regions controlling canine host range determine canine transferrin receptor binding by canine and feline parvoviruses. *J. Virol.*, 77(18):10099–10105, Sep 2003.
- [220] Hueffer, K., Parker, J. S., Weichert, W. S., Geisel, R. E., Sgro, J. Y., and Parrish, C. R. The natural host range shift and subsequent evolution of canine parvovirus resulted from virus-specific binding to the canine transferrin receptor. *J. Virol.*, 77(3):1718–1726, Feb 2003.
- [221] Ilyina, T. V. and Koonin, E. V. Conserved sequence motifs in the initiator proteins for rolling circle DNA replication encoded by diverse replicons from eubacteria, eucaryotes and archaebacteria. *Nucleic Acids Res.*, 20(13):3279–3285, Jul 1992.
- [222] Im, D. S. and Muzyczka, N. The AAV origin binding protein Rep68 is an ATP-dependent site-specific endonuclease with DNA helicase activity. *Cell*, 61(3):447–457, May 1990.
- [223] Itah, R., Tal, J., and Davis, C. Host cell specificity of minute virus of mice in the developing mouse embryo. *J. Virol.*, 78(17):9474–9486, Sep 2004.
- [224] Jindal, H. K., Yong, C. B., Wilson, G. M., Tam, P., and Astell, C. R. Mutations in the NTP-binding motif of minute virus of mice (MVM) NS-1 protein uncouple ATPase and DNA helicase functions. *J. Biol. Chem.*, 269(5):3283–3289, Feb 1994.
- [225] Johnson, F. B., Fenn, L. B., Owens, T. J., Faucheuix, L. J., and Blackburn, S. D. Attachment of bovine parvovirus to sialic acids on bovine cell membranes. *J. Gen. Virol.*, 85(Pt 8):2199–2207, Aug 2004.
- [226] Jones, M. S., Kapoor, A., Lukashov, V. V., Simmonds, P., Hecht, F., and Delwart, E. New DNA viruses identified in patients with acute viral infection syndrome. *J. Virol.*, 79(13):8230–8236, Jul 2005.
- [227] Jongeneel, C. V., Sahli, R., McMaster, G. K., and Hirt, B. A precise map of splice junctions in the mRNAs of minute virus of mice, an autonomous parvovirus. *J. Virol.*, 59(3):564–573, Sep 1986.
- [228] Kalderon, D., Richardson, W. D., Markham, A. F., and Smith, A. E. Sequence requirements for nuclear location of simian virus 40 large-T antigen. *Nature*, 311(5981):33–38, 1984.
- [229] Kalderon, D., Roberts, B. L., Richardson, W. D., and Smith, A. E. A short amino acid sequence able to

- specify nuclear location. *Cell*, 39(3 Pt 2):499–509, Dec 1984.
- [230] Kaludov, N., Brown, K. E., Walters, R. W., Zabner, J., and Chiorini, J. A. Adeno-associated virus serotype 4 (AAV4) and AAV5 both require sialic acid binding for hemagglutination and efficient transduction but differ in sialic acid linkage specificity. *J. Virol.*, 75(15):6884–6893, Aug 2001.
- [231] Kamerling, J. P. and Gerwig, G. J. Structural analysis of naturally occurring sialic acids. *Methods Mol. Biol.*, 347:69–91, 2006.
- [232] Kannagi, R. Molecular mechanism for cancer-associated induction of sialyl Lewis X and sialyl Lewis A expression-The Warburg effect revisited. *Glycoconj. J.*, 20(5):353–364, 2004.
- [233] Kasamatsu, H. and Nakanishi, A. How do animal DNA viruses get to the nucleus? *Annu. Rev. Microbiol.*, 52:627–686, 1998.
- [234] Kashiwakura, Y., Tamayose, K., Iwabuchi, K., Hirai, Y., Shimada, T., Matsumoto, K., Nakamura, T., Watanabe, M., Oshimi, K., and Daida, H. Hepatocyte growth factor receptor is a coreceptor for adeno-associated virus type 2 infection. *J. Virol.*, 79(1):609–614, Jan 2005.
- [235] Kaufmann, B., Baxa, U., Chipman, P. R., Rossmann, M. G., Modrow, S., and Seckler, R. Parvovirus B19 does not bind to membrane-associated globoside in vitro. *Virology*, 332(1):189–198, Feb 2005.
- [236] Kaufmann, B., Lopez-Bueno, A., Mateu, M. G., Chipman, P. R., Nelson, C. D., Parrish, C. R., Almendral, J. M., and Rossmann, M. G. Minute virus of mice, a parvovirus, in complex with the Fab fragment of a neutralizing monoclonal antibody. *J. Virol.*, 81(18):9851–9858, Sep 2007.
- [237] Kawase, M., Momoeda, M., Young, N. S., and Kajigaya, S. Modest truncation of the major capsid protein abrogates B19 parvovirus capsid formation. *J. Virol.*, 69(10):6567–6571, Oct 1995.
- [238] Kilham, L. and Olivier, L. J. A latent virus of rats isolated in tissue culture. *Virology*, 7(4):428–437, Apr 1959.
- [239] Kimsey, P. B., Engers, H. D., Hirt, B., and Jongeneel, C. V. Pathogenicity of fibroblast- and lymphocyte-specific variants of minute virus of mice. *J. Virol.*, 59(1):8–13, Jul 1986.
- [240] King, A. M. Q., Adams, M. J., Carstens, E. B., and Lefkowitz, E. J. *Virus taxonomy: Ninth report of the International Committee on Taxonomy of Viruses*. Elsevier Academic Press, San Diego, CA, 2012.
- [241] King, J. A., Dubielzig, R., Grimm, D., and Kleinschmidt, J. A. DNA helicase-mediated packaging of adeno-associated virus type 2 genomes into preformed capsids. *EMBO J.*, 20(12):3282–3291, Jun 2001.
- [242] Kisary, J. Experimental infection of chicken embryos and day-old chickens with parvovirus of chicken origin. *Avian Pathol.*, 14(1):1–7, Jan 1985.
- [243] Kisary, J., Nagy, B., and Bitay, Z. Presence of parvoviruses in the intestine of chickens showing stunting syndrome. *Avian Pathol.*, 13(2):339–343, Apr 1984.
- [244] Kisary, J., Avalosse, B., Miller-Faures, A., and Rommelalaere, J. The genome structure of a new chicken virus identifies it as a parvovirus. *J. Gen. Virol.*, 66 (Pt 10):2259–2263, Oct 1985.
- [245] Kleinschmidt, J. A. and King, J. A. Molecular interactions involved in assembling the viral particle and packaging the genome. In Kerr, J. R., Bloom, M. E., Cotmore, S. F., Linden, R. M., and Parrish, C. R., eds., *Parvoviruses*, pp. 305–319. Hodder Arnold, London, UK, 2006.
- [246] Kontou, M., Govindasamy, L., Nam, H. J., Bryant, N., Llamas-Saiz, A. L., Foces-Foces, C., Hernando, E., Rubio, M. P., McKenna, R., Almendral, J. M., and Agbandje-McKenna, M. Structural determinants of tissue tropism and in vivo pathogenicity for the parvovirus minute virus of mice. *J. Virol.*, 79(17):10931–10943, Sep 2005.
- [247] Koo, B. S., Lee, H. R., Jeon, E. O., Han, M. S., Min, K. C., Lee, S. B., Bae, Y. J., Cho, S. H., Mo, J. S., Kwon, H. M., Sung, H. W., Kim, J. N., and Mo, I. P. Genetic characterization of three novel chicken parvovirus strains based on analysis of their coding sequences. *Avian Pathol.*, 44(1):28–34, Feb 2015.
- [248] Koonin, E. V. and Ilyina, T. V. Computer-assisted dissection of rolling circle DNA replication. *BioSystems*, 30(1-3):241–268, 1993.
- [249] Kotin, R. M., Siniscalco, M., Samulski, R. J., Zhu, X. D., Hunter, L., Laughlin, C. A., McLaughlin, S., Muzyczka, N., Rocchi, M., and Berns, K. I. Site-specific integration by adeno-associated virus. *Proc. Natl. Acad. Sci. U.S.A.*, 87(6):2211–2215, Mar 1990.

- [250] Kotin, R. M., Menninger, J. C., Ward, D. C., and Berns, K. I. Mapping and direct visualization of a region-specific viral DNA integration site on chromosome 19q13-qter. *Genomics*, 10(3):831–834, Jul 1991.
- [251] Kotin, R. M., Linden, R. M., and Berns, K. I. Characterization of a preferred site on human chromosome 19q for integration of adeno-associated virus DNA by non-homologous recombination. *EMBO J.*, 11(13):5071–5078, Dec 1992.
- [252] Kresse, J. I., Taylor, W. D., Stewart, W. W., and Eernisse, K. A. Parvovirus infection in pigs with necrotic and vesicle-like lesions. *Vet. Microbiol.*, 10(6):525–531, Dec 1985.
- [253] Kronenberg, S., Bottcher, B., von der Lieth, C. W., Bleker, S., and Kleinschmidt, J. A. A conformational change in the adeno-associated virus type 2 capsid leads to the exposure of hidden VP1 N termini. *J. Virol.*, 79(9):5296–5303, May 2005.
- [254] Kudo, N., Wolff, B., Sekimoto, T., Schreiner, E. P., Yoneda, Y., Yanagida, M., Horinouchi, S., and Yoshida, M. Leptomycin B inhibition of signal-mediated nuclear export by direct binding to CRM1. *Exp. Cell Res.*, 242(2):540–547, Aug 1998.
- [255] Kupfer, B., Vehreschild, J., Cornely, O., Kaiser, R., Plum, G., Viazov, S., Franzen, C., Tillmann, R. L., Simon, A., Muller, A., and Schildgen, O. Severe pneumonia and human bocavirus in adult. *Emerging Infect. Dis.*, 12(10):1614–1616, Oct 2006.
- [256] Labieniec-Pintel, L. and Pintel, D. The minute virus of mice P39 transcription unit can encode both capsid proteins. *J. Virol.*, 57(3):1163–1167, Mar 1986.
- [257] Laemmli, U. K. Cleavage of structural proteins during the assembly of the head of bacteriophage T4. *Nature*, 227(5259):680–685, Aug 1970.
- [258] Lau, S. K., Woo, P. C., Tse, H., Fu, C. T., Au, W. K., Chen, X. C., Tsui, H. W., Tsang, T. H., Chan, J. S., Tsang, D. N., Li, K. S., Tse, C. W., Ng, T. K., Tsang, O. T., Zheng, B. J., Tam, S., Chan, K. H., Zhou, B., and Yuen, K. Y. Identification of novel porcine and bovine parvoviruses closely related to human parvovirus 4. *J. Gen. Virol.*, 89(Pt 8):1840–1848, Aug 2008.
- [259] Laufs, J., Jupin, I., David, C., Schumacher, S., Heyraud-Nitschke, F., and Gronenborn, B. Gemini-virus replication: genetic and biochemical characterization of Rep protein function, a review. *Biochimie*, 77(10):765–773, 1995.
- [260] Lavoie, M., Sharp, C. P., Pepin, J., Pennington, C., Fouppouapouognigni, Y., Pybus, O. G., Njouom, R., and Simmonds, P. Human parvovirus 4 infection, Cameroon. *Emerging Infect. Dis.*, 18(4):680–683, Apr 2012.
- [261] Lederman, M., Patton, J. T., Stout, E. R., and Bates, R. C. Virally coded noncapsid protein associated with bovine parvovirus infection. *J. Virol.*, 49(2):315–318, Feb 1984.
- [262] Legendre, D. and Rommelaere, J. Terminal regions of the NS-1 protein of the parvovirus minute virus of mice are involved in cytotoxicity and promoter trans inhibition. *J. Virol.*, 66(10):5705–5713, Oct 1992.
- [263] Legrand, C., Rommelaere, J., and Caillet-Fauquet, P. MVM(p) NS-2 protein expression is required with NS-1 for maximal cytotoxicity in human transformed cells. *Virology*, 195(1):149–155, Jul 1993.
- [264] Leisi, R., Ruprecht, N., Kempf, C., and Ros, C. Parvovirus B19 uptake is a highly selective process controlled by VP1u, a novel determinant of viral tropism. *J. Virol.*, 87(24):13161–13167, Dec 2013.
- [265] Li, B., Ma, J., Xiao, S., Wen, L., Ni, Y., Zhang, X., Fang, L., and He, K. Genome sequence of a highly prevalent porcine partetavivirus in Mainland China. *J. Virol.*, 86(3):1899, Feb 2012.
- [266] Li, L., Pesavento, P. A., Woods, L., Clifford, D. L., Luff, J., Wang, C., and Delwart, E. Novel amodovirus in gray foxes. *Emerging Infect. Dis.*, 17(10):1876–1878, Oct 2011.
- [267] Li, L., Cotmore, S. F., and Tattersall, P. Maintenance of the flip sequence orientation of the ears in the parvoviral left-end hairpin is a nonessential consequence of the critical asymmetry in the hairpin stem. *J. Virol.*, 86(22):12187–12197, Nov 2012.
- [268] Li, X. and Rhode, S. L. Mutation of lysine 405 to serine in the parvovirus H-1 NS1 abolishes its functions for viral DNA replication, late promoter trans activation, and cytotoxicity. *J. Virol.*, 64(10):4654–4660, Oct 1990.
- [269] Li, X. D., Lankinen, H., Putkuri, N., Vapalahti, O., and Vaheri, A. Tula hantavirus triggers pro-apoptotic signals of ER stress in Vero E6 cells. *Virology*, 333(1):180–189, Mar 2005.

- [270] Ling, C., Lu, Y., Kalsi, J. K., Jayandharan, G. R., Li, B., Ma, W., Cheng, B., Gee, S. W., McGoogan, K. E., Govindasamy, L., Zhong, L., Agbandje-McKenna, M., and Srivastava, A. Human hepatocyte growth factor receptor is a cellular coreceptor for adeno-associated virus serotype 3. *Hum. Gene Ther.*, 21(12):1741–1747, Dec 2010.
- [271] Linser, P., Bruning, H., and Armentrout, R. W. Specific binding sites for a parvovirus, minute virus of mice, on cultured mouse cells. *J. Virol.*, 24(1):211–221, Oct 1977.
- [272] Lippincott-Schwartz, J., Yuan, L., Tipper, C., Amherdt, M., Orci, L., and Klausner, R. D. Brefeldin A's effects on endosomes, lysosomes, and the TGN suggest a general mechanism for regulating organelle structure and membrane traffic. *Cell*, 67(3):601–616, Nov 1991.
- [273] Littlefield, J. W. Three degrees of guanylic acid - inosinic acid pyrophosphorylase deficiency in mouse fibroblasts. *Nature*, 203:1142–1144, Sep 1964.
- [274] Llamas-Saiz, A. L., Agbandje-McKenna, M., Wikoff, W. R., Bratton, J., Tattersall, P., and Rossmann, M. G. Structure determination of minute virus of mice. *Acta Crystallogr. D Biol. Crystallogr.*, 53(Pt 1):93–102, Jan 1997.
- [275] Lochelt, M., Delius, H., and Kaaden, O. R. A novel replicative form DNA of Aleutian disease virus: the covalently closed linear DNA of the parvoviruses. *J. Gen. Virol.*, 70 (Pt 5):1105–1116, May 1989.
- [276] Lombardo, E., Ramirez, J. C., Agbandje-McKenna, M., and Almendral, J. M. A beta-stranded motif drives capsid protein oligomers of the parvovirus minute virus of mice into the nucleus for viral assembly. *J. Virol.*, 74(8):3804–3814, Apr 2000.
- [277] Lombardo, E., Ramirez, J. C., Garcia, J., and Almendral, J. M. Complementary roles of multiple nuclear targeting signals in the capsid proteins of the parvovirus minute virus of mice during assembly and onset of infection. *J. Virol.*, 76(14):7049–7059, Jul 2002.
- [278] Lopez-Bueno, A., Mateu, M. G., and Almendral, J. M. High mutant frequency in populations of a DNA virus allows evasion from antibody therapy in an immunodeficient host. *J. Virol.*, 77(4):2701–2708, Feb 2003.
- [279] Lopez-Bueno, A., Rubio, M. P., Bryant, N., McKenna, R., Agbandje-McKenna, M., and Almendral, J. M. Host-selected amino acid changes at the sialic acid binding pocket of the parvovirus capsid modulate cell binding affinity and determine virulence. *J. Virol.*, 80 (3):1563–1573, Feb 2006.
- [280] Lopez-Bueno, A., Segovia, J. C., Bueren, J. A., O'Sullivan, M. G., Wang, F., Tattersall, P., and Almendral, J. M. Evolution to pathogenicity of the parvovirus minute virus of mice in immunodeficient mice involves genetic heterogeneity at the capsid domain that determines tropism. *J. Virol.*, 82(3):1195–1203, Feb 2008.
- [281] Lorson, C., Pearson, J., Burger, L., and Pintel, D. J. An Sp1-binding site and TATA element are sufficient to support full transactivation by proximally bound NS1 protein of minute virus of mice. *Virology*, 240(2):326–337, Jan 1998.
- [282] Lou, H. J., Brister, J. R., Li, J. J., Chen, W., Muzychka, N., and Tan, W. Adeno-associated virus Rep78/Rep68 promotes localized melting of the rep binding element in the absence of adenosine triphosphate. *Chembiochem*, 5(3):324–332, Mar 2004.
- [283] Lou, S., Xu, B., Huang, Q., Zhi, N., Cheng, F., Wong, S., Brown, K., Delwart, E., Liu, Z., and Qiu, J. Molecular characterization of the newly identified human parvovirus 4 in the family Parvoviridae. *Virol.ogy*, 422(1):59–69, Jan 2012.
- [284] Luby-Phelps, K. Cytoarchitecture and physical properties of cytoplasm: volume, viscosity, diffusion, intracellular surface area. *Int. Rev. Cytol.*, 192:189–221, 2000.
- [285] Lukashov, V. V. and Goudsmit, J. Evolutionary relationships among parvoviruses: virus-host coevolution among autonomous primate parvoviruses and links between adeno-associated and avian parvoviruses. *J. Virol.*, 75(6):2729–2740, Mar 2001.
- [286] Luo, M., Tsao, J., Rossmann, M. G., Basak, S., and Compans, R. W. Preliminary X-ray crystallographic analysis of canine parvovirus crystals. *J. Mol. Biol.*, 200(1):209–211, Mar 1988.
- [287] Lusby, E., Fife, K. H., and Berns, K. I. Nucleotide sequence of the inverted terminal repetition in adeno-associated virus DNA. *J. Virol.*, 34(2):402–409, May 1980.
- [288] Lusby, E. W. and Berns, K. I. Mapping of the 5' termini of two adeno-associated virus 2 RNAs in the left half of the genome. *J. Virol.*, 41(2):518–526, Feb 1982.

- [289] Lux, K., Goerlitz, N., Schlemminger, S., Perabo, L., Goldnau, D., Endell, J., Leike, K., Kofler, D. M., Finke, S., Hallek, M., and Buning, H. Green fluorescent protein-tagged adeno-associated virus particles allow the study of cytosolic and nuclear trafficking. *J. Virol.*, 79(18):11776–11787, Sep 2005.
- [290] Ma, X., Endo, R., Ishiguro, N., Ebihara, T., Ishiko, H., Ariga, T., and Kikuta, H. Detection of human bocavirus in Japanese children with lower respiratory tract infections. *J. Clin. Microbiol.*, 44(3):1132–1134, Mar 2006.
- [291] Madadlou, A., O’Sullivan, S., and Sheehan, D. Fast protein liquid chromatography. *Methods Mol. Biol.*, 681:439–447, 2011.
- [292] Mani, B., Baltzer, C., Valle, N., Almendral, J. M., Kempf, C., and Ros, C. Low pH-dependent endosomal processing of the incoming parvovirus minute virus of mice virion leads to externalization of the VP1 N-terminal sequence (N-VP1), N-VP2 cleavage, and uncoating of the full-length genome. *J. Virol.*, 80(2):1015–1024, Jan 2006.
- [293] Mani, B., Gerber, M., Lieby, P., Boschetti, N., Kempf, C., and Ros, C. Molecular mechanism underlying B19 virus inactivation and comparison to other parvoviruses. *Transfusion*, 47(10):1765–1774, Oct 2007.
- [294] Maniatis, T. Mechanisms of alternative pre-mRNA splicing. *Science*, 251(4989):33–34, Jan 1991.
- [295] Manning, A., Russell, V., Eastick, K., Leadbetter, G. H., Hallam, N., Templeton, K., and Simmonds, P. Epidemiological profile and clinical associations of human bocavirus and other human parvoviruses. *J. Infect. Dis.*, 194(9):1283–1290, Nov 2006.
- [296] Manning, A., Willey, S. J., Bell, J. E., and Simmonds, P. Comparison of tissue distribution, persistence, and molecular epidemiology of parvovirus B19 and novel human parvoviruses PARV4 and human bocavirus. *J. Infect. Dis.*, 195(9):1345–1352, May 2007.
- [297] Maroto, B., Ramirez, J. C., and Almendral, J. M. Phosphorylation status of the parvovirus minute virus of mice particle: mapping and biological relevance of the major phosphorylation sites. *J. Virol.*, 74(23):10892–10902, Dec 2000.
- [298] Maroto, B., Valle, N., Saffrich, R., and Almendral, J. M. Nuclear export of the nonenveloped parvovirus virion is directed by an unordered protein signal exposed on the capsid surface. *J. Virol.*, 78(19):10685–10694, Oct 2004.
- [299] Mastrobattista, E., van der Aa, M. A., Hennink, W. E., and Crommelin, D. J. Artificial viruses: a nanotechnological approach to gene delivery. *Nat Rev Drug Discov*, 5(2):115–121, Feb 2006.
- [300] Mattaj, I. W. and Englmeier, L. Nucleocytoplasmic transport: the soluble phase. *Annu. Rev. Biochem.*, 67:265–306, 1998.
- [301] Maxwell, I. H., Spitzer, A. L., Maxwell, F., and Pintel, D. J. The capsid determinant of fibrotropism for the MVMP strain of minute virus of mice functions via VP2 and not VP1. *J. Virol.*, 69(9):5829–5832, Sep 1995.
- [302] McKenna, R., Olson, N. H., Chipman, P. R., Baker, T. S., Booth, T. F., Christensen, J., Aasted, B., Fox, J. M., Bloom, M. E., Wolfinbarger, J. B., and Agbandje-McKenna, M. Three-dimensional structure of Aleutian mink disease parvovirus: implications for disease pathogenicity. *J. Virol.*, 73(8):6882–6891, Aug 1999.
- [303] McKeown, M. Alternative mRNA splicing. *Annu. Rev. Cell Biol.*, 8:133–155, 1992.
- [304] McMaster, G. K., Beard, P., Engers, H. D., and Hirt, B. Characterization of an immunosuppressive parvovirus related to the minute virus of mice. *J. Virol.*, 38(1):317–326, Apr 1981.
- [305] Meehan, B. M., Creelan, J. L., McNulty, M. S., and Todd, D. Sequence of porcine circovirus DNA: affinities with plant circoviruses. *J. Gen. Virol.*, 78 (Pt 1):221–227, Jan 1997.
- [306] Mengeling, W. L. Prenatal infection following maternal exposure to porcine parvovirus on either the seventh or fourteenth day of gestation. *Can. J. Comp. Med.*, 43(1):106–109, Jan 1979.
- [307] Mengeling, W. L. and Cutlip, R. C. Reproductive disease experimentally induced by exposing pregnant gilts to porcine parvovirus. *Am. J. Vet. Res.*, 37(12):1393–1400, Dec 1976.
- [308] Merchlinsky, M. J., Tattersall, P. J., Leary, J. J., Cotmore, S. F., Gardiner, E. M., and Ward, D. C. Construction of an infectious molecular clone of the autonomous parvovirus minute virus of mice. *J. Virol.*, 47(1):227–232, Jul 1983.
- [309] Metcalf, J. B., Bates, R. C., and Lederman, M. Interaction of virally coded protein and a cell cycle-regulated cellular protein with the bovine parvovirus left terminus ori. *J. Virol.*, 64(11):5485–5490, Nov 1990.

- [310] Miller, C. L. and Pintel, D. J. The NS2 protein generated by the parvovirus minute virus of mice is degraded by the proteasome in a manner independent of ubiquitin chain elongation or activation. *Virology*, 285(2):346–355, Jul 2001.
- [311] Miller, C. L. and Pintel, D. J. Interaction between parvovirus NS2 protein and nuclear export factor Crm1 is important for viral egress from the nucleus of murine cells. *J. Virol.*, 76(7):3257–3266, Apr 2002.
- [312] Mingoza, F. and High, K. A. Therapeutic in vivo gene transfer for genetic disease using AAV: progress and challenges. *Nat. Rev. Genet.*, 12(5):341–355, May 2011.
- [313] Misaghi, S., Sun, Z. Y., Stern, P., Gaudet, R., Wagner, G., and Ploegh, H. Structural and functional analysis of human cytomegalovirus US3 protein. *J. Virol.*, 78(1):413–423, Jan 2004.
- [314] Mizukami, H., Young, N. S., and Brown, K. E. Adeno-associated virus type 2 binds to a 150-kilodalton cell membrane glycoprotein. *Virology*, 217(1):124–130, Mar 1996.
- [315] Molitor, T. W., Joo, H. S., and Collett, M. S. Identification and characterization of a porcine parvovirus nonstructural polypeptide. *J. Virol.*, 55(3):554–559, Sep 1985.
- [316] Momoeda, M., Wong, S., Kawase, M., Young, N. S., and Kajigaya, S. A putative nucleoside triphosphate-binding domain in the nonstructural protein of B19 parvovirus is required for cytotoxicity. *J. Virol.*, 68(12):8443–8446, Dec 1994.
- [317] Morgan, W. R. and Ward, D. C. Three splicing patterns are used to excise the small intron common to all minute virus of mice RNAs. *J. Virol.*, 60(3):1170–1174, Dec 1986.
- [318] Morishima, T., McClintock, P. R., Aulakh, G. S., Billups, L. C., and Notkins, A. L. Genomic and receptor attachment differences between mengovirus and encephalomyocarditis virus. *Virology*, 122(2):461–465, Oct 1982.
- [319] Morishima, T., McClintock, P. R., Billups, L. C., and Notkins, A. L. Expression and modulation of virus receptors on lymphoid and myeloid cells: relationship to infectivity. *Virology*, 116(2):605–618, Jan 1982.
- [320] Mouw, M. and Pintel, D. J. Amino acids 16–275 of minute virus of mice NS1 include a domain that specifically binds (ACCA)2-3-containing DNA. *Virology*, 251(1):123–131, Nov 1998.
- [321] Muller, D. E. and Siegl, G. Maturation of parvovirus LuIII in a subcellular system. II. Isolation and characterization of nucleoprotein intermediates. *J. Gen. Virol.*, 64(Pt 5):1055–1067, May 1983.
- [322] Munakata, Y., Saito-Ito, T., Kumura-Ishii, K., Huang, J., Kodera, T., Ishii, T., Hirabayashi, Y., Koyanagi, Y., and Sasaki, T. Ku80 autoantigen as a cellular coreceptor for human parvovirus B19 infection. *Blood*, 106(10):3449–3456, Nov 2005.
- [323] Muzyczka, N. and Berns, K. I. Parvoviridae: the viruses and their replication. In Knipe, D. M. and Howley, P. M., eds., *Fields virology*, pp. 2327–2359. Lippincott Williams and Wilkins, Philadelphia, PA, 4 edition, 2001.
- [324] Nachury, M. V. and Weis, K. The direction of transport through the nuclear pore can be inverted. *Proc. Natl. Acad. Sci. U.S.A.*, 96(17):9622–9627, Aug 1999.
- [325] Naeger, L. K., Cater, J., and Pintel, D. J. The small nonstructural protein (NS2) of the parvovirus minute virus of mice is required for efficient DNA replication and infectious virus production in a cell-type-specific manner. *J. Virol.*, 64(12):6166–6175, Dec 1990.
- [326] Naeger, L. K., Schoborg, R. V., Zhao, Q., Tullis, G. E., and Pintel, D. J. Nonsense mutations inhibit splicing of MVM RNA in cis when they interrupt the reading frame of either exon of the final spliced product. *Genes Dev.*, 6(6):1107–1119, Jun 1992.
- [327] Naeger, L. K., Salome, N., and Pintel, D. J. NS2 is required for efficient translation of viral mRNA in minute virus of mice-infected murine cells. *J. Virol.*, 67(2):1034–1043, Feb 1993.
- [328] Nam, H. J., Gurda-Whitaker, B., Gan, W. Y., Ilaria, S., McKenna, R., Mehta, P., Alvarez, R. A., and Agbandje-McKenna, M. Identification of the sialic acid structures recognized by minute virus of mice and the role of binding affinity in virulence adaptation. *J. Biol. Chem.*, 281(35):25670–25677, Sep 2006.
- [329] Nüesch, J. P. Regulation of non-structural protein functions by differential synthesis, modification and trafficking. In Kerr, J. R., Bloom, M. E., Cotmore, S. F., Linden, R. M., and Parrish, C. R., eds., *Parvoviruses*, pp. 275–289. Hodder Arnold, London, UK, 2006.
- [330] Nüesch, J. P. and Rommelaere, J. NS1 interaction with CKII alpha: novel protein complex mediating parvovirus-induced cytotoxicity. *J. Virol.*, 80(10):4729–4739, May 2006.

- [331] Nüesch, J. P., Lachmann, S., and Rommelaere, J. Selective alterations of the host cell architecture upon infection with parvovirus minute virus of mice. *Virology*, 331(1):159–174, Jan 2005.
- [332] Nüesch, J. P., Bar, S., Lachmann, S., and Rommelaere, J. Ezrin-radixin-moesin family proteins are involved in parvovirus replication and spreading. *J. Virol.*, 83(11):5854–5863, Jun 2009.
- [333] Ni, J., Qiao, C., Han, X., Han, T., Kang, W., Zi, Z., Cao, Z., Zhai, X., and Cai, X. Identification and genomic characterization of a novel porcine parvovirus (PPV6) in china. *Virol. J.*, 11(1):203, Dec 2014.
- [334] Ni, T. H., McDonald, W. F., Zolotukhin, I., Melendy, T., Waga, S., Stillman, B., and Muzyczka, N. Cellular proteins required for adeno-associated virus DNA replication in the absence of adenovirus coinfection. *J. Virol.*, 72(4):2777–2787, Apr 1998.
- [335] Nigg, E. A. Nucleocytoplasmic transport: signals, mechanisms and regulation. *Nature*, 386(6627):779–787, Apr 1997.
- [336] Nonnenmacher, M. and Weber, T. Adeno-associated virus 2 infection requires endocytosis through the CLIC/GEEC pathway. *Cell Host Microbe*, 10(6):563–576, Dec 2011.
- [337] Nuesch, J. P. and Tattersall, P. Nuclear targeting of the parvoviral replicator molecule NS1: evidence for self-association prior to nuclear transport. *Virology*, 196(2):637–651, Oct 1993.
- [338] Nuesch, J. P., Cotmore, S. F., and Tattersall, P. Sequence motifs in the replicator protein of parvovirus MVM essential for nicking and covalent attachment to the viral origin: identification of the linking tyrosine. *Virology*, 209(1):122–135, May 1995.
- [339] Nuesch, J. P., Christensen, J., and Rommelaere, J. Initiation of minute virus of mice DNA replication is regulated at the level of origin unwinding by atypical protein kinase C phosphorylation of NS1. *J. Virol.*, 75(13):5730–5739, Jul 2001.
- [340] Ohkuma, S. and Poole, B. Fluorescence probe measurement of the intralysosomal pH in living cells and the perturbation of pH by various agents. *Proc. Natl. Acad. Sci. U.S.A.*, 75(7):3327–3331, Jul 1978.
- [341] Ohshima, T., Nakajima, T., Oishi, T., Imamoto, N., Yoneda, Y., Fukamizu, A., and Yagami, K. i. CRM1 mediates nuclear export of nonstructural protein 2 from parvovirus minute virus of mice. *Biochem. Biophys. Res. Commun.*, 264(1):144–150, Oct 1999.
- [342] Ojala, P. M., Sodeik, B., Ebersold, M. W., Kutay, U., and Helenius, A. Herpes simplex virus type 1 entry into host cells: reconstitution of capsid binding and uncoating at the nuclear pore complex in vitro. *Mol. Cell. Biol.*, 20(13):4922–4931, Jul 2000.
- [343] Olofsson, S. and Bergstrom, T. Glycoconjugate glycans as viral receptors. *Ann. Med.*, 37(3):154–172, 2005.
- [344] Oppenheim, A., Sandalon, Z., Peleg, A., Shaul, O., Nicolis, S., and Ottolenghi, S. A cis-acting DNA signal for encapsidation of simian virus 40. *J. Virol.*, 66(9):5320–5328, Sep 1992.
- [345] Orozco, B. M., Miller, A. B., Settlage, S. B., and Hanley-Bowdoin, L. Functional domains of a geminivirus replication protein. *J. Biol. Chem.*, 272(15):9840–9846, Apr 1997.
- [346] Ozawa, K., Ayub, J., Hao, Y. S., Kurtzman, G., Shimada, T., and Young, N. Novel transcription map for the B19 (human) pathogenic parvovirus. *J. Virol.*, 61(8):2395–2406, Aug 1987.
- [347] Padgett, R. A., Grabowski, P. J., Konarska, M. M., Seiler, S., and Sharp, P. A. Splicing of messenger RNA precursors. *Annu. Rev. Biochem.*, 55:1119–1150, 1986.
- [348] Padron, E., Bowman, V., Kaludov, N., Govindasamy, L., Levy, H., Nick, P., McKenna, R., Muzyczka, N., Chiorini, J. A., Baker, T. S., and Agbandje-McKenna, M. Structure of adeno-associated virus type 4. *J. Virol.*, 79(8):5047–5058, Apr 2005.
- [349] Page, R. K., Fletcher, O. J., Rowland, G. N., Gaudry, D., and Villegas, P. Malabsorption syndrome in broiler chickens. *Avian Dis.*, 26(3):618–624, 1982.
- [350] Palermo, L. M., Hueffer, K., and Parrish, C. R. Residues in the apical domain of the feline and canine transferrin receptors control host-specific binding and cell infection of canine and feline parvoviruses. *J. Virol.*, 77(16):8915–8923, Aug 2003.
- [351] Panning, M., Kobbe, R., Vollbach, S., Drexler, J. F., Adjei, S., Adjei, O., Drosten, C., May, J., and Eis-Hubinger, A. M. Novel human parvovirus 4 genotype 3 in infants, Ghana. *Emerging Infect. Dis.*, 16(7):1143–1146, Jul 2010.
- [352] Panté, N. and Kann, M. Nuclear pore complex is able to transport macromolecules with diameters of about 39 nm. *Mol. Biol. Cell*, 13(2):425–434, Feb 2002.

- [353] Paradiso, P. R. Infectious process of the parvovirus H-1: correlation of protein content, particle density, and viral infectivity. *J. Virol.*, 39(3):800–807, Sep 1981.
- [354] Paradiso, P. R., Williams, K. R., and Costantino, R. L. Mapping of the amino terminus of the H-1 parvovirus major capsid protein. *J. Virol.*, 52(1):77–81, Oct 1984.
- [355] Park, B., Kim, Y., Shin, J., Lee, S., Cho, K., Fruh, K., Lee, S., and Ahn, K. Human cytomegalovirus inhibits tapasin-dependent peptide loading and optimization of the MHC class I peptide cargo for immune evasion. *Immunity*, 20(1):71–85, Jan 2004.
- [356] Park, G. S., Best, S. M., and Bloom, M. E. Two mink parvoviruses use different cellular receptors for entry into CRFK cells. *Virology*, 340(1):1–9, Sep 2005.
- [357] Parker, J. S. and Parrish, C. R. Cellular uptake and infection by canine parvovirus involves rapid dynamin-regulated clathrin-mediated endocytosis, followed by slower intracellular trafficking. *J. Virol.*, 74(4):1919–1930, Feb 2000.
- [358] Parker, J. S., Murphy, W. J., Wang, D., O'Brien, S. J., and Parrish, C. R. Canine and feline parvoviruses can use human or feline transferrin receptors to bind, enter, and infect cells. *J. Virol.*, 75(8):3896–3902, Apr 2001.
- [359] Parrish, C. R. and Carmichael, L. E. Characterization and recombination mapping of an antigenic and host range mutation of canine parvovirus. *Virology*, 148(1):121–132, Jan 1986.
- [360] Parrish, C. R., Aquadro, C. F., and Carmichael, L. E. Canine host range and a specific epitope map along with variant sequences in the capsid protein gene of canine parvovirus and related feline, mink, and raccoon parvoviruses. *Virology*, 166(2):293–307, Oct 1988.
- [361] Parrish, C. R., Aquadro, C. F., Strassheim, M. L., Evermann, J. F., Sgro, J. Y., and Mohammed, H. O. Rapid antigenic-type replacement and DNA sequence evolution of canine parvovirus. *J. Virol.*, 65(12):6544–6552, Dec 1991.
- [362] Pass, D. A., Robertson, M. D., and Wilcox, G. E. Runting syndrome in broiler chickens in Australia. *Vet. Rec.*, 110(16):386–387, Apr 1982.
- [363] Pemberton, L. F. and Paschal, B. M. Mechanisms of receptor-mediated nuclear import and nuclear export. *Traffic*, 6(3):187–198, Mar 2005.
- [364] Perez, R., Castellanos, M., Rodriguez-Huete, A., and Mateu, M. G. Molecular determinants of self-association and rearrangement of a trimeric intermediate during the assembly of a parvovirus capsid. *J. Mol. Biol.*, 413(1):32–40, Oct 2011.
- [365] Perros, M., Deleu, L., Vanacker, J. M., Kherrouche, Z., Spruyt, N., Faisst, S., and Rommelaere, J. Upstream CREs participate in the basal activity of minute virus of mice promoter P4 and in its stimulation in ras-transformed cells. *J. Virol.*, 69(9):5506–5515, Sep 1995.
- [366] Pettersen, E. F., Goddard, T. D., Huang, C. C., Couch, G. S., Greenblatt, D. M., Meng, E. C., and Ferrin, T. E. UCSF Chimera—a visualization system for exploratory research and analysis. *J Comput Chem*, 25(13):1605–1612, Oct 2004.
- [367] Pintel, D., Dadachanji, D., Astell, C. R., and Ward, D. C. The genome of minute virus of mice, an autonomous parvovirus, encodes two overlapping transcription units. *Nucleic Acids Res.*, 11(4):1019–1038, Feb 1983.
- [368] Pitluk, Z. W. and Ward, D. C. Unusual Sp1-GC box interaction in a parvovirus promoter. *J. Virol.*, 65(12):6661–6670, Dec 1991.
- [369] Poole, B. and Ohkuma, S. Effect of weak bases on the intralysosomal pH in mouse peritoneal macrophages. *J. Cell Biol.*, 90(3):665–669, Sep 1981.
- [370] Praefcke, G. J. and McMahon, H. T. The dynamin superfamily: universal membrane tubulation and fission molecules? *Nat. Rev. Mol. Cell Biol.*, 5(2):133–147, Feb 2004.
- [371] Prasad, K. M. and Trempe, J. P. The adeno-associated virus Rep78 protein is covalently linked to viral DNA in a preformed virion. *Virology*, 214(2):360–370, Dec 1995.
- [372] Prevelige, P. E. New approaches for antiviral targeting of HIV assembly. *J. Mol. Biol.*, 410(4):634–640, Jul 2011.
- [373] Previsani, N., Fontana, S., Hirt, B., and Beard, P. Growth of the parvovirus minute virus of mice MVMP3 in EL4 lymphocytes is restricted after cell entry and before viral DNA amplification: cell-specific differences in virus uncoating in vitro. *J. Virol.*, 71(10):7769–7780, Oct 1997.

- [374] Pujol, A., Deleu, L., Nuesch, J. P., Cziepluch, C., Jauniaux, J. C., and Rommelaeere, J. Inhibition of parvovirus minute virus of mice replication by a peptide involved in the oligomerization of nonstructural protein NS1. *J. Virol.*, 71(10):7393–7403, Oct 1997.
- [375] Qing, K., Mah, C., Hansen, J., Zhou, S., Dwarki, V., and Srivastava, A. Human fibroblast growth factor receptor 1 is a co-receptor for infection by adeno-associated virus 2. *Nat. Med.*, 5(1):71–77, Jan 1999.
- [376] Qiu, J., Cheng, F., Burger, L. R., and Pintel, D. The transcription profile of Aleutian mink disease virus in CRFK cells is generated by alternative processing of pre-mRNAs produced from a single promoter. *J. Virol.*, 80(2):654–662, Jan 2006.
- [377] Qiu, J., Cheng, F., Johnson, F. B., and Pintel, D. The transcription profile of the bocavirus bovine parvovirus is unlike those of previously characterized parvoviruses. *J. Virol.*, 81(21):12080–12085, Nov 2007.
- [378] Qui, J., Yoto, Y., Tullis, G., and Pintel, D. J. Parvovirus RNA processing strategies. In Kerr, J. R., Bloom, M. E., Cotmore, S. F., Linden, R. M., and Parrish, C. R., eds., *Parvoviruses*, pp. 253–273. Hodder Arnold, London, UK, 2006.
- [379] Ramirez, J. C., Fairen, A., and Almendral, J. M. Parvovirus minute virus of mice strain i multiplication and pathogenesis in the newborn mouse brain are restricted to proliferative areas and to migratory cerebellar young neurons. *J. Virol.*, 70(11):8109–8116, Nov 1996.
- [380] Reguera, J., Carreira, A., Riolobos, L., Almendral, J. M., and Mateu, M. G. Role of interfacial amino acid residues in assembly, stability, and conformation of a spherical virus capsid. *Proc. Natl. Acad. Sci. U.S.A.*, 101(9):2724–2729, Mar 2004.
- [381] Rhode, S. L. trans-Activation of parvovirus P38 promoter by the 76K noncapsid protein. *J. Virol.*, 55(3): 886–889, Sep 1985.
- [382] Richards, R., Linser, P., and Armentrout, R. W. Kinetics of assembly of a parvovirus, minute virus of mice, in synchronized rat brain cells. *J. Virol.*, 22(3): 778–793, Jun 1977.
- [383] Riolobos, L., Reguera, J., Mateu, M. G., and Almendral, J. M. Nuclear transport of trimeric assembly intermediates exerts a morphogenetic control on the icosahedral parvovirus capsid. *J. Mol. Biol.*, 357(3): 1026–1038, Mar 2006.
- [384] Robbins, J., Dilworth, S. M., Laskey, R. A., and Dingwall, C. Two interdependent basic domains in nucleoplasmin nuclear targeting sequence: identification of a class of bipartite nuclear targeting sequence. *Cell*, 64(3):615–623, Feb 1991.
- [385] Ron, D. and Tal, J. Spontaneous curing of a minute virus of mice carrier state by selection of cells with an intracellular block of viral replication. *J. Virol.*, 58(1): 26–30, Apr 1986.
- [386] Ros, C. and Kempf, C. The ubiquitin-proteasome machinery is essential for nuclear translocation of incoming minute virus of mice. *Virology*, 324(2):350–360, Jul 2004.
- [387] Ros, C., Burckhardt, C. J., and Kempf, C. Cytoplasmic trafficking of minute virus of mice: low-pH requirement, routing to late endosomes, and proteasome interaction. *J. Virol.*, 76(24):12634–12645, Dec 2002.
- [388] Rose, J. A., Berns, K. I., Hoggan, M. D., and Koczot, F. J. Evidence for a single-stranded adenovirus-associated virus genome: formation of a DNA density hybrid on release of viral DNA. *Proc. Natl. Acad. Sci. U.S.A.*, 64(3):863–869, Nov 1969.
- [389] Rossmann, M. G. and Johnson, J. E. Icosahedral RNA virus structure. *Annu. Rev. Biochem.*, 58:533–573, 1989.
- [390] Rubio, M. P., Lopez-Bueno, A., and Almendral, J. M. Virulent variants emerging in mice infected with the apathogenic prototype strain of the parvovirus minute virus of mice exhibit a capsid with low avidity for a primary receptor. *J. Virol.*, 79(17):11280–11290, Sep 2005.
- [391] Ruffing, M., Zentgraf, H., and Kleinschmidt, J. A. Assembly of viruslike particles by recombinant structural proteins of adeno-associated virus type 2 in insect cells. *J. Virol.*, 66(12):6922–6930, Dec 1992.
- [392] Ryan, K. J. and Wente, S. R. The nuclear pore complex: a protein machine bridging the nucleus and cytoplasm. *Curr. Opin. Cell Biol.*, 12(3):361–371, Jun 2000.
- [393] Sahli, R., McMaster, G. K., and Hirt, B. DNA sequence comparison between two tissue-specific variants of the autonomous parvovirus, minute virus of mice. *Nucleic Acids Res.*, 13(10):3617–3633, May 1985.

- [394] Saif, Y. M., Barnes, H. J., Glisson, J. R., Fadly, A. M., McDougald, L. R., and Swayne, D. E. *Diseases of Poultry 11th edn.* Wiley-Blackwell, Hoboken, NJ, 2003. pp 1171–1180.
- [395] Saknimit, M., Inatsuki, I., Sugiyama, Y., and Yagami, K. Virucidal efficacy of physico-chemical treatments against coronaviruses and parvoviruses of laboratory animals. *Jikken Dobutsu*, 37(3):341–345, Jul 1988.
- [396] Salzman, L. A. and Jori, L. A. Characterization of the Kilham rat virus. *J. Virol.*, 5(2):114–122, Feb 1970.
- [397] Samulski, R. J., Chang, L. S., and Shenk, T. Helper-free stocks of recombinant adeno-associated viruses: normal integration does not require viral gene expression. *J. Virol.*, 63(9):3822–3828, Sep 1989.
- [398] Samulski, R. J., Zhu, X., Xiao, X., Brook, J. D., Housman, D. E., Epstein, N., and Hunter, L. A. Targeted integration of adeno-associated virus (AAV) into human chromosome 19. *EMBO J.*, 10(12):3941–3950, Dec 1991.
- [399] Sauerbrei, A. and Wutzler, P. Testing thermal resistance of viruses. *Arch. Virol.*, 154(1):115–119, 2009.
- [400] Schmidt, M. and Chiorini, J. A. Gangliosides are essential for bovine adeno-associated virus entry. *J. Virol.*, 80(11):5516–5522, Jun 2006.
- [401] Schoborg, R. V. and Pintel, D. J. Accumulation of MVM gene products is differentially regulated by transcription initiation, RNA processing and protein stability. *Virology*, 181(1):22–34, Mar 1991.
- [402] Schwartz, D., Green, B., Carmichael, L. E., and Parrish, C. R. The canine minute virus (minute virus of canines) is a distinct parvovirus that is most similar to bovine parvovirus. *Virology*, 302(2):219–223, Oct 2002.
- [403] Schwarz, T. F., Serke, S., Von Brunn, A., Hottentrager, B., Huhn, D., Deinhardt, F., and Roggendorf, M. Heat stability of parvovirus B19: kinetics of inactivation. *Zentralbl. Bakteriol.*, 277(2):219–223, Jul 1992.
- [404] Segovia, J. C., Bueren, J. A., and Almendral, J. M. Myeloid depression follows infection of susceptible newborn mice with the parvovirus minute virus of mice (strain i). *J. Virol.*, 69(5):3229–3232, May 1995.
- [405] Segovia, J. C., Gallego, J. M., Bueren, J. A., and Almendral, J. M. Severe leukopenia and dysregulated erythropoiesis in SCID mice persistently infected with the parvovirus minute virus of mice. *J. Virol.*, 73(3):1774–1784, Mar 1999.
- [406] Segovia, J. C., Guenechea, G., Gallego, J. M., Almendral, J. M., and Bueren, J. A. Parvovirus infection suppresses long-term repopulating hematopoietic stem cells. *J. Virol.*, 77(15):8495–8503, Aug 2003.
- [407] Seiler, M. P., Miller, A. D., Zabner, J., and Halbert, C. L. Adeno-associated virus types 5 and 6 use distinct receptors for cell entry. *Hum. Gene Ther.*, 17(1):10–19, Jan 2006.
- [408] Seisenberger, G., Ried, M. U., Endress, T., Buning, H., Hallek, M., and Brauchle, C. Real-time single-molecule imaging of the infection pathway of an adeno-associated virus. *Science*, 294(5548):1929–1932, Nov 2001.
- [409] Seksek, O., Biwersi, J., and Verkman, A. S. Translational diffusion of macromolecule-sized solutes in cytoplasm and nucleus. *J. Cell Biol.*, 138(1):131–142, Jul 1997.
- [410] Shackelton, L. A. and Holmes, E. C. Phylogenetic evidence for the rapid evolution of human B19 erythrovirus. *J. Virol.*, 80(7):3666–3669, Apr 2006.
- [411] Shackelton, L. A., Parrish, C. R., Truyen, U., and Holmes, E. C. High rate of viral evolution associated with the emergence of carnivore parvovirus. *Proc. Natl. Acad. Sci. U.S.A.*, 102(2):379–384, Jan 2005.
- [412] Sharp, C. P., LeBreton, M., Kantola, K., Nana, A., Diffo, J. l. e. D., Djoko, C. F., Tamoufe, U., Kiyang, J. A., Babila, T. G., Ngole, E. M., Pybus, O. G., Delwart, E., Delaporte, E., Peeters, M., Soderlund-Venermo, M., Hedman, K., Wolfe, N. D., and Simmonds, P. Widespread infection with homologues of human parvoviruses B19, PARV4, and human bocavirus of chimpanzees and gorillas in the wild. *J. Virol.*, 84(19):10289–10296, Oct 2010.
- [413] Sharp, C. P., Lail, A., Donfield, S., Gomperts, E. D., and Simmonds, P. Virologic and clinical features of primary infection with human parvovirus 4 in subjects with hemophilia: frequent transmission by virally inactivated clotting factor concentrates. *Transfusion*, 52(7):1482–1489, Jul 2012.
- [414] Shein, H. M. and Enders, J. F. Multiplication and cytopathogenicity of Simian vacuolating virus 40 in cultures of human tissues. *Proc. Soc. Exp. Biol. Med.*, 109:495–500, Mar 1962.

- [415] Shen, S., Bryant, K. D., Brown, S. M., Randell, S. H., and Asokan, A. Terminal N-linked galactose is the primary receptor for adeno-associated virus 9. *J. Biol. Chem.*, 286(15):13532–13540, Apr 2011.
- [416] Simmons, R., Sharp, C., McClure, C. P., Rohrbach, J., Kovari, H., and et al. Parvovirus 4 infection and clinical outcome in high-risk populations. *J. Infect. Dis.*, 205(12):1816–1820, Jun 2012.
- [417] Simmons, R., Sharp, C., Levine, J., Bowness, P., Simmonds, P., Cox, A., and Klenerman, P. Evolution of CD8+ T cell responses after acute PARV4 infection. *J. Virol.*, 87(6):3087–3096, Mar 2013.
- [418] Simpson, A. A., Chipman, P. R., Baker, T. S., Tijsen, P., and Rossmann, M. G. The structure of an insect parvovirus (*Galleria mellonella densovirus*) at 3.7 Å resolution. *Structure*, 6(11):1355–1367, Nov 1998.
- [419] Simpson, A. A., Chandrasekar, V., Hebert, B., Sullivan, G. M., Rossmann, M. G., and Parrish, C. R. Host range and variability of calcium binding by surface loops in the capsids of canine and feline parvoviruses. *J. Mol. Biol.*, 300(3):597–610, Jul 2000.
- [420] Slepchenko, B. M., Semenova, I., Zaliapin, I., and Rondonov, V. Switching of membrane organelles between cytoskeletal transport systems is determined by regulation of the microtubule-based transport. *J. Cell Biol.*, 179(4):635–641, Nov 2007.
- [421] Smith, A. L. and Tignor, G. H. Host cell receptors for two strains of Sindbis virus. *Arch. Virol.*, 66(1):11–26, 1980.
- [422] Smith, C. W., Patton, J. G., and Nadal-Ginard, B. Alternative splicing in the control of gene expression. *Annu. Rev. Genet.*, 23:527–577, 1989.
- [423] Snyder, R. O., Im, D. S., and Muzyczka, N. Evidence for covalent attachment of the adeno-associated virus (AAV) rep protein to the ends of the AAV genome. *J. Virol.*, 64(12):6204–6213, Dec 1990.
- [424] Sonntag, F., Bleker, S., Leuchs, B., Fischer, R., and Kleinschmidt, J. A. Adeno-associated virus type 2 capsids with externalized VP1/VP2 trafficking domains are generated prior to passage through the cytoplasm and are maintained until uncoating occurs in the nucleus. *J. Virol.*, 80(22):11040–11054, Nov 2006.
- [425] Spalholz, B. A. and Tattersall, P. Interaction of minute virus of mice with differentiated cells: strain-dependent target cell specificity is mediated by intracellular factors. *J. Virol.*, 46(3):937–943, Jun 1983.
- [426] Spalholz, B. A., Bratton, J., Ward, D. C., and Tattersall, P. *Tumor Viruses and Differentiation*. Academic Press, New York, NY, 1982.
- [427] Stahnke, S., Lux, K., Uhrig, S., Kreppel, F., Hosel, M., Coutelle, O., Ogris, M., Hallek, M., and Buning, H. Intrinsic phospholipase A2 activity of adeno-associated virus is involved in endosomal escape of incoming particles. *Virology*, 409(1):77–83, Jan 2011.
- [428] Stammes, M. Regulating the actin cytoskeleton during vesicular transport. *Curr. Opin. Cell Biol.*, 14(4):428–433, Aug 2002.
- [429] Stoffler, D., Fahrenkrog, B., and Aeby, U. The nuclear pore complex: from molecular architecture to functional dynamics. *Curr. Opin. Cell Biol.*, 11(3):391–401, Jun 1999.
- [430] Streck, A. F., Bonatto, S. L., Homeier, T., Souza, C. K., Goncalves, K. R., Gava, D., Canal, C. W., and Truyen, U. High rate of viral evolution in the capsid protein of porcine parvovirus. *J. Gen. Virol.*, 92(Pt 11):2628–2636, Nov 2011.
- [431] Su, H. L., Liao, C. L., and Lin, Y. L. Japanese encephalitis virus infection initiates endoplasmic reticulum stress and an unfolded protein response. *J. Virol.*, 76(9):4162–4171, May 2002.
- [432] Siikkanen, S., Saajarvi, K., Hirsimaki, J., Valilehto, O., Reunanen, H., Vihtinen-Ranta, M., and Vuento, M. Role of recycling endosomes and lysosomes in dynein-dependent entry of canine parvovirus. *J. Virol.*, 76(9):4401–4411, May 2002.
- [433] Siikkanen, S., Aaltonen, T., Nevalainen, M., Valilehto, O., Lindholm, L., Vuento, M., and Vihtinen-Ranta, M. Exploitation of microtubule cytoskeleton and dynein during parvoviral traffic toward the nucleus. *J. Virol.*, 77(19):10270–10279, Oct 2003.
- [434] Siikkanen, S., Antila, M., Jaatinen, A., Vihtinen-Ranta, M., and Vuento, M. Release of canine parvovirus from endocytic vesicles. *Virology*, 316(2):267–280, Nov 2003.
- [435] Summerford, C. and Samulski, R. J. Membrane-associated heparan sulfate proteoglycan is a receptor for adeno-associated virus type 2 virions. *J. Virol.*, 72(2):1438–1445, Feb 1998.

- [436] Summerford, C., Bartlett, J. S., and Samulski, R. J. $\alpha_V\beta_5$ -integrin: a co-receptor for adeno-associated virus type 2 infection. *Nat. Med.*, 5(1):78–82, Jan 1999.
- [437] Tardif, K. D., Mori, K., Kaufman, R. J., and Siddiqui, A. Hepatitis C virus suppresses the IRE1-XBP1 pathway of the unfolded protein response. *J. Biol. Chem.*, 279(17):17158–17164, Apr 2004.
- [438] Tattersall, P. Replication of the parvovirus MVM. I. Dependence of virus multiplication and plaque formation on cell growth. *J. Virol.*, 10(4):586–590, Oct 1972.
- [439] Tattersall, P. The evolution of parvovirus taxonomy. In Kerr, J. R., Bloom, M. E., Cotmore, S. F., Linden, R. M., and Parrish, C. R., eds., *Parvoviruses*, p. 9. Hodder Arnold, London, UK, 2006.
- [440] Tattersall, P. and Bratton, J. Reciprocal productive and restrictive virus-cell interactions of immunosuppressive and prototype strains of minute virus of mice. *J. Virol.*, 46(3):944–955, Jun 1983.
- [441] Tattersall, P. and Cotmore, S. F. The nature of parvoviruses. In Pattison, J. R., ed., *Parvoviruses and Human Diseases*, pp. 5–41. CRC Press, Inc., Boca Raton, FL, 1988.
- [442] Tattersall, P. and Gardiner, E. M. Autonomous parvovirus-host-cell interactions. In Tijssen, P., ed., *Handbook of parvoviruses*, vol. 1, pp. 111–121. CRC Press, Inc., Boca Raton, FL, 1990.
- [443] Tattersall, P. and Ward, D. C. Rolling hairpin model for replication of parvovirus and linear chromosomal DNA. *Nature*, 263(5573):106–109, Sep 1976.
- [444] Tattersall, P. and Ward, D. C. The parvoviruses - an introduction. In Ward, D. C. and Tattersall, P., eds., *Replication of mammalian parvoviruses*, pp. 3–12. Cold Spring Harbor Laboratory Press, Cold Spring Harbor, NY, 1978.
- [445] Tattersall, P., Cawte, P. J., Shatkin, A. J., and Ward, D. C. Three structural polypeptides coded for by minute virus of mice, a parvovirus. *J. Virol.*, 20(1):273–289, Oct 1976.
- [446] Tattersall, P., Shatkin, A. J., and Ward, D. C. Sequence homology between the structural polypeptides of minute virus of mice. *J. Mol. Biol.*, 111(4):375–394, Apr 1977.
- [447] Tennant, R. W., Layman, K. R., and Hand, R. E. Effect of cell physiological state on infection by rat virus. *J. Virol.*, 4(6):872–878, Dec 1969.
- [448] Thacker, T. C. and Johnson, F. B. Binding of bovine parvovirus to erythrocyte membrane sialylglycoproteins. *J. Gen. Virol.*, 79 (Pt 9):2163–2169, Sep 1998.
- [449] Tijssen, P. *Handbook of parvoviruses*, vol. 1. CRC Press, Inc., Boca Raton, FL, 1990.
- [450] Tijssen, P. Molecular and structural basis of the evolution of parvovirus tropism. *Acta Vet. Hung.*, 47(3):379–394, 1999.
- [451] Tijssen, P., Szelei, J., and Zádori, Z. Phospholipase A₂ domains in structural proteins of parvoviruses. In Kerr, J. R., Bloom, M. E., Cotmore, S. F., Linden, R. M., and Parrish, C. R., eds., *Parvoviruses*, pp. 95–105. Hodder Arnold, London, UK, 2006.
- [452] Trampel, D. W., Kinden, D. A., Solorzano, R. F., and Stogsdill, P. L. Parvovirus-like enteropathy in Missouri turkeys. *Avian Dis.*, 27(1):49–54, 1983.
- [453] Tresnan, D. B., Southard, L., Weichert, W., Sgro, J. Y., and Parrish, C. R. Analysis of the cell and erythrocyte binding activities of the dimple and canyon regions of the canine parvovirus capsid. *Virology*, 211 (1):123–132, Aug 1995.
- [454] Truyen, U., Agbandje, M., and Parrish, C. R. Characterization of the feline host range and a specific epitope of feline panleukopenia virus. *Virology*, 200 (2):494–503, May 1994.
- [455] Tsao, J., Chapman, M. S., Agbandje, M., Keller, W., Smith, K., Wu, H., Luo, M., Smith, T. J., Rossmann, M. G., and Compans, R. W. The three-dimensional structure of canine parvovirus and its functional implications. *Science*, 251(5000):1456–1464, Mar 1991.
- [456] Tsao, J., Chapman, M. S., Wu, H., Agbandje, M., Keller, W., and Rossmann, M. G. Structure determination of monoclinic canine parvovirus. *Acta Crystallogr., B*, 48 (Pt 1):75–88, Feb 1992.
- [457] Tse, H., Tsoi, H. W., Teng, J. L., Chen, X. C., Liu, H., Zhou, B., Zheng, B. J., Woo, P. C., Lau, S. K., and Yuen, K. Y. Discovery and genomic characterization of a novel ovine partetetravirus and a new genotype of bovine partetetravirus. *PLoS ONE*, 6(9):e25619, 2011.
- [458] Tullis, G. E., Burger, L. R., and Pintel, D. J. The trypsin-sensitive RVER domain in the capsid proteins

- of minute virus of mice is required for efficient cell binding and viral infection but not for proteolytic processing in vivo. *Virology*, 191(2):846–857, Dec 1992.
- [459] Tullis, G. E., Burger, L. R., and Pintel, D. J. The minor capsid protein VP1 of the autonomous parvovirus minute virus of mice is dispensable for encapsidation of progeny single-stranded DNA but is required for infectivity. *J. Virol.*, 67(1):131–141, Jan 1993.
- [460] Valle, N., Riolobos, L., and Almendral, J. M. Synthesis, post-translational modification and trafficking of the parvovirus structural polypeptides. In Kerr, J. R., Bloom, M. E., Cotmore, S. F., Linden, R. M., and Parrish, C. R., eds., *Parvoviruses*, pp. 291–304. Hodder Arnold, London, UK, 2006.
- [461] van Leengoed, L. A., Vos, J., Gruys, E., Rondhuis, P., and Brand, A. Porcine Parvovirus infection: review and diagnosis in a sow herd with reproductive failure. *Vet Q*, 5(3):131–141, Jul 1983.
- [462] Vandenberghe, L. H., Xiao, R., Lock, M., Lin, J., Korn, M., and Wilson, J. M. Efficient serotype-dependent release of functional vector into the culture medium during adeno-associated virus manufacturing. *Hum. Gene Ther.*, 21(10):1251–1257, Oct 2010.
- [463] Varki, N. M. and Varki, A. Diversity in cell surface sialic acid presentations: implications for biology and disease. *Lab. Invest.*, 87(9):851–857, Sep 2007.
- [464] Vasudevacharya, J. and Compans, R. W. The NS and capsid genes determine the host range of porcine parvovirus. *Virology*, 187(2):515–524, Apr 1992.
- [465] Vicente, D., Cilla, G., Montes, M., Perez-Yarza, E. G., and Perez-Trallero, E. Human bocavirus, a respiratory and enteric virus. *Emerging Infect. Dis.*, 13(4): 636–637, Apr 2007.
- [466] Vihinen-Ranta, M., Kakkola, L., Kalela, A., Vilja, P., and Vuento, M. Characterization of a nuclear localization signal of canine parvovirus capsid proteins. *Eur. J. Biochem.*, 250(2):389–394, Dec 1997.
- [467] Vihinen-Ranta, M., Kalela, A., Makinen, P., Kakkola, L., Marjomaki, V., and Vuento, M. Intracellular route of canine parvovirus entry. *J. Virol.*, 72(1):802–806, Jan 1998.
- [468] Vihinen-Ranta, M., Yuan, W., and Parrish, C. R. Cyttoplasmic trafficking of the canine parvovirus capsid and its role in infection and nuclear transport. *J. Virol.*, 74(10):4853–4859, May 2000.
- [469] Vihinen-Ranta, M., Wang, D., Weichert, W. S., and Parrish, C. R. The VP1 N-terminal sequence of canine parvovirus affects nuclear transport of capsids and efficient cell infection. *J. Virol.*, 76(4):1884–1891, Feb 2002.
- [470] Vihinen-Ranta, M., Suikkanen, S., and Parrish, C. R. Pathways of cell infection by parvoviruses and adeno-associated viruses. *J. Virol.*, 78(13):6709–6714, Jul 2004.
- [471] Walker, S. L., Wonderling, R. S., and Owens, R. A. Mutational analysis of the adeno-associated virus type 2 Rep68 protein helicase motifs. *J. Virol.*, 71(9): 6996–7004, Sep 1997.
- [472] Walters, R. W., Yi, S. M., Keshavjee, S., Brown, K. E., Welsh, M. J., Chiorini, J. A., and Zabner, J. Binding of adeno-associated virus type 5 to 2,3-linked sialic acid is required for gene transfer. *J. Biol. Chem.*, 276(23):20610–20616, Jun 2001.
- [473] Wang, X. S., Ponnazhagan, S., and Srivastava, A. Rescue and replication of adeno-associated virus type 2 as well as vector DNA sequences from recombinant plasmids containing deletions in the viral inverted terminal repeats: selective encapsidation of viral genomes in progeny virions. *J. Virol.*, 70(3):1668–1677, Mar 1996.
- [474] Wang, X. S., Qing, K., Ponnazhagan, S., and Srivastava, A. Adeno-associated virus type 2 DNA replication in vivo: mutation analyses of the D sequence in viral inverted terminal repeats. *J. Virol.*, 71(4): 3077–3082, Apr 1997.
- [475] Ward, D. C. and Tattersall, P. Minute virus of mice. In Foster, H. L., Small, J. D., and Fox, J. G., eds., *The mouse in biomedical research*, vol. 2, pp. 313–334. Academic Press, Inc., New York, NY, 1982.
- [476] Weichert, W. S., Parker, J. S., Wahid, A. T., Chang, S. F., Meier, E., and Parrish, C. R. Assaying for structural variation in the parvovirus capsid and its role in infection. *Virology*, 250(1):106–117, Oct 1998.
- [477] Weigel-Kelley, K. A., Yoder, M. C., and Srivastava, A. Recombinant human parvovirus B19 vectors: erythrocyte P antigen is necessary but not sufficient for successful transduction of human hematopoietic cells. *J. Virol.*, 75(9):4110–4116, May 2001.
- [478] Weigel-Kelley, K. A., Yoder, M. C., and Srivastava, A. $\alpha_5\beta_1$ -integrin as a cellular co-receptor for human parvovirus B19: requirement of functional activation of β_1 -integrin for viral entry. *Blood*, 102(12):3927–3933, Dec 2003.

- [479] Weiner, H. L., Drayna, D., Averill, D. R., and Fields, B. N. Molecular basis of reovirus virulence: role of the S1 gene. *Proc. Natl. Acad. Sci. U.S.A.*, 74(12): 5744–5748, Dec 1977.
- [480] Weiner, H. L., Ault, K. A., and Fields, B. N. Interaction of reovirus with cell surface receptors. I. Murine and human lymphocytes have a receptor for the hemagglutinin of reovirus type 3. *J. Immunol.*, 124(5):2143–2148, May 1980.
- [481] Weis, K. Nucleocytoplasmic transport: cargo trafficking across the border. *Curr. Opin. Cell Biol.*, 14(3): 328–335, Jun 2002.
- [482] Weiss, N., Stroh-Dege, A., Rommelaere, J., Dinsart, C., and Salome, N. An in-frame deletion in the NS protein-coding sequence of parvovirus H-1PV efficiently stimulates export and infectivity of progeny virions. *J. Virol.*, 86(14):7554–7564, Jul 2012.
- [483] Weller, M. L., Amornphimoltham, P., Schmidt, M., Wilson, P. A., Gutkind, J. S., and Chiorini, J. A. Epidermal growth factor receptor is a co-receptor for adeno-associated virus serotype 6. *Nat. Med.*, 16(6): 662–664, Jun 2010.
- [484] Whittaker, G. R., Kann, M., and Helenius, A. Viral entry into the nucleus. *Annu. Rev. Cell Dev. Biol.*, 16:627–651, 2000.
- [485] Wichman, H. A., Badgett, M. R., Scott, L. A., Boulian, C. M., and Bull, J. J. Different trajectories of parallel evolution during viral adaptation. *Science*, 285(5426):422–424, Jul 1999.
- [486] Willwand, K. and Hirt, B. The minute virus of mice capsid specifically recognizes the 3' hairpin structure of the viral replicative-form DNA: mapping of the binding site by hydroxyl radical footprinting. *J. Virol.*, 65(9):4629–4635, Sep 1991.
- [487] Willwand, K. and Hirt, B. The major capsid protein VP2 of minute virus of mice (MVM) can form particles which bind to the 3'-terminal hairpin of MVM replicative-form DNA and package single-stranded viral progeny DNA. *J. Virol.*, 67(9):5660–5663, Sep 1993.
- [488] Willwand, K., Baldauf, A. Q., Deleu, L., Mumtsidu, E., Costello, E., Beard, P., and Rommelaere, J. The minute virus of mice (MVM) nonstructural protein NS1 induces nicking of MVM DNA at a unique site of the right-end telomere in both hairpin and duplex conformations in vitro. *J. Gen. Virol.*, 78 (Pt 10): 2647–2655, Oct 1997.
- [489] Willwand, K., Moroianu, A., Horlein, R., Stremmel, W., and Rommelaere, J. Specific interaction of the nonstructural protein NS1 of minute virus of mice (MVM) with [ACCA](2) motifs in the centre of the right-end MVM DNA palindrome induces hairpin-primed viral DNA replication. *J. Gen. Virol.*, 83(Pt 7):1659–1664, Jul 2002.
- [490] Wilson, G. M., Jindal, H. K., Yeung, D. E., Chen, W., and Astell, C. R. Expression of minute virus of mice major nonstructural protein in insect cells: purification and identification of ATPase and helicase activities. *Virology*, 185(1):90–98, Nov 1991.
- [491] Wimmer, E., ed. *Cellular receptors for animal viruses*. Cold Spring Harbor Press, Cold Spring Harbor, NY, 1994.
- [492] Wistuba, A., Kern, A., Weger, S., Grimm, D., and Kleinschmidt, J. A. Subcellular compartmentalization of adeno-associated virus type 2 assembly. *J. Virol.*, 71(2):1341–1352, Feb 1997.
- [493] Wong, S., Momoeda, M., Field, A., Kajigaya, S., and Young, N. S. Formation of empty B19 parvovirus capsids by the truncated minor capsid protein. *J. Virol.*, 68(7):4690–4694, Jul 1994.
- [494] Wu, H. and Rossmann, M. G. The canine parvovirus empty capsid structure. *J. Mol. Biol.*, 233(2):231–244, Sep 1993.
- [495] Wu, H., Keller, W., and Rossmann, M. G. Determination and refinement of the canine parvovirus empty-capsid structure. *Acta Crystallogr. D Biol. Crystallogr.*, 49(Pt 6):572–579, Nov 1993.
- [496] Wu, Z., Asokan, A., Grieger, J. C., Govindasamy, L., Agbandje-McKenna, M., and Samulski, R. J. Single amino acid changes can influence titer, heparin binding, and tissue tropism in different adeno-associated virus serotypes. *J. Virol.*, 80(22):11393–11397, Nov 2006.
- [497] Wu, Z., Miller, E., Agbandje-McKenna, M., and Samulski, R. J. Alpha2,3 and alpha2,6 N-linked sialic acids facilitate efficient binding and transduction by adeno-associated virus types 1 and 6. *J. Virol.*, 80 (18):9093–9103, Sep 2006.
- [498] Xiao, C. T., Gimenez-Lirola, L. G., Jiang, Y. H., Halbur, P. G., and Opriessnig, T. Characterization of a novel porcine parvovirus tentatively designated PPV5. *PLoS ONE*, 8(6):e65312, 2013.

- [499] Xiao, C. T., Halbur, P. G., and Opriessnig, T. Complete Genome Sequence of a Novel Porcine Parvovirus (PPV) Provisionally Designated PPV5. *Genome Announc.*, 1(1), Jan 2013.
- [500] Xiao, W., Warrington, K. H., Hearing, P., Hughes, J., and Muzyczka, N. Adenovirus-facilitated nuclear translocation of adeno-associated virus type 2. *J. Virol.*, 76(22):11505–11517, Nov 2002.
- [501] Xie, Q. and Chapman, M. S. Canine parvovirus capsid structure, analyzed at 2.9 Å resolution. *J. Mol. Biol.*, 264(3):497–520, Dec 1996.
- [502] Xie, Q., Bu, W., Bhatia, S., Hare, J., Somasundaram, T., Azzi, A., and Chapman, M. S. The atomic structure of adeno-associated virus (AAV-2), a vector for human gene therapy. *Proc. Natl. Acad. Sci. U.S.A.*, 99(16):10405–10410, Aug 2002.
- [503] Yan, Z., Zak, R., Luxton, G. W., Ritchie, T. C., Bantel-Schaal, U., and Engelhardt, J. F. Ubiquitination of both adeno-associated virus type 2 and 5 capsid proteins affects the transduction efficiency of recombinant vectors. *J. Virol.*, 76(5):2043–2053, Mar 2002.
- [504] Young, P. J., Jensen, K. T., Burger, L. R., Pintel, D. J., and Lorson, C. L. Minute virus of mice NS1 interacts with the SMN protein, and they colocalize in novel nuclear bodies induced by parvovirus infection. *J. Virol.*, 76(8):3892–3904, Apr 2002.
- [505] Yu, X., Zhang, J., Hong, L., Wang, J., Yuan, Z., Zhang, X., and Ghildyal, R. High prevalence of human parvovirus 4 infection in HBV and HCV infected individuals in shanghai. *PLoS ONE*, 7(1):e29474, 2012.
- [506] Zadori, Z., Szelei, J., Lacoste, M. C., Li, Y., Gariepy, S., Raymond, P., Allaire, M., Nabi, I. R., and Tijssen, P. A viral phospholipase A2 is required for parvovirus infectivity. *Dev. Cell*, 1(2):291–302, Aug 2001.
- [507] Zadori, Z., Szelei, J., and Tijssen, P. SAT: a late NS protein of porcine parvovirus. *J. Virol.*, 79(20):13129–13138, Oct 2005.
- [508] Zhao, Q., Schoborg, R. V., and Pintel, D. J. Alternative splicing of pre-mRNAs encoding the nonstructural proteins of minute virus of mice is facilitated by sequences within the downstream intron. *J. Virol.*, 68(5):2849–2859, May 1994.
- [509] Zhao, Q., Gersappe, A., and Pintel, D. J. Efficient excision of the upstream large intron from P4-generated pre-mRNA of the parvovirus minute virus of mice requires at least one donor and the 3' splice site of the small downstream intron. *J. Virol.*, 69(10):6170–6179, Oct 1995.
- [510] Zhao, Q., Mathur, S., Burger, L. R., and Pintel, D. J. Sequences within the parvovirus minute virus of mice NS2-specific exon are required for inclusion of this exon into spliced steady-state RNA. *J. Virol.*, 69(9):5864–5868, Sep 1995.
- [511] Zhong, L., Li, B., Jayandharan, G., Mah, C. S., Govindasamy, L., Agbandje-McKenna, M., Herzog, R. W., Weigel-Van Aken, K. A., Hobbs, J. A., Zolotukhin, S., Muzyczka, N., and Srivastava, A. Tyrosine-phosphorylation of AAV2 vectors and its consequences on viral intracellular trafficking and transgene expression. *Virology*, 381(2):194–202, Nov 2008.
- [512] Zhong, L., Li, B., Mah, C. S., Govindasamy, L., Agbandje-McKenna, M., Cooper, M., Herzog, R. W., Zolotukhin, I., Warrington, K. H., Weigel-Van Aken, K. A., Hobbs, J. A., Zolotukhin, S., Muzyczka, N., and Srivastava, A. Next generation of adeno-associated virus 2 vectors: point mutations in tyrosines lead to high-efficiency transduction at lower doses. *Proc. Natl. Acad. Sci. U.S.A.*, 105(22):7827–7832, Jun 2008.
- [513] Zlotnick, A. and Mukhopadhyay, S. Virus assembly, allostery and antivirals. *Trends Microbiol.*, 19(1):14–23, Jan 2011.
- [514] Zsak, L., Strother, K. O., and Kisary, J. Partial genome sequence analysis of parvoviruses associated with enteric disease in poultry. *Avian Pathol.*, 37(4):435–441, Aug 2008.

Declaration of consent

on the basis of Article 28 para. 2 of the RSL05 phil.-nat.

Name/First Name:

Matriculation Number:

Study program:

Bachelor

Master

Dissertation

Title of the thesis:

Supervisor:

I declare herewith that this thesis is my own work and that I have not used any sources other than those stated. I have indicated the adoption of quotations as well as thoughts taken from other authors as such in the thesis. I am aware that the Senate pursuant to Article 36 para. 1 lit. r of the University Act of 5 September, 1996 is authorised to revoke the title awarded on the basis of this thesis. I allow herewith inspection in this thesis.

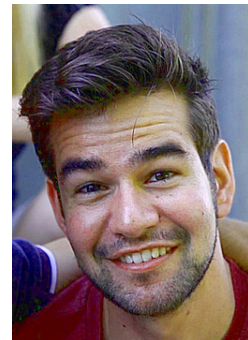
Place/Date

Signature

Curriculum Vitae

Personal Details

First Name	Raphael
Surname	Wolfisberg
Date of Birth	14. May 1988
Nationality	Swiss
E-mail	raphael.w@hotmail.com
Mobile	+41 79 837 19 62



Education

Mar. 2012 - present	Ph.D. at the Department of Chemistry and Biochemistry (DCB) University of Bern, Switzerland Title of the Ph.D. thesis: "Characterization of the prelytic active egress of a non-enveloped virus." Supervisors: Dr. Carlos Ros and Prof. Dr. Christoph Kempf
Oct. - Dec. 2013	Scientific exchange at Centro de Biología Molecular Severo Ochoa Universidad Autónoma de Madrid Collaboration with Prof. Dr. José María Almendral del Río
Sept. 2010 - Jan. 2012	Master of Science (MSc) in Chemistry and Molecular Science DCB, University of Bern, Switzerland Title of the master thesis: "Changing the surface of human parvovirus B19." Supervisors: Dr. Carlos Ros and Prof. Dr. Christoph Kempf
Sept. 2007 - Aug. 2010	Bachelor of Science (BSc) in Chemistry or Biochemistry DCB, University of Bern, Switzerland Title of the bachelor thesis: "Die Suche nach dem NMD Mechanismus in <i>Trypanosoma brucei</i> ." Supervisor: Prof. Dr. André Schneider
Aug. 2003 - Aug. 2007	Grammar school at the Kantonsschule Reussbühl, Lucerne Main subjects: physics and applied mathematics

Skills

Languages	German	Mother tongue
	English	Advanced
	French	Intermediate level
	Spanish	Basic knowledge
Operating Systems	Microsoft Windows Apple OS X	
Programs	Typesetting	Apple iWork \LaTeX
		Microsoft Office
	Molecular modeling	PyMOL UCSF Chimera
	Data processing	GraphPad Prism Mathcad